AN EXPERIMENTAL INVESTIGATION OF HEAT TRANSFER AND PRESSURE DROP IN THE TRANSITION REGION FOR A HORIZONTAL TUBE WITH DIFFERENT INLETS AND UNIFORM WALL HEAT FLUX

By

LAP MOU TAM

Bachelor of Science
National Chiao Tung University
Hsinchu, Taiwan, Republic of China
1989

Master of Science
Oklahoma State University
Stillwater, Oklahoma
1990

Submitted to the Faculty of the
Graduate College of the
Oklahoma State University
in partial fulfillment of
the requirements for
the Degree of
DOCTOR OF PHILOSOPHY
December, 1995

AN EXPERIMENTAL INVESTIGATION OF HEAT TRANSFER AND PRESSURE DROP IN THE TRANSITION REGION FOR A HORIZONTAL TUBE WITH DIFFERENT INLETS AND UNIFORM WALL HEAT FLUX

Thesis Approved :

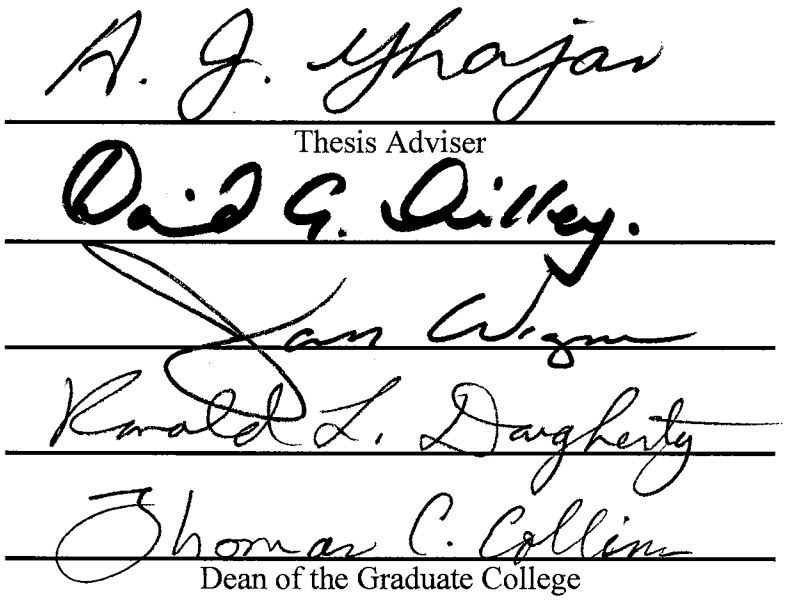

Thesis Adviser

Dean of the Graduate College

ACKNOWLEDGMENTS

I would like to express my sincere appreciation to my adviser, Dr. A. J. Ghajar, for his intelligent supervision and advice throughout the progress of this research. My sincere appreciation extends to my committee members, Dr. J. Wagner, Dr. D. Lilley and Dr. R. Dougherty whose valuable suggestion and guidance are invaluable.

Moreover, I would like to express my sincere gratitude to my close friends who provided suggestions and assistance for this study: Dr. Ming-Chun Dong, Dr. Ye Tian, Dr. Jiaqi Cai, Dr. Tzer-Kun Lin, Dr. G. X. Chen, and Mr. Wen-Cheih Tang.

Special gratitude and appreciation is expressed to my loving wife, Yut Ching Kan, for her support, understanding, and sacrifices throughout this whole process. I deeply appreciate the encouragement and financial support given by my family, Mr. Kuok Kuong Tam, Mrs. Chau Mei Heng Tam, Ms. Man Man Tam, and Ms. Ian Ian Tam.

Finally, I would like to thank the School of Mechanical and Aerospace Engineering for the financial support during these four and one-half years of study.

TABLE OF CONTENTS

LIST OF TABLES

LIST OF FIGURES

NOMENCLATURE

English Letters

C_f	fully developed skin friction coefficient (fanning friction factor), (= $\Delta PD/2L\rho V^2$), dimensionless
D	inside diameter of the test section, cm
f	Darcy fully developed friction factor, dimensionless
f_{app}	Darcy apparent friction factor, dimensionless
g	acceleration of gravity, m/s^2
Gr	local bulk Grashof number, $g\beta\rho^2D^3(T_{wi} - T_b)/\mu^2$
h	heat transfer coefficient, W/m^2-K
h_b	peripheral heat transfer coefficient at the bottom of the tube, W/m^2-K
h_t	peripheral heat transfer coefficient at the top of the tube, W/m^2-K
I	current carried by the test section, Amperes
k	thermal conductivity of the test fluid evaluated at T_b, W/m-K
L	length of the test section (tube), m
m	an exponent; see Table II
Nu	local average or fully developed peripheral Nusselt number (= hD/k), dimensionless
Nu_l	local average or fully developed peripheral laminar Nusselt number, dimensionless
Nu_t	local average or fully developed peripheral turbulent Nusselt number, dimensionless

Nu_{tr} local average or fully developed peripheral transitional Nusselt number, dimensionless

Pr local bulk Prandtl number (= $\mu c_p/k$), dimensionless

Re local bulk Reynolds number (= $\rho VD/\mu$), dimensionless

St Stanton number (= Nu/(RePr))

T_b local bulk temperature of the test fluid, ^oC

T_{wi} local peripheral tube inside wall temperature, ^oC

V average velocity in the test section, m/s

x local distance along the test section from the inlet, m

Greek Symbols

β coefficient of thermal expansion of the test fluid evaluated at T_b, K^{-1}

ΔP pressure difference, Pa

μ_b absolute viscosity of the test fluid evaluated at T_b, Pa-s

μ_w absolute viscosity of the test fluid evaluated at T_{wi}, Pa-s

ρ density of the test fluid evaluated at T_b, kg/m^3

Subscripts

app refers to apparent

b refers to the bottom

cal refers to the calculated value

exp refers to the experimental value

forced refers to forced convection

mixed refers to mixed convection

t refers to the top

CHAPTER I

INTRODUCTION

A large amount of experimental, numerical and analytical work is available for fluid flow through tubes in the laminar and turbulent flow regimes. However, very little has been done in the entrance region of a transitional flow. An important design problem in industrial heat exchangers arises when the flow inside the tube falls into the transition region. The usual recommendation is to avoid design and operation in this flow regime; however, this is not always feasible under design constraints. Much of the information available in the literature deals with the fully developed flow from the entrance, or involves entrance effects downstream from highly idealized entrances. Due to the non-linear terms in the Navier-Stokes equation and the intermittent behavior of the transition region, it is difficult to examine the problem analytically or numerically. Hence, an experimental approach seems to be suitable for this type of problem. In this study, attention will be paid to heat transfer transitional flow in the entrance region and pressure drop transition flow under non-isothermal flow condition. This chapter is devoted to the descriptions of the background, the literature survey of related studies, and the objectives of the work.

1.1 Background

In this section, three key factors which are very important to the investigation of the transitional flow will be presented. These factors are the inlet configuration, the entrance region, and the effect of combined forced and free convection.

1.1.1 Effect of the Inlet Configuration

The usually cited transition Reynolds number of about 2100 applies to a very steady flow with a rounded entrance. If the flow has a disturbed entrance typical of heat exchangers, in which there is a sudden contraction and possibly even a reentrant entrance, this transition Reynolds number may be completely different. The heat transfer and pressure drop characteristics are different from fully developed laminar and turbulent regions. In order to investigate the transition region, the transition Reynolds number (from laminar to transition and from transition to turbulent) needs to be defined.

1.1.2 Entrance Region

The development of the velocity and temperature profiles in the entrance region is strongly dependent on the nature of the inlet and the previous history of the flow field. Inside a heat exchanger, the entrance to the tubes is usually of a disturbed type, like square-edged or reentrant. Due to the complexity of the entrance flow and the interactions between momentum and energy transfer, entrance effects are usually ignored and only fully developed momentum and energy transfer are considered. This lack of consideration of the entrance effects may be suitable for turbulent flow since its entrance length is short. When the tube is short and the flow is in the transition region, neglecting the entrance

effects may cause serious problems. Up to now, there have been only qualitative but not quantitative information about heat transfer in the entrance region of the transitional flow. Hence, the influence of entrance should be investigated.

1.1.3 The Effect of Combined Forced and Free Convection

Mixed convection flow received considerable attention in the late 1970s. Heating a fluid flowing in a horizontal pipe produces a secondary flow. The fluid near the pipe wall due to its higher temperature and lower density, circulates upward, and the fluid near the central region of the pipe having a lower temperature and higher density circulates downward. In the laminar and transition regions these counterrotating transverse vortices that are superimposed on the stream-wise main flow due to free convection effects can increase the forced convection heat transfer significantly. In the turbulent region, the influence of buoyancy is completely overwhelmed by the turbulent motion. This is contrary to the cases of laminar and transition flows. Actually, buoyancy forces are present in any forced convection flow, and for design purposes, it is of interest to know when they can be neglected and when they have to be accounted for. The traditional criterion is to use the ratio Gr/Re^2. When this ratio is close to unity, free convection effect should be considered. However, a lot of inconsistency shows up when this ratio is applied. In fact, the buoyant effect depends on not only Reynolds number and Grashof number, but also depends on the flow regime, Prandtl number, axial location, and the type of inlet configuration. It is important to investigate how these parameters influence the buoyant effect in the transition region.

From the information above, it is obvious that our understanding of pipe flow in the transition region is far from complete. Very little information is available for a design engineer to predict the heat transfer coefficient and pressure drop in the transition region for a tube with a disturbed entrance. The main goal of this study is to create an accurate and broad forced and mixed convection heat transfer and pressure drop data base across all flow regimes for a wide range of Reynolds, Prandtl, and Grashof numbers in the entrance and fully developed regions of a circular horizontal tube under uniform wall heat flux boundary condition. Three different inlet configurations (reentrant, square-edged, and bell-mouth) will be considered. Experimental data can be used to investigate the effect of inlet configuration, entrance region, and buoyancy force effects quantitatively. By understanding all those factors, accurate correlations in the transition region can be developed for engineering purposes.

1.2 Literature Survey

The local heat transfer and pressure drop characteristics in horizontal pipes for both laminar and turbulent flow regimes have been treated extensively in the past including many analytical and numerical solutions for combined forced and free convection in horizontal tubes. In this section a brief review of many of the most important and pertinent works related to this study will be given. At the end of this section, the most recommended and relevant correlations for heat transfer and pressure drop for all flow regimes are tabulated.

1.2.1 Heat Transfer

Using air as a test fluid in a uniformly heated horizontal tube, McComas and Eckert (1966) investigated free convection heat transfer for laminar flow Reynolds numbers from 100 to 900 and Grashof numbers from 0.33 to 1000. By comparing high Grashof number runs with low Grashof number runs at equal Reynolds numbers, they found that buoyancy created secondary flow increase with the ratio of Grashof to Reynolds numbers.

Mori et al. (1966) studied the effect of buoyancy on fully developed forced convection heat transfer in horizontal tubes with uniform heat flux. For air at Reynolds numbers from 100 to 13000 in a brass tube with nichrome wires wound at constant pitch for nearly uniform heat flux, they developed a correlation for the Nusselt number in the fully developed laminar flow region. They observed that when the product of Reynolds and Rayleigh numbers is more than 10^4, the secondary flow is stronger. They also pointed out that secondary flow has no effect on Nusselt number in the turbulent region.

Petukhov and Polyakov (1967a,1967b) using distilled water in a tube heated with internal electrical wall resistance (using AC current) studied local heat transfer coefficient. By measuring the temperature at both axial and radial locations, they plotted average Nusselt numbers as a function of the reduced length ((x/D) / (RePr)) and showed that the local Nusselt numbers are a strong function of Rayleigh number. They also observed that the thermal entry length decreased when Rayleigh number increased.

Shannon and Depew (1968,1969) investigated natural convection effects for a wall resistance (DC current) heated stainless steel tube that also incorporated an unheated

calming section. They used two fluids (water and ethylene glycol) to cover a Reynolds number range of 6 to 2300. Their results showed the influence of free convection and were correlated using the parameter $GrPr^{0.25}/NuGz$ where NuGz is the theoretical local Nusselt number found from Siegel et al. (1958). They concluded that when $GrPr^{0.25}/NuGz$ was less than 2, the free convection effect was unimportant.

Siegwarth et al. (1969) analyzed the effect of secondary flow on the temperature field and primary flow at the outlet of a long electrically-heated tube. They developed a model for the flow field by dimensional reasoning and found that the secondary flow controls the rate of heat transfer. Their model showed good agreement with the data measured by Readal (1969).

Hussain and McComas (1970) researched the effect of free convection for Reynolds numbers between 670 and 3800 for air flowing through a uniformly heated horizontal circular tube. They found that below Reynolds numbers of 1200 and far downstream of the entrance, the heat transfer was below the pure forced convection prediction. For larger Reynolds numbers the results were higher than predicted by forced convection theory. In their experiments, they experienced significant wall temperature variation in the circumferencial direction.

Using a flow visualization technique, Bergles and Simonds (1971) studied the effects of free convection on laminar water flow in a horizontal circular tube with uniform heat flux. The tubes were Pyrex E-C coated tubes with four thermocouples placed 90 degrees apart in the peripheral direction. Heat was generated in the Pyrex E-C coating to provide a constant heat flux with nearly zero radial conduction, and their results were similar to Petukhov and Polyakov (1967b).

Morcos and Bergles (1975) investigated the effects of fluid property variations for laminar flow heat transfer with a fully developed velocity profile in a horizontal tube with uniform heat flux. They used both glass and steel tubes in their study. They argued that the traditional viscosity correction factor $(\mu_b/\mu_w)^{0.14}$ could not account for the variable property effect even when the exponent was varied. Hence they used the film temperature for evaluation of all fluid properties and developed a correlation using the method introduced by Churchill and Usagi (1972) for fully developed mixed convection flow.

Gnielinski (1976) used experimental data from the literature to develop a correlation which cover Reynolds numbers from 2300 to 100000. He used a modified version of Petukhov and Popov's (1963) correlation. The correlation is limited to fully developed forced convection flow.

Churchill (1977) used the asymptotic method introduced by Churchill and Usagi (1972) to construct a correlation for the entire flow regime. However, this correlation is only for the highly idealized round entrance (no disturbance) and for fully developed forced flow.

Shah and Johnson (1980) carried out an extensive review of available correlations. They recommended Gnielinski's (1976) correlation for Reynolds numbers greater than 2300 and, hence, the correlation can be applied in the transition region.

Al-Arabi (1982) investigated the turbulent heat transfer in the entrance region of a tube for different inlet configurations. In his studies for a bell-mouth entrance, the

boundary layer along the tube wall is at first laminar and then changes through a transition region to the turbulent condition causing a dip in the h-x/D curve.

Ogawa and Kawamura (1987) experimented with air flow in the transition region for Reynolds numbers ranging from 1940 to 9120. They used a vertical steel tube subjected to a nearly uniform heat flux provided by electric sheath heaters and studied the effect produced by four entrance configurations (providing different levels of disturbance) using 16 thermocouples and three pressure taps. They also gathered intermittency data in the transition region for Reynolds numbers of 566 to 16500 using a hot wire anemometer. Their results indicated that the intermittency factor is slightly influenced by the local bulk Reynolds number and is primarily dependent upon the entrance condition. Additionally, their results were not influenced by free convection as Rayleigh number experienced in their study was confined to values below 15. For the heat transfer results they present both laminar and turbulent heat transfer correlations in terms of Stanton number. In the transition flow region, an interpolating equation using the intermittency factor as a weighting factor is proposed. Their data are claimed to agree with the correlation. However by using air as the test fluid, their correlation is limited to a narrow range of Prandtl number (0.7~0.8).

Chen (1988) investigated local heat transfer in a horizontal tube with a square-edged entrance for laminar, transition, and turbulent flows. He used an electrically-heated horizontal circular tube and accounted for the peripheral conduction of heat by using eight and four thermocouples in the circular direction. Using water and diethylene glycol, he covered a Reynolds number range from 121 to 12400 and a Prandtl number

range from 3.5 to 282.4. He developed correlations for the heat transfer data and his correlation predicted his experimental data well.

Ghajar et al. (1990) using distilled water and a mixture of ethylene glycol and water as the test fluid experimented in the transition region for two different inlet configurations under the uniform wall heat flux boundary condition. In their experiments, the local bulk Reynolds number ranged from 281 to 50529, local bulk Prandtl number ranged from 3.44 to 157.8, the local bulk Grashof number ranged from 1031 to 2.25×10^6 and the local bulk Nusselt number ranged from 12.9 to 232. In their research, they found that the free convection effect is present in the lower transition region and this effect changes the heat transfer characteristic totally from the forced convection situation. The fully developed heat transfer results for the square-edged and reentrant inlet configurations used in their study showed that the range of Reynolds number for which transition flow exists is in the range of 2400 to 9000 and 2200 to 7500, respectively. In the laminar flow region, mixed convection was the dominant mode of heat transfer. They obtained two correlations in the transition region for the two different inlet configurations. However, these two correlations are only good for fully developed flow.

Laurens (1995) used three different inlet configurations to investigate the effect of different heating rates in the laminar and turbulent regions. His results show that in the laminar region, the heat transfer characteristics of the flow are very sensitive to the different magnitude of heating rates. At a very low heating rate (0.5 kW/m^2), he experimentally obtained the laminar Nusselt number to be very close to the classical Nusselt number (Nu = 4.364). As heating rate increases, the corresponding Nusselt number has an almost parallel shift from the classical Nu = 4.364 value. The shift is more

pronounced when the heating rate is large. In the turbulent region, his results show that no significant influence is observed.

Eckert & Diaguila (1954) used a short vertical tube as their test section and air as their test fluid to define the boundary between free, forced, and mixed convection. The determination of the limits between these regimes requires somewhat arbitrary definitions. They defined the boundary between the free, forced, and mixed convection, based on the criterion that mixed convection is present if the measured or calculated heat transfer coefficient is 10 percent greater than the corresponding heat transfer coefficient calculated for the case of pure free or forced convection. Metais (1963) and Metais & Eckert (1964) developed a flow map for vertical and horizontal tubes based on the same criterion. However, this flow map was constructed under the uniform wall temperature boundary condition, and the effect of inlet configuration on the transition region was not taken into consideration.

The pertinent results of these studies and other similar studies are presented in Table I in the form of heat transfer correlations. In this table, the correlations by Morcos and Bergles (1975), Gnielinski (1976) and Churchill (1977) are recommended according to the "Handbook of Single-Phase Convective Heat Transfer" by Kakac et al. (1987). The correlations by Gnielinki (1976) are also recommended strongly by Shah and Johnson (1980). The correlations by Chen (1988) and Ghajar et al. (1990) are also included since their work is closely related to the present study. From this brief review, it is important to point out that most of the previous works (with the exception of the works of Chen (1988) and Ghajar et al. (1990)) are restricted to an ideal round entrance, and no work has been done to investigate the influence of inlet configuration on the free convection

TABLE I

HEAT TRANSFER CORRELATIONS FOR A SMOOTH CIRCULAR DUCT

INVESTIGATOR	CORRELATION	RANGE
Morcos & Bergles (1975)	$Nu_f = \{(4.36)^2 + [0.055(\frac{Gr_f\, Pr_f^{1.35}}{P_w^{0.25}})^{0.4}]^2\}^{0.5}$ $P_w = (hd_2/K_w t)$	$Ra = 3x10^4$ to 10^6 $Pr = 4$ to 175 $P_w = 2$ to 66
Gnielinski (1976)	$Nu = \frac{(f/2)(Re - 1000)Pr}{1 + 12.7(f/2)^{0.5}(Pr^{2/3} - 1)}$	$Re = 2300$ to $5x10^4$ $Pr = 0.5$ to 2000
Churchill (1977)	$Nu^{10} = Nu_l^{10} + \{\frac{\exp[(2200 - Re)/365]}{Nu_l^2} + \frac{1}{Nu^2}\}^{-5}$ where $Nu_l = 4.364$ $Nu_t = 6.3 + \frac{0.079(f/2)^{1/2}\, Re\, Pr}{(1 + Pr^{4/5})^{5/10}}$	for all Re and Pr
Chen (1988)	(a) $Nu = [4.364 + 0.00106Re^{0.81}Pr^{0.45}(1 + 14e^{-0.063x/D}) + 0.268(GrPr)^{1/4}(1 - e^{-0.042x/D})](\mu/\mu_w)^{0.14}$	$Re = 121$ to 2100 $Pr = 3.5$ to 282.4 $Gr = 930$ to 67300
	(b) $Nu = 0.0039RePr^{1/3}(1 + 1.19e^{-0.308x/D})(\mu/\mu_w)^{0.14}$	$Re = 4600$ to 7000 $Pr = 3.5$ to 7.4 $Gr = 45570$ to $1.04x10^6$
	(c) $Nu = 0.01426Pr^{0.86}Pr^{1/3}[1 + 1.15e^{-x/(3D)}](\mu/\mu_w)^{0.14}$	$Re = 7000$ to 2400 $Pr = 3.5$ to 7.4 $Gr = 45570$ to $1.04x10^6$
	$Nu = [(1-y)Nu_l + yNu_t]$	$Re = 2100$ to 4600 Nu_l = eq(a), Nu_t = eq(b).

TABLE I (Continued)

Ghajar et al. (1990)	$Nu = Nu_l + \{\frac{\exp((a - Re)/b)}{Nu_l^2} + \frac{1}{Nu_t^2}\}^{-1/2}$ where $Nu_l = 14.5$ $Nu_t = 6.3 + [\frac{0.079(f)^{0.5} Re Pr}{(1 + Pr^{0.8})^{5/6}}]$ $(f)^{0.5} = [\frac{1}{2.21\ln(Re/7)}]$ a = 2311, b = 534 for reentrant inlet a = 2685, b = 298 for square-edged inlet	for all flow regimes

effects. A few researchers provided criterion to examine the existence of buoyancy, but they are only good for the uniform wall temperature boundary condition. There are no correlations for the developing transition region when mixed convection is present.

1.2.2 Pressure Drop

Schiller (1922) reasoned that the velocity profile in the hydrodynamically developing region could be treated as having two regions, a boundary layer developing near the wall and a central inviscid fluid core. He used a parabolic velocity profile in the boundary layer and Bernoulli's equation in the inviscid core to determine the pressure distribution in the axial direction. He neglected the effect of viscous dissipation in the flow cross section, so this method provides poor results downstream as confirmed by experimental results.

Shapiro and Smith (1947) conducted both experimental and analytical studies for determination of friction factor in the laminar hydrodynamic entrance region of a smooth round tube with a bell-mouth entrance. The range of Reynolds number was from 39,000 to 590,000 with air and water. Their data were correlated with

$$f_{app} = 3.44/[Re(x^+)^{0.5}] \; ; \; x^+ = x/[D(Re)]$$

Shapiro and Smith (1947) postulated that, near the entrance, where the boundary layer is thin compared to diameter of the pipe, its behavior is very similar to flow over a flat plate. Their arguments were qualitative. They said quantitative arguments could not be made because the two flows are fundamentally different. For ducts, drag includes both shear stress and momentum flux changes, whereas for flat plates, drag represents only

shearing stress. A duct flow has a pressure gradient in the direction of flow while it is shown for a flat plate that dp/dx = 0. This boundary layer they said undergoes a transition to turbulent flow (remembering their Re based on tube diameter was greater than the 2000~3000 range). This transition was found to occur at Reynolds number based on "x" at somewhat the same Reynolds number as for a flat plate, i.e. $Re_X = 5x10^5$.

Campbell and Slattery (1963) refined Schiller's solution by considering energy loss due to viscous dissipation within the fluid. This improvement due to Campbell and Slattery showed considerably better agreement with the experimental data than the earlier results of Shapiro and Smith (1947).

As mentioned above Shapiro and Smith (1947) correlated their data in the laminar hydrodynamic region for $10^{-5} < x^+ < 10^{-3}$, where $x^+ = x/[D(Re)]$, with $f_{app} = 3.44/Re_D (x^+)^{0.5}$ where the range of Reynolds number was 51,000 to 113,000. Bender (see Shah 1978) then theoretically obtained an equation for the whole tube length.

Shah (1978) modified the "C" term in Bender's equation from 0.00018 to 0.00021 for a circular duct in the equation

$$f_{app} = \frac{1}{Re}\left[\frac{3.44}{(x^+)^{0.5}} + \frac{\frac{0.31}{x^+} + 16 - \frac{3.44}{(x^+)^{0.5}}}{1 + \frac{0.00021}{(x^+)^2}}\right]$$

This correlation is based on uniform velocity profile at the entrance of the duct. Henc e, the applicability of this equation for a disturbed type of entrance is questionable.

Deissler (1951) carried out experiments in a circular tube. He obtained relations for the prediction of radial distributions of velocity and temperature for fully developed laminar flow of gases and of liquid metals in tubes with fluid properties variable along

the radius. For the friction coefficient, Deissler used the property ratio method and used the following equation:

$$\frac{C_{f_{vp}}}{C_{f_{cp}}} = \left[\frac{\mu_b}{\mu_w}\right]^m$$

where subscript "vp" refers to variable-property due to heating and subscript "cp" refers to constant property associated with isothermal conditions. Deissler indicated that m=-0.58 for heating and m=-0.50 for cooling.

Test (1968) conducted not only an analytical but also an experimental studies of heat transfer and pressure drop in the laminar flow region. His studies cover the case of both heating and cooling of a liquid. The analytical approach was a numerical solution of the momentum, continuity, and energy equations. The experimental approach involved the use of the hot wire technique for the determination of the velocity profile. He obtained a correlation for the Nusselt number and skin friction coefficient in the laminar region. Test used oil as the working fluid in his experiments. His correlation for the non-isothermal skin friction coefficients is very similar to what Deissler (1951) proposed.

Shannon and Depew (1969) investigated the influence of free convection and variable viscosity on forced laminar flow. Their theoretical analysis established that the condition for fully developed flow in the absence of free convection required an exponential variation of viscosity with temperature or the viscosity ratio, μ_b/μ_w. The experimental setup was similar to the setup for the present study using an electrically heated horizontal circular tube with a water-ethylene glycol mixture as the working fluid.

However, they did not propose any skin friction coefficient correlations based on their investigation.

Allen and Eckert (1964) conducted measurements of overall test section friction coefficient and local heat transfer coefficient for the case in which fully developed turbulent flow of water entered a uniformly heated circular tube. They reported that their variable property fully developed skin friction coefficients can be correlated with the form identical to what Deissler (1951) used when the value of "m" = -0.25.

Morcos and Bergles (1975) investigated the effects of property variations on fully developed laminar flow heat transfer and pressure drop in horizontal tubes. They developed a facility to test electrically heated glass and stainless steel tubes, with distilled water and ethylene glycol as working fluids. They reported a correlation for skin friction coefficient. However, their correlation is only applicable to very low Reynolds numbers.

Ghajar and Augustine (1990) conducted pressure drop measurements in a horizontal circular straight tube with a square-edged entrance under isothermal flow conditions. The experiments covered a Reynolds number range from 512 to 14970. Their results showed that the range of Reynolds number for which transition flow exists is between 2070 and 2840. Comparison of their experimental data in the transition region with the available fully developed friction factor correlations showed that the data were not predicted well by the existing correlations. This was primarily due to the influence of the inlet configuration used in their study on the onset of transition. Based on the experimental data, they developed an empirical correlation for friction factor in the fully developed transition region. In the entrance region, they observed that the length required

for the friction factor to become fully developed in both the laminar and turbulent flow regimes was found to be inversely proportional to the Reynolds number.

Ghajar and Madon (1992) conducted pressure drop measurements in a horizontal circular straight tube with a reentrant and bell-mouth inlet under isothermal flow conditions. The experiments covered a Reynolds number range from about 500 to 15000. From their experimental data, they concluded that the range of Reynolds number for which transition flow exists is from 1980 to 2600 for the reentrant inlet and 2125 to 3200 for the bell-mouth inlet. The experimental friction factors in the fully developed laminar and turbulent flow regimes compared within $\pm 5\%$ of the established correlations. In the transition region, their experimentally obtained fully developed skin friction coefficients showed excellent agreement with Churchill's (1977) correlation. No comparison in the transition region of square-edged and reentrant inlets was made, since no correlation is available for inlet configurations other than bell-mouth. They developed empirical correlations for the skin friction coefficient in the form of a second-order polynomials based on their fully developed data in the transition region for the reentrant, square-edged, and bell-mouth inlets. Qualitative results for the variation of laminar apparent friction factor along the entire length of the tube for different inlets were also presented. Their results indicated that for low laminar Reynolds numbers, the "f_{app}(Re)" factor is not just a function of "Re(x/D)" as predicted by other investigators, but is a strong function of Reynolds number as well.

Achmadi (1993) investigated the heating effect on pressure drop measurements for a bell-mouth inlet. He used three different heating rates and showed that heating has a significant effect on pressure drop in the laminar and transition regions. However, he did

not provide good explanation for this effect. In the turbulent region, he found that the effect of heating on pressure drop measurement was not pronounced.

Febransyah (1994) used a sensitive pressure transducer to measure the pressure drop in the entrance region for a bell-mouth inlet. His fully developed data showed good agreement with the results of other investigators in all flow regimes. In his report, he also showed that the hydrodynamic entry length is inversely proportional to Reynolds number. However, in the entrance region for all flow regimes, he did not provide any correlations to predict the apparent friction factor.

Warnecker (1995) used different inlet configurations (reentrant and square-edged) to investigate the effect of heating on fully developed skin friction coefficient in the laminar, transition, and turbulent flow regions. He shows that heating has a significant effect on the fully developed skin friction coefficient in the laminar and transition regions. In the turbulent region, the effect of heating on fully developed skin friction coefficient is not pronounced. However, no correlations are provided in the flow regimes which is influenced by the effect of heating.

In order to predict the pumping power in a heat exchanger, many researchers presented their result in form of friction factor correlations. In Table II, the presently available friction factor correlations are shown. In this table, only Shah's (1978) correlation is for apparent friction factor in the laminar region for a bell-mouth entrance. It is important to know that there are no apparent friction factor correlations for the transition and turbulent regions. In the table, there are six available correlations for predicting fully developed skin friction coefficients in the transition region. These correlations were developed by Bhatti and Shah (1987), Churchill (1977), Hrycak and

TABLE II

FRICTION FACTOR CORRELATIONS FOR A SMOOTH CIRCULAR DUCT

INVESTIGATOR	CORRELATION	RANGE
Shah (1978)	$f_{app} = \frac{1}{Re}[\frac{3.44}{\zeta^{0.5}} + \frac{0.31/\zeta + 16 - 3.44/\zeta^{0.5}}{1 + 0.00021/\zeta^2}]$ where $\zeta = (x/D)/Re$, fapp = apparent friction factor	laminar
Churchill (1977)	$\frac{2}{C_f} = \{\frac{1}{[(8/Re)^{10} + (Re/36500)^{20}]^{0.5}} + [2.21 \ln(\frac{Re}{7})]^{10}\}^{\frac{1}{5}}$	all flow regimes
Hrycak & Andrushkiw (1974)	$C_f = -3.10\times10^{-3} + 7.125\times10^{-6}Re - 9.70\times10^{-10}Re^2$	Re = 2100 to 4500
Bhatti & Shah (1987)	$C_f = A + \frac{B}{Re^{1/m}}$ where A = 0.0054, B= 2.3×10^{-8}, m = -2/3 for 2300 ≤ Re ≤ 4000 and A = 1.28×10^{-3} B = 0.01143, m = 3.2154 for 4000≤ Re ≤10^7	Re = 2300 to 10^7
Ghajar & Augustine (1990)	$C_f = -2.56\times10^{-2} + 2.49\times10^{-5}Re - 4.25\times10^{-9}Re^2$	Re = 2070 to 2840 for square-edged inlet
Ghajar & Madon (1992)	$C_f = -9.89\times10^{-3} + 1.15\times10^{-5}Re - 1.29\times10^{-9}Re^2$ $C_f = -8.03\times10^{-3} + 1.05\times10^{-5}Re - 1.47\times10^{-9}Re^2$	Re = 1950 to 2650 for reentrant inlet Re = 2075 to 3450 for bell-mouth inlet

TABLE II (Continued)

Blasius (1913)	$C_f = 0.0791 Re^{-0.25}$	$Re = 4x10^3$ to 10^5
Test (1968)	$C_f = \frac{16}{Re}\frac{1}{k}\left[\frac{\mu_b}{\mu_w}\right]^m$ where k = 0.89, m = 0.2	Laminar flow
Deissler (1951)	$C_f = \frac{16}{Re}\left[\frac{\mu_b}{\mu_w}\right]^m$ where m = -0.58	Laminar flow
Allen & Eckert (1964)	$C_f = 0.0791\ Re^{-0.25}\ [\mu_b/\mu_w]^m$ where m = -0.25	Turbulent flow

Andrushkiw (1974), Ghajar and Augustine (1990) and Ghajar and Madon (1992), and they are only good for an ideal round entrance, except the correlation by Ghajar and Augustine (1990) for a square-edged inlet and Ghajar and Madon (1992) for a reentrant inlet. For Reynolds number ranging from 4000 to 100000, the well established Blasius (1913) turbulent skin friction coefficient correlation can be used. For non-isothermal skin friction coefficient, in the laminar region, the correlations proposed by Test (1968) and Deissler (1951) are available. In the turbulent region, the correlation proposed by Allen and Eckert (1964) for non-isothermal skin friction coefficient is also available. However, the applicability of the non-isothermal skin friction coefficient correlations still needs to be verified. For a smooth round tube with disturbed types of entrances, the limit of this correlation is not well defined. Most of the work done in the past did not include the influence of inlet configuration or flow disturbance and the effect of heating, and these effects should be investigated.

1.3 Objectives of the Research

In the previous sections, the shortcomings of the previous works related to heat transfer and pressure drop have been discussed. The specific objectives of this research can be summarized as follows:

1. Investigate the heat transfer behavior in the developing and fully developed regions for all flow regimes by using three different inlet configurations with different degrees of disturbance.

2. Investigate the pressure drop behavior in the fully developed region for all flow regimes by using three different inlet configurations with different degrees of disturbance.
3. Investigate the effect of buoyancy (secondary flow) on heat transfer. The focus of this investigation would be to look at the influence of flow regime, inlet configuration, and pipe length on the buoyancy and development of guidelines for determination of this effect.
4. Investigate the influence of heating on pressure drop (friction factor) by using the available non-isothermal pressure drop data. The main purpose of this investigation would be to identify the key heat transfer parameter(s) influencing the pressure drop measurements.
5. Finally, develop accurate correlations for prediction of heat transfer and skin friction coefficient in circular pipes to be used for heat exchanger design purposes.

CHAPTER II

EXPERIMENTAL SETUP AND FACILITIES

A schematic diagram of the experimental apparatus for the heat transfer and pressure drop measurements is shown in Fig. 2.1. This versatile experimental setup was built and instrumented by Augustine (1990) and Strickland (1990). In order to perform the experiments proposed in this study, the inlet section for each test section was redesigned, and the method for pressure drop measurements in the entrance section was changed. A computer program FRIC (see Appendix A) is developed for the pressure drop measurement and data reduction purposes. The uncertainty analysis of the overall experimental procedures using the method of Kline and McClintock (1953) showed that there was a maximum of 10% uncertainty for heat transfer coefficient calculations and a maximum of 5% uncertainty for skin friction coefficient calculations. The maximum error in the experimental measurements of the heat transfer coefficient and skin friction coefficient is presented in Appendix B. Presented in this chapter is a description of the experimental apparatus used including the necessary instrumentation details. Following the apparatus description is the explanation of the calibration processes. Finally, this section will cover the data reduction techniques and the computer programs assisting in this research.

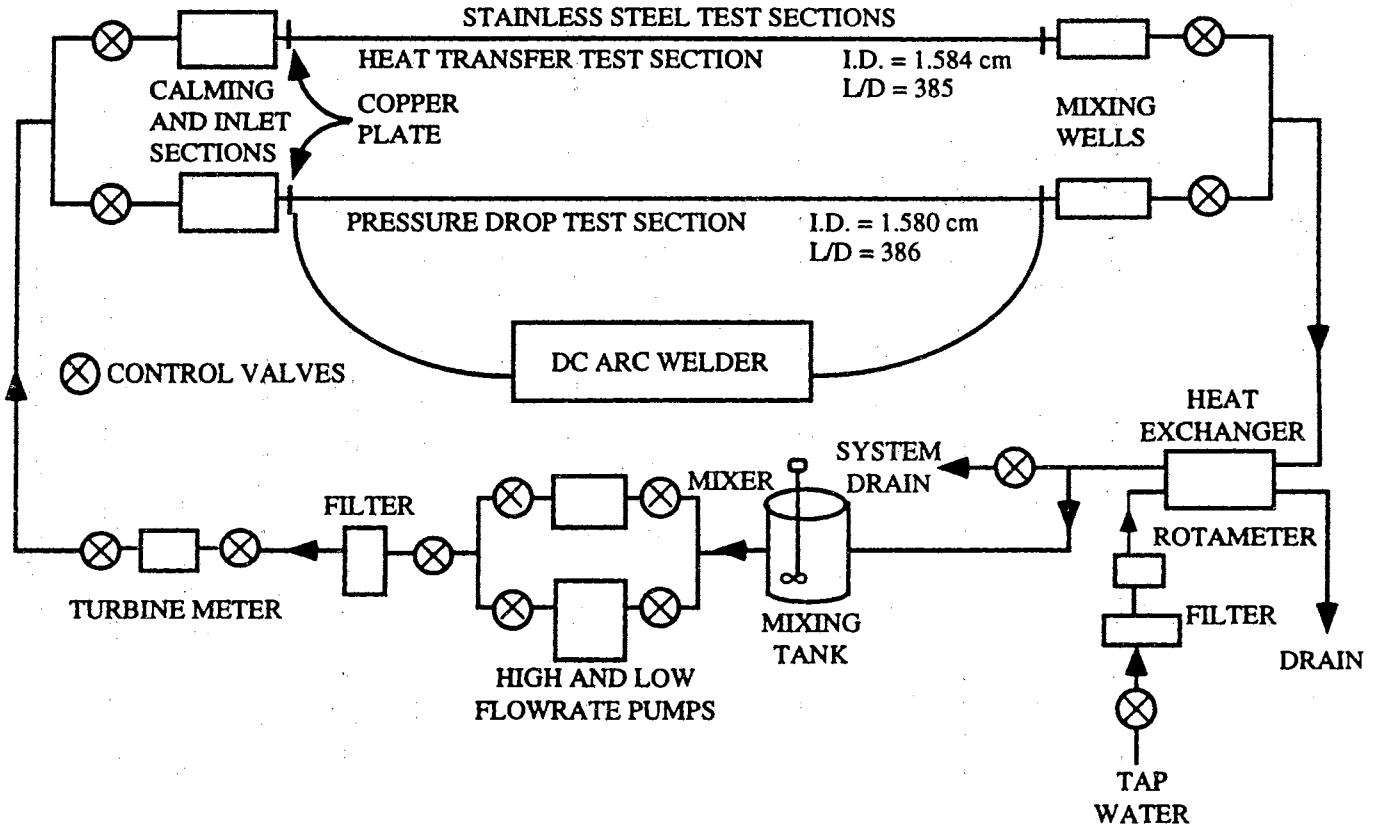

Figure 2.1 Schematic Diagram of the Experimental Setup.

2.1 Description of the Equipment

This section will introduce all of the equipment. The equipment was used to perform the pressure drop and heat transfer measurements.

2.1.1 Test Section

The test sections for the heat transfer and pressure drop are horizontal seamless 316 stainless steel circular tubes with an average inside diameter of 15.84 mm for the heat transfer section (15.8 mm for the pressure drop section). The outside diameter of the tube is 19 mm for the heat transfer section (19.1 mm for the pressure drop section). The length of each test section is 5.86 m providing a maximum length to diameter ratio (L/D) of 385 and 386 for the heat transfer and pressure drop section.

In order to apply the uniform wall heat flux boundary condition to the test section, copper plates are silver soldered to the inlet (0.635x25.4x25.4 cm) and exit (0.635x12.7x22.86 cm) of the test sections. Welding cables are attached to the copper plates. The heat source is a Lincoln Idealarc DC-600 three-phase rectified type electric welder and is used with a variable voltage to produce a DC electric current through the test section. The welder is rated for a 100% duty cycle at 600 amps and 44 volts at either 50/60 Hz giving a maximum power output of 26.4 kW. A General Electric dropping resistor was used when the experiments were conducted with the current below 150 amps. This resistor was placed in series with the electric welder. To ensure minimal room heating and vibrational effects from the welder, it is located at an external wall where it exhausts hot air (outside) through a square duct, and brings in cooler air through a duct

protected by a steel grate. Much of the exhaust noise is alleviated in this manner. A plywood box fitting flush with the external wall and layered on all internal sides with duct insulation isolates the vibration effects due to the welder's operation. To control transmission of vibration through the floor the welder is placed on rubber damping pads.

The entire length of the test sections are surrounded with fiberglass pipe wrap insulation, followed by a thin polymer vapor seal to prevent moisture penetration. An approximate total thickness of the insulation materiel is 3.175 cm.

2.1.2 Calming and Inlet Sections

The calming section serves as a flow straightening and turbulence reduction device (see Fig. 2.2). The calming section consists of a 17.8 cm diameter acrylic plastic cylinder with three perforated acrylic plastic plates with an open area ratio of 0.312 (73 holes per plate, hole diameter 1.1 cm) followed by tightly packed soda straws (inside diameter 0.57 cm, length 10.2 cm, open area ratio 0.915) sandwiched between fine plastic mesh screens (strand diameter 0.03 cm, mesh width 0.14 cm, open area ratio 0.65). Before leaving the calming section, test fluid passes through two more fine plastic mesh screens. The total length of the calming section is 61.6 cm. Two other mesh screens with open area ratios of 0.759 and 0.825 will be used for the bell-mouth inlet in order to investigate the unusual boundary layer changing effect in heat transfer mentioned in Al-Arabi (1982). Also mesh screens with an open area ratio of 0.825 will be used for different inlet configurations to investigate the effect of screen size on the fully developed skin friction coefficient. To investigate the effect of screen size on the pressure drop and heat transfer, only the last two sets of screens were varied (the set which sandwiched the

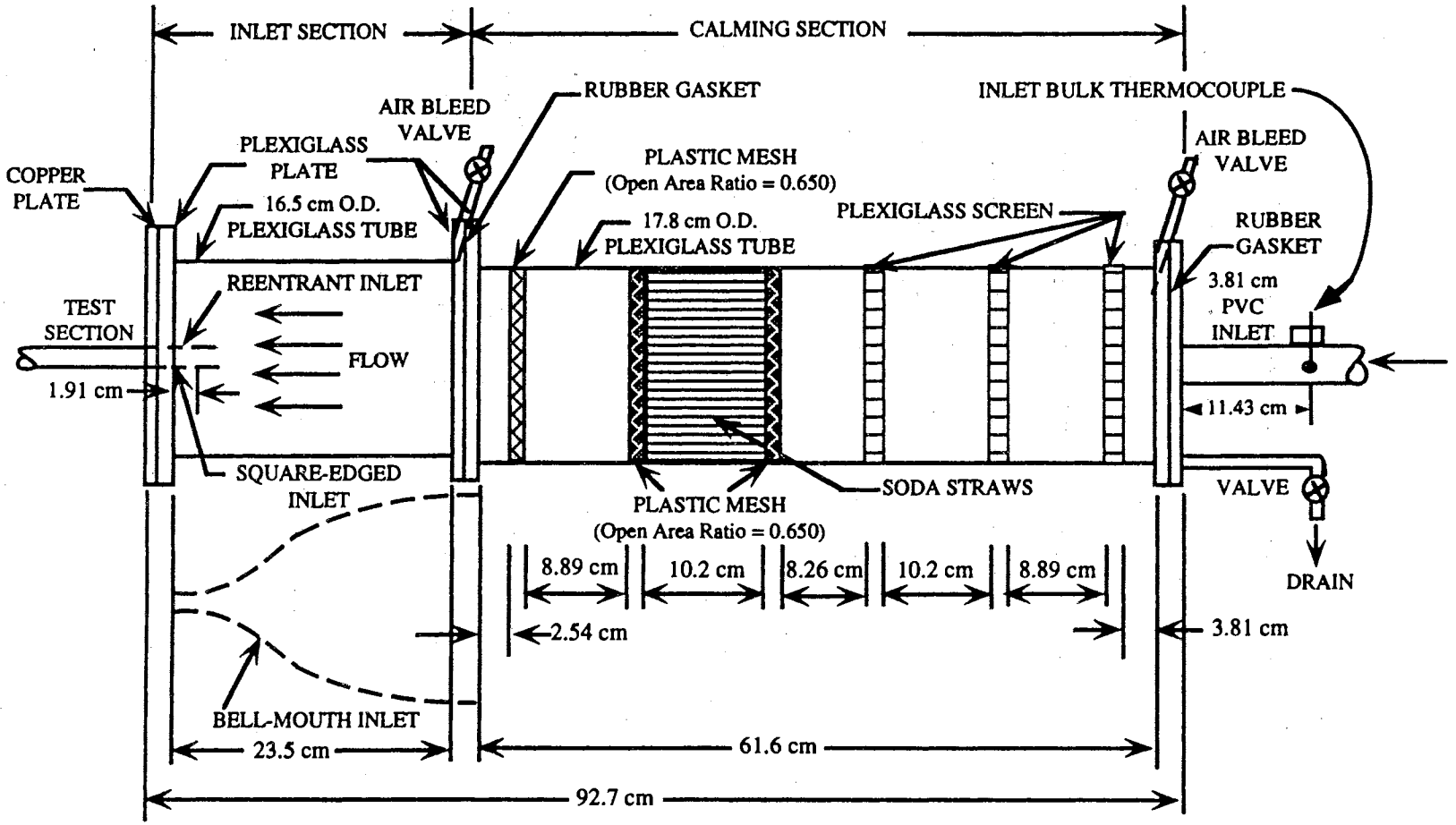

Figure 2.2 Schematic of Calming and Inlet Sections.

tightly packed soda straws and the set before the inlet section). The specific mesh screen used in different cases will be indicated carefully in the later chapters where the results are discussed.

The aim of this proposed study is to investigate the effect of different inlet configurations on the developing transitional flow. Hence, three different inlets, namely, reentrant, square-edged, and bell mouth will be used.

The inlet section has the versatility of being modified to incorporate a reentrant or a bell-mouth entrance (see Fig. 2.2). The reentrant entrance is simulated by sliding 1.91 cm of the tube entrance length into the inlet section (Fig. 2.2), which is otherwise the square-edged (sudden contraction) entrance. For the bell-mouth entrance, a fiberglass nozzle constructed by Madon (1990), replaces the inlet section of Fig. 2.2. The nozzle has a contraction ratio of 10.7 and a total length of 23.5 cm. Due to the leakage problems in the inlet sections and the difficulty encountered in changing the inlet configurations, the connection between the inlet and calming sections has been redesigned. Two aluminum circular flanges were used, one for the calming section and the other for the inlet section. In between, an o-ring is placed in an annular gap and flanges are tightened to compress the o-ring to prevent leakage.

Air-escape valves are located on both the calming and inlet sections in order to release the pressure due to any accumulation of air.

2.1.3 Thermocouples for the Heat Transfer Test Section

In the heat transfer test section, Omega TT-T-30 copper-constantan insulated T-type thermocouple wires were cemented with Omegabond 101 to the outside wall of the

test section. OMEGA EXPP-T-20 extension wire were used for relay to the data acquisition system. Thermocouples are placed on the outer surface of the tube wall at close intervals near the entrance region and at greater intervals further downstream (see Fig. 2.3). There are 31 stations in the test section. All stations up to and including station 22 have four thermocouples. They are labeled looking at the tail of the fluid flow with peripheral location number one located at the top of the tube, two at 90 degrees in the clockwise sense, three at the bottom of the tube, and four 90 degrees from the bottom in the clockwise sense (see Fig. 2.3). Starting with station number 23 and including just the odd stations, terminating at station 31, only two thermocouples are used. For these stations, location number one is at the top and number two is at the bottom (see Fig. 2.3). All the thermocouples were monitored with a Cole-Parmer MAC-14 datalogger.

The inlet and exit bulk temperatures are measured by OMEGA TJ36-CPSS-14U-12 thermocouple probes inserted in the calming section and mixing well, respectively. Thermocouples and thermocouple probes are accurate within $\pm 0.4\ ^{o}C$.

2.1.4 Pressure Taps

Twenty-one holes of 0.198 cm diameter are drilled in the test section to accommodate twenty-one pressure taps. The hole spacing and pressure tap orientation is shown in Fig. 2.4. The pressure taps are standard saddle type self-tapping valves with the tapping core removed. Vinyl tubing (0.635cm) is used to connect the pressure taps to the pressure tap manifold.

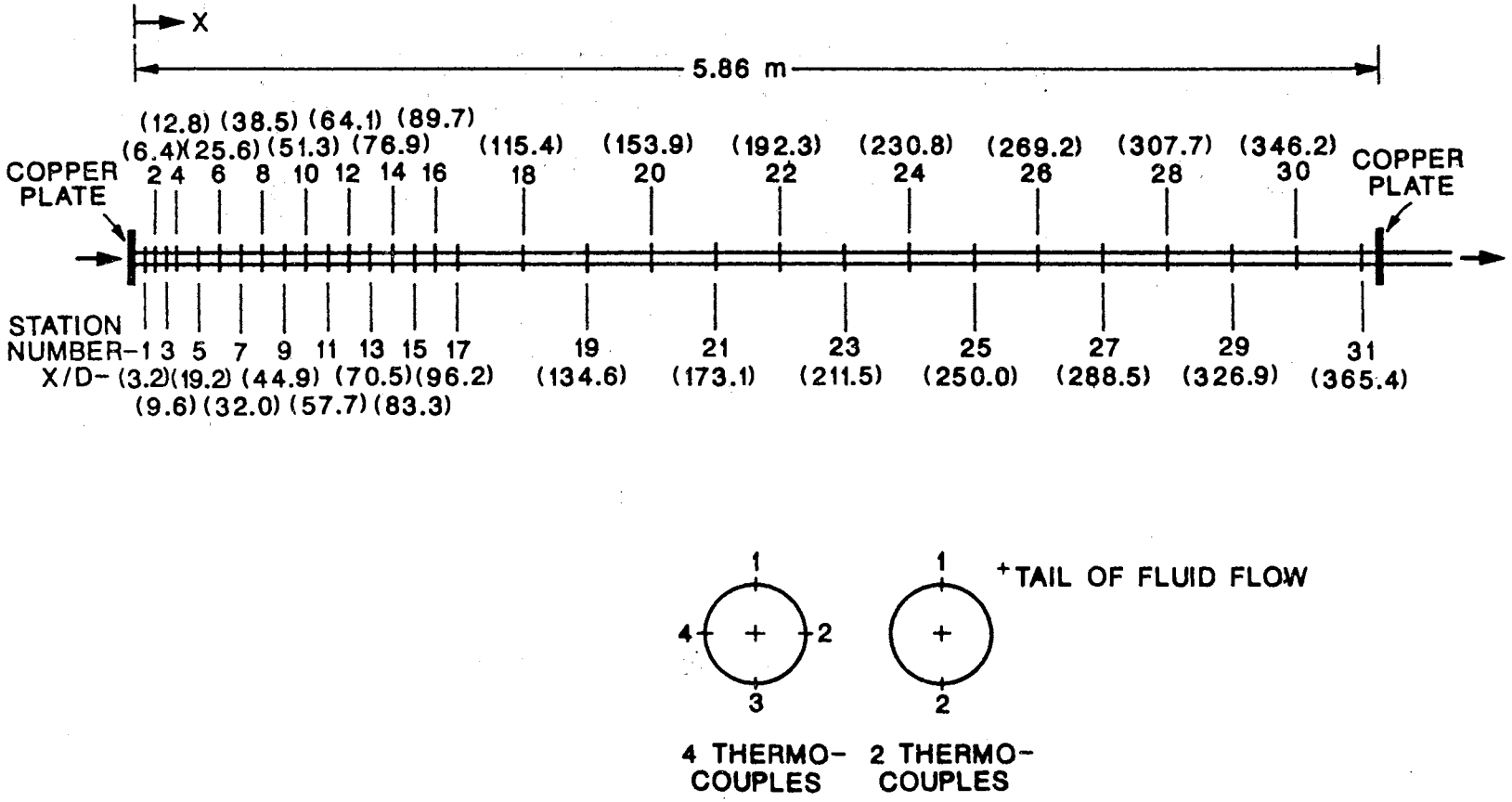

Figure 2.3 Heat Transfer Test Section Thermocouple Distribution.

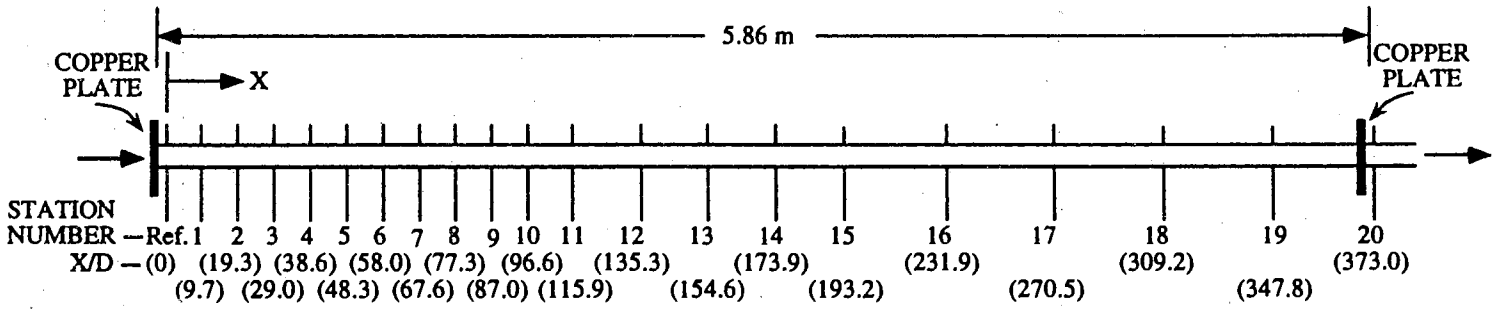

Figure 2.4 Pressure Drop Test Section Pressure Tap Distribution.

2.1.5 Thermocouples for the Pressure Drop Test Section

In order to investigate the effect of heating on pressure drop measurements in the fully developed region, four thermocouples were placed at pressure stations 16, 17, and 18 of the test section to measure the outside wall temperature. Omega TT-T-30 copper-constantan insulated T-type thermocouple wires were cemented with Omegabond 101 to the outside wall of the test section. Omega EXPP-TT-20 extension wires were used for relay to the data acquisition system. The thermocouples were labeled looking at the tail of the fluid flow with peripheral location number one at the top of the tube, two at 90 degrees in the clockwise direction, three at the bottom of the tube, and four at 90 degrees from the bottom in clockwise direction. The same arrangement of thermocouples were placed 11.43 cm before the entrance to the calming section in the 3.81 cm PVC pipe and at the exit of the mixing well to measure the inlet and outlet bulk temperatures of the test fluid. Two more thermocouples of the same type were placed inside a black plastic tube and were used to monitor the average room temperature during the experiments. All the thermocouples were monitored with an Electronic Controls Design forty channel data logger (model ECD 5100)

2.1.6 Pressure Tap Manifold

A pressure tap manifold is used to make sequential pressure drop measurements down the test section. This apparatus is shown in Fig. 2.5. The manifold consists of five sections containing four valves each. The valves are PVC ball valves with 0.635 cm NPT threads on one end and a 0.635 to 0.953 cm hose barb on the other. Each section is essentially a 3.81x2.54x20.32 cm aluminum block with a 0.3175 cm hole drilled through

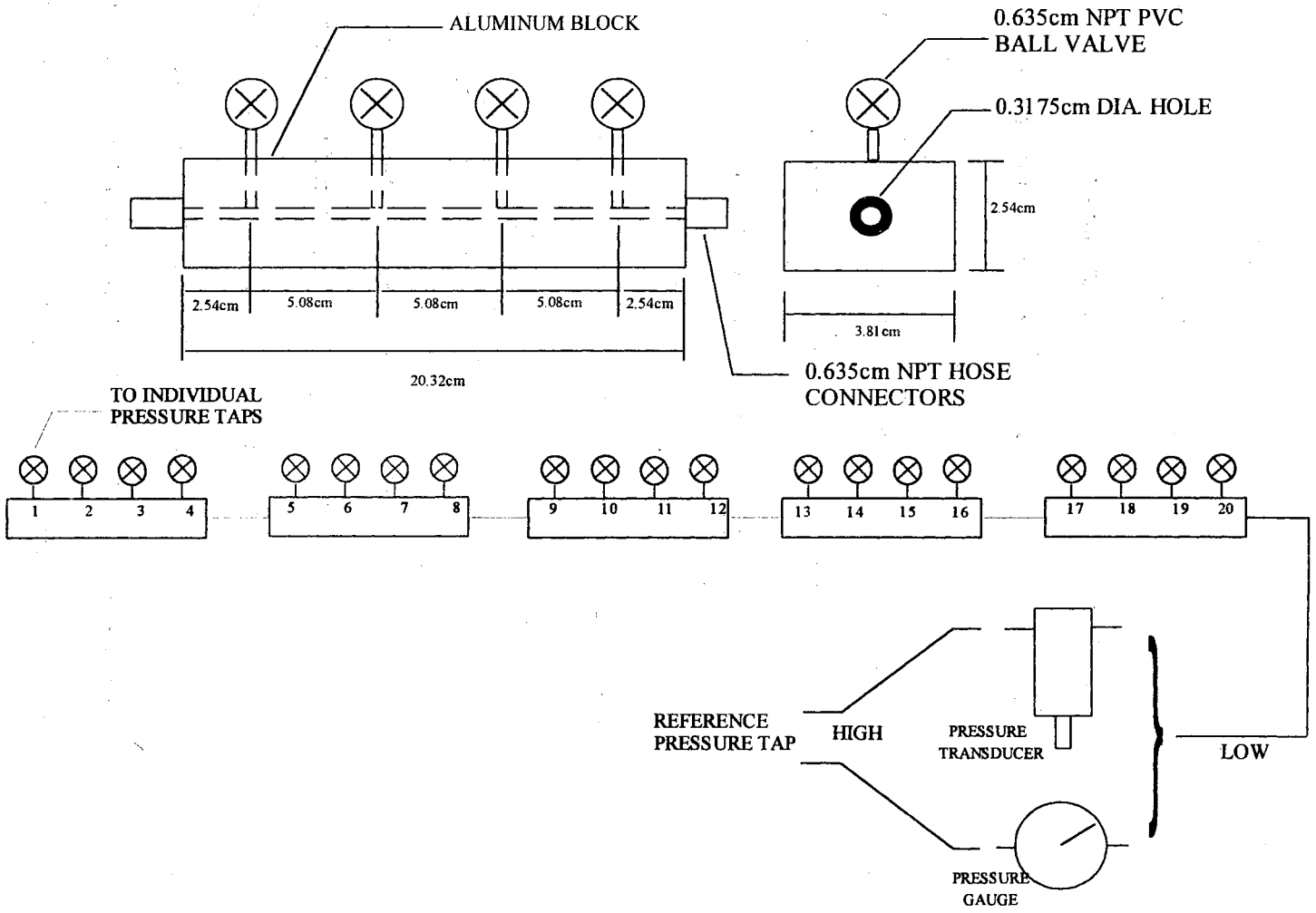

Figure 2.5 Schematic of the Pressure Tap Manifold.

the center. Four holes are drilled through the top and tapped to accommodate the ball valves.

2.1.7 Pressure Transducers

The previous pressure drop measurements of Augustine (1990) and Madon (1990) involved the use of three analog differential pressure gauges. The scale of the first gauge ranged from 0 to 1 inch of water, the second ranged from 0 to 5 inches of water and the third ranged from 0 to 20 inches of water. Acquiring pressure drop measurements using the analog gauges over the entire test section took a long time and more importantly, the pressure drop in the transition region is always fluctuating. For this reason, it is impossible to capture the instantaneous pressure fluctuation and have an average pressure reading using the traditional pressure gauges. In order to investigate the pressure drop in the transition flow region, two differential pressure transducers are used.

The pressure transducers are Validyne model P305D and model DP15 wet-wet differential pressure transducers. The pressure range of the model P305D pressure transducer is $\pm$22.2 inches of water. When the pressure is greater than $\pm$22.2 inches of water, the model DP15 pressure transducer is used since it is able to handle pressures up to $\pm$55 inches of water. Both pressure transducers are accurate to $\pm$0.25% of full scale, including linearity, hysteresis and repeatability. They can also be over pressured by 200%. The output of the transducers is bi-directional $\pm$5 volts at 0.5 mA. The pressure transducer is connected to the computer through an A/D board model CI0-AD08 manufactured by Computer Board Inc. A schematic of the pressure transducer plumbing is shown in Fig. 2.6.

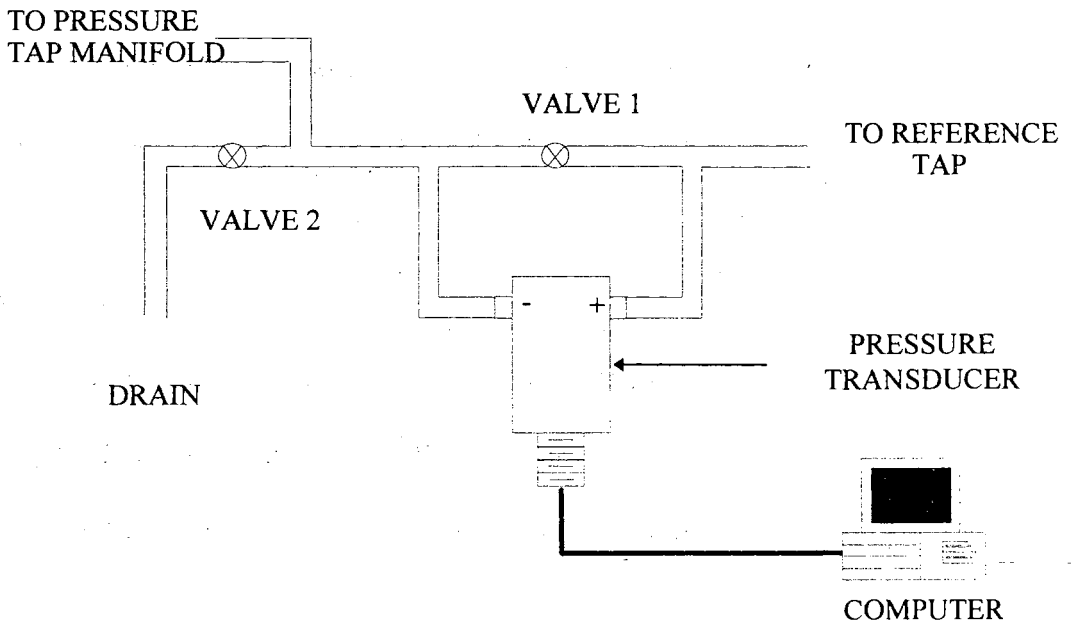

Figure 2.6 Schematic of Plumbing for Pressure Transducers.

2.1.8 Manometer

For differential pressures greater than 20 inches of water, the differential pressures could be accurately measured with a mercury manometer. For this case, a 20 inch U-tube mercury manometer manufactured by the Meriam Instrument Corporation, model 10AA25WM was used.

2.1.9 Data Acquisition System

For the heat transfer test section, a Cole-Parmer MAC-14 ninety-six channel input datalogger interfaced with a personal computer provided digital data acquisition for the temperature measurements. The data acquisition system accepts input voltages from 0.3 micro-volts to 10 volts, has an accuracy of $\pm$0.02% of volts, and has 16 bit resolution. Connection to the computer is through shielded cable to an RS232 port, and to the printer via the printer port. Menu driven software (MS), is used in conjunction with signal conditioning (SC), real time graphics (RTG), and printer driver (PD) software to handle data input.

The IBM compatible personal computer with an 80286 CPU has a 40 MB hard drive, dual floppy disk drives, an EGA monitor, an 80827-8 coprocessor, and a Panasonic 1091i printer. The computer is used for datalogging and printer interfacing, data storage and reduction, and for graphics and text production.

2.1.10 Supplemental Data Acquisition

An Electronics Controls Design (ECD) model 5100 digital data logger with forty channel capacity was used to support the temperature recording capabilities of the MAC-

14 by storing fluid bulk inlet and exit temperatures. Using PC-PLUS, the model 5100 datalogger can interface with the personal computer through a shielded cable to a second RS232 port. The model 5100 datalogger has a resolution of 0.06 °C, over a temperature range of -106 to 400 °C and a +0.06 °C conformity error over a range of -76 to 204 °C.

The model 5100 digital data logger was also used to monitor the fluid bulk inlet and exit temperatures, the outside wall temperatures at stations 16, 17, and 18, and the average room temperature when the pressure drop measurement was concerned.

2.1.11 Mixing Well

To ensure a uniform fluid bulk temperature at the exit of the test section, a mixing well was utilized. Alternating acrylic baffles were placed first from the top, blocking nearly 60% of the flow area and then from the bottom also blocking approximately 60% of the flow area. This provides an overlapping baffled passage forcing the fluid to encounter flow reversal and swirling regions.

2.1.12 Voltmeter

An HP 3468B digital multimeter was used to measure the actual voltage drop across the test section. The range for voltage measurement is 1 microvolt to 300 volt with an accuracy of 1% of the reading, and a resolution of 10 microvolt.

2.1.13 DC Ammeter

The current passing through the test section wall was measured with a Weston Instruments ammeter placed in parallel with a 50 millivolt shunt. The accuracy is about 1% of the 750 amp full scale reading.

2.1.14 Heat Exchanger

An ITT Standard model BCF 4036 one shell and two tube pass heat exchanger was used to cool the test fluid to an allowable bulk temperature.

2.1.15 Fluid Reservoir

A 61 liter cylindrical polyethylene tank, with approximate dimensions of 40.64 cm diameter and 53.34 cm height was used as a fluid reservoir. To ensure uniform temperature distribution in the reservoir, a 19 watt mixer with a 1550 rpm motor was used.

2.1.16 Pumps

For low flow rates a pump with 4.5 GPM at 3100 rpm was used. The pump has a 1/12 HP motor. At high flow rates another pump with a 1/3 HP rating producing 11 GPM at 3450 rpm was used. Flexible hoses connect the pump at both upstream and downstream ends to prevent vibrations from being transmitted to the fluid return tubing. Both pumps are mounted inside a wood housing. Rubber cushions are used to prevent vibration of the pumps from being transmitted to the test section. Fiberglass lines the inside wall surface of the housing to reduce noise.

2.1.17 Turbine Meters

For small flow rates, a 1.27 cm turbine meter was used over a frequency range of 140 to 1625 Hz, giving flow rates from 0.75 to 7.5 GPM. For larger flow rates, a 2.54 cm turbine meter was used over a frequency range of 50 to 150 Hz for flow rates up to approximately 10.5 GPM. The turbine meters have an accuracy of $\pm 0.5\%$ of reading and

repeatability of less than ±1.0% of reading.

2.1.18 Frequency Meter

The output of the turbine meters was read using a Hewlett-Packard model 5314A universal counter. The counter could cater to a range of input frequencies from 10Hz to 100 MHz with a sensitivity of 25 millivolts rms for 100 MHz.

There was a problem using the frequency meter to read output from the turbine meters at low frequencies. To counter this problem a variable gain amplifier was used which has a possible gain from 1 to 5.

2.1.19 Test Fluids

The test fluids used in this study were distilled water, ethylene glycol and a mixture of ethylene glycol and distilled water (30 to 90% by mass fraction).

2.1.20 Hydrometer

A Fisher 11-540A hydrometer with scale values from 1.000 to 1.220 (calibrated at 15.56 ^{o}C) was used to ascertain the specific gravity of the test fluid used. The exact mass concentration then can be calculated.

2.2 Calibration Processes

In the setup used, four key pieces of equipment need to be calibrated. They are (1) ECD 5100 datalogger, (2) thermocouples, (3) pressure transducers, and (4) turbine meters. The calibration processes of the equipment will be presented here.

2.2.1 Calibration of ECD 5100 Datalogger

The model 5100 data logger required a calibration procedure outlined in the operation manual to ensure correct readings from the thermocouples. To perform the calibration a standard DC voltage was required. To begin the calibration, it was required to perform the setup procedure as described in the manual. With the datalogger held on channel number one, a 2.0000 volt $\pm$ 10 microvolts standard voltage was applied to the channel. On the accessory card, the R32 unit in the datalogger was adjusted until the mainframe display indicated exactly 2.0000 volts.

2.2.2 Calibration of Thermocouples

The thermocouples connected to the system were calibrated by means of a constant temperature bath. A steady state condition was accomplished with no heat addition when all thermocouples indicated nearly the same temperatures (within 0.4 ^{o}C). Eleven sets of data were collected. An average test section temperature and deviation from the temperature for each thermocouple location was calculated for all eleven data sets. The average deviation was then calculated and stored for each thermocouple location to correct the thermocouple data.

2.2.3 Calibration of Pressure Transducers

To calibrate the pressure transducers, a volt-meter and an inclined manometer are required. A "T" tubing connector was used to connect the pressure transducer, the inclined manometer and a pressurized device. The pressure readings from the manometer were recorded versus the voltage readings from the transducers as shown in Fig. 2.7. A

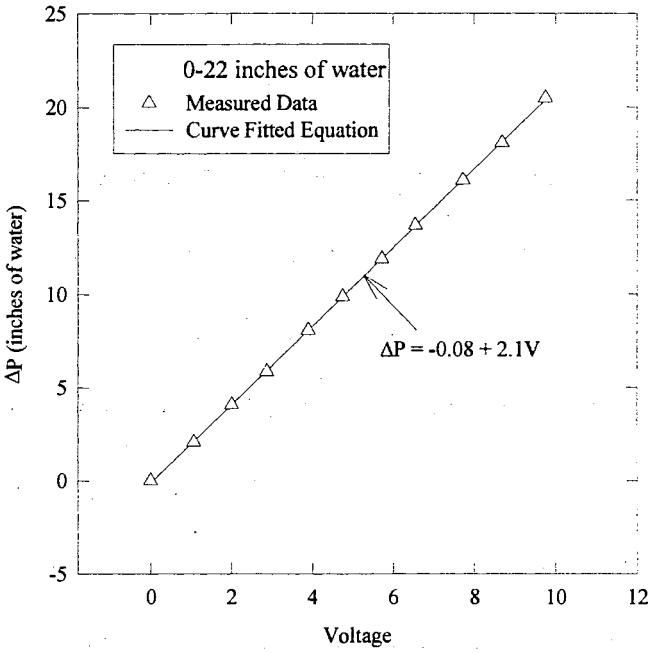

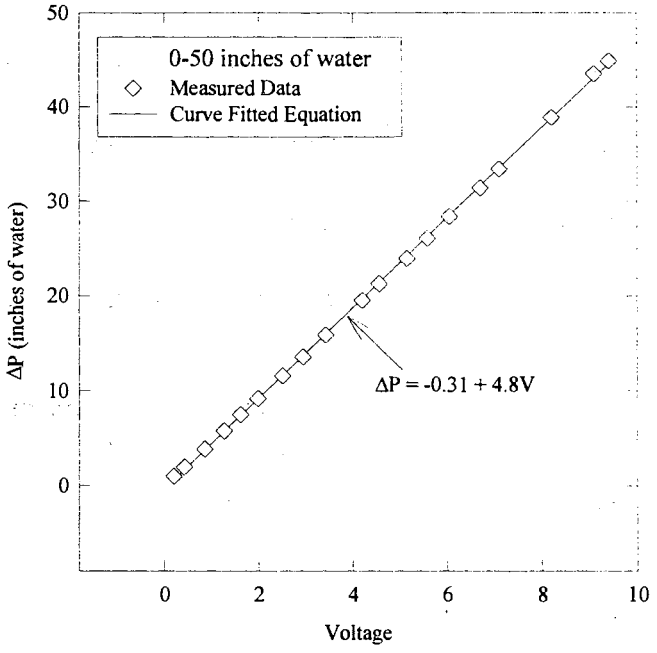

Figure 2.7 Calibration of Pressure Transducers.

linear equation was fitted to the pressure and the voltage reading. The correlation coefficient of the linear curve-fitted equation is 0.98.

2.2.4 Calibration of Turbine Meters

The flow rate through the two turbine meters was calibrated against the frequency of impeller rotation. The calibration required a stopwatch, a frequency meter, and a graduated cylinder. The pump was switched on and the fluid passed through the turbine meter. The fluid was retrieved by the graduated cylinder. The frequency indicated by the meter was recorded during the fluid collection process. When roughly two liters of fluid were collected in the graduated cylinder, or a reasonable period had elapsed for the considered flow rate, the stopwatch and the pump were simultaneously stopped. The volumetric flow rate was then calculated for the specific frequency. The procedure was repeated at representative values over the available frequency range of each turbine meter. This provided data of volumetric flow rate versus average frequency. The data were curve-fitted to a linear equation. The curve-fitted equation was used to calculate the flow rate in the data taking process. Figures 2.8 shows the data collected from the calibration and the correlated linear fit using small and large turbine meters.

2.3 Major Data Reduction Programs

Three major computer programs were used in this study. The functions of these programs will be introduced in this section.

2.3.1 Program HNEW

A computer program called HNEW is the major data reduction tool. For details on

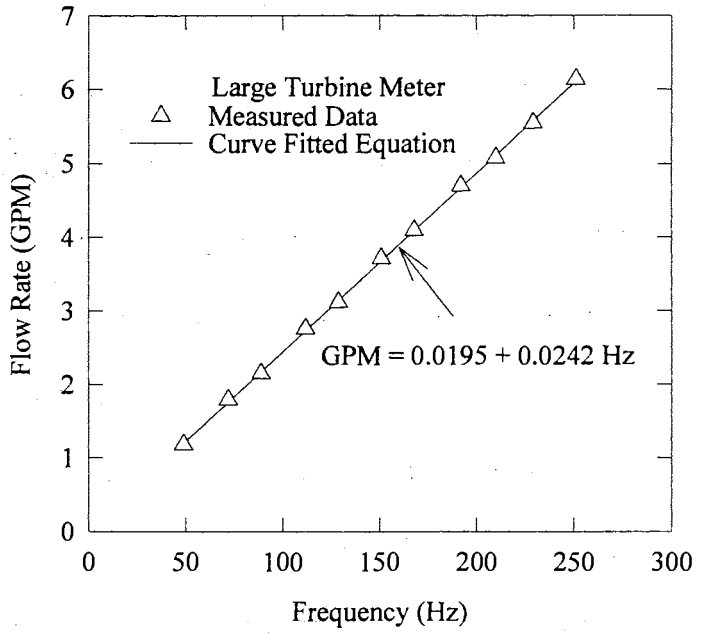

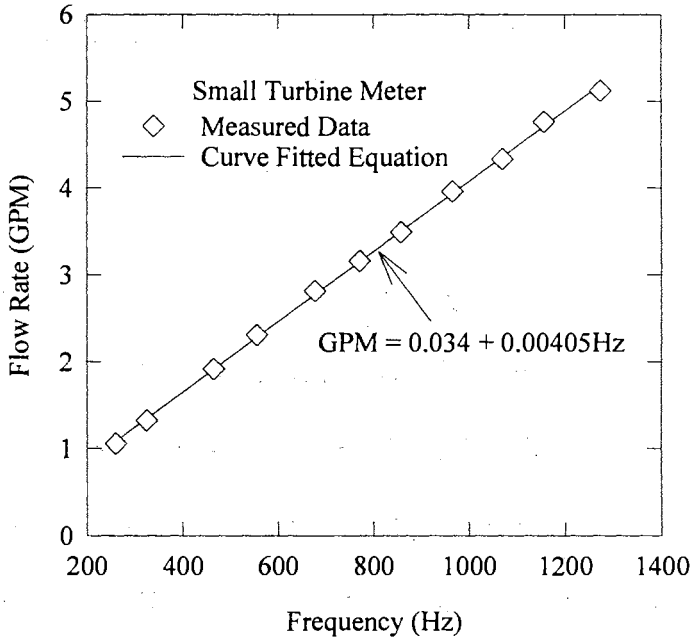

Figure 2.8 Calibration of Turbine Meters.

this program refer to Appendix A. The inputs of this program include the type of test fluid used, the voltage drop across the tube, the current carried by the tube, the volumetric flow rate, the bulk fluid temperatures at the inlet and exit, and the outside wall temperature data for all stations. The data file reduced by HNEW program is the 'reduced' file obtained by using the KRED96 program detailed in Appendix B of Strickland (1990). The program HNEW uses a finite-difference method to calculate the inside wall temperature. Fluid bulk temperature is assumed to vary linearly along the axial direction. The program generates two output files, the first one has the extension OUT and gives a complete listing of all output calculations. The second output file has the extension SUM and gives summary output in a headingless table for easy input to graphic software or curve fitting programs. In the SUM files, the values of heat transfer coefficient, wall temperature, Reynolds, Prandtl, and Grashof numbers at each axial location are given.

2.3.2 Program RQ

The program called RQ (see Appendix A) is a curve fitting program. This program uses a nonlinear regression algorithm to fit the experimental data. The algorithm of this program was developed by Dr. J. P. Chandler of the OSU Computer Science Department, and later modification for interactive use on PC was done by D. R. Maiello and L.M. Tam. The format of the input file of this program can be the same as the SUM file of program HNEW mentioned before. The maximum size of the input file is seven hundred rows and six columns of data.

2.3.3 Program FRIC

A computer program FRIC (see Appendix A) was developed for the pressure drop measurement and data reduction purposes. This program has three functions. The first one is the fluid properties calculation. This part utilizes the correlations developed by Bohn et al. (1984) to calculate density, absolute viscosity, thermal conductivity, Reynolds number, Prandtl number, Grashof number and average velocity of the test fluid. The inputs for this part are the mass concentration of the test fluid, the average fluid bulk temperature, the wall temperature, and the flow rate.

The second function of this program is to read the voltage from the pressure transducer through the A/D board at a user defined number of samples and delay (in milliseconds) between each sampling. The delay determines the sampling rate (number of samples per second). The pressure transducer calibration equation is then used to obtain the pressure corresponding to a specific location along the test section. Each test location is sampled at a user defined number of samples, and the samples were taken by the computer, averaged, and recorded as the pressure reading for that location. The averaged values were used for the friction factor calculations. It is important to point out that the delay and number of samples used are very critical in the transition region. In the laminar and turbulent regions, the pressure reading is stable, hence, the delay and number of samples used are not critical. In these regions, the number of samples and delay used in this study were 1500 and 200 milliseconds, respectively. This gave a sampling rate of 5 samples per second. Hence, 1500 pressure drop data for each location were obtained in a 5 minute time period. However, in the transition region, the pressure reading is

fluctuating. A small delay time and a large number of samples should be used in order to capture the characteristics of the transition region. In this region, the number of samples and delay used in this study were 12000 and 100 milliseconds, respectively. By delaying 100 milliseconds between each sampling, this gave a sampling rate of 10 samples per second. Hence, 12000 data at each location were obtained in a 20 minute time period.

The third function of the program is to calculate the skin friction coefficient. The data obtained in the first and second part is sent to this part and the x/D values for each pressure tap are stored in the program, hence, the skin friction coefficient at each location can be obtained. The skin friction coefficient at each test location is filed in a user defined file name.

CHAPTER III

HEAT TRANSFER RESULTS AND DISCUSSION

In order to investigate the effect of inlet configuration on heat transfer in laminar, transition and turbulent flow regimes, one hundred and twenty six sets of heat transfer data for a bell-mouth entrance were experimentally obtained. For the other two inlet configurations, seventy data sets for square-edged inlet from Strickland (1990) and forty-four data sets for reentrant inlet from Kuppuraju (1990) were used. In addition, 80 experimental data sets from Laurens (1995) in the laminar flow region for three different inlet configurations (reentrant, square-edged, and bell-mouth) were also used for the development of the laminar correlation. Summary of the experimental data is listed in Appendix C. For the experiments, the local bulk Reynolds number ranged from about 280 to 49,000, the local bulk Prandtl number varied from about 4 to 158, the local bulk Grashof number range was from 1000 to 2.5×10^5, and the local bulk Nusselt number varied from 13 to 258. The data sets cover the laminar, transition and turbulent flow regimes. The boundary condition of the experiment for these three inlet configurations is uniform wall heat flux. Heat balance errors were calculated for all experimental runs by taking a percent difference between two methods of calculating the heat addition. The product of the voltage drop across the test section and the current carried by the tube was the primary method, while the fluid enthalpy rise from inlet to exit was the second

method. The heat balance error between the two methods in all cases was less than 5%. Experiments under the same conditions were conducted periodically to ensure the repeatability. The difference between the duplicated experimental runs were within ±5%. The uncertainty analysis (see Appendix B) of the overall experimental procedures using the method of Kline and McClintock (1953) showed that there was a maximum of 10% uncertainty for heat transfer coefficient calculations.

This chapter will present the heat transfer results in the developing and fully developed regions. The general trend of heat transfer coefficient along the pipe for three different inlet configurations will be discussed first, then the effect of inlet configuration on heat transfer modes (forced convection and mixed convection) and on the start and end of the heat transfer transition region will be discussed. After understanding the role of inlet configuration, a detailed discussion of how the inlet configuration changes the flow regime will be presented; and a flow regime map and useful heat transfer correlations will be introduced. Finally, the unusual heat transfer boundary layer changing behavior of the bell-mouth inlet will be discussed.

3.1 Trend of Heat Transfer Coefficient Variation along the Pipe

It is well known that the heat transfer coefficient decreases along a horizontal tube and approaches a constant value after a certain length. Figure 3.1 shows the general shape of the curve. The local heat transfer coefficient decreases with tube length asymptotically. The local heat transfer coefficient is very large at the entrance. This is because at the entrance, the thermal boundary thickness is zero and the temperature gradient at the wall is infinite. The general shape of this curve is very much the same for the square-edged,

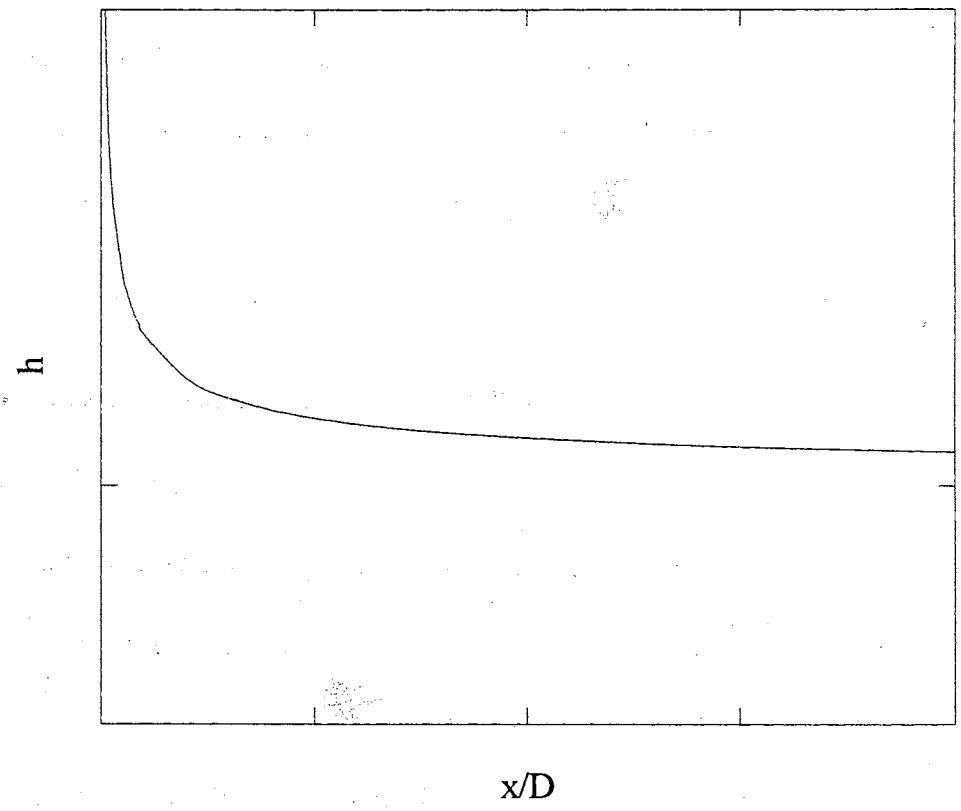

Figure 3.1 General Trend of Heat Transfer Coefficient in the Laminar Region.

the reentrant, and the bell-mouth inlets in the laminar region. In the turbulent region, for the square-edged and reentrant inlets, the trend of the heat transfer coefficient along the pipe is almost the same. The only difference between them is that for laminar flow, it requires a longer entrance length for heat transfer coefficient to approach a constant value. For turbulent flow in a tube, the entry region usually tends to be of minor interest because it is short. However, for the bell-mouth inlet, the trend of heat transfer coefficient along the pipe in the turbulent region is completely different from that in the laminar region. Figure 3.2 shows the general trend of heat transfer coefficient along the pipe for a bell-mouth inlet in the turbulent region. According to Al-Arabi (1982), for a bell-mouth inlet configuration, the boundary layer is at first laminar and then passes through a transition region to the turbulent condition causing a dip in the h-x/D curve.

3.2 Forced and Mixed Convection Heat Transfer Boundary

Transfer of heat through the tube wall produces a temperature difference in the fluid. The fluid near the tube wall has a higher temperature and lower density than the fluid close to the centerline of the tube. This temperature difference may produce a secondary flow due to free convection, and the peripheral temperatures around the tube become nonuniform. When secondary flow is not present, the peripheral temperatures around the tube wall should be uniform. If the tube wall temperatures are uniform, the heat transfer coefficients around the tube wall theoretically should be the same. The ratio of the local peripheral heat transfer coefficient at the top of the tube to the local peripheral heat transfer coefficient at the bottom of the tube (h_t/h_b) could be used to distinguish between forced and mixed convection. For forced convection the ratio of heat transfer

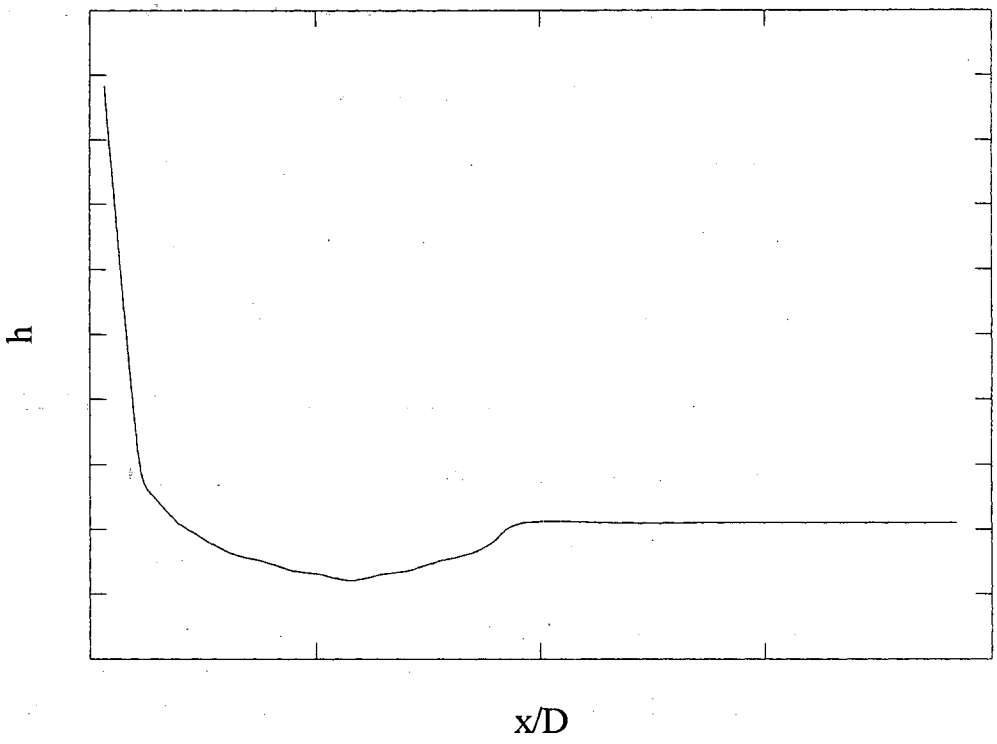

Figure 3.2 General Trend of Heat Transfer Coefficient in the Turbulent Region for a Bell-mouth Inlet.

coefficients (h_t/h_b) is close to unity (0.8~1.0) and for mixed convection is much less than unity (<0.8). Figure 3.3 shows the general trend of peripheral heat transfer coefficients along the dimensionless locations for the reentrant, square-edged and the bell-mouth inlets in the laminar and lower transition flow regimes. This figure shows four curves for each inlet. One curve is for the heat transfer coefficients being measured at the top of the tube, the other three curves represent the heat transfer coefficients being measured at both sides of the tube and the bottom of the tube 90 degrees aparts. As seen in this figure, approximately at the first fifty x/D locations, the peripheral heat transfer coefficients behave very much the same, after that, these curves do not overlap. The heat transfer coefficients at the top always have lower values than the other three locations. The heat transfer coefficients for the two sides of the tube and the bottom of the tube are always close to each other, but the bottom one almost always has the highest value. This can be explained because the mode of heat transfer in the laminar and lower transition regions is not forced convection when x/D is greater than 50. A considerable starting length appears necessary for the establishment of the free convection effect. When the secondary flow is established, an increase in heat transfer occurs due to the circulation introduced by the free convection effect. This circulation is superimposed on the main flow and assists the main flow in removing heat from the tube wall. Mixed convection heat transfer, in addition to being dependent on Reynolds and Prandtl numbers, is also dependent upon the Grashof number (which accounts for the variation in density of the test fluid).

To further illustrate and explain the different heat transfer modes (mixed and forced convection) encountered for the three inlets during the experiments, Fig. 3.4 is presented. This figure shows the different trends in the heat transfer coefficient ratio h_t/h_b.

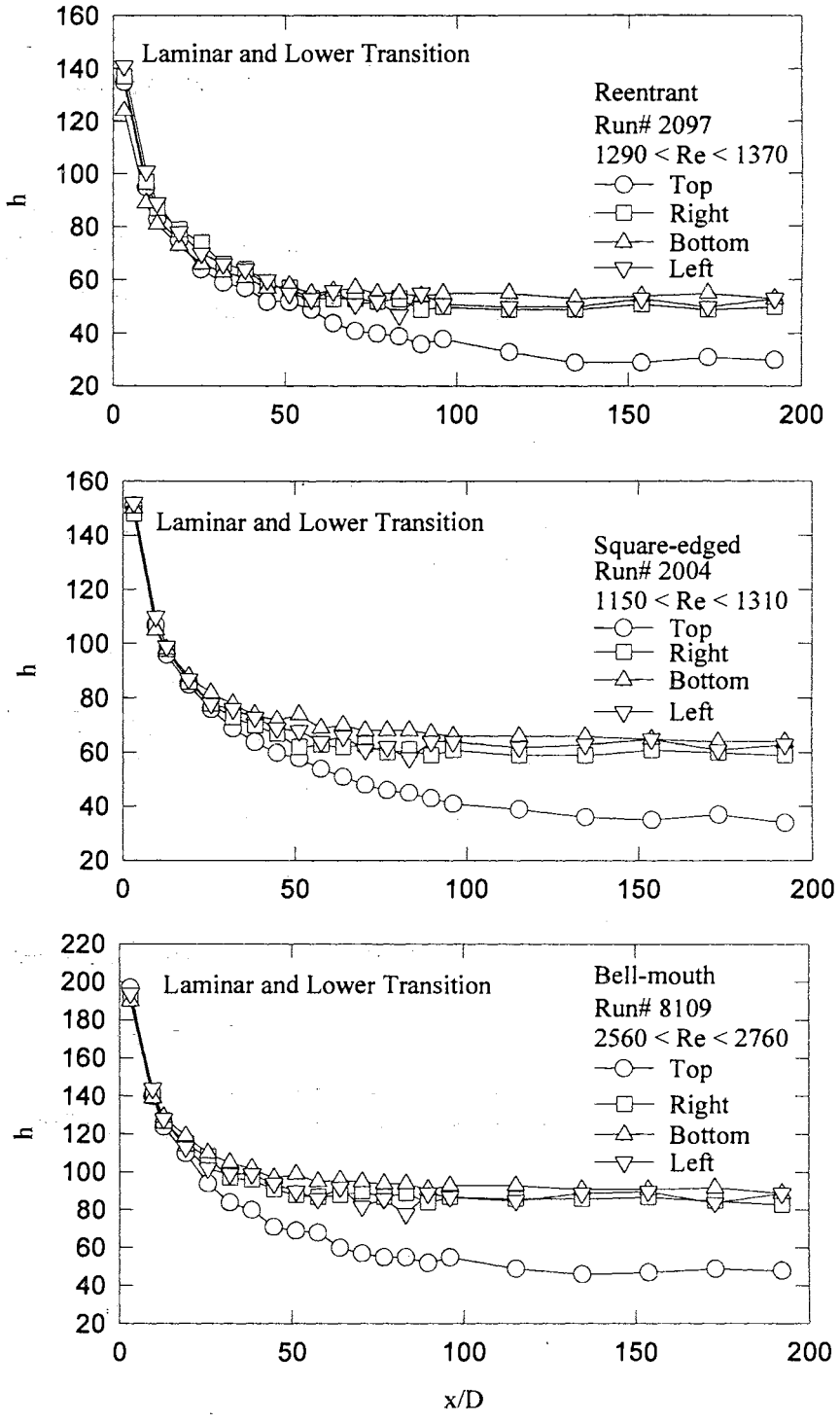

Figure 3.3 Peripheral Heat Transfer Coefficient for Different Inlets in the Laminar and Lower Transition Regions.

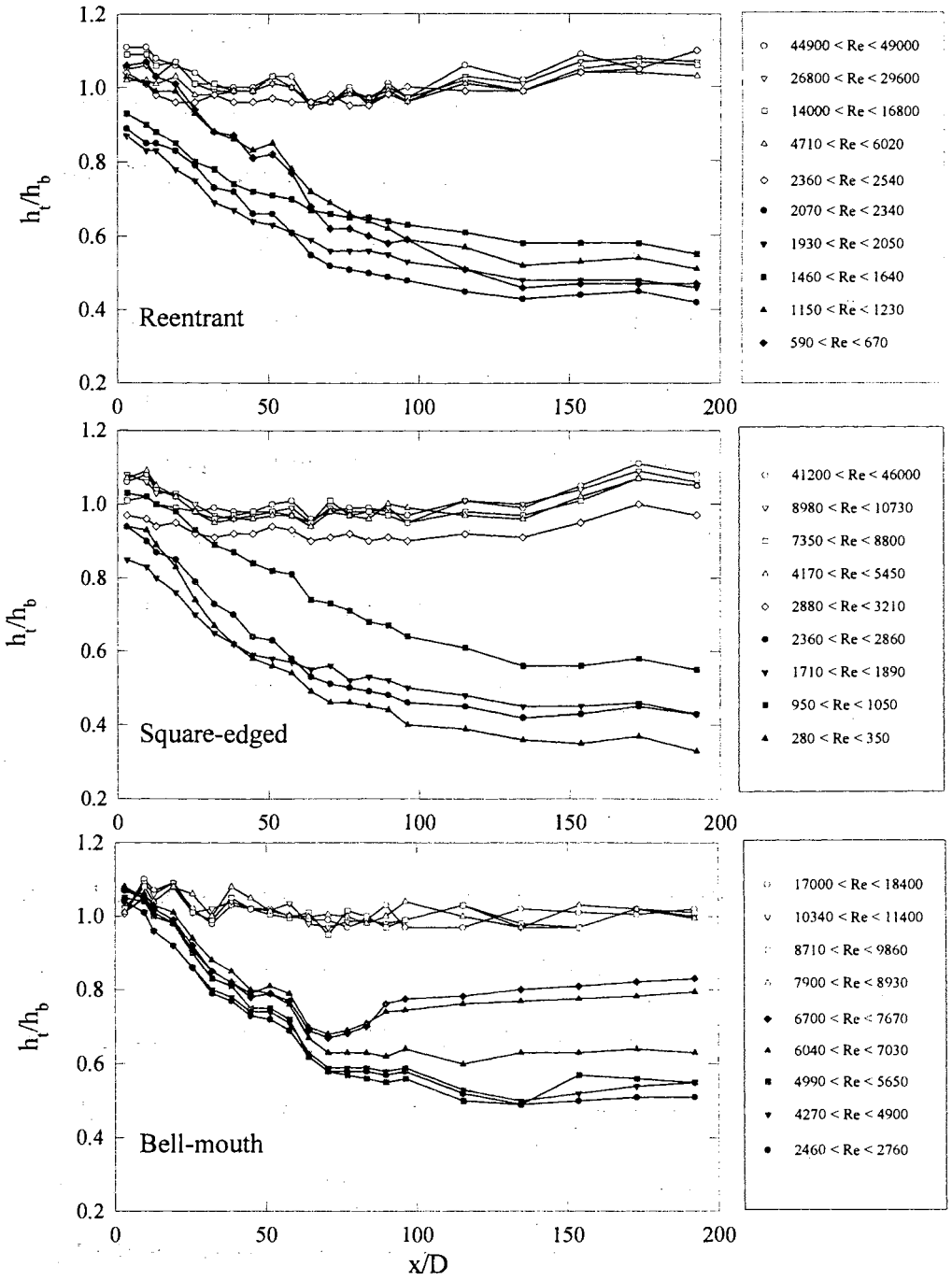

Figure 3.4 Effect of Secondary Flow on Heat Transfer Coefficient for Different Inlets and Flow Regimes.

It includes representative Reynolds number ranges from laminar to fully turbulent flow for the three inlets (Re = 280-49000). As shown in the figure, the boundary between forced and mixed convection heat transfer is inlet dependent. For the reentrant, square-edged, and bell-mouth inlets when the Reynolds numbers (based on the first test station) were greater than 2360, 2880, and 7900, respectively, the flows were dominated by forced convection heat transfer, and the heat transfer coefficient ratios did not fall below 0.8-0.9 and at times exceeded unity due to heat loss at the end of the pipe and non-uniformity of the input heat flux in addition to the thermal couple error. The flows dominated by mixed convection heat transfer had heat transfer coefficient ratios beginning near unity but dropping off rapidly as the length-to-diameter ratio increased. Beyond about 125 diameters from the tube entrance, the ratio was almost invariant, with x/D indicating a much less dominant role for forced convection heat transfer and an increased free convection activity.

In reference to Fig. 3.4, it is interesting to observe that the starting length necessary for the establishment of the free convection effect for low Reynolds number flows was also inlet-dependent. When the secondary flow was established, a sharp decrease in h_t/h_b occurred for large values of x/D (x/D > 100). Depending on the type of inlet configuration, for low Reynolds number flows (Re<2360 for reentrant, Re<2880 for square-edged, and Re<7900 for bell-mouth), the flow can be considered to be dominated by forced convection over the first 20-70 diameters from the entrance to the tube.

It is also interesting to see how the peripheral heat transfer coefficients change along the pipe in the upper transition and turbulent regions. A plot similar to Fig. 3.3 (Fig. 3.5) shows the peripheral heat transfer coefficients variation for the three different

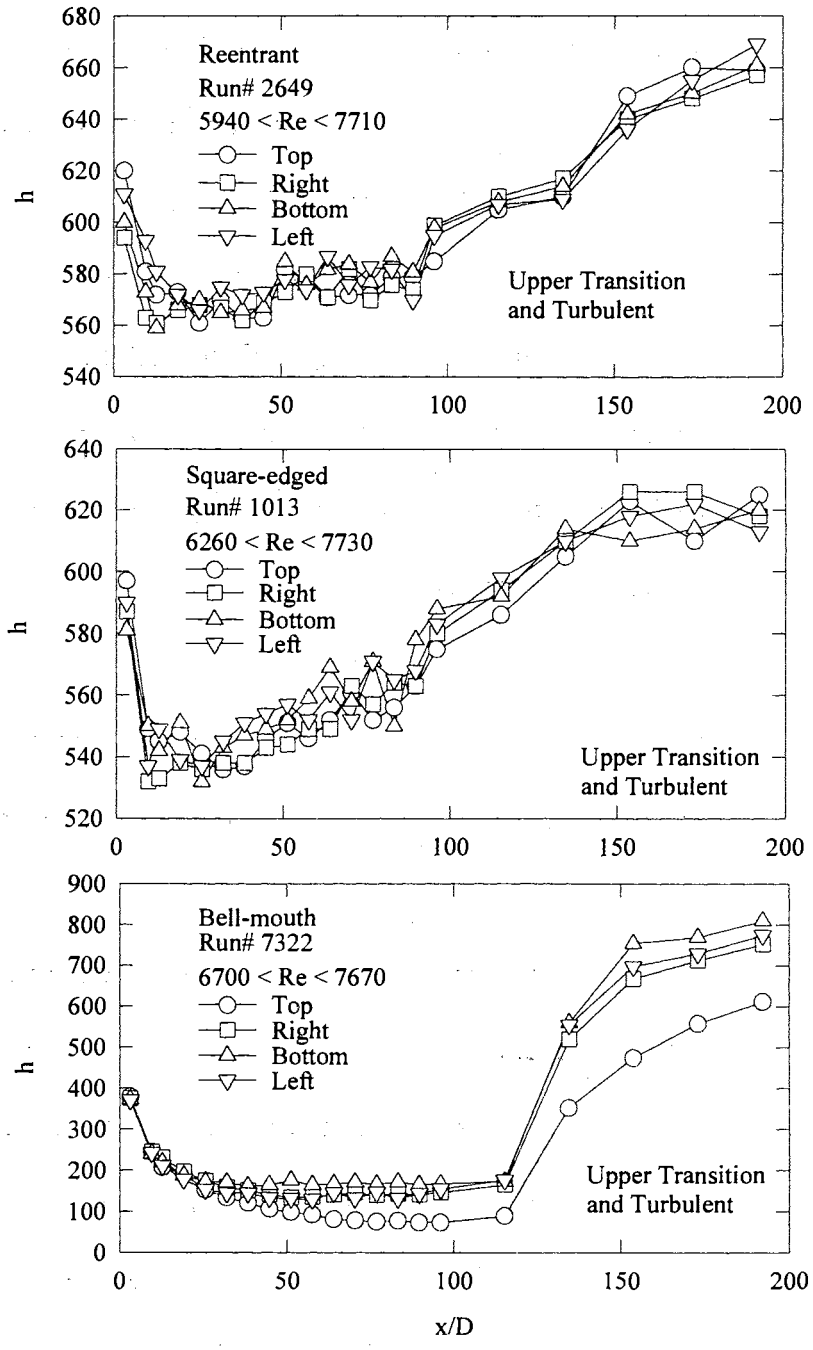

Figure 3.5 Peripheral Heat Transfer Coefficients for Different Inlets in the Upper Transition and Turbulent Regions.

inlet configurations in these regions. Theoretically, when the heat transfer coefficient reaches a minimum value, it should stay at this value along the tube. In Figure 3.5, for the reentrant and square-edged inlets, the heat transfer coefficient has a minimum value at x/D approximately equal to 25 and increases monotonically along the tube rather than staying at a constant value. As seen in this figure, the heat transfer coefficient at the last station is even larger than the heat transfer coefficient at the first station.

The reason for the heat transfer coefficient shifting upward can be explained as follows. The inside wall temperature and the fluid bulk temperature increase monotonically after they have reached their fully developed values but the fluid bulk temperature has a larger rate of increase. The smaller rate of increase of the inside wall temperature is due to the heat lost from the wall to the surroundings (perfect insulation is impossible to achieve). The heat transfer coefficient increases along the pipe due to the decrease of the wall to fluid temperature difference. The chaotic behavior of the peripheral heat transfer coefficients for the reentrant and square-edged inlets are solely due to the turbulent motion. In these regions, the heat transfer coefficient ratio (h_t/h_b) is always greater than 0.8, hence, the secondary flow is totally overwhelmed by the turbulent motion and the heat transfer mode is always forced convection.

For the bell-mouth inlet in the upper transition and the turbulent regions, the behavior of the heat transfer coefficients along the periphery of the tube is completely different from the reentrant and the square-edged inlets (refer to Fig. 3.5). The heat transfer coefficients for this particular inlet behave exactly the same as they behaved in the laminar region at the first 100 diameters (mixed convection is the dominant heat transfer mode). When the tube length is greater than approximately 100 diameters, the

heat transfer characteristic changes. The heat transfer coefficients at the peripheral locations are no longer constant and they increase along the pipe. According to Al-Arabi (1982), for a bell-mouth inlet configuration in the turbulent flow, the boundary layer is at first laminar and then changes through a transition region to the turbulent condition causing a dip in the h-x/D curve. The length and depth of this dip decreases with the increase of Reynolds number. This behavior, of course, is the characteristic of this special inlet configuration. If one uses a short tube with a bell-mouth inlet in a heat exchanger and expects turbulent heat transfer behavior in high Reynolds number region, the heat exchanger will perform very poorly (refer to Fig. 3.5, the laminar heat transfer behavior in the first 100 x/D locations). Due to this significant reason, the last section of this chapter will have an in-depth discussion about this unusual heat transfer behavior.

3.3 Influence of Inlet on Heat Transfer Transition Region

In order to show the influence of inlet configuration on the beginning and end of the heat transfer transition region, Fig. 3.6 is used. The local average peripheral heat transfer coefficients in terms of the Colburn j factor ($StPr^{0.667}$) are plotted as a function of local bulk Reynolds number for all flow regimes at the length-to-diameter ratio of 192. The solid symbols represent the start and end of the heat transfer transition region for each inlet configuration. As shown by the solid symbols, the lower and upper limits of the heat transfer transition Reynolds number range are dependent on the inlet configuration.

Figure 3.6, for comparison purposes, also shows the typical fully developed pipe flow forced convection heat transfer correlations for turbulent flow by Sieder and Tate (1936) and laminar flow (Nu = 4.364) under the uniform wall heat flux boundary

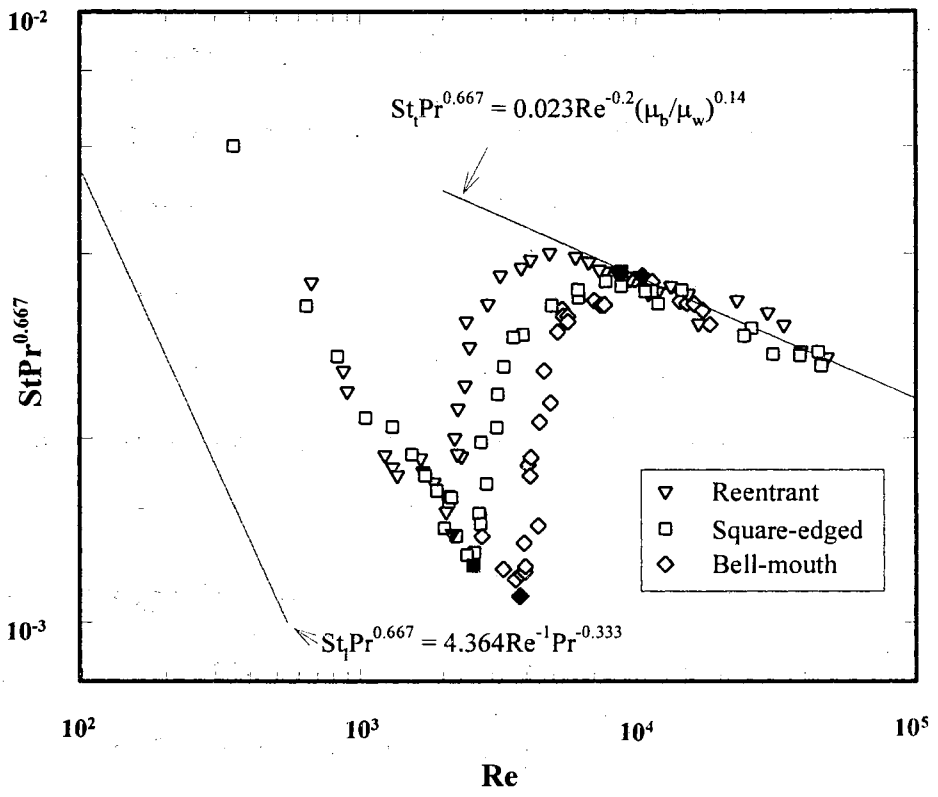

Figure 3.6 Influence of Different Inlets on Heat Transfer Transition Region at x/D = 192. (The solid symbols indicate the start and end of the transition region.)

condition. In the turbulent flow regime for Reynolds numbers greater than about 8500-10,500 (depending on the inlet type), the experimental data appear on the turbulent heat transfer line (within ± 8%). However, in the laminar region, for Reynolds numbers less than about 2000-3800 (depending on the inlet type), the data appear to have a pronounced and almost parallel shift above the accepted laminar heat transfer line. This is directly due to the strong influence of buoyancy forces (free convection) on forced convection (mixed convection), giving rise to mixed convection heat transfer. This in turn results in a higher fully developed laminar uniform wall heat flux Nusselt number than the accepted 4.364 value (a value of about 14.5 is estimated from the data). It should be noted that in the fully developed laminar flow region, no forced convection data could be obtained. At the time the data were taken, the minimum welder current setting was approximately 150 Amps. At this setting, the heat generated at the tube wall was enough to bring about peripheral temperature variations extensive enough to cause secondary flow. It should be noted that Laurens (1995) used a resistor in the same experimental setup and reduced the current setting to approximately 50 Amps. However, he still could not obtain the pure forced convection laminar Nusselt (Nu = 4.364). The fully developed Nusselt number he obtained by using the resistor is around 6 which is about 40 percent greater than the theoretically obtained Nusselt number (4.364).

As shown by the solid symbols in Fig. 3.6, the lower and upper limits of heat transfer transition Reynolds number range depend on inlet configuration. In addition, these transition Reynolds number limits are x/D-dependent. Figure 3.4 demonstrates that after a certain length-to-diameter ratio (depending on the inlet), secondary flow will dominate. This is particularly true in the laminar and lower transition regions. The

presence of the secondary flow and the fact that the wall and fluid bulk temperatures increase along the pipe cause the fluid kinematic viscosity to decrease with an increase in x/D. This in turn causes the local bulk Reynolds number (i.e., lower and upper limits of heat transfer transition Reynolds number range) to increase along the pipe. To determine the range of heat transfer transition Reynolds number along the pipe ($3 \leq x/D \leq 192$), figures similar to Figure 3.6 were developed for 20 other x/D locations. Figure 3.7 depicts the variation of the lower and the upper limits of heat transfer transition Reynolds number along the pipe for each inlet. In fact, to determine the Reynolds number for the start and end of the transition, the most reliable way is to measure the intermittency factor. However, it is not feasible due to the limitations of the experimental setup. The Reynolds number for the start of the transition region is defined as the Reynolds number corresponding to the first abrupt change in the Colburn j factor ($StPr^{0.667}$). The Reynolds number for the end of the transition region corresponds to the Reynolds number of the Colburn j factor ($StPr^{0.667}$) that first reaches the Sieder and Tate's (1936) fully developed turbulent line, or agrees with their line within 5% deviation. Based on the experimental results, the limits of the heat transfer transition Reynolds number range for each inlet over the entire tube ($3 < x/D < 192$) can be summarized as

Reentrant	$2000 < Re < 8500$
Square-edged	$2400 < Re < 8800$
Bell-mouth	$3800 < Re < 10{,}500$

The above limits for the heat transfer transition Reynolds number indicate that the inlet that caused the most disturbance (reentrant) produced an early transition (Re =

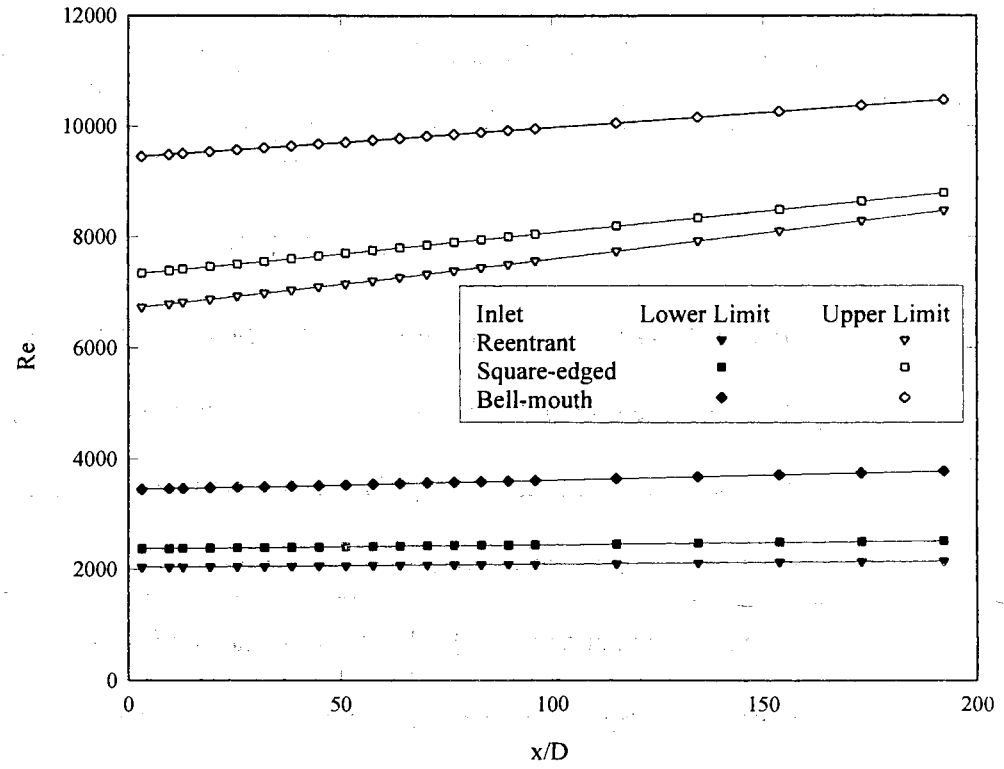

Figure 3.7 Variation of the Lower and Upper Limits of Heat Transfer Transition Reynolds Number Along the Pipe for Different Inlets.

2000), and the inlet with the least disturbance (bell-mouth) did not go into transition below a Reynolds number of about 3800. The square-edged inlet, which causes less disturbance than the reentrant inlet but more than the bell-mouth inlet, produced a transition Reynolds number of about 2500. It should be pointed out that the reported lower (at x/D = 3) and upper (at x/D = 192) limits of heat transfer transition Reynolds number are not influenced by the presence of mixed convection (see Fig. 3.4). However, as the flow travels the pipe length required for the establishment of secondary flow, the beginning of the transition region will be influenced by the presence of mixed convection.

3.4 Flow Regime Map

Metais and Eckert (1964) have recommended the use of the flow regime map of Figure 3.8 for determining the boundary between mixed and forced convection in horizontal pipes under a uniform wall temperature boundary condition. For the identified pure forced or mixed convection heat transfer regime, a heat transfer correlation for the laminar or turbulent flow has been offered on the map. The boundary between laminar forced and mixed convection regions in their flow regime map was apparently either based on the correlations of Kern and Othmer (1943) or Eubank and Proctor (1951). Metais (1963), gave no clear explanation in his report as to which correlation was used. In the turbulent region, the boundary between forced and mixed convection regions was based on the correlations of Metais and Kraussold (see Metais (1963)). In the development of the flow regime map, Metais and Eckert (1964) utilized the mentioned laminar and turbulent forced and mixed convection correlations using the following general relationship:

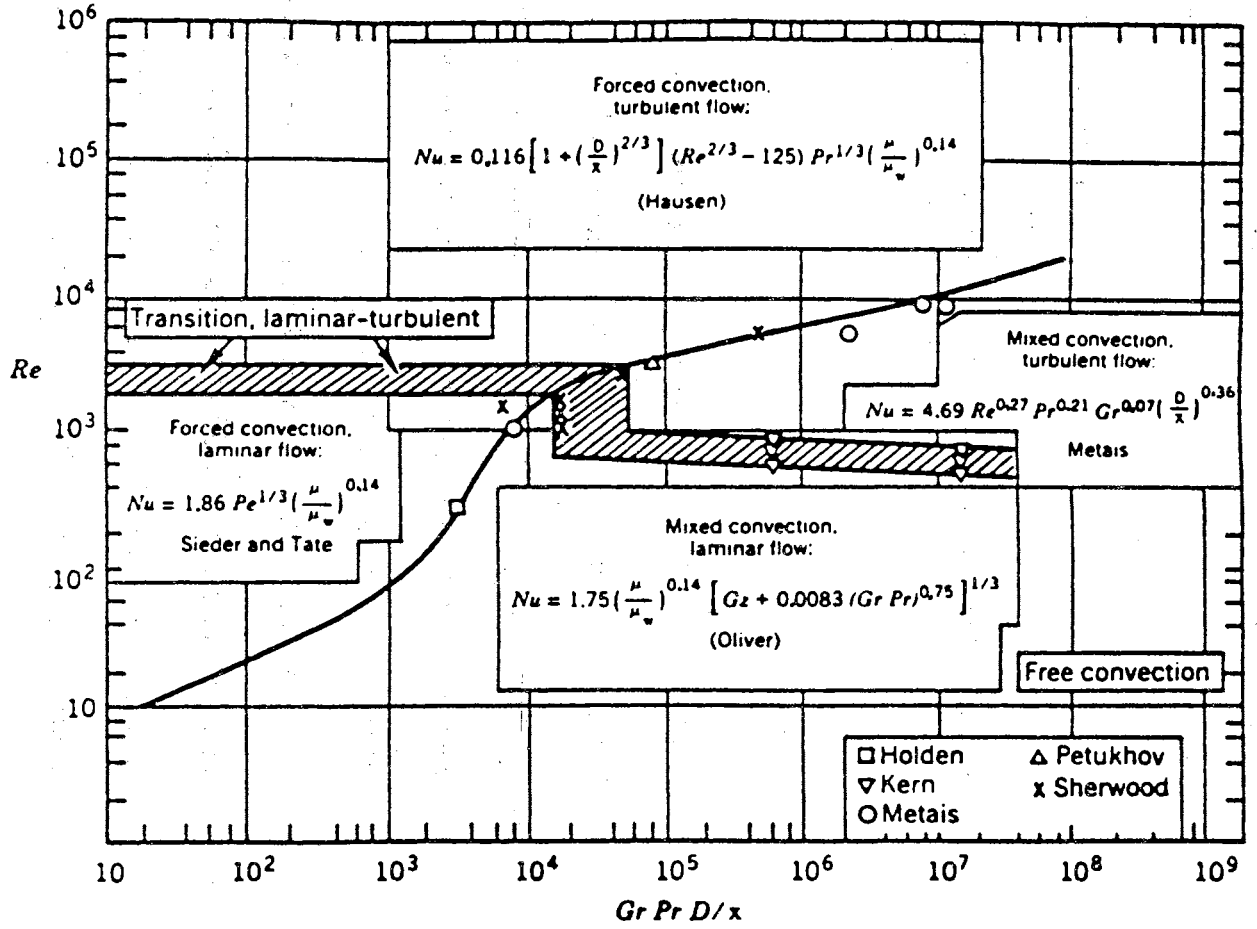

Figure 3.8 Free, Forced, and Mixed Convection Regimes for Flow in Horizontal Circular Tubes for $10^{-2} < PrD/x < 1$ and Uniform Wall Temperature Boundary Condition Taken from Kakac et al. (1987).

$$Nu_{mixed} = Nu_{forced} \times (\text{Correction Factor}) \quad (3.1)$$

The correction factor (F) is a function of Gr, Pr, and Re. To find the boundary between forced and mixed convection regions, Metais and Eckert (1964) arbitrarily set the correction factor to 10%. In other words, Nu_{mixed} was set to be 10% greater than Nu_{forced}. In this fashion, Eq. (3.1) becomes

$$Nu_{mixed}/Nu_{forced} = 1.1 = F(Gr,Pr,Re) \quad (3.2)$$

Equation (3.2) can be rearranged such that Reynolds number can be represented as a function of Grashof and Prandtl numbers

$$Re = f(Gr,Pr) \quad (3.3)$$

Equation (3.3) represents the general form of the expression used by Metais (1963) to develop equations for the boundaries between the laminar and turbulent forced and mixed convection regions. These equations are represented in Fig. 3.8 by the solid line. In reference to Fig. 3.8, it is also interesting to note that, although the solid line separating the laminar and turbulent forced and mixed convection regions was based on specific forced and mixed convection heat transfer correlations, only one of the correlations used (Metais' correlation for the turbulent mixed convection) has been recommended on the flow regime map. The other recommended correlations on the flow regime map were those of Sieder and Tate for laminar forced convection, Oliver for laminar mixed convection, and Hausen for turbulent forced convection (see Metais (1963)). In addition, the flow regime map doesn't offer a heat transfer correlation for the forced or mixed

convection transition regions. As pointed out earlier, the details on the transition region in the flow regime map (shaded area) are very sketchy, and the reported transition Reynolds number ranges in the forced and mixed convection regions are not justified. This was primarily due to the lack of reliable experimental data in these regions.

The flow regime map provided by Metais (1963) can be used to assist the heat exchanger designer in determining the influence of buoyancy in a horizontal circular tube with the uniform wall temperature boundary condition. However, this flow regime map cannot be used with the uniform wall heat flux boundary condition. The dependency of the heat transfer transition region on the type of the inlet configuration should be incorporated into the flow regime map, and the boundary between laminar and transition forced and mixed convection regions should be redefined. For this purpose, our experimental data for the three inlets were utilized.

Development of the new boundary required laminar and transition forced and mixed convection data. As pointed out in reference to Fig. 3.4, secondary flow needs a certain length for development. Our experimental data indicated that for x/D less than 70, pure forced convection is still dominant in the laminar and lower transition regions. The experimental data for development of this new boundary between laminar and transition forced and mixed convection regions can be identified by using the criterion that the ratio of the local peripheral heat transfer coefficient at the top of the tube to the local peripheral heat transfer coefficient at the bottom of the tube (h_t/h_b) should be greater than or equal to 0.8 for forced convection and less than 0.8 for mixed convection (see Fig. 3.4). This way, 51 data points (at $h_t/h_b = 0.8$) which represent the boundary between laminar and transition forced and mixed convection for the three inlets used in our experiments were

identified. Figure 3.9 shows the data points plotted on the flow regime map coordinates (Re vs. GrPr). To obtain a smooth boundary between the laminar and transition forced and mixed convection regions, the data points for the three inlets were curve-fitted in the form given by Equation (3.4) using a least squares curve fitting program. The recommended equation for the forced and mixed convection regions in the flow regime map is

$$Re = 2674 + 5.35x10^{-13}(GrPr)^{2.5} - 1.85x10^{-16}(GrPr)^{3} - 2.64x10^{14}(GrPr)^{-2} \quad (3.4)$$

Equation (3.4) correlates the 51 data points with a correlation coefficient of 0.96 (see Fig. 3.9).

The boundary between laminar and transition forced and mixed convection regions given in Metais and Eckert's (1964) original flow regime map (see Fig. 3.8) and replotted as Fig. 3.9 should be replaced with Equation (3.4) when the uniform wall heat flux boundary condition is used. In addition, the heat transfer transition Reynolds number ranges for the three inlets should be incorporated into the flow regime map. These changes appear in the revised version of the flow regime map given as Fig. 3.10. In this figure, there is a common boundary for all three inlets separating the laminar forced and mixed convection regions. However, for the transition forced and mixed convection regions, the boundaries are inlet configuration dependent. The lower and upper bounds of heat transfer transition Reynolds number for each inlet shown in Fig. 3.10 were based on the results at x/D = 3 and 192, respectively.

The proposed flow regime map (see Fig. 3.10) was verified with our experimental data for the three inlets. The results of these comparisons are shown in Figs. 3.11, 3.12,

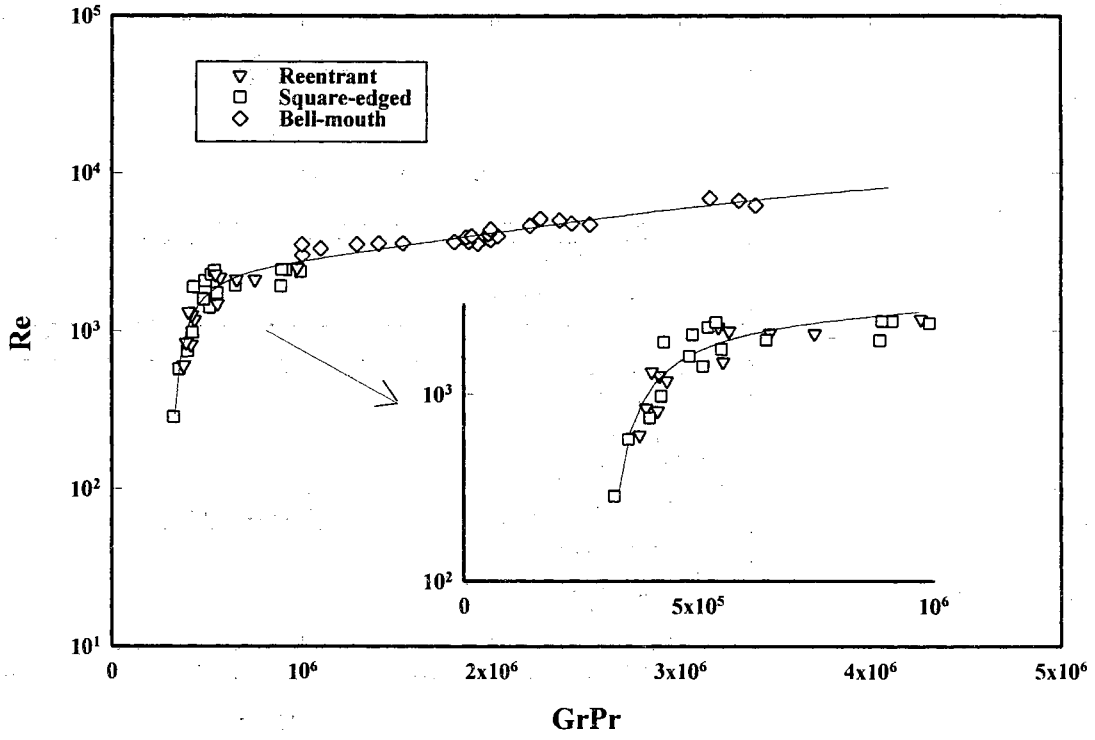

Figure 3.9 The Boundary Between Forced and Mixed Convection.

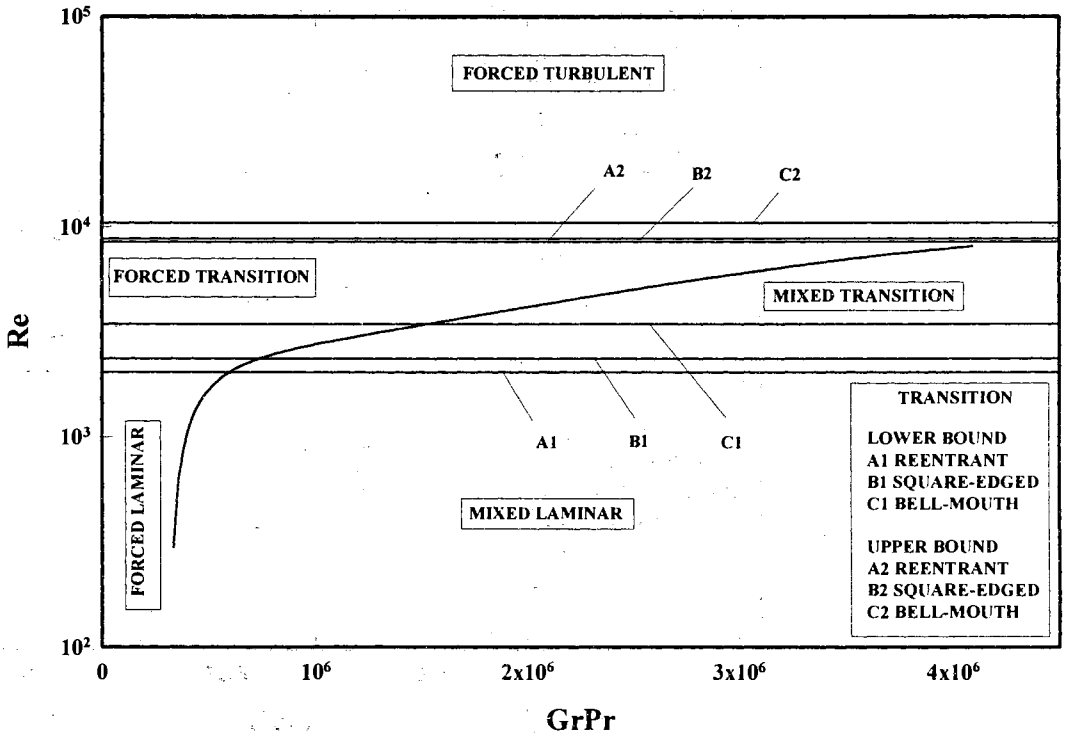

Figure 3.10 The New Flow Regime Map for Flow in Horizontal Tubes with Three Different Inlet Configurations and Uniform Wall Heat Flux.

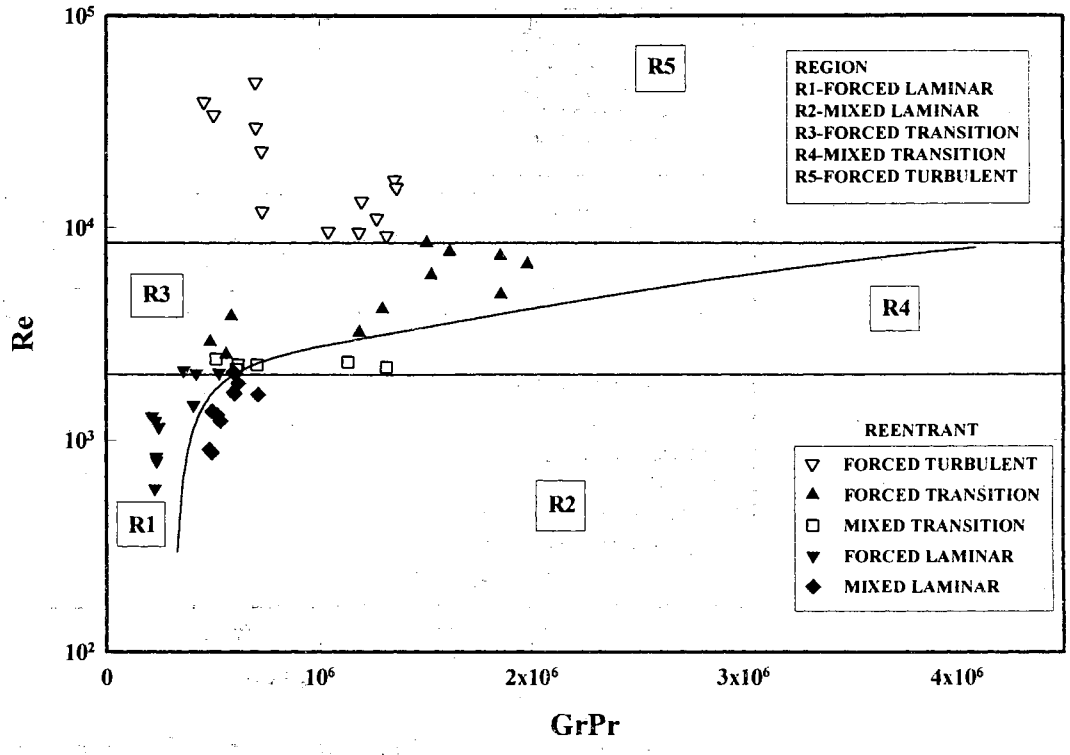

Figure 3.11 Comparison of Experimental Data for a Reentrant Inlet with the New Flow Regime Map.

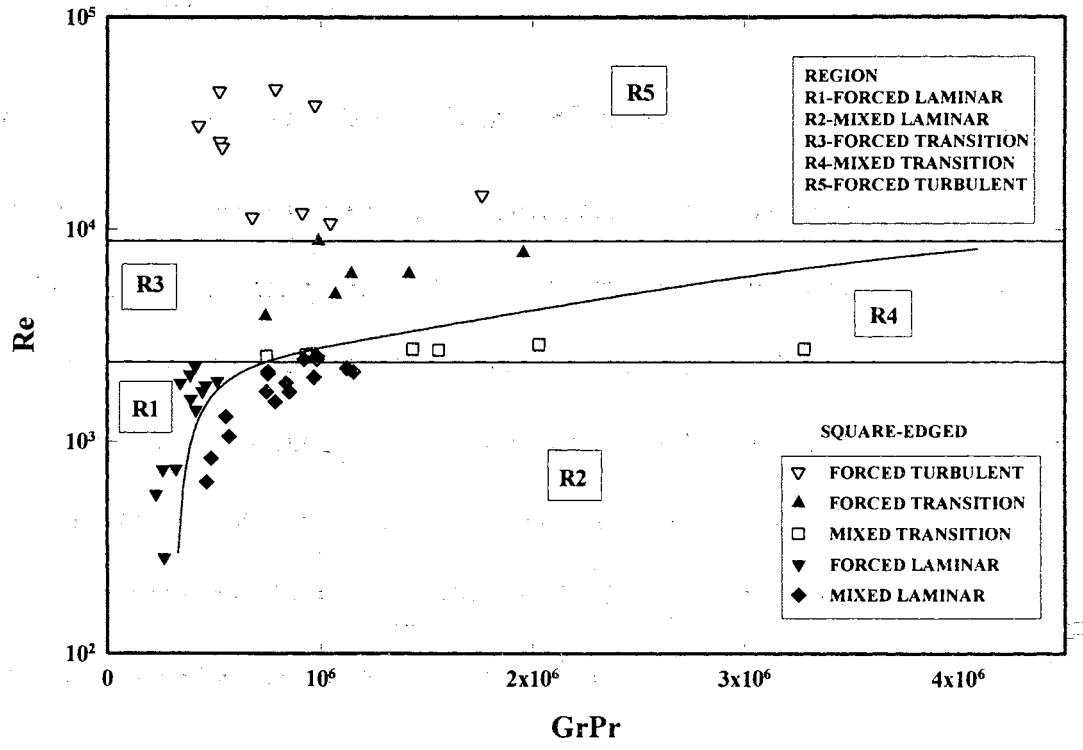

Figure 3.12 Comparison of Experimental Data for a Square-edged Inlet with the New Flow Regime Map.

and 3.13 for the reentrant, square-edged, and the bell-mouth inlets, respectively. As shown in these figures, the experimental data for all applicable flow regimes are predicted correctly by the revised flow regime map. In addition, Fig. 3.14 shows an independent check of the revised flow regime map with experimental data of Chen (1988) who used a completely different experimental setup for a square-edged inlet. Again, the revised flow regime map predicted the flow regimes correctly.

3.5 Heat Transfer Correlation for the Laminar Region

As pointed out in reference to Fig. 3.4, the modes of heat transfer in the laminar flow region can be divided into forced and mixed convection. Pure forced convection can be observed near the entrance, since secondary flow needs a certain length for development. To develop a heat transfer correlation in the entrance and fully developed laminar regions, we used the mixed and forced convection data in these regions. A correlation similar to the one proposed by Martineli and Boelter (1942) was curve-fitted to our data using a least squares curve-fitting program. The correlation is

$$Nu_l = 0.61[(RePrD/x)+0.025(GrPr)^{0.8}]^{0.4}(\mu_b/\mu_w)^{0.14} \qquad (3.5)$$

where

$3 \leq x/D \leq 192$, $280 \leq Re \leq 3800$, $13 \leq Pr \leq 160$,

$1000 \leq Gr \leq 2.0x10^5$, $1.2 \leq \mu_b/\mu_w \leq 3.8$

Equation (3.5) is applicable to laminar forced and mixed convection in the entrance and fully developed regions and can be used for all three inlets. It should be noted that two coefficients are common between the proposed correlation and Martineli-

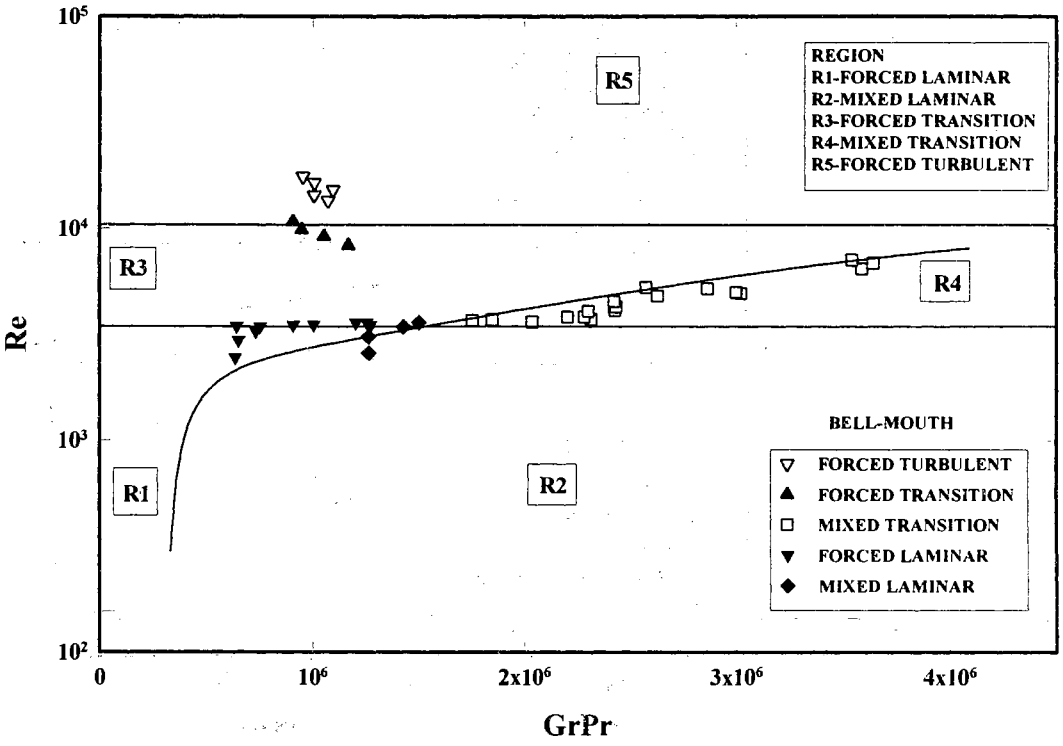

Figure 3.13 Comparison of Experimental Data for a Bell-mouth Inlet with the New Flow Regime Map.

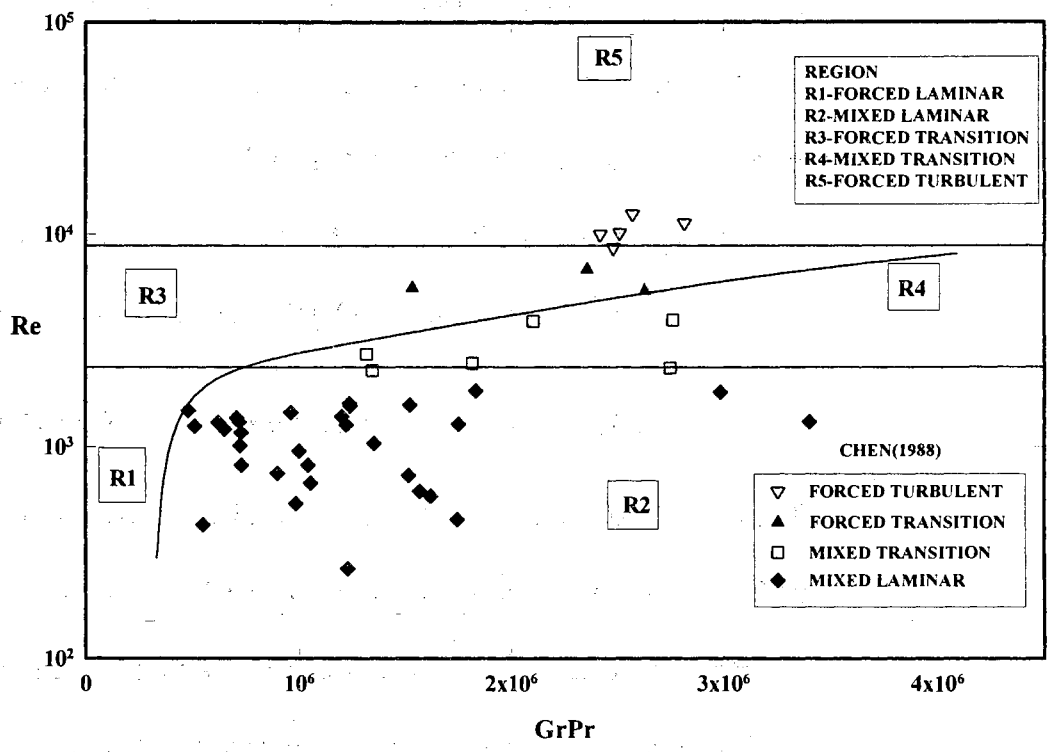

Figure 3.14 Comparison of Experimental Data of Chen (1988) for a Square-edged Inlet With the New Flow Regime Map.

Boelter's correlation. They are the leading coefficient of the Grashof and Prandtl numbers product (0.025) and the power of the viscosity ratio (0.14). The equation gives a representation of the experimental data to within +18% and -18%. In the development of the correlation, a total of 1545 experimental data points were used. It is worth mentioning that the data used in the development of the proposed correlation was gathered by four different investigators in a period of six years. The absolute average deviation between the results predicted by the correlation and the experimental data is 6.4%. About 22% of the data (348 data points) were predicted with more than $\pm 10\%$ deviation, and 78% of the data (1197 data points) with less than $\pm 10\%$ deviation. Figure 3.15 compares the predicted Nusselt numbers obtained from Equation (3.5) with measurements.

3.6 Heat Transfer Correlation for the Turbulent Region

In the turbulent flow region (refer to Fig. 3.4, the ratios of heat transfer coefficients at the top and bottom of the tube are close to unity), the effect of free convection on our data is insignificant and the flow is considered to be dominated by forced convection effects. Using the entrance and fully developed turbulent forced convection data for all three inlets, a correlation similar to the Sieder and Tate correlation (1936) with two extra terms was curve-fitted to our experimental data. The extra terms are x/D and μ_b/μ_w. The x/D term is used to include the entrance effect and the μ_b/μ_w term is used to include the influence of variation of axial and radial properties. The proposed correlation is

$$Nu_t = 0.023Re^{0.8}\, Pr^{0.385}(x/D)^{-0.0054}(\mu_b/\mu_w)^{0.14} \qquad (3.6)$$

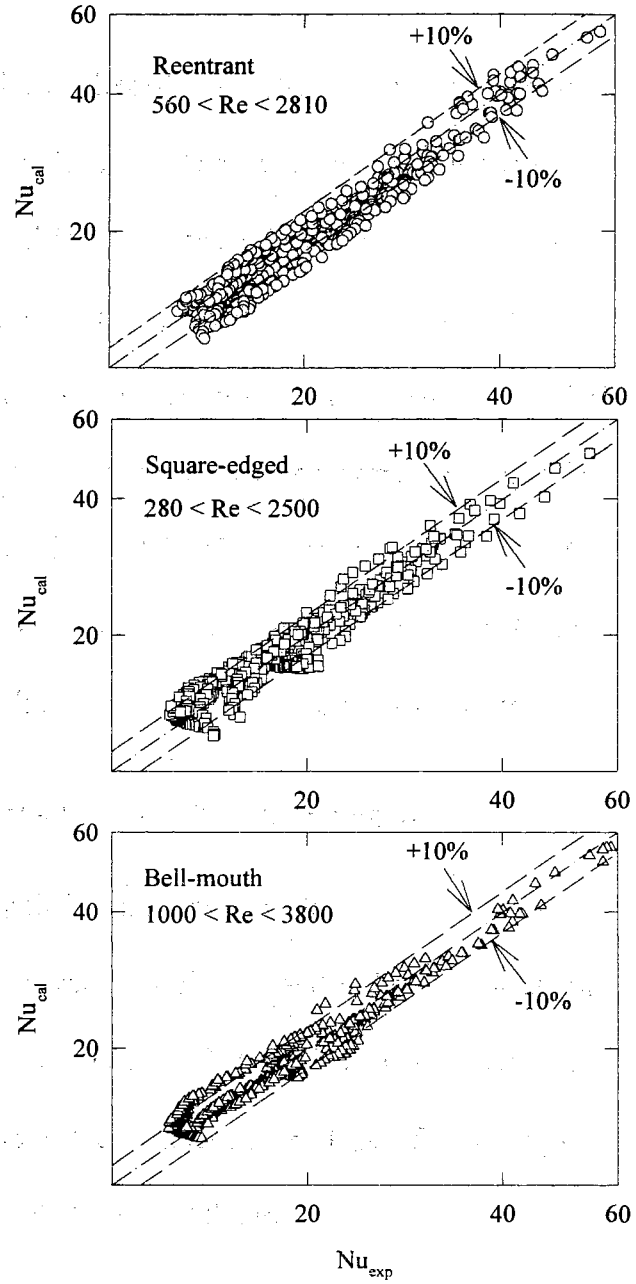

Figure 3.15 Comparison Between Experimental Nusselt Numbers and Those Predicted by the Proposed Laminar Region Heat Transfer Correlation.

where

$3 \leq x/D \leq 192$, $7000 \leq Re \leq 49{,}000$

$4 \leq Pr \leq 34$, $1.1 \leq \mu_b/\mu_w \leq 1.7$

Equation (3.6) is applicable to turbulent forced convection in the entrance and fully developed regions and can be used for all three inlets. It should be noted that the power for the Prandtl number is also modified from the original Sieder and Tate's correlation. The equation correlates the experimental data within +11.5% and -12.8%. In the development of the correlation, 1261 experimental data points were used. The absolute average deviation between the results predicted by the correlation and the experimental data is 3.7%. The correlation predicted 92% of the experimental data (1160 data points) within ±10% deviation and 71% of the data within ±5% deviation. Figure 3.16 compares the Nusselt number obtained from Equation (3.6) with measurements.

3.7 Heat Transfer Correlation for the Transition Region

In the transition region, flow has both laminar and turbulent characteristics. In addition, the type of inlet configuration influences the beginning and end of the transition region. Thus a single correlation for this region cannot predict the data, and a correlation for each inlet should be developed. The form of the correlation developed for this region is similar to the one proposed by Churchill (1977) and is of the form

$$Nu_{tr} = Nu_l + \{\exp[(a-Re)/b] + Nu_t^c\}^c \qquad (3.7)$$

The equations for Nu_l and Nu_t are the same as Eqs. (3.5) and (3.6), respectively. The exponential term in the equation describes the steep change in the transitional heat

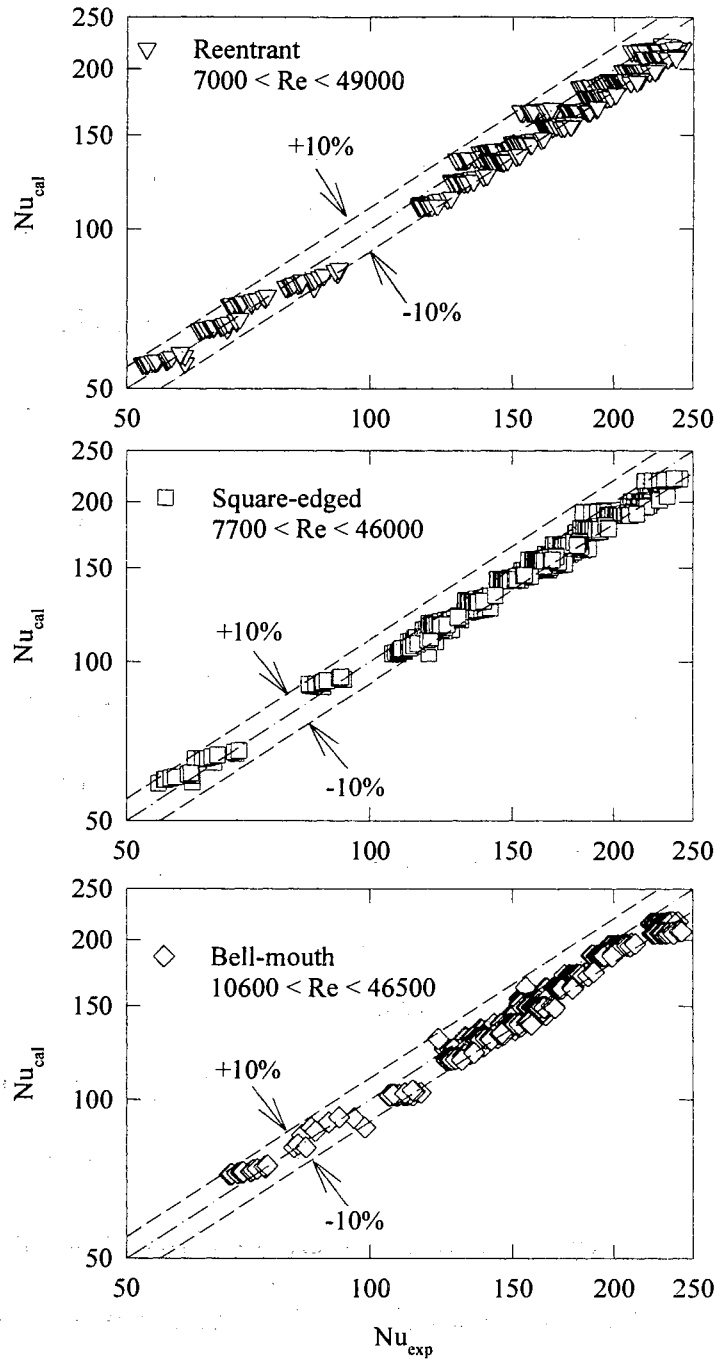

Figure 3.16 Comparison Between Experimental Nusselt Numbers and Those Predicted by the Proposed Turbulent Region Heat Transfer Correlation.

transfer behavior of the flow from laminar to turbulent (see Fig. 3.6). Equation (3.7) was curve-fitted to our experimental data in the transition region, and the following constants were obtained for each inlet.

Reentrant

$a = 1766, b=276, c=-0.955$

where

$3 \leq x/D \leq 192, 1700 \leq Re \leq 9100, 5 \leq Pr \leq 51$

$4000 \leq Gr \leq 2.1x105, 1.2 \leq \mu_b/\mu_w \leq 2.2$

Square-edged

$a = 2617, b=207, c = -0.950$

where

$3 \leq x/D \leq 192, 1600 \leq Re \leq 10{,}700, 5 \leq Pr \leq 55$

$4000 \leq Gr \leq 2.5x105, 1.2 \leq \mu_b/\mu_w \leq 2.6$

Bell-mouth

$a = 6628, b = 237, c = -0.980$

where

$3 \leq x/D \leq 192, 3300 \leq Re \leq 11{,}100, 13 \leq Pr \leq 77$

$6000 \leq Gr \leq 1.1x105, 1.2 \leq \mu_b/\mu_w \leq 3.1$

Equation (3.7) is applicable to the heat transfer transition region. It is able to predict the heat transfer coefficient in the entrance and fully developed regions and should be used with an appropriate set of constants for each inlet configuration. For the development of the transition region correlation for the reentrant inlet, 441 experimental

data points were used. The correlation gave a representation of the experimental data to within +25.1% and -23% and had an absolute deviation of 8%. Three percent of the data (13 data points) were predicted with more than ±20% deviation, 29% (129 data points) with ±10-20% deviation, and 68% (299 data points) with less than ±10% deviation. For the square-edged inlet, 416 experimental data points were used for the development of the correlation. The equation correlated the experimental data to within +24.3% and -23.9% and had an absolute average deviation of 7.2%. Three percent of the data (12 data points) were predicted with more than ±20% deviation, 26% (106 data points) with ±10-20% deviation, and 72% (298 data points) with less than ±10% deviation. The correlation for the bell-mouth inlet was based on 433 experimental data points. The correlation represented the experimental data to within +18.5% and -22% and had an absolute average deviation of 8.1%. Less than 1% of the data (four data points) were predicted with more than ±20% deviation, 24% (104 data points) with ±10-20% deviation, and 75% (325 data points) with less than ±10% deviation. Figure 3.17 compares the predicted Nusselt numbers obtained from Eq. (3.7) for each inlet with measurements.

In summary, five new forced and mixed heat transfer correlations for the three inlets have been developed corresponding to the entrance and fully developed data for each flow region. Common correlations were used in the laminar and turbulent regions for the three inlets. Because the transition region is dependent on inlet configuration, three separate correlations were developed in the transition region, one for each inlet. To have a continuous prediction from the proposed correlations for each inlet across all flow regimes, the limits of each correlation were stretched as much as possible without loss of accuracy into the other regions. These correlations can be applied in the appropriate

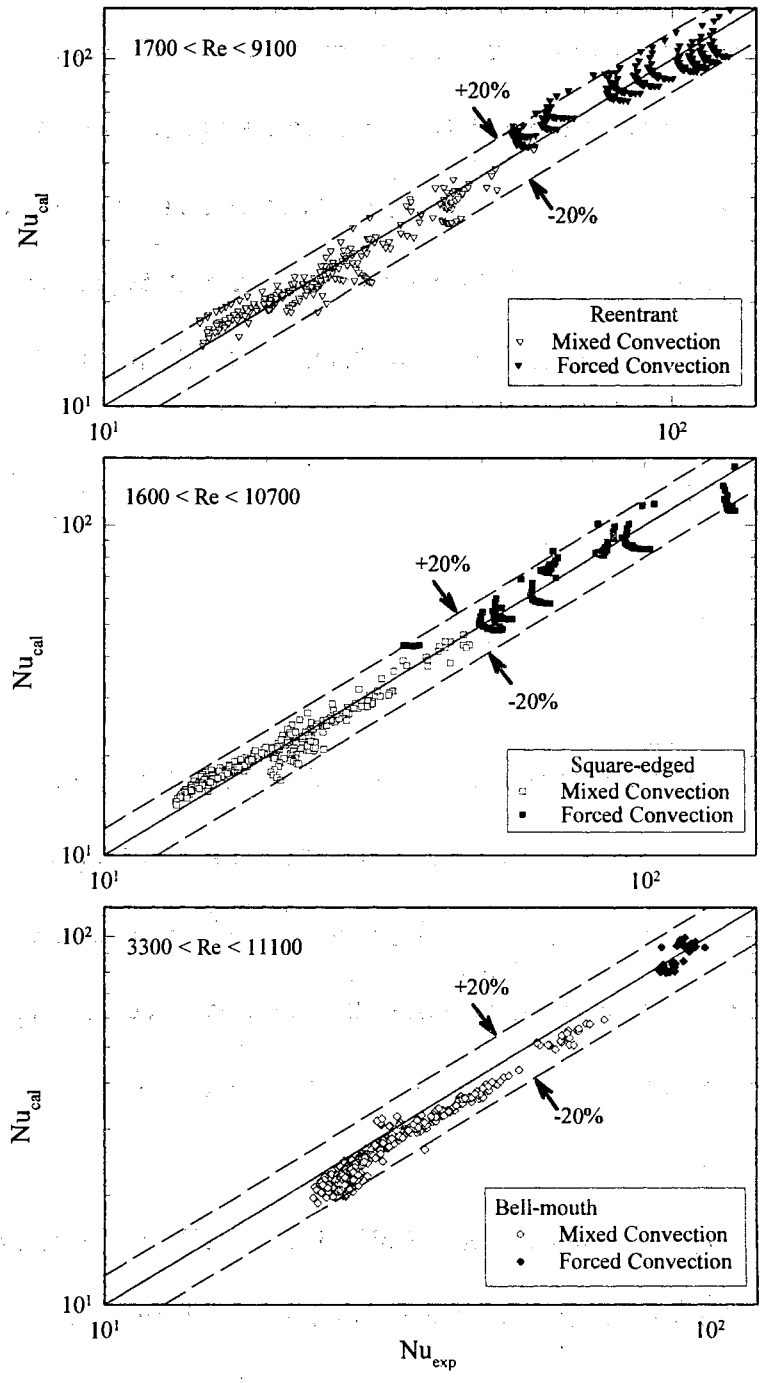

Figure 3.17 Comparison between Experimental Nusselt Numbers and Those Predicted by the Proposed Transition Region Heat Transfer Correlation.

region in the flow regime map.

3.8 Comparison of Available Correlations with Experiments

A large number of fully developed forced convection heat transfer correlations for pipes with a rounded entrance have been compared by Shah and Johnson (1980), and these comparison have been extended by Kakac et al. (1987). Based on these extensive comparisons, the following fully developed forced convection correlation developed by Gnielinski (1976) for $2300 \leq Re \leq 5x10^4$ and $0.5 \leq Pr \leq 2000$ was recommended:

$$Nu = \frac{(f/2)(Re-1000)Pr}{11+12.7(f/2)^{0.5}(Pr^{2/3}-1)} \tag{3.8}$$

where

$$f = (1.58 \ln Re - 3.28)^{-2}$$

Gnielinski's correlation was compared with our fully developed forced convection heat transfer data in the transition and turbulent regions for all three inlets (see Fig. 3.18). The correlation predicted our experimental data within ±20%. Since Gnielinski's correlation was based on experimental data for a smooth entrance (bell-mouth), the accuracy of the correlation improved to well within ±10% when the experimental data for the bell-mouth inlet were used.

Another correlation recommended by Kakac et al. (1987) was the one developed by Churchill (1977). This correlation is based on asymptotic solutions/correlations and was constructed for $0 \leq Pr \leq 10^6$ and $10 \leq Re \leq 10^6$, spanning the laminar, transition, and turbulent flow regimes. Churchill's correlation is restricted to fully developed forced

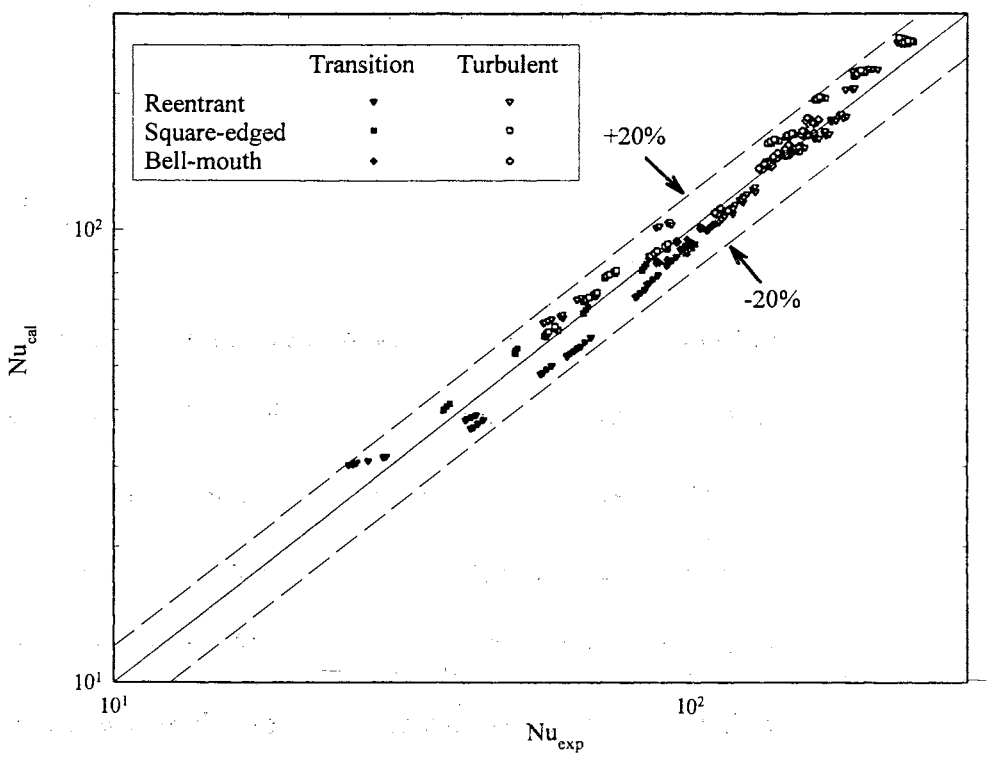

Figure 3.18 Comparison between Experimental Fully Developed Forced Convective Heat Transfer Data for All Three Inlets and Correlation of Gnielinski (1976).

convection heat transfer in pipes with a rounded entrance. The correlation for uniform wall heat flux boundary condition is of the form

$$Nu^{10} = Nu_l^{10} + \left[\frac{\exp[(2200 - Re)/365]}{Nu_l^2} + \frac{1}{Nu_t^2} \right]^{-5} \tag{3.9}$$

where

$$Nu_l = 4.364$$

$$Nu_t = 6.3 + \frac{0.079(f/2)^{1/2}\, Re\, Pr}{(1 + Pr^{4/5})^{5/6}}$$

Churchill's correlation was compared with our fully developed forced convection heat transfer data for all three inlets (see Fig. 3.19). For the bell-mouth inlet, the correlation predicted our experimental data within ±10%. However, for the other two inlets the predictions were not as accurate. For Re > 4000 the correlation predicted the reentrant and square-edged data with an accuracy of ±30%. For Re < 4000, the accuracy of the correlation deteriorated with a decrease in the Reynolds number, and underpredicted the experimental data by 40-80%. This was due to the strong influence of inlet configuration on the heat transfer coefficient in the laminar and lower transition regions, which was not accounted for in Churchill's correlation.

The comparisons shown in Figs. 3.18 and 3.19 indicate that the correlations do a good job of predicting the fully developed forced convection Nusselt numbers in the upper transition and turbulent regions for different inlets. The accuracy of the predictions improved when the correlations were compared with the data for a rounded entrance (bell-mouth). However, the correlations have a limited range of application and cannot be

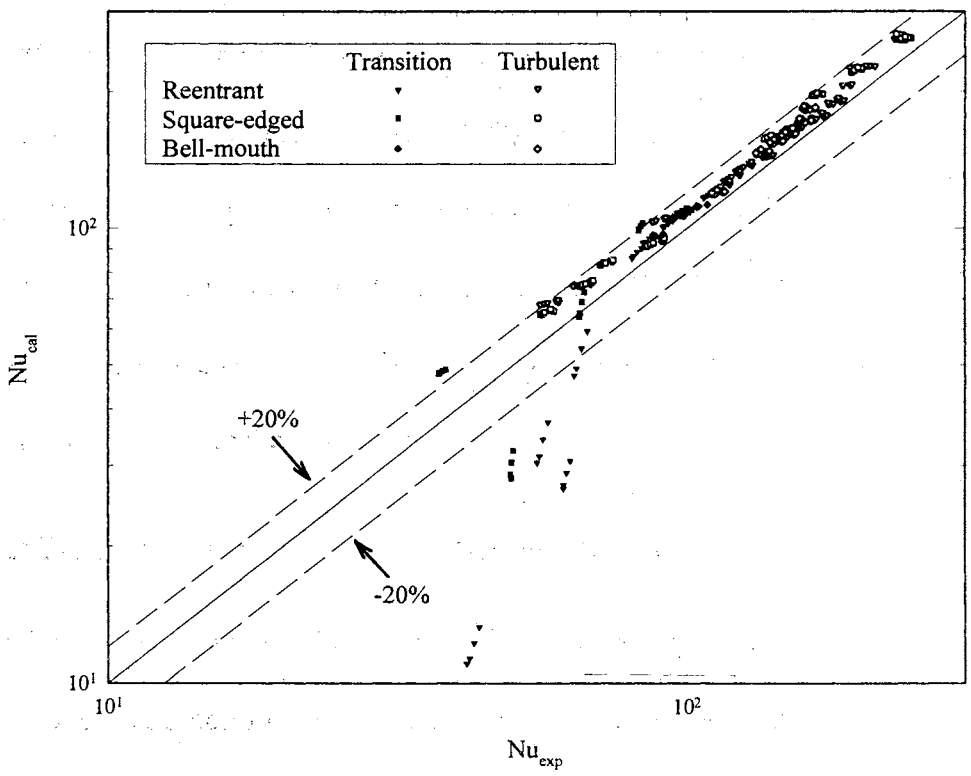

Figure 3.19 Comparison between Experimental Fully Developed Forced Convective Heat Transfer Data for All Three Inlets and Correlation of Churchill (1977).

applied to flows where mixed convection and inlet and entrance effects are important. For these flows the correlations developed in this study are recommended; see Eqs. (3.5)-(3.7).

It should be noted that the experimental data in the laminar and transition regions for the reentrant and square-edged inlets were also compared with other correlations presented in Kakac et al. (1987), and the results of these comparisons showed no clear trend (see Ghajar and Strickland (1990) and Ghajar et al. (1990)). For a given flow regime, no single correlation predicted the experimental data with any consistency. This was particularly true for the mixed laminar and lower transition regions. This lack of prediction was attributed to the strong influence of secondary flow and the shape of inlet configuration on the heat transfer coefficient in these regions.

3.9 Unusual Heat Transfer Characteristic of the Bell-mouth Inlet

From the previous section, it is obvious that the heat transfer characteristics in the upper transition and turbulent region for a bell-mouth inlet are completely different from the square-edged and reentrant inlets. Referring to Fig. 3.5, at approximately the first 50 diameters, forced convection is the dominant heat transfer mode; so the heat transfer coefficient at the top is close to the heat transfer coefficient at the bottom. Between 50 and 100 diameters, the free convection effect is established; so the heat transfer coefficient at the top and the heat transfer coefficient at the bottom are not close to each other. When x/D is greater than 100, the heat transfer coefficients increase as x/D increases. This unusual trend can be explained as follows. Using a highly disturbed inlet, like the reentrant and square-edged, the free stream turbulence is severe. A turbulent

boundary layer forms immediately at the entrance of the test section. Using a bell-mouth inlet configuration, the velocity and temperature profiles are uniform when the flow enters the test section. A laminar boundary layer initially forms at the entrance of the tube. This is very similar to the behavior of a flat plate. The free stream passes through the leading edge of the plate and a laminar boundary layer is formed. Then, at some distance from the entrance of the tube, possibly dependent on the degree of initial turbulence, the flow becomes unstable, and a transition to a turbulent boundary layer takes place. The turbulent boundary layer would then spread until it reaches the center of the tube and becomes a fully turbulent flow.

To further investigate this unusual behavior, three different screen sizes were used in the last section of calming section for this inlet. The first one was a coarse mesh screen with an open area ratio of 0.825. The second one was a medium mesh screen with an open area ratio of 0.759, and the third one was a fine mesh screen with an open area ratio of 0.650. The idea of using different mesh screens is to see the unusual heat transfer behavior responses to three different inlet turbulence levels. As we know, if the screen is fine, the inlet turbulence is low. Figures 3.20, 3.21, and 3.22 plot the local Nusselt number along the dimensionless x/D locations for the bell-mouth inlet with the coarse, medium, and fine mesh screens respectively. For the coarse mesh screen, the unusual heat transfer behavior is observed in the Reynolds number range from about 3430 to 7700. For Reynolds numbers less than 3430, the local Nusselt number along the dimensionless x/D locations is exactly the same as it behaved in the laminar region. When Reynolds number is greater than 3430 (see Fig. 3.20), the local Nusselt number seems to shift upward at x/D greater than 100 and causes a dip in the Nu-x/D curve. According to this figure, the

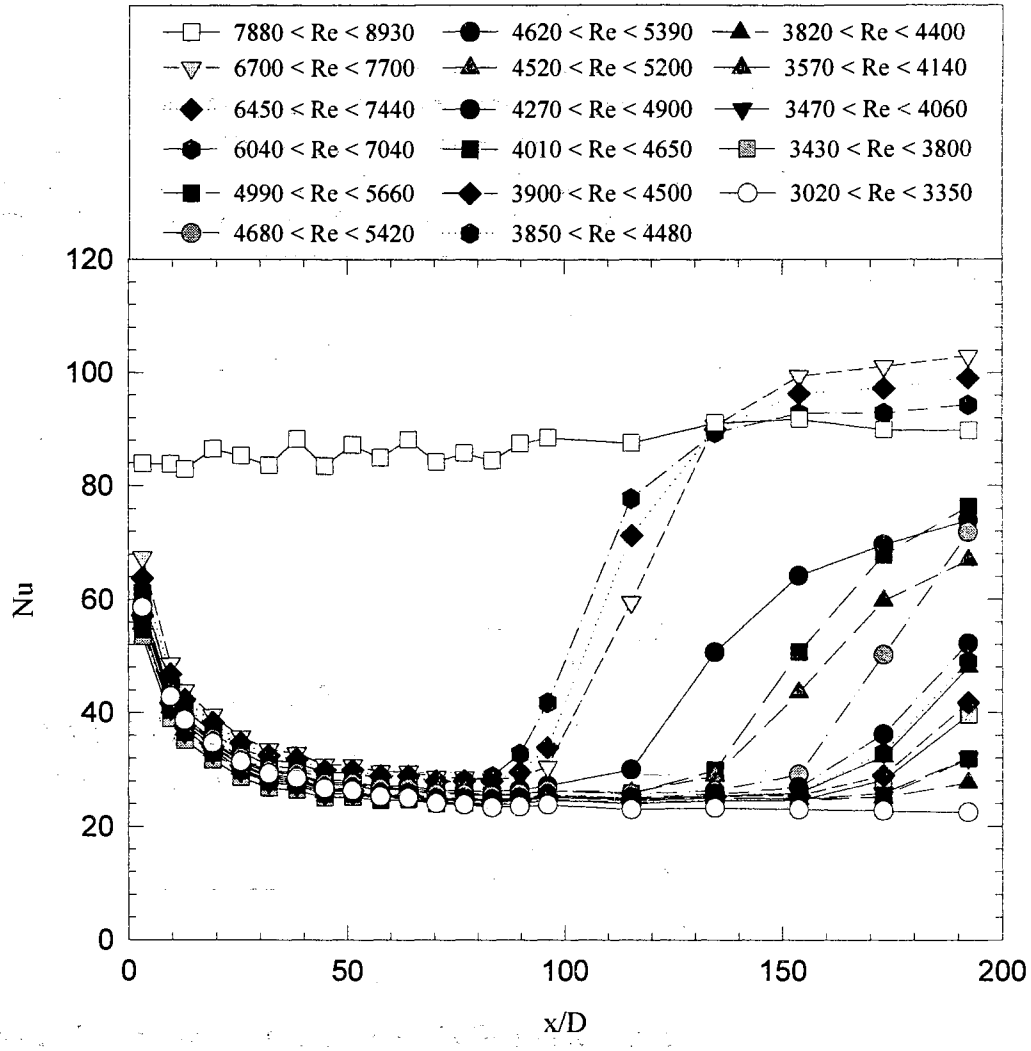

Figure 3.20 Boundary Layer Changing Behavior of a Bell-mouth Inlet with Coarse Mesh Screen.

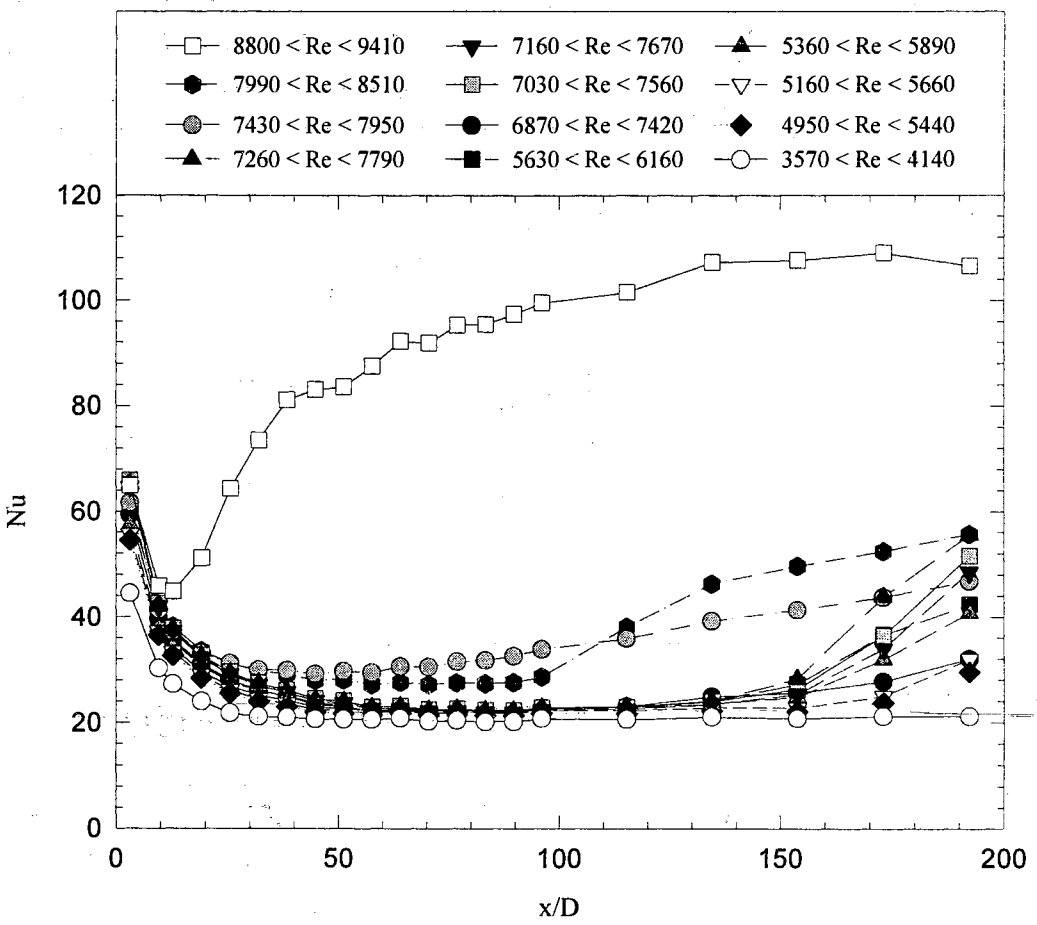

Figure 3.21 Boundary Layer Changing Behavior of a Bell-mouth Inlet with Medium Mesh Screen.

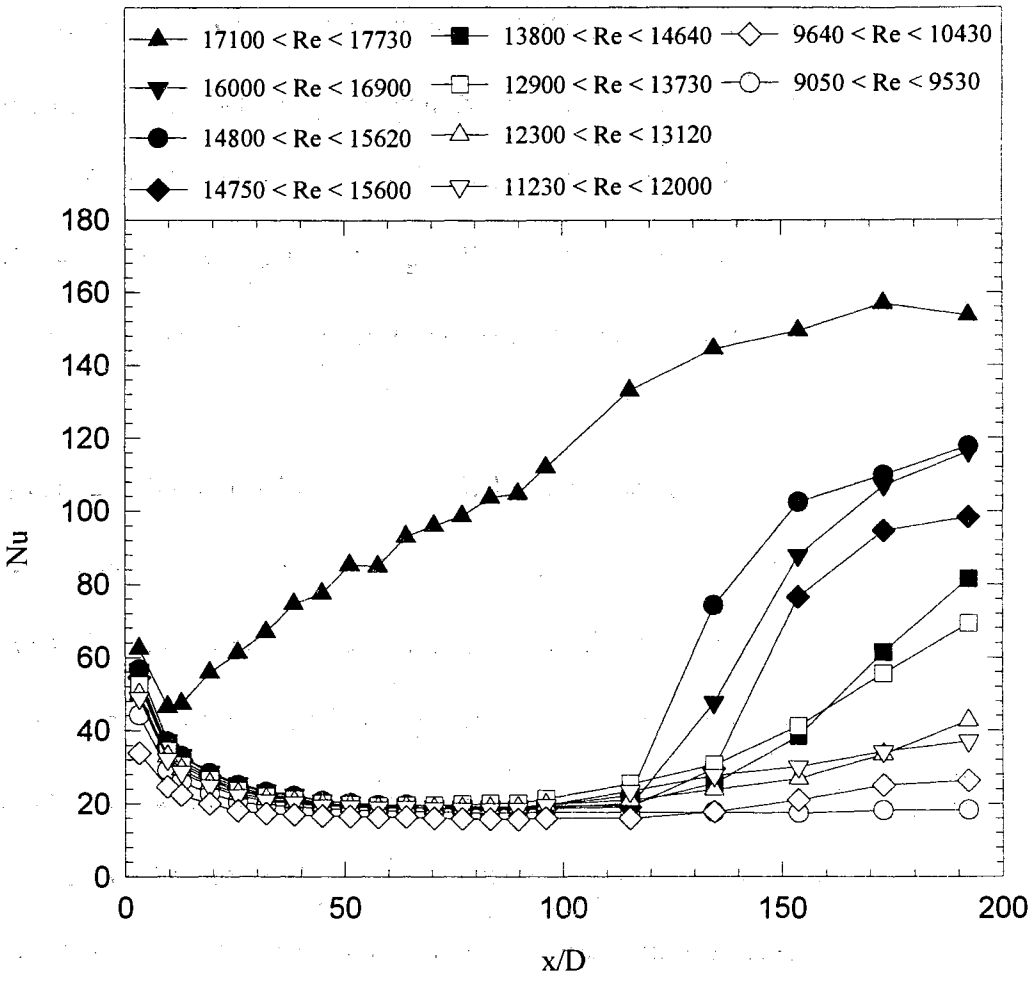

Figure 3.22 Boundary Layer Changing Behavior of a Bell-mouth Inlet with Fine Mesh Screen.

local Nusselt number starts to shift upward when x/D equals to 173 at a Reynolds number of about 3430. This means that the laminar boundary layer becomes unstable and it starts to change from laminar to turbulent at this location. As Reynolds number increases, the dimensionless location for which the local Nusselt number starts to shift upward decreases. This behavior tells us that the location for which the boundary changes from laminar to turbulent decreases as Reynolds number increases. The band of the dip reaches the smallest value when x/D approximately equals to 100 at a Reynolds number of about 7700. For Reynolds numbers greater than 7700, this unusual behavior can no longer be observed.

For the medium mesh screen, the unusual heat transfer behavior is observed when Reynolds number ranges from about 4950 to 8510. For Reynolds numbers less than 4950, the local Nusselt number along the dimensionless x/D locations is exactly the same as it behaved in the laminar region. When Reynolds number is greater than 4950 (refer to Fig. 3.21), the local Nusselt number starts to shift upward at x/D approximately equal to 173 and causes a dip in the Nu-x/D curve. Similar to the situation for the coarse mesh screen, as Reynolds number increases, the x/D location for which the local Nusselt number starts to shift upward decreases. When Reynolds number reaches approximately 8510, the dip reaches its smallest value at x/D approximately equal to 100. For Reynolds numbers greater than 8510 for this case, the dip can no longer be observed.

For the fine mesh screen, the unusual heat transfer behavior is observed when Reynolds number ranges from about 9640 to 16,900. For Reynolds numbers less than 9640, the local Nusselt number along the dimensionless x/D locations is exactly the same as it behaved in the laminar region. When Reynolds number is greater than 9640 (refer to

Fig. 3.22), the local Nusselt number starts to shift upward at x/D approximately equal to 173 and cause a dip in the Nu-x/D curve. Similar to the situation for the coarse mesh screen, as Reynolds number increases, the x/D location for which the local Nusselt number starts to shift upward decreases. When Reynolds number reaches approximately 16,900, the dip reaches its smallest value at x/D approximately equal to 100. For Reynolds numbers greater than 16,900 for this case, the dip can no longer be observed.

Referring to Figs. 3.20, 3.21 and 3.22, there are several common key factors.

1. The dimensionless location x/D for which the local Nusselt number starts to shift upward is approximately a constant (x/D = 173). This means that the laminar boundary layer exists up to x/D = 173. Then, the boundary layer becomes unstable and starts to change from laminar to turbulent.
2. The dimensionless location x/D for which the dip becomes smallest is approximately a constant (x/D = 100). The band of the dip gets smaller as the Reynolds number increases. This means that the distance required for the boundary layer change decreases as the Reynolds number increases.
3. For all three different screen sizes, the dip can no longer be detected when it reaches the smallest value at x/D = 100.
4. The local heat transfer coefficient has laminar behavior for these three different screen sizes for the first 100 x/D locations. This means that the boundary layer does not change from laminar to turbulent until the flow goes beyond x/D = 100.
5. The Reynolds number for which the unusual heat transfer behavior begins is inlet condition dependent. For a high inlet turbulence level (coarse screen), the Reynolds number is 3430. For a low inlet turbulence level (fine screen), the Reynolds number is

9640. For a moderate inlet turbulence level (medium screen), the Reynolds number is 4950.

In order to verify that the flow is actually going through a boundary layer changing process, special attention was paid to the peripheral temperatures profile during the data taking process. When the flow is in the laminar boundary layer region ($x/D < 100$), the peripheral wall temperature profiles are highly non-uniform (see Fig. 3.23). The temperature at the top has the highest value and the bottom temperature has the lowest value for this region. This means that strong mixed convection is present in this region. In the region in which the Nusselt number starts to shift upward, the peripheral wall temperature has an intermittent behavior (laminar boundary layer becomes unstable, and transition from laminar to turbulent is taking place). Most of the time, the peripheral wall temperatures profile is highly non-uniform which means the heat transfer mode is mixed convection, and at a certain moment, the peripheral wall temperatures become highly uniform which means that the heat transfer mode is pure forced convection (see Fig. 3.24). Whether the uniform peripheral wall temperature profile appears often or not is based on the Reynolds number range for these three different screen sizes. If Reynolds number is high, the uniform peripheral wall temperature profile appears more. Figure 3.25 shows the intermittent behavior of the peripheral wall temperature at a fixed location for a specific experimental run. As we know, turbulent heat transfer is much larger than laminar heat transfer. When the peripheral wall temperatures profile becomes intermittent, we can say that the heat transfer is oscillating between laminar and turbulent heat transfer characteristics. This is a typical transitional heat transfer behavior. Hence, the magnitude of the heat transfer coefficient lies between laminar and turbulent values.

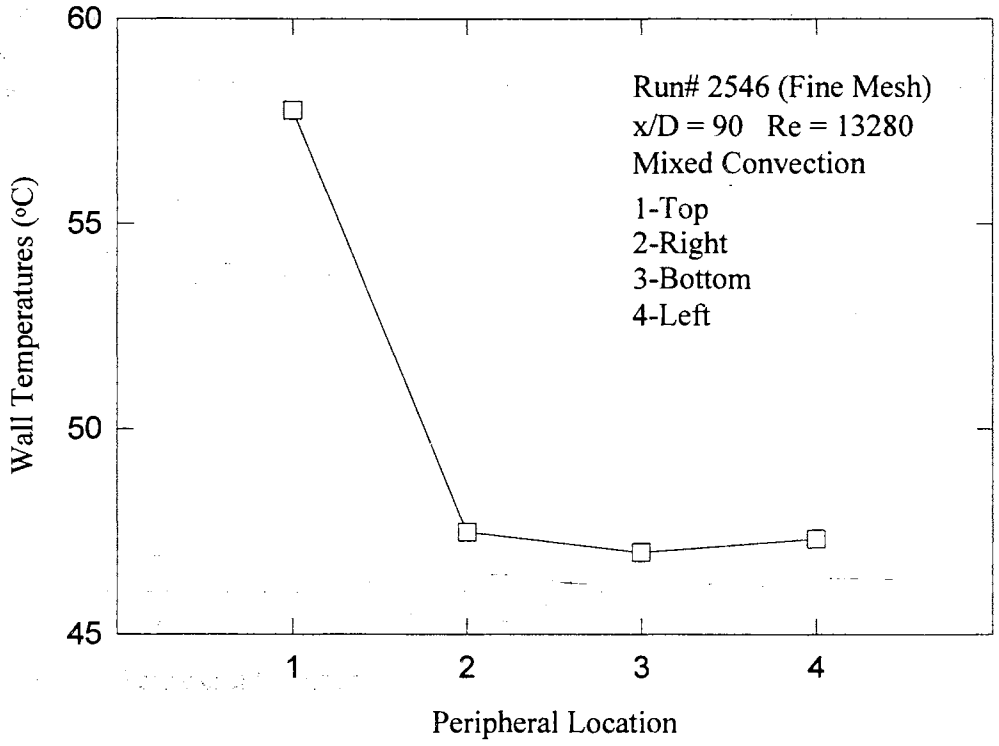

Figure 3.23 Peripheral Temperatures Trend for Mixed Convection.

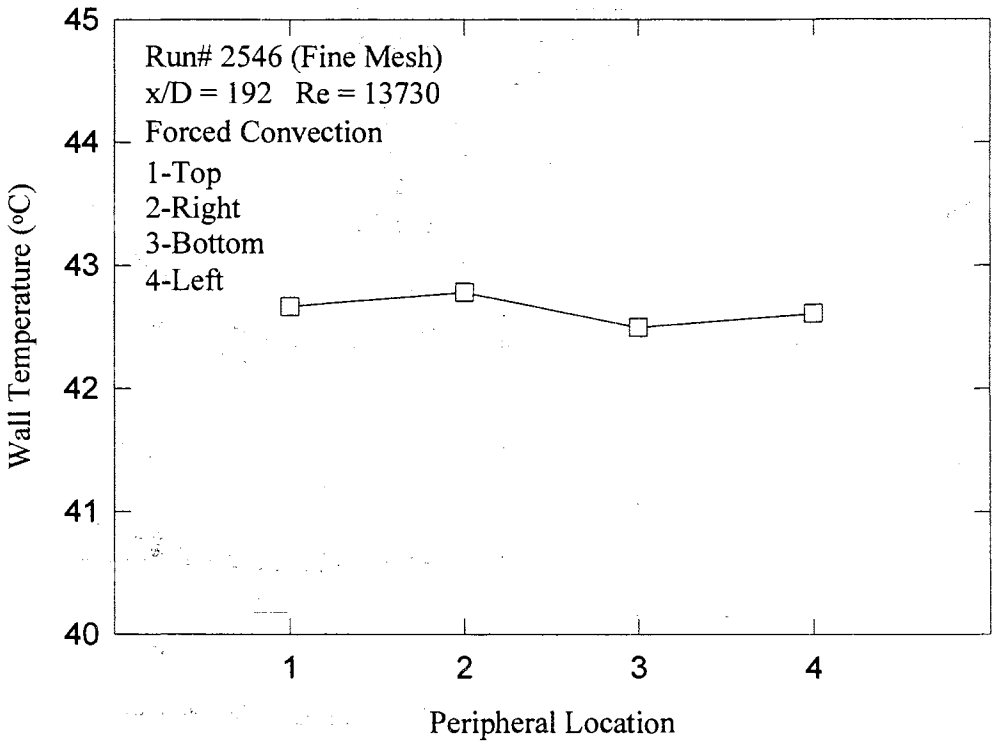

Figure 3.24 Peripheral Temperatures Trend for Forced Convection.

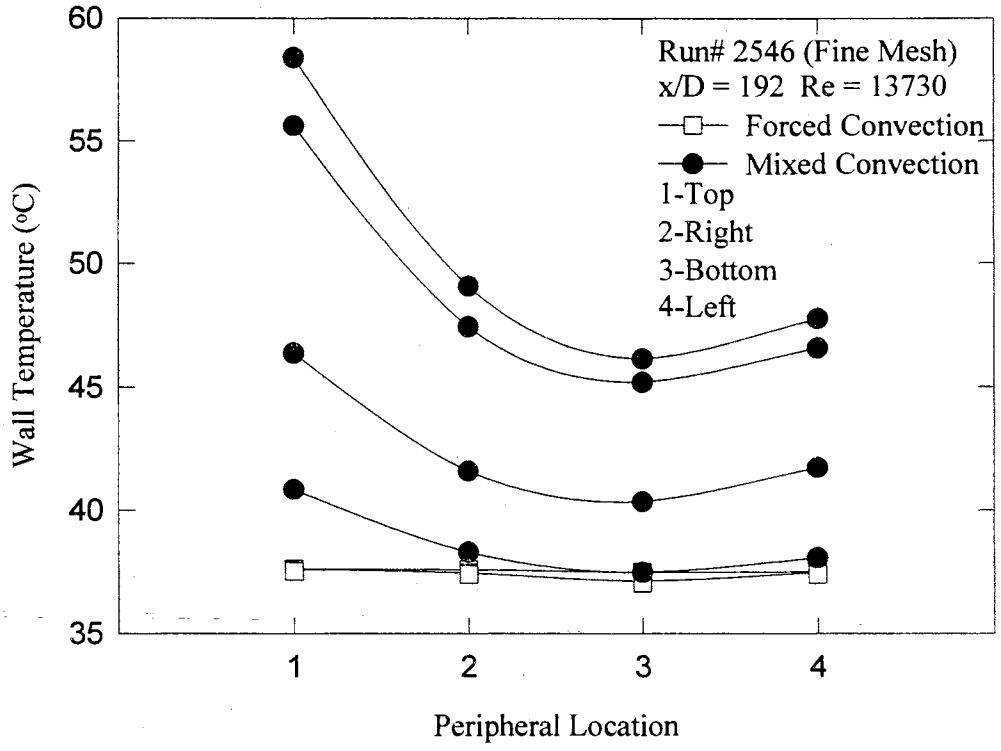

Figure 3.25 Peripheral Temperatures Trend for Intermittent Heat Transfer.

When this transitional heat transfer behavior ends, completely turbulent heat transfer can be observed.

CHAPTER IV

PRESSURE DROP RESULTS AND DISCUSSION

In order to investigate the effect of inlet configuration (reentrant, square-edged, and bell-mouth) and heating on fully developed skin friction coefficient in laminar, transition, and turbulent flow regimes, 79 sets of skin friction coefficient data for a bell-mouth entrance under isothermal and non-isothermal (uniform wall heat flux) flow conditions were experimentally obtained. For the other two inlet configurations, 122 sets of data for reentrant inlet and 132 sets of data for square-edged inlet under isothermal and non-isothermal flow conditions from Warnecker (1995) were used. Summary of the experimental data is listed in Appendix C. For the experiments, the local bulk Reynolds number ranged from about 1000 to 17000, the local bulk Prandtl number varied from about 6 to 30, the local bulk Grashof number ranged from 0 (isothermal condition) to 965000. The data sets covered the laminar, transition, and turbulent flow regimes. The uncertainty analysis (see Appendix B) of the overall experimental procedures using the method of Kline and McClintock (1953) showed that there was a maximum of 5% uncertainty for skin friction coefficient calculations. The isothermal flow conditions were ensured when the inlet and outlet bulk temperatures were nearly equal (within 0.4 ^{o}C of each other). For the non-isothermal runs, the heat balance errors were calculated similar to the calculations described for the heat transfer experiments (refer to Chapter III). The

heat balance error for the non-isothermal experimental runs was less than 5%. Experiments under the same conditions were conducted periodically to ensure the repeatability. The difference between the duplicated experimental runs were within ±5%.

In this chapter, the results for isothermal and non-isothermal skin friction coefficients will be discussed. First of all, the effect of calming section will be investigated. Secondly, the effect of inlet configuration on skin friction coefficient in all flow regimes will be discussed. After understanding the roles of calming section and inlet configuration, the effect of heating on pressure drop will be introduced. Finally, the experimental data used in this study will be compared with the available correlations, and new correlations for fully-developed skin friction coefficient will be introduced.

4.1 Effect of Calming Section on the Transition Region

In order to investigate the effect of calming section, only isothermal fully developed skin friction data for the reentrant, square-edged, and bell-mouth inlets were used. The effect of a calming section is always important since it serves as a flow straightening and turbulent reduction device and it will directly influence what happens downstream. Figures 4.1, 4.2, and 4.3 show two different curves for the same type of inlet configuration using different calming sections under isothermal flow condition. In the figures, the data with the fine mesh screen for reentrant and square-edged inlets were taken by Warnecker (1995) and for the bell-mouth inlet are based on the present study. The data with the coarse mesh screen for the reentrant, square-edged, and bell-mouth inlets were taken by Madon (1990), Augustine (1990), and Febransyah (1994), respectively. The difference between the coarse and fine mesh screens is discussed in

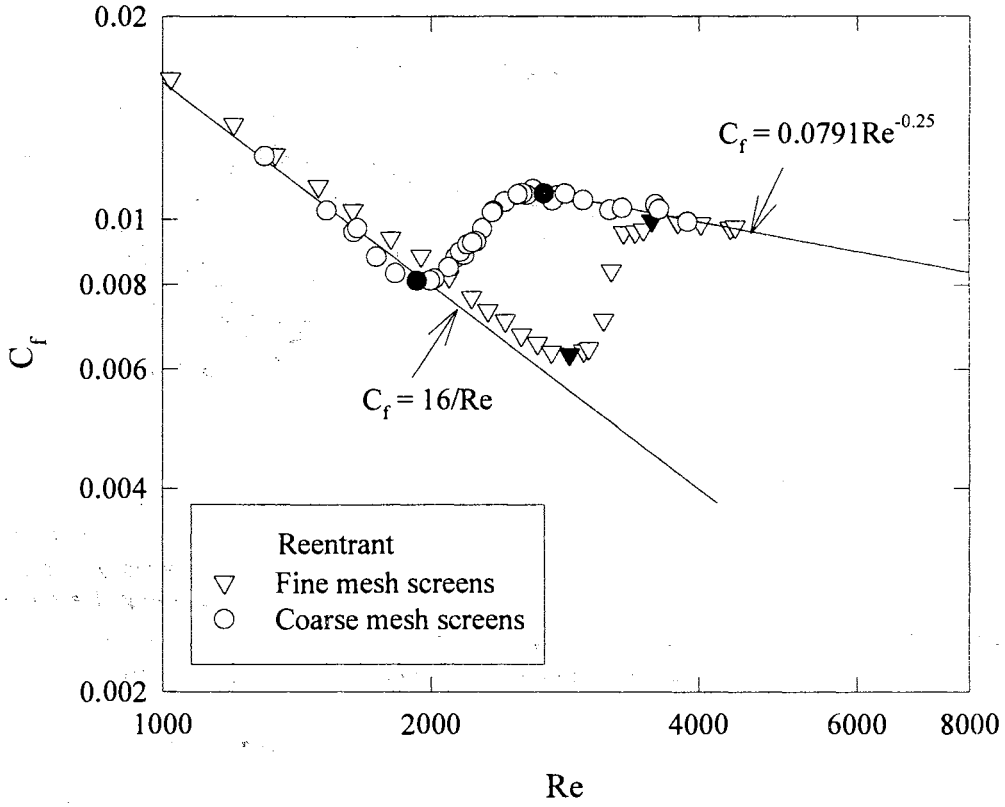

Figure 4.1 Effect of Screen Size on Fully Developed Skin Friction Coefficients for a Reentrant Inlet. (The solid symbols indicate the start and end of the transition region.)

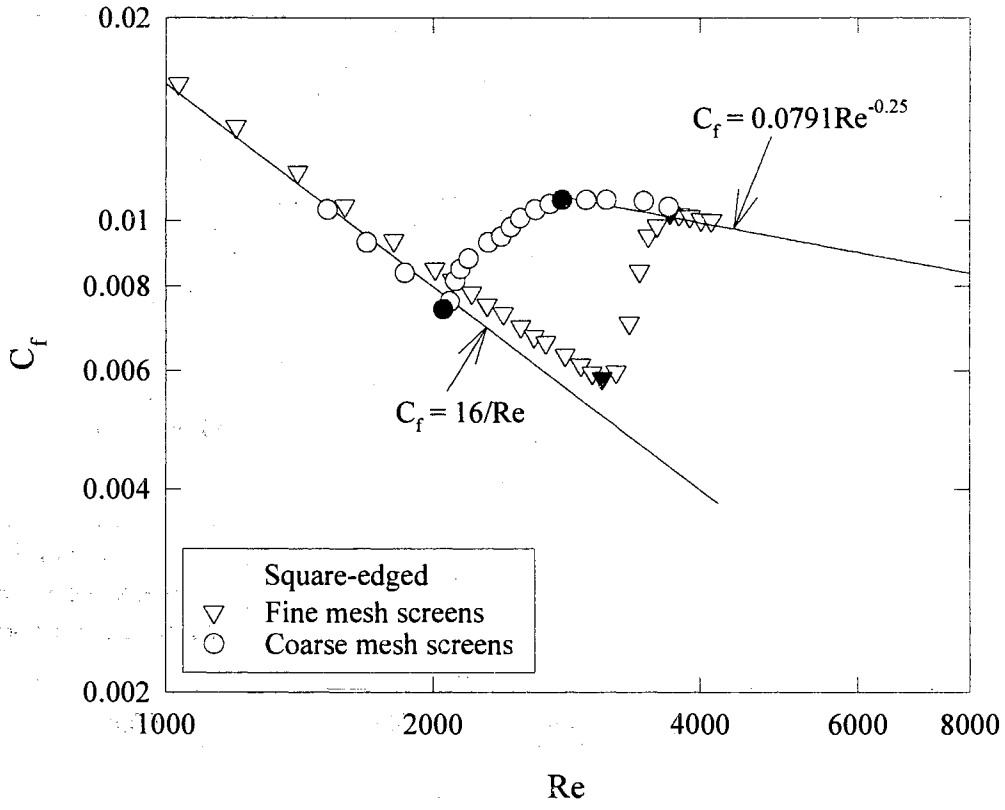

Figure 4.2 Effect of Screen Size on Fully Developed Skin Friction Coefficients for a Square-edged Inlet. (The solid symbols indicate the start and end of the transition region.)

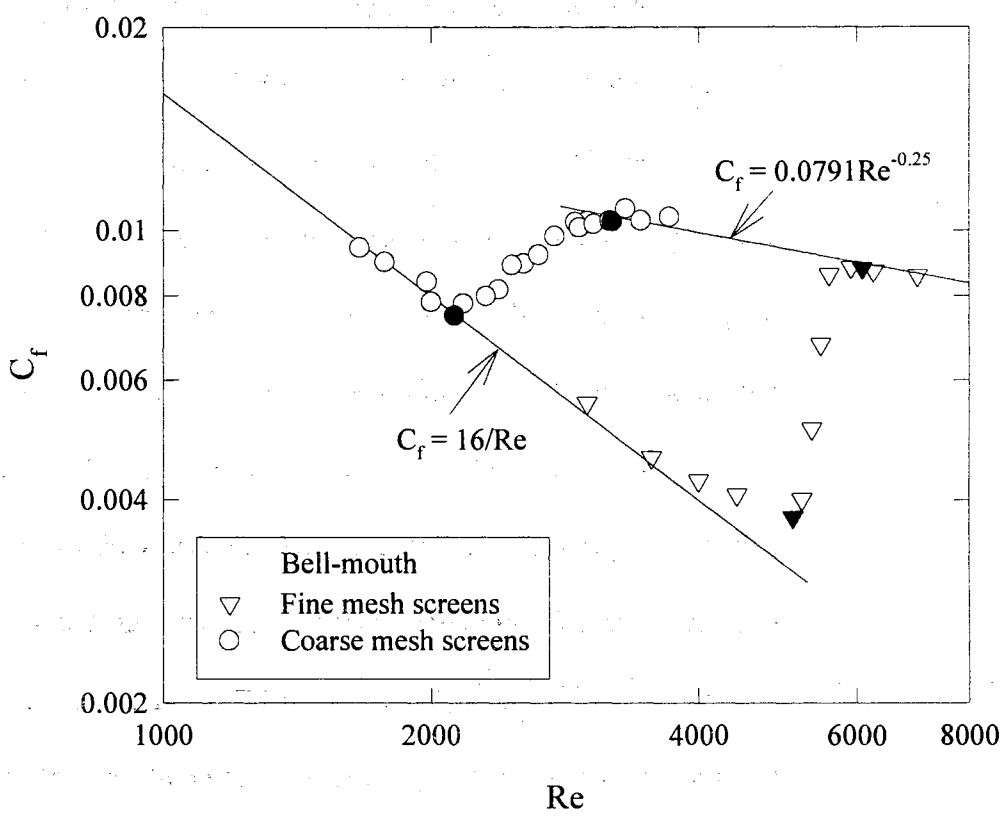

Figure 4.3 Effect of Screen Size on Fully Developed Skin Friction Coefficients for a Bell-mouth Inlet. (The solid symbols indicate the start and end of the transition region.)

Chapter II. From Figures 4.1 to 4.3, it is obvious that the pressure drop data behave differently in the laminar and transition regions. For the reentrant, square-edged, and bell-mouth inlets, the data taken with coarse screens followed the Poiseuille's equation in the laminar region very closely, then it went into the transition region. The transition Reynolds number range for the pressure drop data with coarse screens was determined to be about 1900-3000 for the reentrant inlet, 2000-3100 for the square-edged inlet, and 2200-3300 for the bell-mouth inlet. The Reynolds number for the start of the transition region is defined as the Reynolds number corresponding to the first abrupt change in the skin friction factor, and the Reynolds number for the end of the transition region corresponds to the Reynolds number of the skin friction coefficient that first reaches the Blasius fully developed turbulent skin friction coefficient line. The solid symbols in the figures indicate the start and end of the transition region. In the turbulent region, the data follow the Blasius' fully developed turbulent skin friction equation. The pressure drop data with fine mesh screens initially follow the Poiseuille's equation, however the data gradually tapers away from the laminar line before increasing sharply and going into the transition region at a much higher Reynolds number than the coarse mesh data. The transition Reynolds number range for the pressure drop data with the fine mesh screens is about 2870-3500 for the reentrant inlet, 3110-3700 for the square-edged inlet, and 5100-6100 for the bell-mouth inlet. In the turbulent region, the data for the fine mesh screens behave the same way as those for the coarse mesh screens.

From the results presented in Figures 4.1 to 4.3, it is obvious that for the same kind of inlet configuration, the transition Reynolds number range was influenced by the type of calming section. In terms of disturbance level, for the same kind of inlet, the type of

calming section using coarse mesh screens (open area ratio = 0.825) disturbs the flow more in comparison to the calming section using fine mesh screens (open area ratio = 0.65). The calming section with fine mesh screens better prepares the flow entering the test section in comparison to the flow with coarse mesh screens, because the size of the screen determines the amount of turbulence reduction, thereby delaying the transition. Therefore, we can conclude that the transition Reynolds number range can be manipulated by using different screen sizes.

As mentioned earlier, in the laminar region the data obtained by using coarse mesh screens follow the Poiseuille's equation well. However, the data obtained by using fine mesh screens gradually tapered away from the laminar line with an increase in the Reynolds number. Similar results have been obtained by Ogawa et. al. (1987) for air flow. In their results, the same tapering up behavior in the laminar region was experimentally observed when a highly undisturbed calming section was used. They stated that the flow is not fully developed when the skin friction coefficient starts tapering away from the laminar line. As we know, the entry length for tube flow in the laminar region is directly proportional to the Reynolds number. An approximation for the length of tube necessary for the development of the laminar velocity profile is

$$\frac{x}{D} = \frac{Re}{a} \tag{4.1}$$

where a is somewhere between 10 to 20. As Reynolds number increases, the entrance length increases. In the case when the skin friction coefficient gradually tapers away from the laminar line, the flow may not be fully developed. Since the investigation of skin

friction coefficient with heat is the main subject of this study, further investigation into this matter for isothermal flow was beyond the scope of this study.

4.2 Effect of Inlet Configuration on the Transition Region

In the previous section, the effect of the calming section has been discussed. In this section, the role of the inlet configuration will be investigated. The effect of inlet configuration was observed by using the same calming section (fine mesh screens) but different inlet configurations, namely, the reentrant, the square-edged, and the bell-mouth inlets. In order to isolate the effect of inlet configuration on the transition region, only the isothermal skin friction coefficient data were used.

A plot of isothermal skin friction coefficient versus Reynolds number for the three inlets is presented as Figure 4.4. In this figure, only the data far downstream from the entrance is used in order to avoid any entrance effects. Measurements in the entrance region for different flow regimes were beyond the scope of this study. The filled symbols represent the start and end of the fully developed transition region for the different inlet configurations. The Reynolds number for the start of the transition region is defined as the Reynolds number corresponding to the first abrupt change in the skin friction factor, and the Reynolds number for the end of the transition region corresponds to the Reynolds number of the skin friction coefficient that first reaches the Blasius fully developed turbulent skin friction coefficient line. From this figure the limits for the transition Reynolds number for these three inlet configurations can be summarized as:

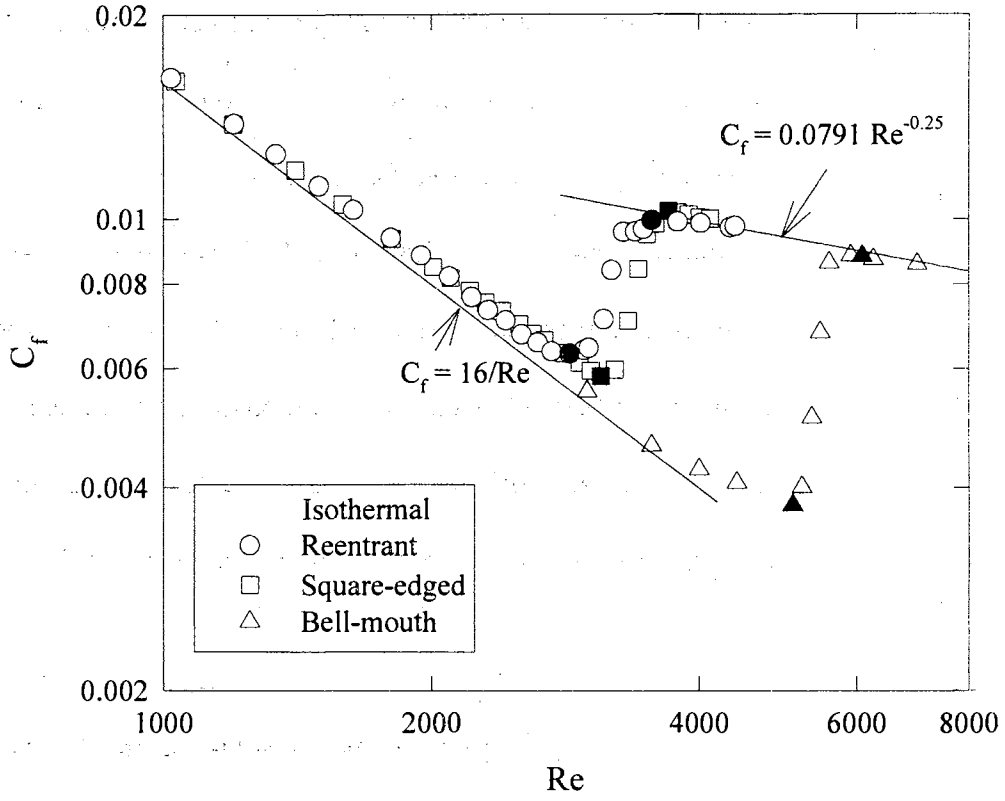

Figure 4.4 Influence of Different Inlets on Fully Developed Skin Friction Coefficients.
(The solid symbols indicate the start and end
of the transition region.)

Inlet Type	Transition Reynolds Numbers
Reentrant	$2870 < Re < 3500$
Square-edged	$3110 < Re < 3700$
Bell-mouth	$5100 < Re < 6100$

Since the calming section is a common factor for all three inlets, the difference between the transition Reynolds number ranges is only due to the effect of different inlet configurations. The above limits for the skin friction coefficient transition Reynolds numbers indicate that the inlet that caused the most disturbance (reentrant) produced an early transition (Re=2870), and the inlet with the least disturbance (bell-mouth) did not go into transition below a Reynolds number of about 5100. The square-edged inlet, which causes less disturbance than the reentrant inlet but more than the bell-mouth inlet, produced a transition Reynolds number of about 3110. From this observation, it is obvious that the transition Reynolds number can be manipulated by using different inlet configurations.

4.3 Effect of Heating on the Transition Region

Most of the flow pressure drop (skin friction coefficient) analyses have been carried out under the assumption that the fluid properties do not vary with temperature throughout the flow field (isothermal flow condition). However, in practical situations, this assumption is obviously an idealization, since the transport properties of most fluids vary with temperature and thus vary through the boundary layer or over the flow cross section of a tube.

Three different heating rates (3, 8, and 16 kW/m^2) were used to investigate the effect of heating on the fully developed skin friction coefficient. A DC welder was used

to approximate the uniform wall heat flux condition. The results presented in Figs. 4.5, 4.6, and 4.7 clearly establish the influence of heating rate on the laminar, transition, and turbulent regions. From the figures, it can be seen that the data for 3, 8, and 16 kW/m^2 in the laminar and transition flow regimes follow an almost parallel shift from the isothermal values. In these regions, heating seems to increase the value of skin friction coefficient for a fixed Reynolds number. The increase is very significant in the transition region. In the turbulent region, it seems that heating did not affect the magnitude of the skin friction coefficient. The significant influence of heating on the values of skin friction coefficient in the laminar and transition regions is directly due to the effect of secondary flow. Application of heat to the tube wall produces a temperature difference in the fluid. The fluid near the tube wall has a higher temperature and lower density than the fluid close to the centerline of the tube. This temperature difference may produce a secondary flow due to free convection. When mixed convection takes place, the velocity profile of the flow changes. In this case, it changes the shear stress and the fluid density of the flow, hence the skin friction coefficient is changed. As the heat flux increases, the shear stress due to the change of the velocity profile increases, density becomes smaller hence the skin friction coefficient increases.

To further illustrate the effect of secondary flow, Figures 4.8, 4.9, and 4.10 plot the heat transfer coefficient in terms of Colburn-j factor versus Reynolds number in the laminar flow region for the reentrant, square-edged, and bell-mouth inlets under different heating rates. These heat transfer coefficients were measured simultaneously with the skin friction coefficients at the same location in the pressure drop test section. For comparison purposes, these figures also show the typical fully developed pipe flow

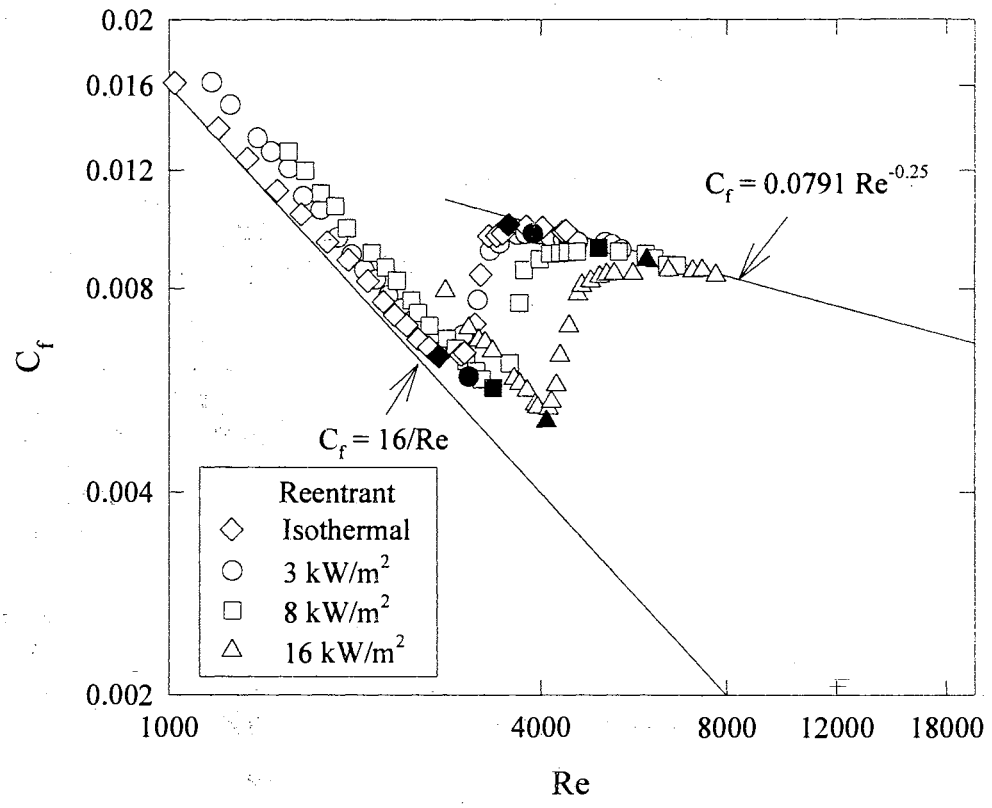

Figure 4.5 Effect of Heating on Fully Developed Skin Friction Coefficients for a Reentrant Inlet. (The solid symbols indicate the start and end of the transition region.)

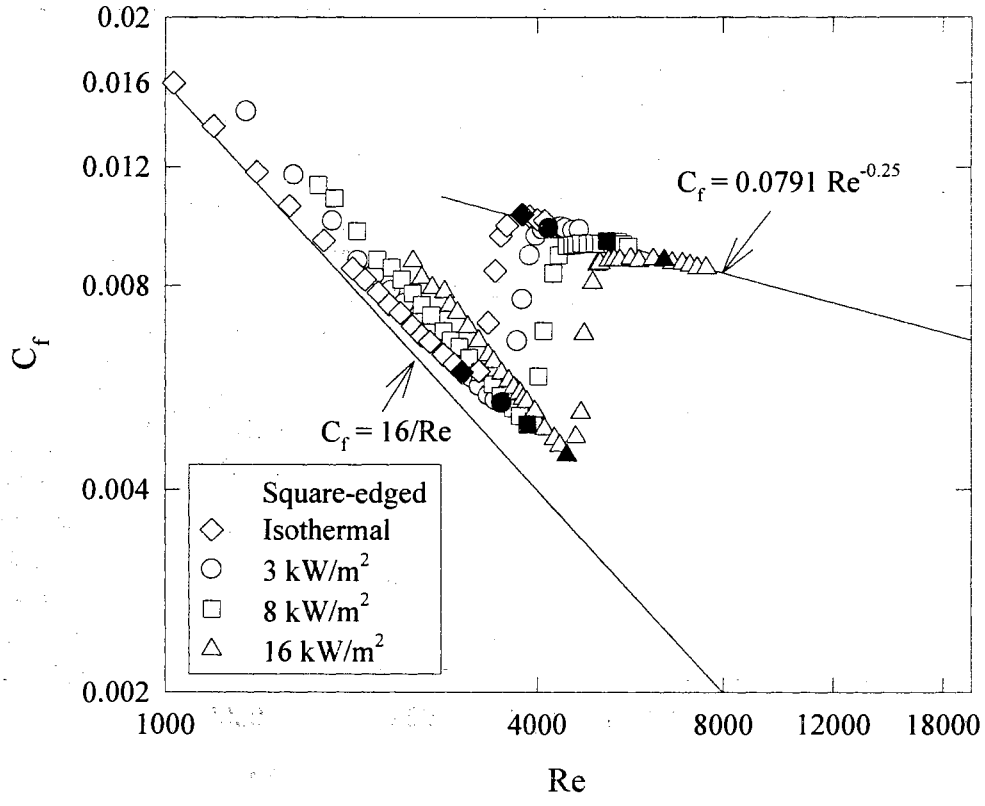

Figure 4.6 Effect of Heating on Fully Developed Skin Friction Coefficients for a Square-edged Inlet. (The solid symbols indicate the start and end of the transition region.)

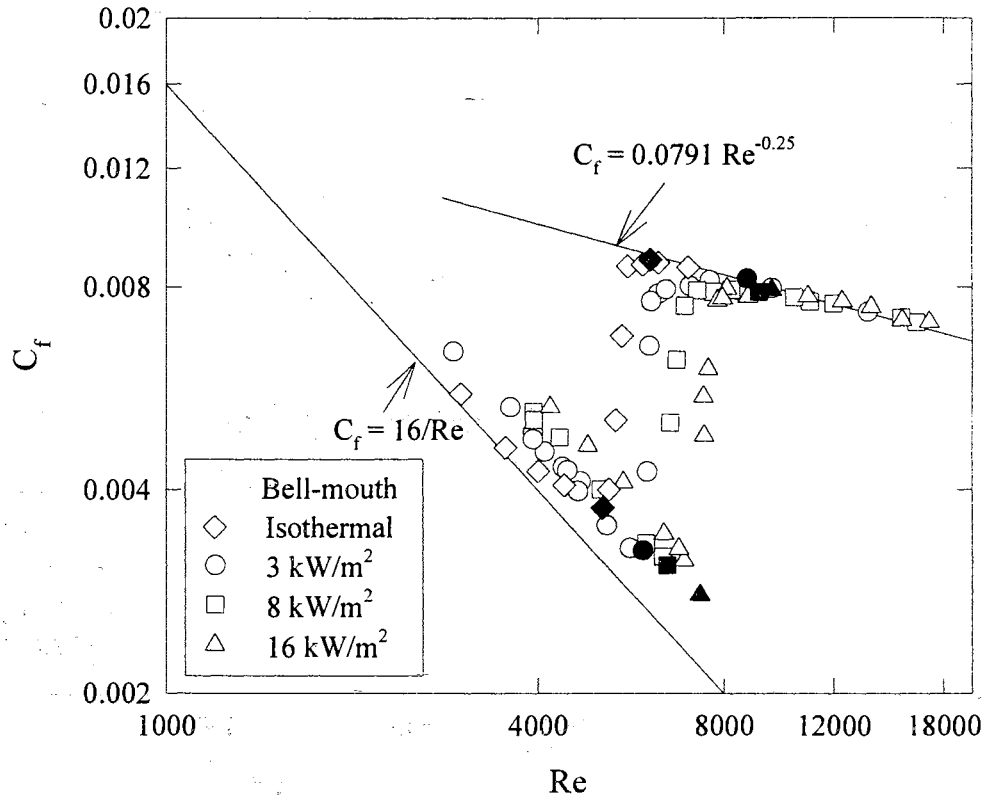

Figure 4.7 Effect of Heating on Fully Developed Skin Friction Coefficients for a Bell-mouth Inlet. (The solid symbols indicate the start and end of the transition region.)

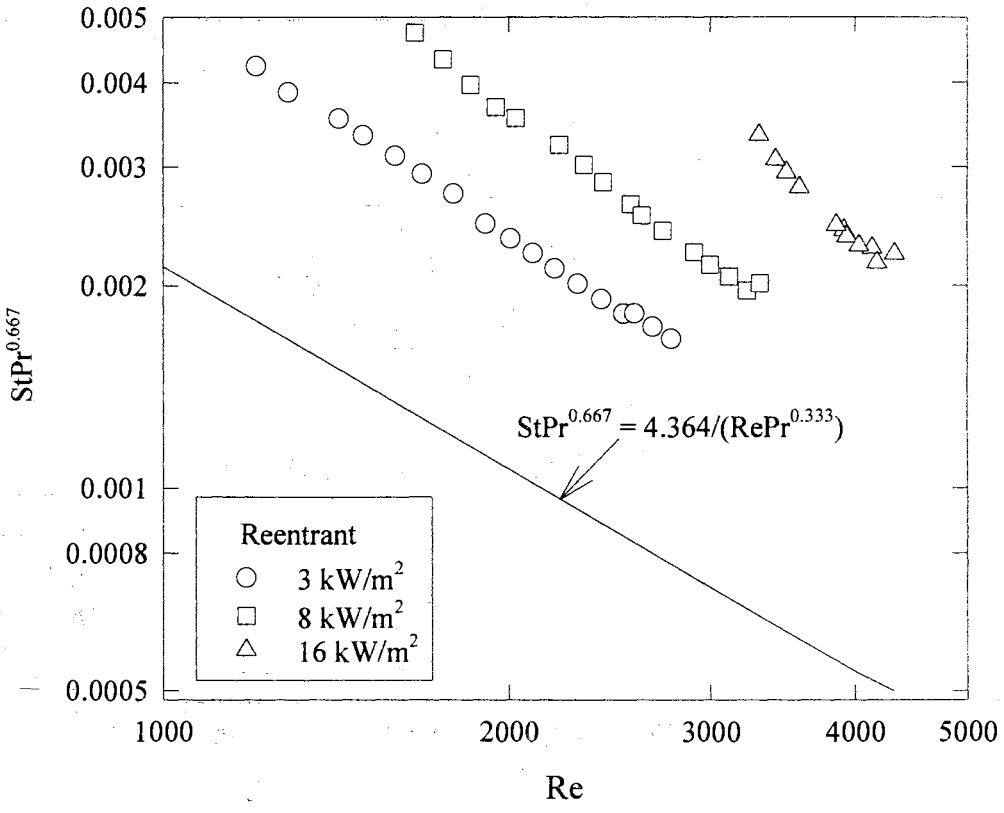

Figure 4.8 Effect of Heating on Laminar Heat Transfer Coefficients for a Reentrant Inlet.

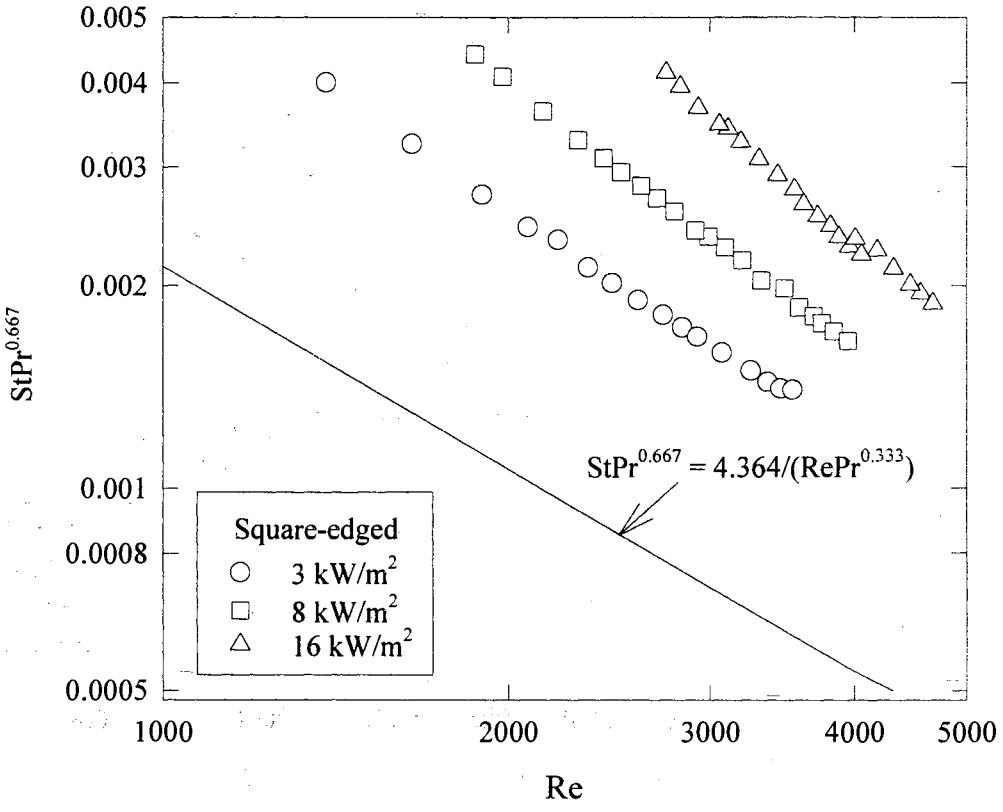

Figure 4.9 Effect of Heating on Laminar Heat Transfer Coefficients for a Square-edged Inlet.

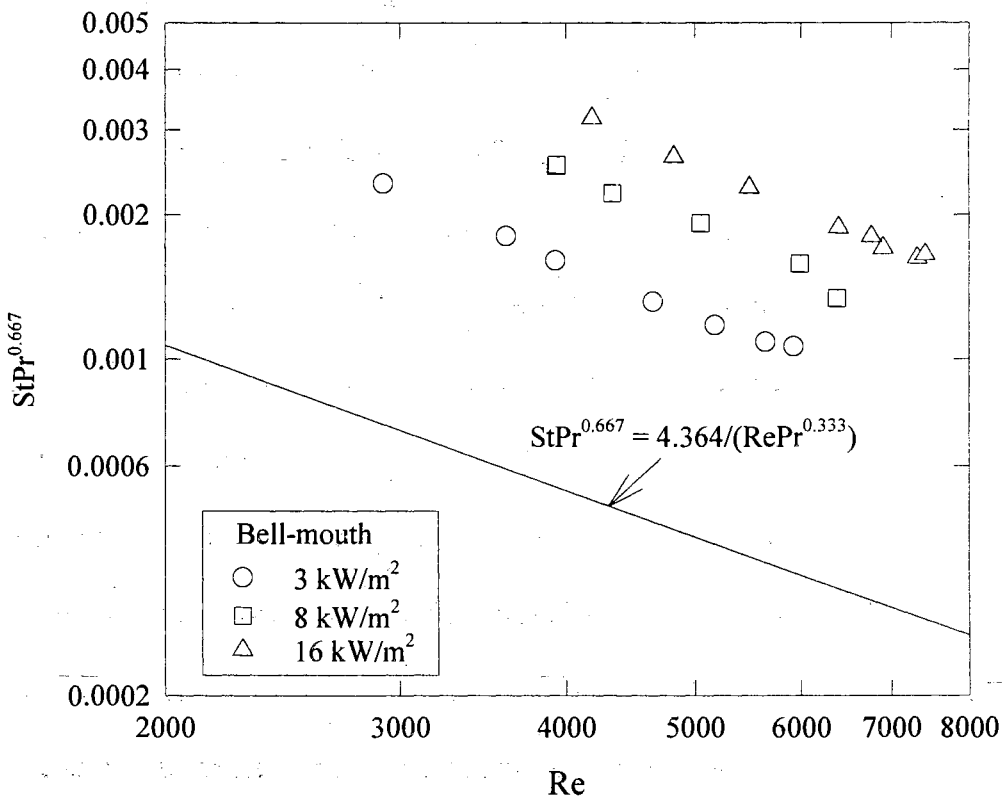

Figure 4.10 Effect of Heating on Laminar Heat Transfer Coefficients for a Bell-mouth Inlet.

forced convection heat transfer correlation for laminar flow (Nu=4.364) under the uniform wall heat flux boundary condition. From the figures, similar to the behavior of skin friction coefficient in the laminar flow region (see Figs. 4.5 to 4.7), it can be seen that the data for 3, 8, and 16 kW/m^2 in this flow region follow an almost parallel shift above the accepted laminar heat transfer line. This enhancement is directly due to the strong influence of buoyancy forces (free convection) on forced convection (mixed convection), giving rise to mixed convection heat transfer (refer to Chapter III).

In the transition region, unlike the laminar region (Nusselt number is constant), no such comparisons can be made. In order to show the effect of secondary flow in the laminar and transition regions, the ratio of local peripheral heat transfer coefficients at the top and bottom of the tube is used. Referring to the discussion in Chapter III, the flow should be considered as mixed convection when the heat transfer coefficient ratio is much less than unity. Figures 4.11 to 4.16 show this heat transfer coefficient ratio versus Reynolds number for the laminar and transition flow regions. In the laminar flow region (see Figs. 4.11 to 4.13), it can be seen that for the same Reynolds number, as heating rate increases, the ratio of the local heat transfer coefficient at the top and bottom of the tube decreases. This means that the effect of secondary flow increases as heating rate increases. In the transition flow region (see Figs. 4.14 to 4.16), it can be seen that in all cases, the flow is influenced by secondary flow in the lower transition region (h_t/h_b much less than unity). As Reynolds number increases, the heat transfer coefficient ratio increases and approaches unity in the upper transition region. In the turbulent region, the secondary flow effect is suppressed by the turbulent motion, hence no shift was observed in this region. The transition Reynolds number ranges for the three different inlets with

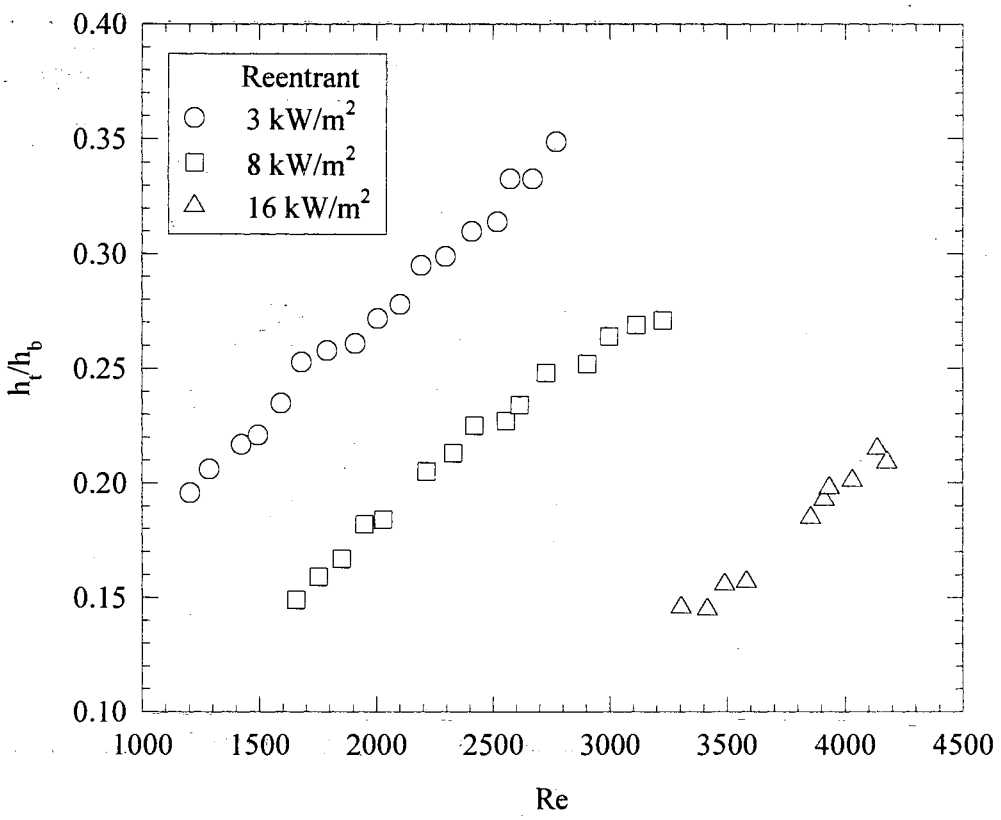

Figure 4.11 Effect of Secondary Flow in the Laminar Region for a Reentrant Inlet.

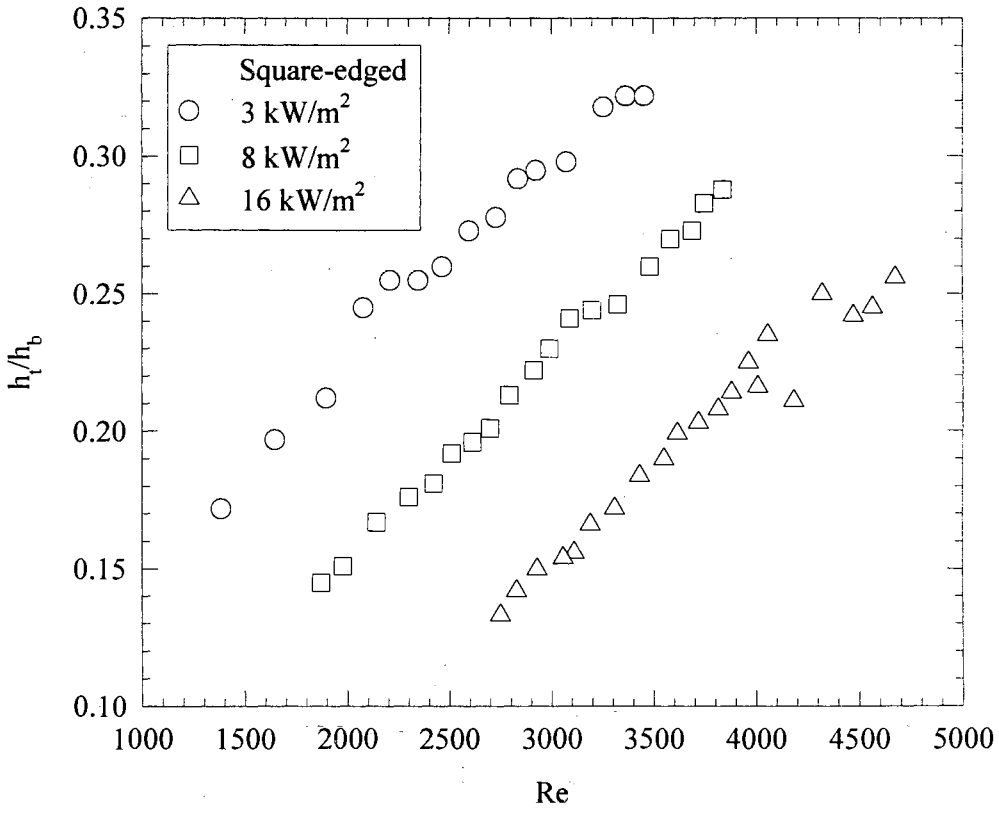

Figure 4.12 Effect of Secondary Flow in the Laminar Region for a Square-edged Inlet.

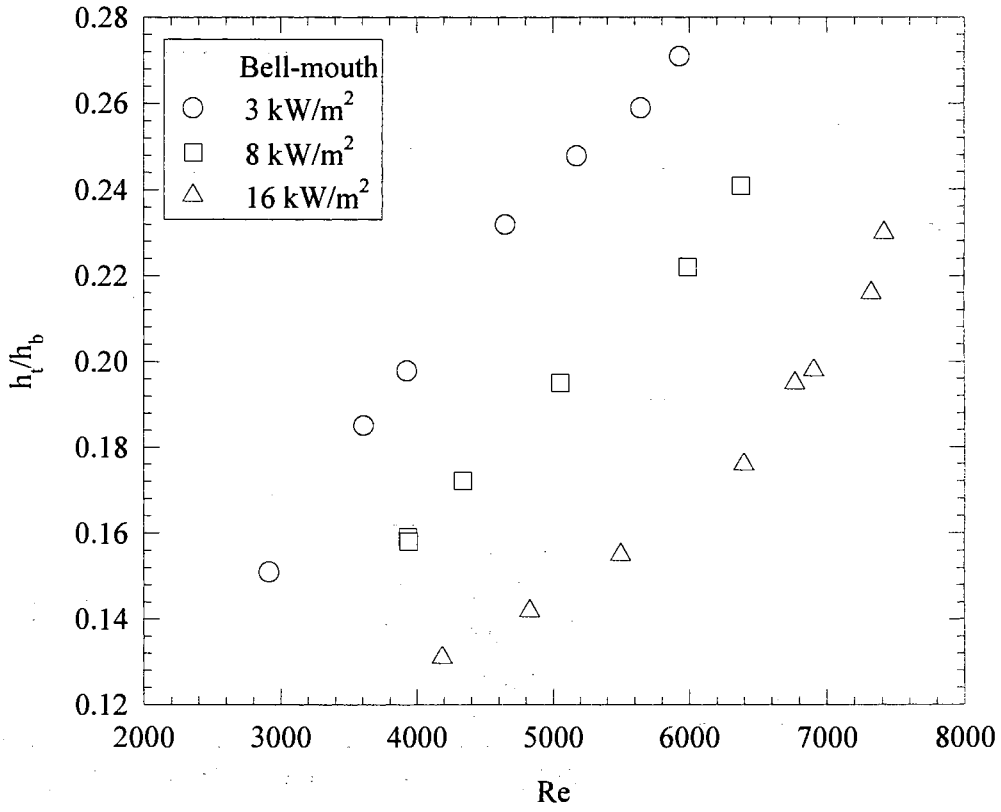

Figure 4.13 Effect of Secondary Flow in the Laminar Region for a Bell-mouth Inlet.

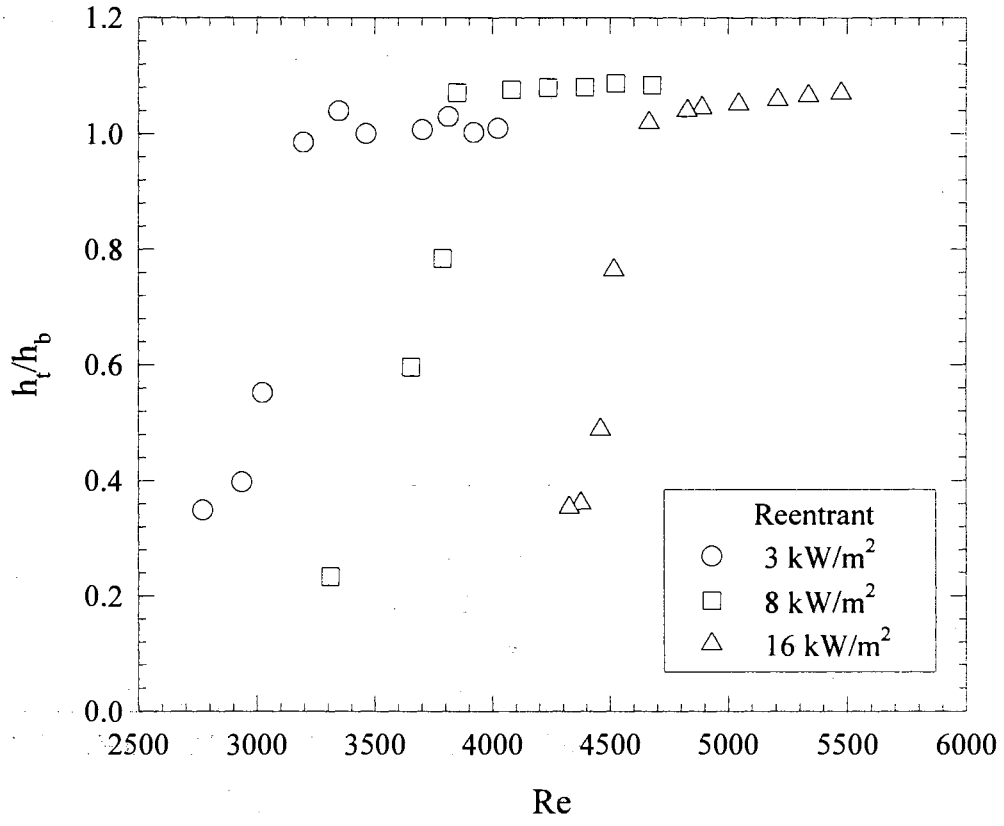

Figure 4.14 Effect of Secondary Flow in the Transition Region for a Reentrant Inlet.

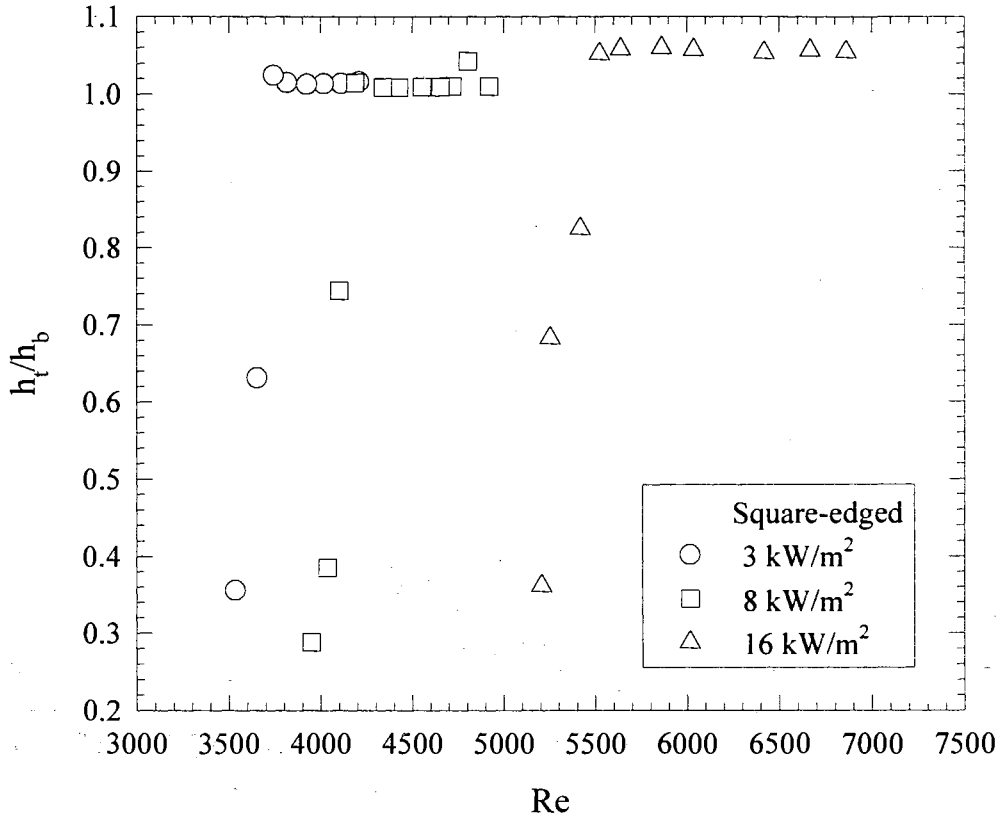

Figure 4.15 Effect of Secondary Flow in the Transition Region for a Square-edged Inlet.

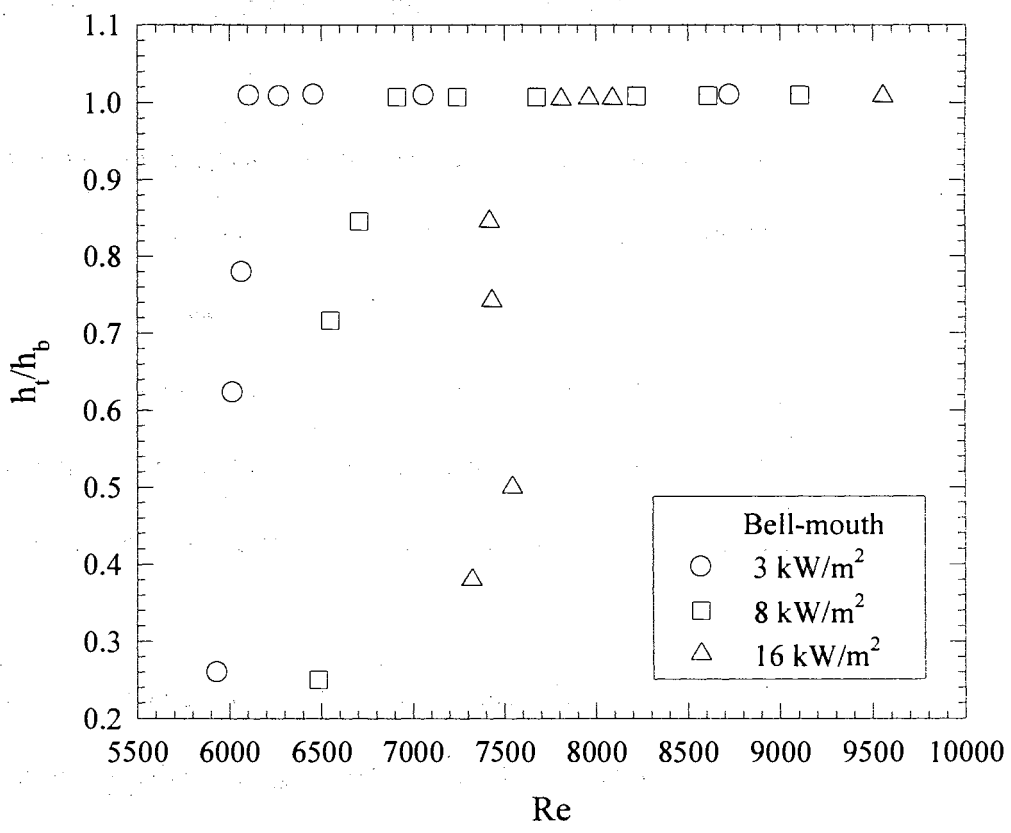

Figure 4.16 Effect of Secondary Flow in the Transition Region for a Bell-mouth Inlet.

three different heating rates used in this study can be summarized as:

Transition Reynolds Numbers

Heat flux	Reentrant	Square-edged	Bell-mouth
3 kW/m^2	3060< Re < 3890	3500 < Re < 4180	5930 < Re < 8730
8 kW/m^2	3350 < Re < 4960	3860 < Re < 5200	6480 < Re < 9110
16 kW/m^2	4090 < Re < 5940	4450 < Re < 6430	7320 < Re < 9560

The above limits for the fully develop skin friction coefficient transition Reynolds numbers indicate that with an increase in the input heat flux, the upper and lower limits of the transition Reynolds number both increase.

Referring to Figs. 4.5 to 4.7, it can be noticed that the effect of heating is to delay the flow transition. The transition Reynolds number increases as the heating rate increases. So, addition of heat in fact stabilizes the flow, hence the flow went into transition later.

Figures 4.17, 4.18, and 4.19 show how the skin friction coefficient changes under the same heating rate for different inlet configurations. From the figures, when the heating rate was the same, the most disturbed inlet (reentrant) still produced an early transition. The disturbance level of the square-edged inlet is greater than the bell-mouth and is less than the reentrant inlet went into transition later than the reentrant. The bell-mouth inlet which is the most undisturbed inlet, went into the transition last. This behavior is identical to the observations made for the isothermal skin friction coefficient (refer to Fig. 4.4).

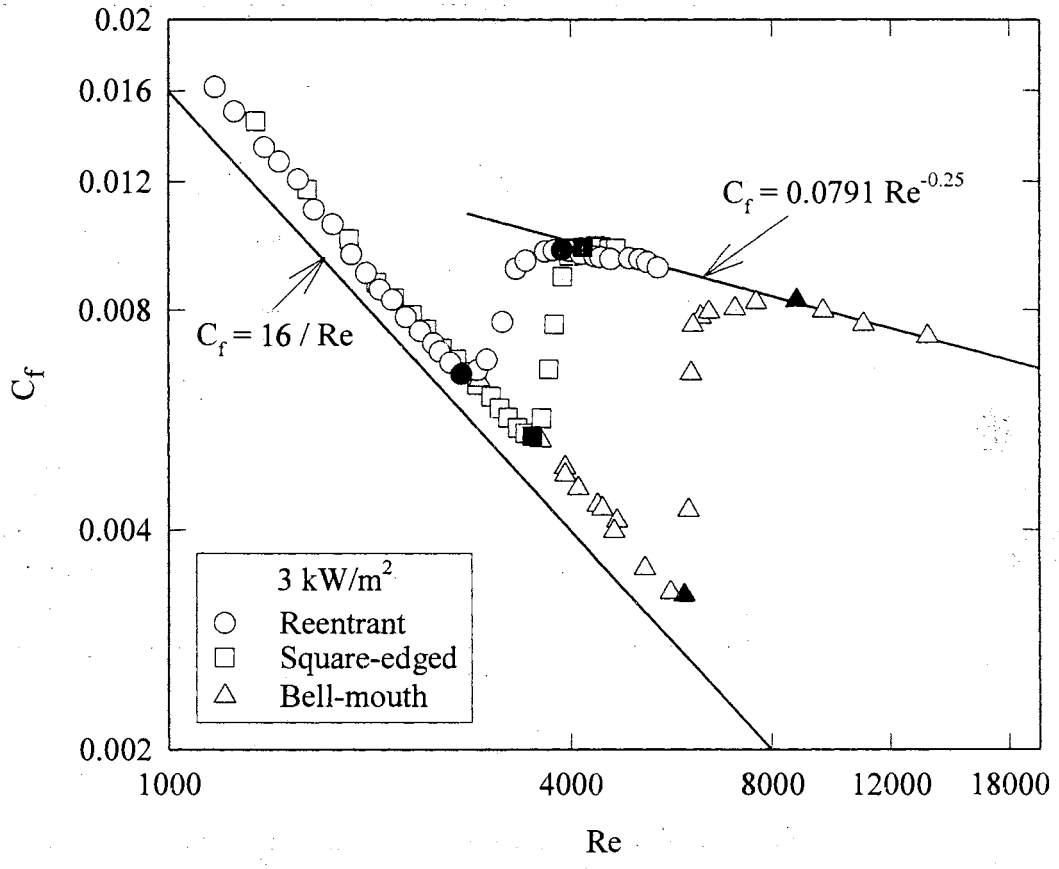

Figure 4.17 Fully Developed Skin Friction Coefficients for Three Different Inlets Under the Same Heating Rate (3 kW/m^2). (The solid symbols indicate the start and end of the transition region.)

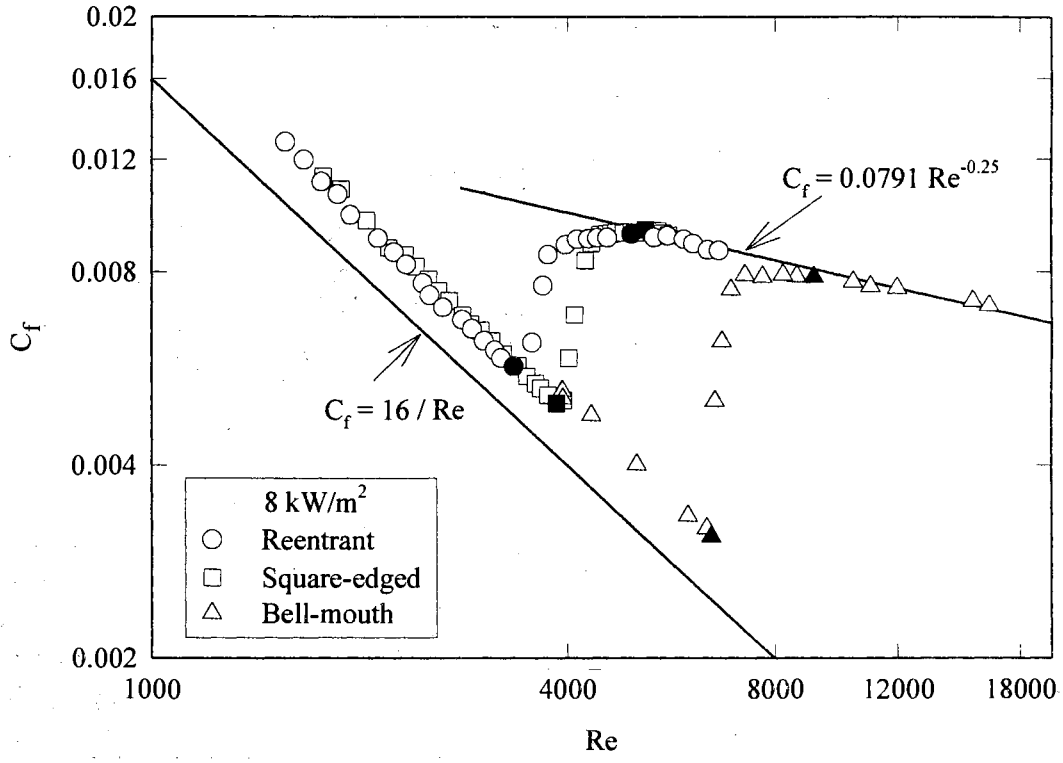

Figure 4.18 Fully Developed Skin Friction Coefficients for Three Different Inlets Under the Same Heating Rate (8 kW/m^2). (The solid symbols indicate the start and end of the transition region.)

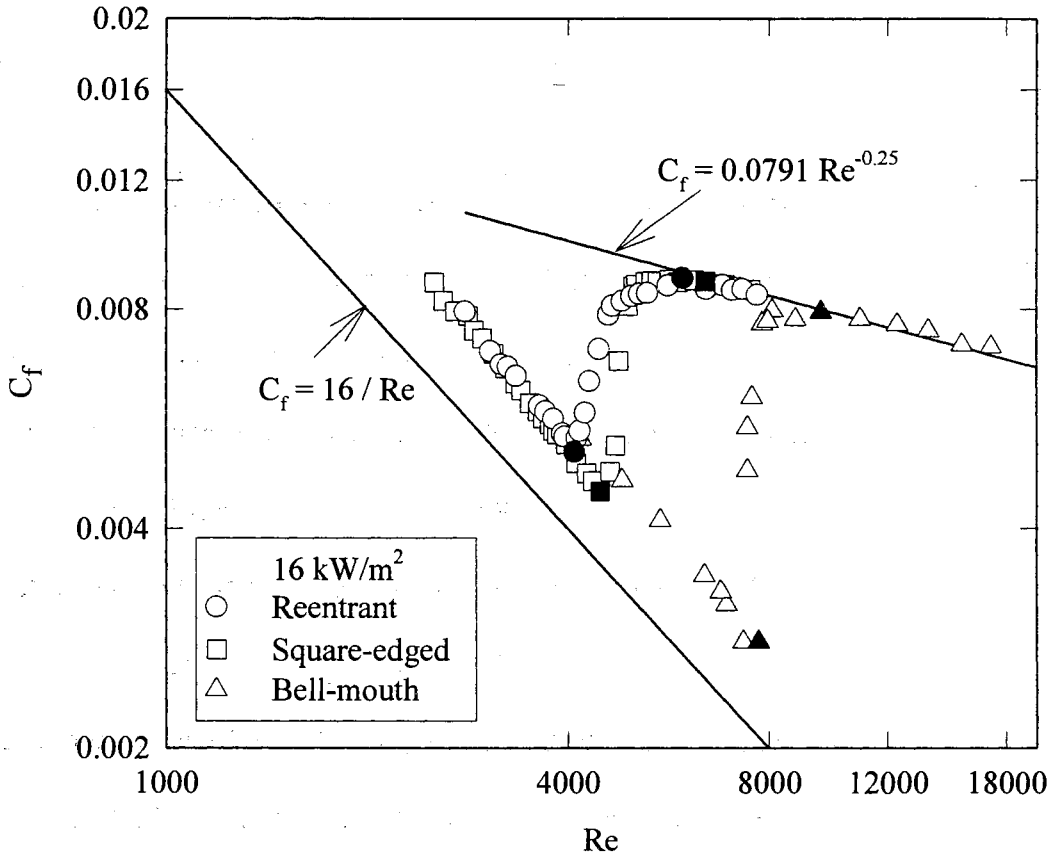

Figure 4.19 Fully Developed Skin Friction Coefficients for Three Different Inlets Under the Same Heating Rate (16 kW/m^2). (The solid symbols indicate the start and end of the transition region.)

4.4 Comparison of the Available Correlations with Experiments

The experimentally obtained non-isothermal laminar fully developed skin friction coefficients were compared with the correlation proposed by Test (1968). His correlation is of the form

$$C_f = \frac{16}{Re}\frac{1}{0.89}\left[\frac{\mu_b}{\mu_w}\right]^m, \text{ where } m=0.2 \qquad (4.2)$$

Figures 4.20, 4.21 and 4.22 show this comparison using the reentrant, square-edged, and bell-mouth inlets respectively. It can be seen that for heating at 3 kW/m^2 the agreement between our experimental data and the results predicted by Test's correlation is considered good (the majority of the data were predicted within 10% with an average absolute deviation of 8.5%). However, for heating at 8 and 16 kW/m^2, Test's correlation under-predicted the non-isothermal fully developed skin friction coefficients with an average absolute deviation of about -18 to -27% respectively. The main reason for the under-predictions is the constant value of m (the correction factor) used in Test's correlation. As discussed previously, heating increases the fully developed skin friction coefficient, and the exponent "m" of the correction factor to the isothermal equation is a strong function of the heating rate. Referring to Figs. 4.5 to 4.7, heating seems to increase the value of skin friction coefficient for a fixed Reynolds number. At low heating rates (3 kW/m^2), the secondary flow effects are not as strong in comparison with the high heating rate (8 and 16 kW/m^2), hence, Test's correlation does a good job. However, with an increase in the heating rate, the secondary flow effects get stronger and the exponent "m" is no longer a constant. In Test's correlation, the value of "m" in the correction factor

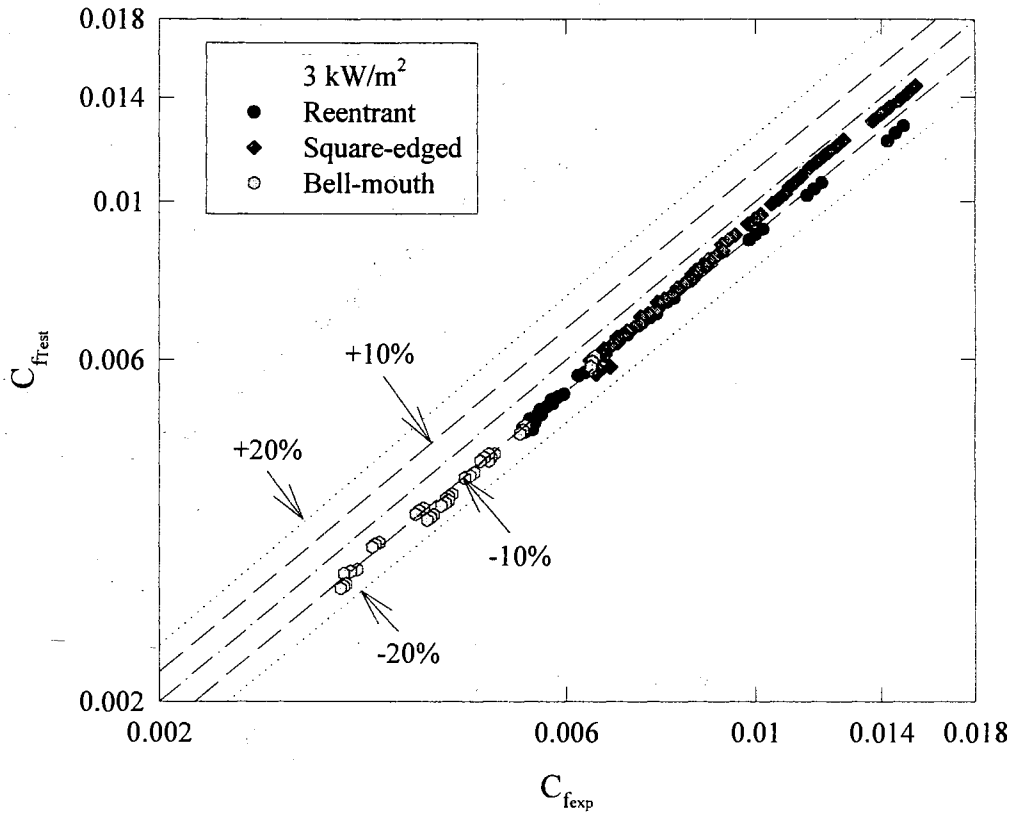

Figure 4.20 Comparison Between Experimental Fully Developed Skin Friction Coefficients at 3 kW/m^2 Heating and Laminar Correlation of Test (1968).

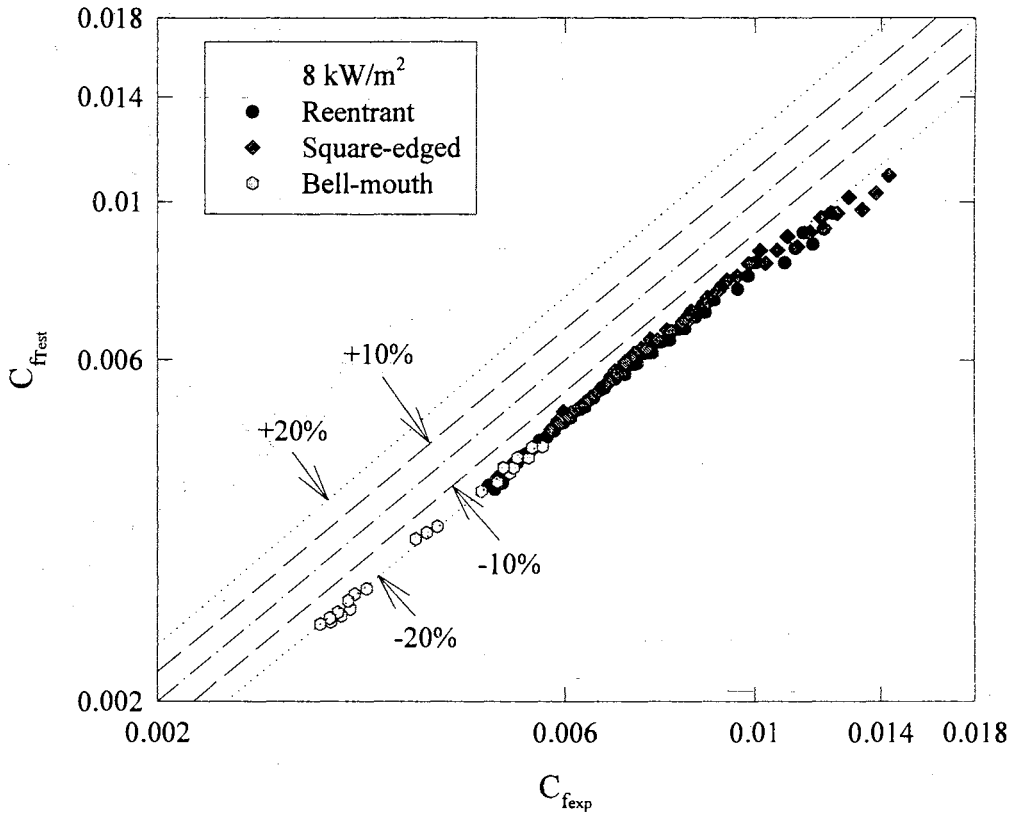

Figure 4.21 Comparison Between Experimental Fully Developed Skin Friction Coefficients at 8 kW/m^2 Heating and Laminar Correlation of Test (1968).

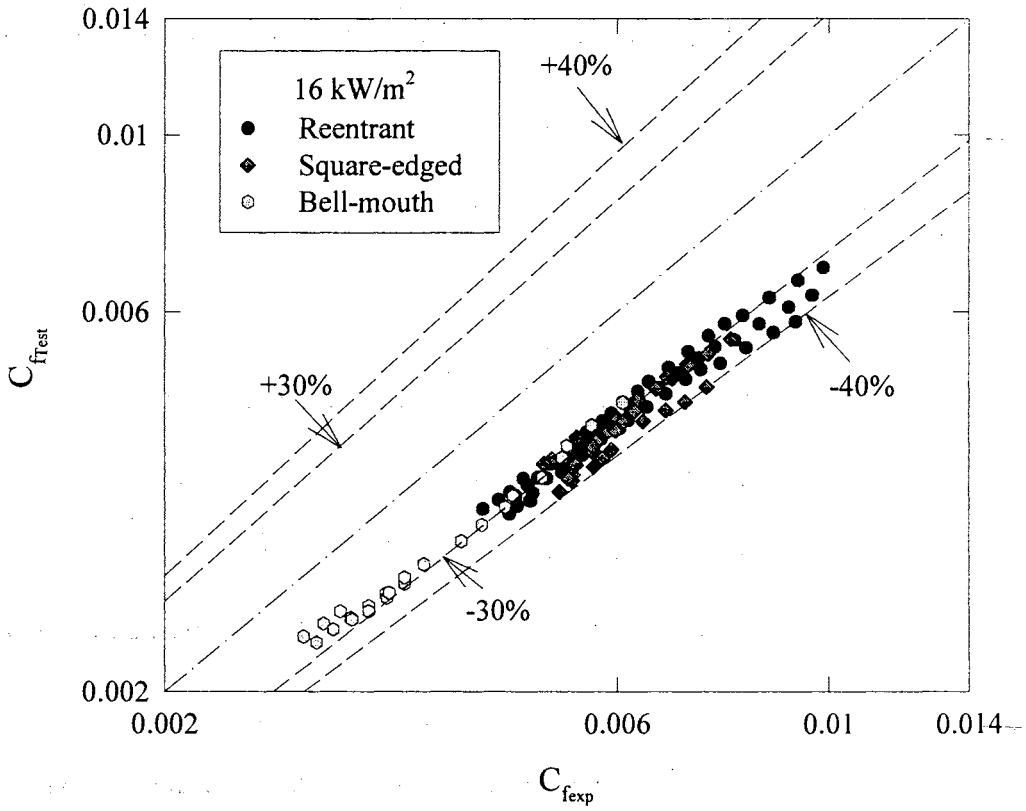

Figure 4.22 Comparison Between Experimental Fully Developed Skin Friction Coefficients at 16 kW/m^2 Heating and Laminar Correlation of Test (1968).

$1/0.89(\mu_b/\mu_w)^m$ always introduces a correction value close to unity which is not appropriate with high heating. Therefore, Test's correlation does not perform well when strong secondary flow (high heating rate) is involved.

The correlation proposed by Deissler (1951) was also used to compare with the laminar non-isothermal fully developed skin friction coefficient experimental data. Deissler's correlation is of the form

$$C_f = \frac{16}{Re}\left[\frac{\mu_b}{\mu_w}\right]^m \text{, where m=-0.58} \qquad (4.3)$$

Figures 4.23 to 4.25 show this comparison. From the figures, Deissler's correlation under predicted the experimental data for 3, 8, and 16 kW/m^2 with an average absolute deviation of about -29% , -42%, and -49%, respectively. The deviation increases as the heating rate increases. The main reason again is the constant value of m used in the correction factor.

The experimentally obtained non-isothermal turbulent fully developed skin friction coefficients for the reentrant, square-edged, and bell-mouth inlets were compared with the correlation proposed by Allen and Eckert (1964). Their correlation is of the form

$$C_f = 0.0791\,Re^{-0.25}\left[\frac{\mu_b}{\mu_w}\right]^m \text{, where m=-0.25} \qquad (4.4)$$

Figure 4.26 shows this comparison. For all heating rates, Allen and Eckert's correlation did a very good job. The majority of the data (84%) were predicted within 6% with a maximum deviation of 7.8%. However, in all the turbulent experimental runs, the average

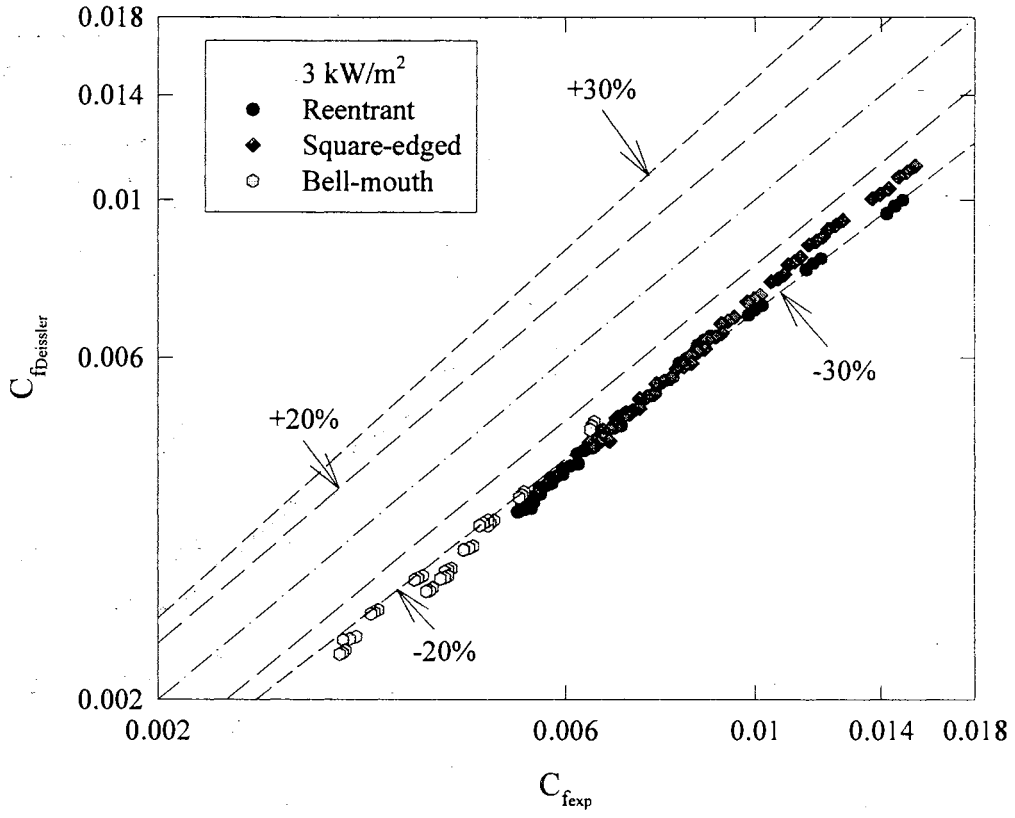

Figure 4.23 Comparison Between Experimental Fully Developed Skin Friction Coefficients at 3 kW/m^2 Heating and Laminar Correlation of Deissler (1951).

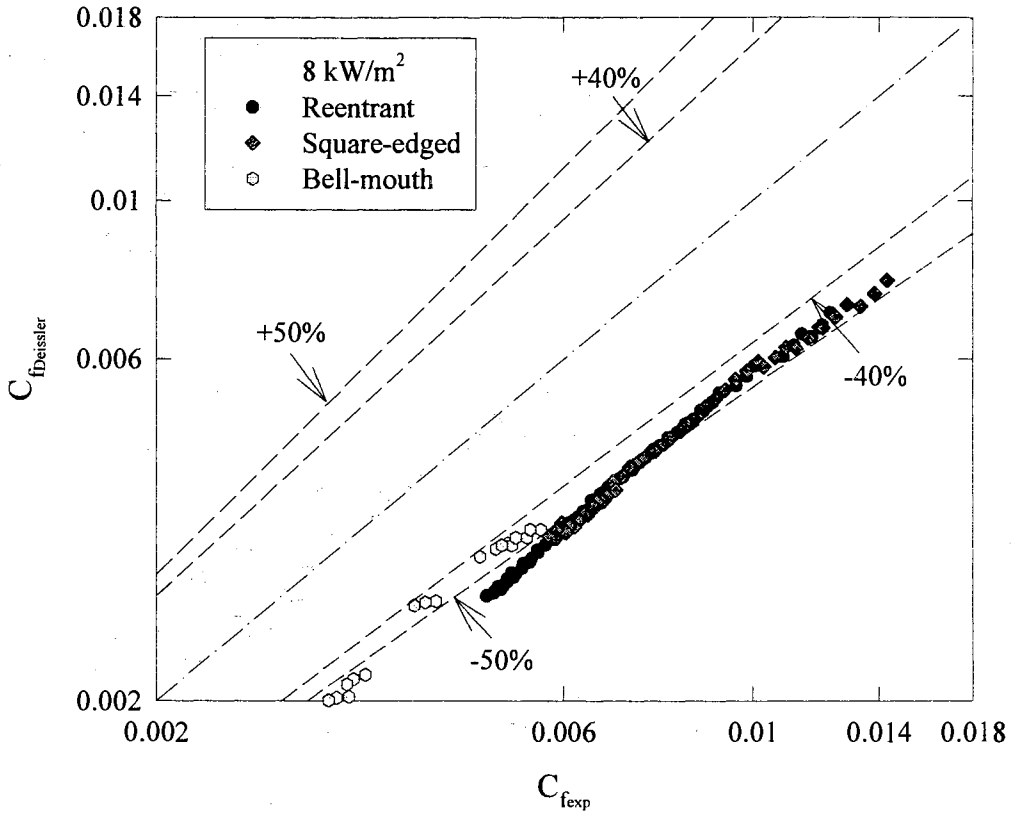

Figure 4.24 Comparison Between Experimental Fully Developed Skin Friction Coefficients at 8 kW/m^2 Heating and Laminar Correlation of Deissler (1951).

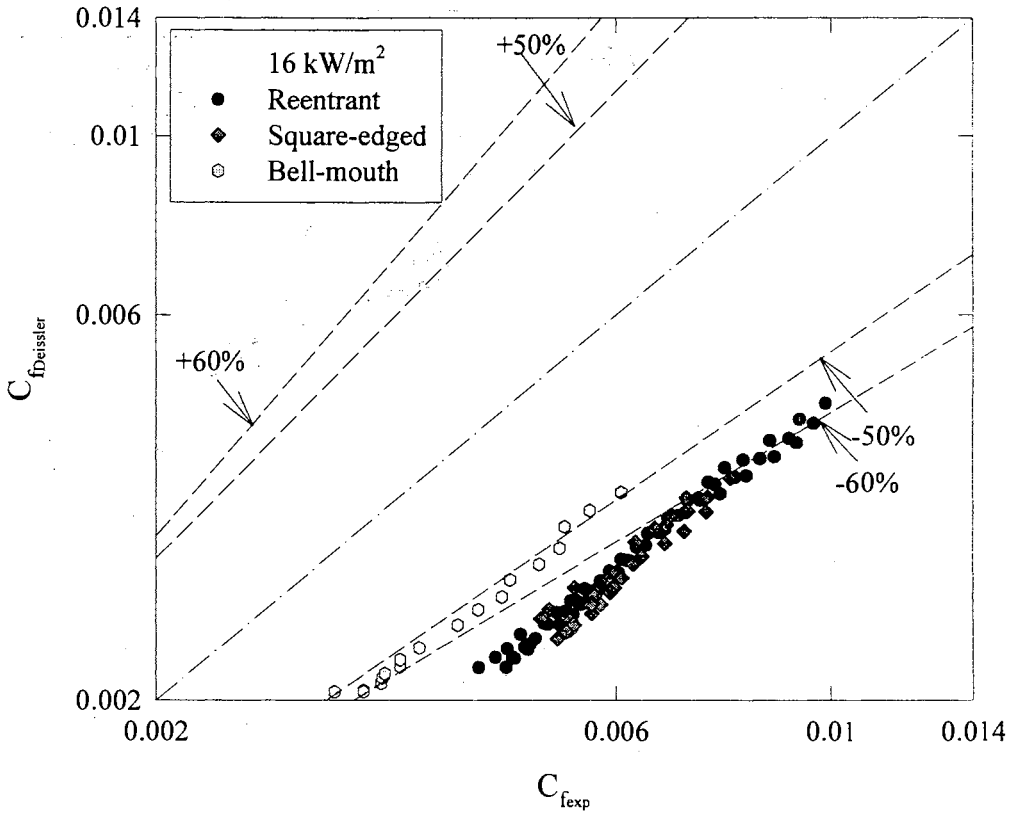

Figure 4.25 Comparison Between Experimental Fully Developed Skin Friction Coefficients at 16 kW/m^2 Heating and Laminar Correlation of Deissler (1951).

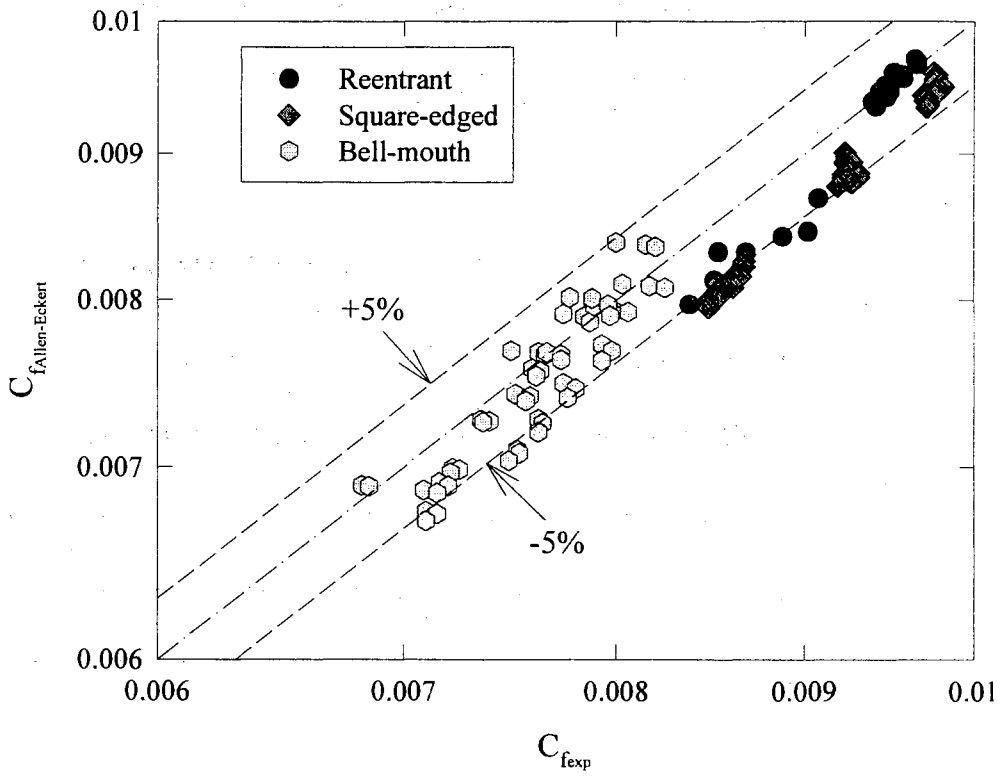

Figure 4.26 Comparison Between Experimental Fully Developed Skin Friction Coefficients and Turbulent Correlation of Allen and Eckert (1964).

of the ratio μ_b/μ_w was equal to 0.86. When the correction factor $(\mu_b/\mu_w)^{-0.25}$ is applied, this correction factor, in fact is extremely close to unity. Referring to section 4.3 where heating effect on fully developed skin friction coefficient was discussed, the turbulent fully developed skin friction coefficient for all three different inlets in all three different heating rates followed the Blasius' equation extremely well (within 5% deviation). This means that in the turbulent region, a correction factor to the established Blasius equation is not necessary.

4.5 New Correlation for the Laminar Skin Friction Coefficient with Heating

In the laminar region, as pointed out in reference to Figs. 4.8 to 4.10, there is an almost upward parallel shift from the isothermal values due to the secondary flow effect. Following the form of the classic relation $C_f = 16/Re$, a correction factor in terms of a viscosity ratio was applied to the laminar isothermal equation to account for the heating effect. The proposed correlation is of the form

$$C_f = \frac{16}{Re}\left[\frac{\mu_b}{\mu_w}\right]^m \tag{4.5}$$

where $m = 1.65 - 0.013Pr^{0.84}\,Gr^{0.17}$, $1100 < Re < 7400$, $6 < Pr < 36$

$17100 < Gr < 95600$, $1.25 < \mu_b/\mu_w < 2.40$

In the above equation, the Prandtl and Grashof numbers in the exponent "m" account for the effect of different heating rates on the fully developed laminar skin friction coefficient. For the lowest (3 kW/m^2) and the highest (16 kW/m^2) heating rates, the correction factor $(\mu_b/\mu_w)^m$ to the isothermal fully developed skin friction coefficient

varied from about 1.15 to 1.40, respectively. This is a 15 to 40% increase in the friction coefficient over the isothermal value due to different heating rates.

Equation (4.5) gives a representation of the experimental data to within +12.1 to -12.6%. In the development of the correlation, a total of 393 experimental data points were used. The absolute average deviation between the results predicted by the correlation and the experimental data is 3%. Eighty percent of the data were predicted with less than 5% deviation. Eighteen percent of the data were predicted within 10% deviation. The performance of the proposed correlation at different heating rates can be summarized as follows. For low heating rate (3 kW/m^2), the correlation predicts the data with an absolute average deviation of 2.1%. The maximum deviation in this heating rate is 8.2%. For moderate heating rate (8 kW/m^2), the correlation predicts the data with an absolute average deviation of 3.1%. The maximum deviation for this particular heating rate is 11.7%. For high heating rate (16 kW/m^2), the correlation predicts the data with an absolute average deviation of 3.7%. The maximum deviation corresponding to this heating rate is 12.6%. Figure 4.27 compares the predicted skin friction coefficients obtained from the proposed equation with measurements.

4.6 New Correlation for the Transition Skin Friction Coefficient with Heating

Since the type of inlet configuration influences the beginning and end of the transition region, a single correlation for this region cannot predict the data, and a correlation for each inlet was developed. The correlation is of the form

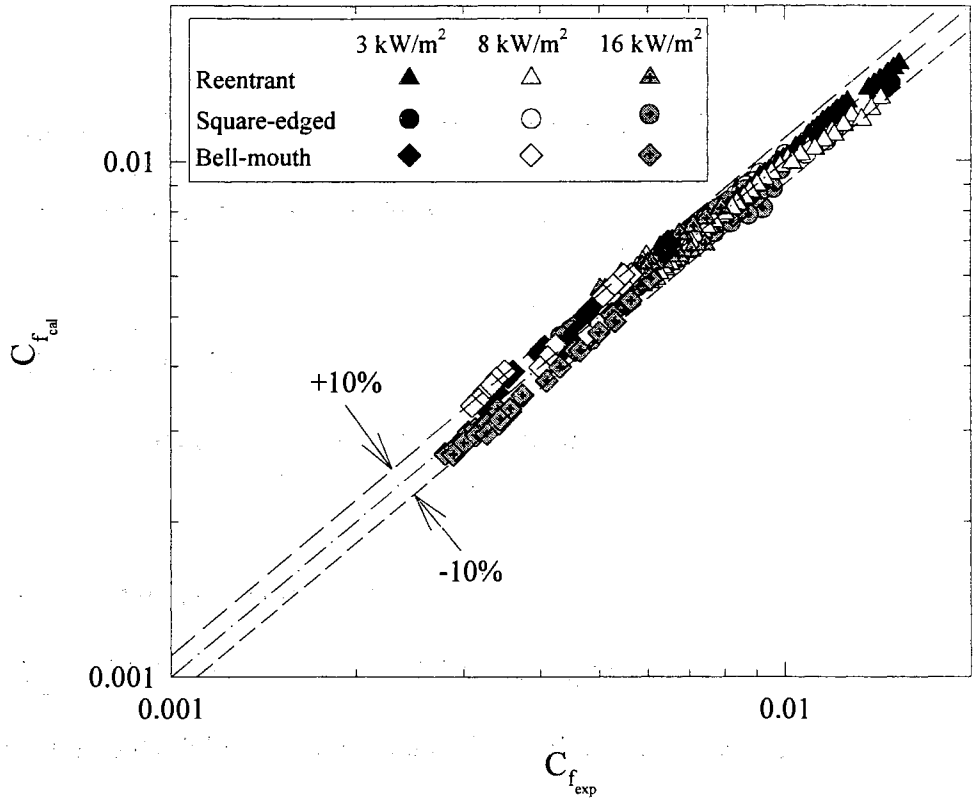

Figure 4.27 Comparison Between Experimental Fully Developed Skin Friction Coefficients and the Proposed Laminar Correlation.

$$C_f = \left[1 + \left(\frac{Re}{a}\right)^b\right]^c \left(\frac{\mu_b}{\mu_w}\right)^m \qquad (4.6)$$

where the coefficients a, b, and m are inlet dependent, and they were obtained separately for each inlet. The coefficients for each inlet are as follows.

Reentrant:

a=5840, b=-0.0145, c=-6.23, and m=-1.1-0.46 $Gr^{-0.133}$ $Pr^{4.1}$

where $2700 < Re < 5500$, $16 < Pr < 35$, $7410 < Gr < 158300$, $1.13 < (\mu_b/\mu_w) < 2.13$

Square-edged:

a=4230, b=-0.16, c=-6.57, and m=-1.13-0.396 $Gr^{-0.16}$ $Pr^{5.1}$

where $3500 < Re < 6900$, $12 < Pr < 29$, $6800 < Gr < 104500$, $1.11 < (\mu_b/\mu_w) < 1.89$

Bell-mouth:

a=5340, b=-0.0990, c=-6.32, and m=-2.58-0.42 $Gr^{-0.41}$ $Pr^{2.46}$

where $5900 < Re < 9600$, $8 < Pr < 15$ $11900 < Gr < 353000$, $1.05 < (\mu_b/\mu_w) < 1.47$

Equation (4.6) is applicable to the fully developed transition region and should be used with an appropriate set of constants for each inlet configuration. For the development of the transition region correlation for the reentrant inlet, thirty experimental data points were used. The correlation gave a representation of the experimental data to within +9.5% and -9% and had an absolute average deviation of 3.4%. All data for the reentrant inlet were predicted with less than 10% deviation. For the square-edged inlet, twenty nine experimental data points were used for the development of the correlation. The equation correlated the experimental data to within +20% to -11.8% and had an absolute average deviation of 8.4%. Twenty eight percent (9 data points) were predicted

with ± 10-20% deviation and 72% (21 data points) were predicted with less than ± 10% deviation. The correlation for the bell-mouth inlet was based on 24 experimental data points. The correlation represented the experimental data to within +20 % to - 23% and had an absolute average deviation of 9%. Eight percent (3 data points) were predicted with more than ± 20% deviation, 20% (5 data points) with ± 10-20% deviation and 72% (17 data points) with less than + 10% deviation. Figures 4.28, 4.29, and 4.30 compare the predicted fully developed skin friction coefficients obtained from Eq. (4.6) for each inlet with measurements.

It should be noted that Eq. (4.6) is unique in a sense that it is the first correlation for the prediction of the non-isothermal fully developed skin friction coefficient. The main purpose for the development of the correlation was to identify the key parameters which influence the skin friction coefficient and obtain a general equation which can describe the behavior of the non-isothermal skin friction coefficient in the transition region.

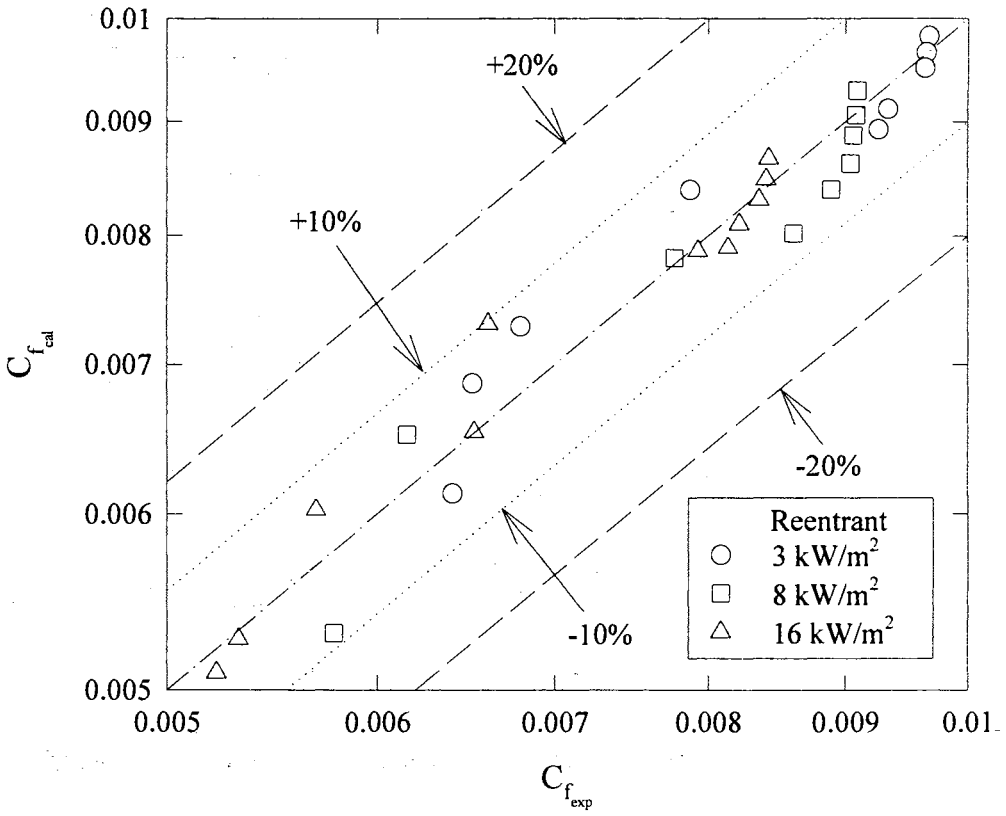

Figure 4.28 Comparison Between Experimental Fully Developed Skin Friction Coefficients for a Reentrant Inlet and the Proposed Transition Correlation.

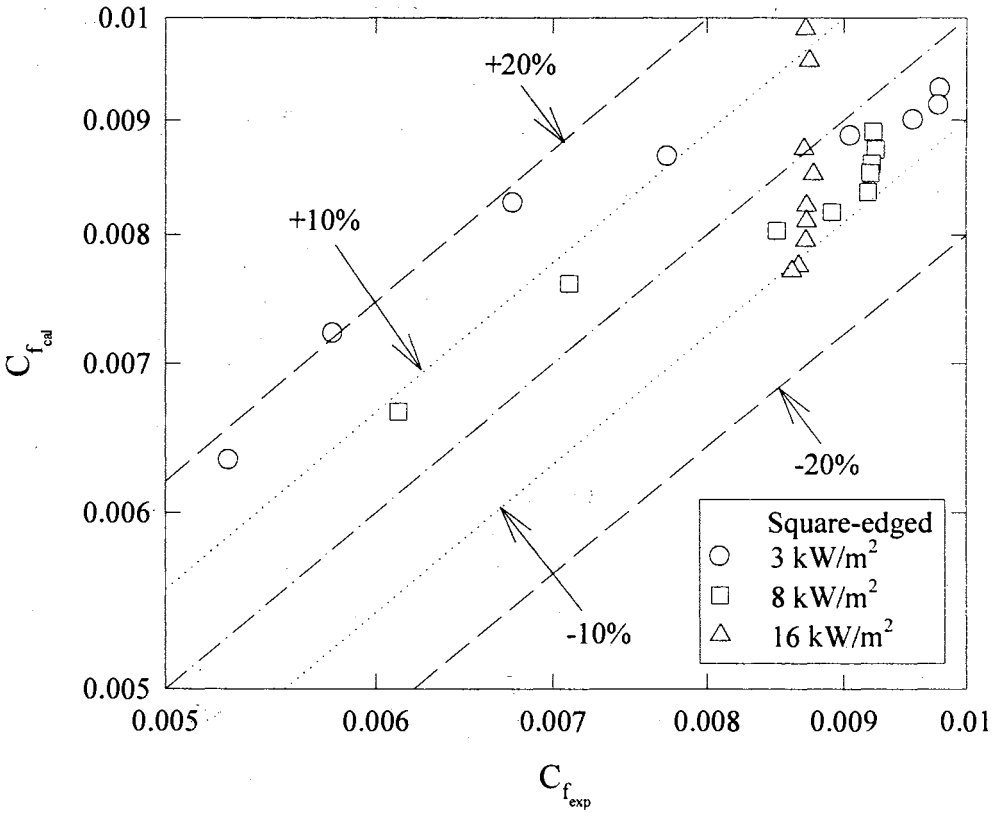

Figure 4.29 Comparison Between Experimental Fully Developed Skin Friction Coefficients for a Square-edged Inlet and the Proposed Transition Correlation.

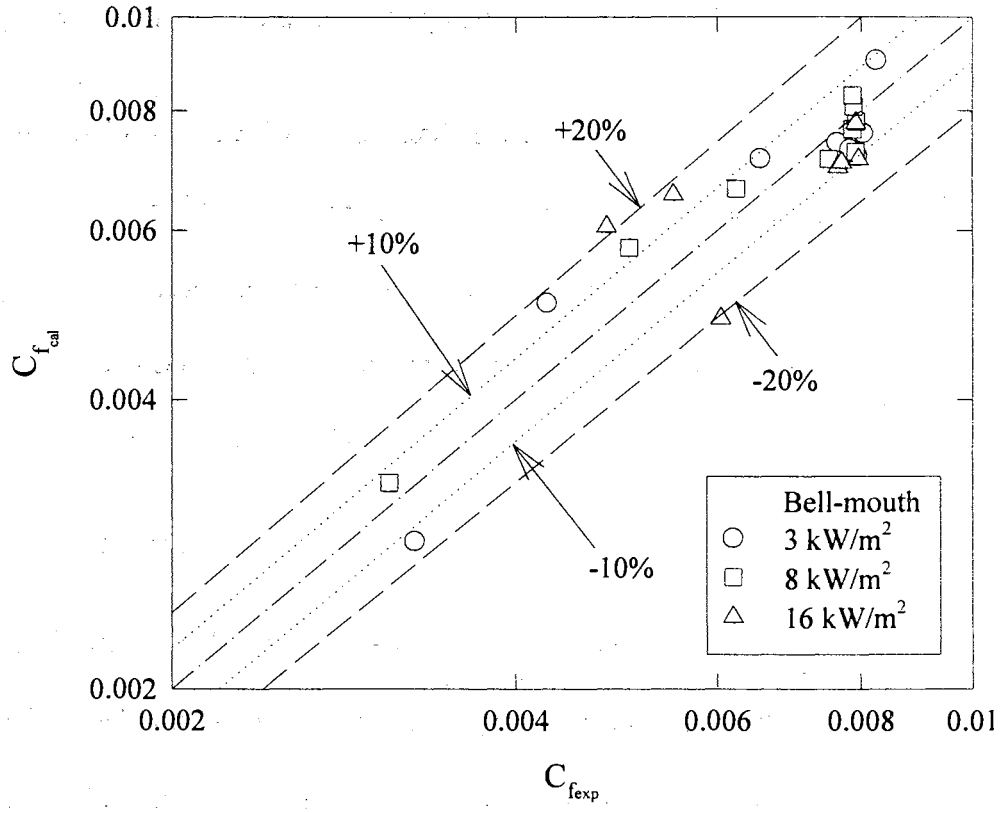

Figure 4.30 Comparison Between Experimental Fully Developed Skin Friction Coefficients for a Bell-mouth Inlet and the Proposed Transition Correlation.

CHAPTER V

CONCLUSIONS AND RECOMMENDATIONS

To obtain a better understanding of the flow characteristics for transitional pipe flow under the uniform wall heat flux condition, a series of experimental studies have been conducted and their results were presented and discussed in detail in Chapters III and IV. In this chapter, the accomplishments of the present study will be summarized and the recommendations for the future work will be specified.

5.1 Conclusions

The general conclusions drawn from this study may be summarized as:

1. Both forced and mixed convection modes of heat transfer were studied. The heat transfer results for three inlets showed that the range of Reynolds number values for which transition flow exists is strongly inlet-dependent. The establishment of secondary flow along the pipe also proved to be inlet configuration dependent. In the laminar and lower transition flow regions, mixed convection was found to be the dominant mode of heat transfer. In the turbulent region, the influence of free convection was found to be negligible, and inlet configuration had a minor influence on the heat transfer coefficient. The boundary between forced and mixed convection also showed a strong dependency on the inlet configuration.

2. A new flow regime map for forced flow in a circular horizontal pipe with three different inlets under uniform wall heat flux is recommended. The flow regime map is unique in the sense that it is the first attempt at developing such a map for the case of a horizontal pipe with uniform wall heat flux. In the development of the flow regime map, particular attention was paid to the role of inlet configuration on the start and end of the heat transfer transition region and the development of secondary flow along the pipe. Experimental data for three different inlet configurations (reentrant, square-edged, and bell-mouth) were used to verify the correctness of the map. The proposed map appears to be very general for the experimental data it was verified with and is applicable to both developing and fully-developed flows. With a knowledge of Re and the parameter GrPr at a particular x/D location, the flow regime map can be used to identify the convection heat transfer flow regime (pure forced or mixed) for any of the three inlets.

3. Based on the obtained experimental data, heat transfer correlations capable of predicting both entrance and fully developed forced and mixed convection heat transfer coefficients in the laminar, transition, and turbulent flow regimes were developed. These correlations are unique in the sense that they include the significant influences of different inlet configurations on the heat transfer coefficient along the pipe. These influences are more pronounced in the laminar and transition region correlations. The heat transfer correlation for the transition region in fact is the first correlation available in the literature which can predict not only the fully-developed region but also the entrance region.

4. Comparison of our fully developed forced convection heat transfer data in the transition and turbulent regions for a bell-mouth inlet showed excellent agreement

with the correlations developed by Gnielinski (1976) and Churchill (1977). However, the accuracy of these correlations deteriorated as the influence of inlet configuration on the heat transfer coefficient became more pronounced. Therefore, caution should be exercised in applying these correlations to tubes with distributed entrances (reentrant and square-edged). In addition, none of the reported correlations in the literature were capable of predicting our entrance and fully developed mixed convective heat transfer data for disturbed entrances in the laminar and transition regions with any consistency. For these flows the correlations developed in this study are recommended.

5. The boundary layer changing behavior was proven to be a characteristic of the bell-mouth inlet. In this study, three different inlet screen sizes were used in order to investigate how those characteristics respond to different inlet conditions. The results showed that the local Nusselt number starts to shift upward at x/D ranges from 100 to 173 and cause a dip in the Nu-x/D curve. The Reynolds number for which the boundary layer starts to change is inlet condition dependent. From the results, when the flow is still in the region ($x/D < 100$), the peripheral wall temperatures profile is highly non-uniform, and when the flow is in the upward shifting region ($x/D > 100$), the peripheral wall temperature profile is intermittent (changing between uniform and non-uniform). We can say that the heat transfer is jumping around between laminar and turbulent heat transfer characteristics. When this transitional heat transfer behavior ends, completely turbulent heat transfer can be observed.

6. The effects of calming section and inlet configuration on pressure drop measurements were investigated. The results show that the transition Reynolds number range is influenced by both calming section and inlet configuration. Three different

heating rates were used to investigate the effect of heating on the fully developed skin friction coefficient. In the laminar and transition flow regions, heating seems to increase the value of skin friction coefficient for a fixed Reynolds number. In the turbulent flow region, it seems that heating did not affect the magnitude of the skin friction coefficient. The significant influence of heating on the values of skin friction coefficient in the laminar and transition regions is directly due to the effect of secondary flow. From the results, the effect of heating is to delay the flow transition. The transition Reynolds number increases as the heating rate increases.

7. The experimental data was used to compare with the available non-isothermal skin friction coefficient correlations. The comparisons showed that none of the available correlations in the laminar region predicted the experimental data with satisfactory accuracy. The accuracy of these correlations deteriorated rapidly as the influence of secondary flow (due to increased heat input) became more pronounced. In the turbulent region, the experimental data agrees well with the correlation proposed by Allen and Eckert (1964). Empirical correlations for prediction of the non-isothermal skin friction coefficients in the laminar and transition flow regions were developed based on the experimental data. The correlation developed for skin friction coefficient in the transition region is unique in the sense that there is no other correlation in this region. The effect of heating in these correlations was accounted for in terms of a viscosity ratio expressed as a function of Prandtl and Grashof numbers.

5.2 Recommendations

Based on the observations and conclusions made during this study, the following recommendations are suggested:

1. Due to the test fluid used in this study, no forced convection data can be obtained in the fully developed laminar and transition flow regions. It is believed that secondary flow can delay the transition, however, it is difficult to draw this conclusion since no forced convection data is available. In order to obtain the forced convection data and make this study more comprehensive in the fully developed laminar and transition regions, different test fluid, probably air should be used.

2. More test locations should be added in the heat transfer test section. By adding more test locations, we should be able to define the location where the boundary layer changes from laminar to transition for a bell-mouth inlet and the length for the free convection effect can be established more accurately.

3. In the non-isothermal pressure drop measurements, due to the limitation of the experimental setup, only the data in the fully developed region can be obtained. It is important to see how heating influences friction coefficient in the entrance region. By adding thermocouples to the entrance region of the test section, we should be able to take the effect of heating on pressure drop into account. The pressure drop test section should be modified to achieve this goal.

4. In the heat transfer measurements, the results show that the peripheral temperature profile is highly non-uniform when secondary flow is present. It would be interesting to see whether the peripheral pressure distribution at that location is uniform

or not when secondary flow is present. Instead of using one pressure tap at each test location, multiple pressure taps around the periphery of the test section should be used.

5. In this study, a straight tube was used to investigate the transitional behavior for heat transfer and pressure drop. For heat exchanger design, instead of straight tube, a U tube is often used. In the literature, no information regarding heat transfer and pressure drop in the transition region for a U tube is available. The heat transfer and pressure drop characteristics for a U tube could be investigated to make the picture more complete.

REFERENCES

Achmadi, F. (1993), Fully Developed Pressure Drop Measurements in a Horizontal Circular Tube with a Bell-mouth Entrance Under Uniform Wall Heat Flux, Masters Report, School of Mechanical and Aerospace Engineering, Oklahoma State University, Stillwater, Oklahoma.

Al-Arabi, M. (1982), Turbulent Heat Transfer In The Entrance Region Of A Tube, Heat Transfer Engineering, v. 3, nos. 3-4, pp. 78-83.

Allen, R. W. and Eckert, E.R.G., (1964), Friction and Heat Transfer Measurements to Turbulent Pipe Flow of Water (Pr = 7 and 8) at Uniform Wall Heat Flux, J. Heat Transfer, v. 86, pp. 301-310.

Augustine, J. R. (1990), Pressure Drop Measurements in the Transition Region for a Circular Tube with a Square-edged Entrance, Masters Thesis, Oklahoma State University, Stillwater, Oklahoma.

Bhatti, M. S., and Shah, R. K. (1987), Turbulent and Transition Flow Convective Heat Transfer in Ducts, in Handbook of Single-Phase Convective Heat Transfer, S. Kakac, R. K. Shah, and W. Aung, Eds., Chapter 4, p. 16, Wiley, New York.

Bergles, A. E., and Simonds, R. R. (1971), Combined Forced and Free Convection for Laminar Flow in Horizontal Tubes with Uniform Heat Flux Int. J. Heat Mass Transfer, v. 14, pp. 1989-2000.

Blasius, H. (1913), Das Ahnlichkeitsgesetz bei Reibungsvorgangen in Flussigkeiten, Forsch. Arb. Ing.-Ves., 131.

Bohn, D., Fischer, S., and Obermeir, E. (1984), Thermal Conductivity, Density, Viscosity, and Prandtl Numbers of Ethylene Glycol-Water Mixtures, Ber Bunsenges. Phys. Chem., v.88, pp. 739-742.

Campbell, W. D. and Slattery, J. C. (1963), Flow in the Entrance Region of Tube, Journal of Basic Engineering Trans. of The ASME, v. 95, pp. 153-158.

Chen, J. (1988), Heat Transfer in High Laminar, Transition and Lower Turbulent Flow Regimes for Square-Edged Contraction Entrance in a Circular Tube, Ph.D. Dissertation, Oklahoma State University, Stillwater, Oklahoma.

Churchill, S. W. (1977), Comprehensive Correlating Equations for Heat, Mass Momentum Transfer in Fully Developed Flow in Smooth Tubes, Ind. Eng. Chem., Fundam., v. 16, pp. 109-115.

Churchill, S. W. and Usagi ,R. (1972), General Expression for the Correlation of Rates of Transfer and Other Phenomena, A.I.Ch.E., v. 18, pp.1121-1128.

Deissler, R. G., (1951), Analytical Investigation of Fully Developed Laminar Flow in Tubes with Heat Transfer with Fluid Properties Variable along the Radius, NACA TN 2410, Washington.

Eckert, E. R. G. and Diaguila A. J. (1954), Convective Heat Transfer for Mixed, Free and Forced Flow Through Tubes, Trans. ASME, v. 76, pp. 497-504.

Eubank, O. C., and Proctor, S. M. (1951), Effect of Natural Convection on Heat Transfer with Laminar Flow, Thesis in Chemical Engineering, MIT, Cambridge, MA.

Febransyah, A. (1994), Pressure Drop Measurements in the Entrance Region for a Circular Tube with a Bell-mouth Entrance Under Isothermal Flow Condition, Masters Report, School of Mechanical and Aerospace Engineering, Oklahoma State University, Stillwater, Oklahoma.

Ghajar, A. J. and Augustine, J. (1990), Pressure Drop Measurements in the Transition Region for a Circular Tube with a Square-Edged Entrance, AIAA Paper No. 90-1500, Presented at the 21st Fluid Dynamics, Plasma Dynamics and Lasers Conference, Seattle, Washington, June 18-20, 1990.

Ghajar, A. J., and Madon, K. F. (1992), Pressure Drop Measurements in the Transition Region for a Circular Tube with Three Different Inlet Configurations, Experimental Thermal and Fluid Science, v. 5, no. 1, pp. 129-135.

Ghajar, A. J. and Strickland, D. T. (1990), Forced and Mixed Convective Heat Transfer Correlations in the Laminar-Transition-Turbulent Regions for a Circular Tube with a Square-Edged Entrance, AIAA Paper No. 90-1762, Presented at the AIAA/ASME 5th Joint Thermophysics and Heat Transfer Conference, Seattle, Washington, June 18-20, 1990.

Ghajar, A. J., Strickland, D. T. and Kuppuraju, S. (1990), Forced and Mixed Convective Heat Transfer Measurements in a Circular Tube with Different Inlets, in Mixed Convection, eds. R.L. Mahajan and R.D. Boyd, ASME, HTD v. 152, pp. 37-45.

Gnielinski, V. (1976), New Equations for Heat and Mass Transfer in Turbulent Pipe and Channel Flow, Int. Chem. Engr., v. 16, no. 2, pp. 359-368.

Hrycak, P. and Andrushkiw, R. (1974), Calculation of Critical Reynolds Numbers in Round Tubes and Infinite Channels and Heat Transfer in the Transition Region. Heat Transfer, v. 2, pp. 183-187.

Hussain, N. A. and McComas, S. T. (1970), Experimental Investigation of Combined Convection in a Horizontal Tube with Uniform Heat Flux, Proceeding of the Int. Heat Mass Transfer Conf. Paris, v. 4, paper no. NC3.4.

Kakac, S., Shah, R. K., and Aung, W. (1987), Handbook of Single-Phase Convective Heat Transfer, Wiley, New York.

Kern, D. Q., and Othmer, D. F. (1943), Effect of Free Convection on Viscous Heat Transfer in Horizontal Tubes, AIChE, v. 39, pp. 517-555.

Kline, S. J. and McClintock, F. A. (1953), Describing Uncertainties in Single-Sample Experiments, Mech. Engr., v. 1, pp. 3-8.

Kuppuraju, S. (1990), Heat Transfer Measurements in the Transition Region for a Horizontal Circular Tube with a Reentrant Entrance, M.S. Report, School of Mechanical and Aerospace Engineering, Oklahoma State University, Stillwater, Oklahoma.

Laurens, M. M. (1995), Effect of Heating Rate and Inlet Configuration on Heat Transfer Characteristics in Laminar and Turbulent Flow Regions of a Horizontal Circular Tube Under Uniform Wall Heat Flux Condition, M.S. Report, School of Mechanical and Aerospace Engineering, Oklahoma State University, Stillwater, Oklahoma.

Madon, K. F. (1990), Pressure Drop Measurements in the Transition Region for a Circular Tube with a Reentrant and Bell-Mouth Entrance, M.S. Report, School of Mechanical and Aerospace Engineering, Oklahoma State University, Stillwater, Oklahoma.

Martinelli, R. C., and Boelter, L. M. K. (1942), The Analytical Prediction of Superposed Free and Forced Viscous Convection in a Vertical Pipe, Univ. Calif. Publ. Eng., v. 5, no. 2, p. 23.

McComas, S. T. and Eckert, E. R. G. (1966), Combined Free and Forced Convection in a Horizontal Circular Tube, Int. J. Heat Mass Transfer Trans., v. 88, pp. 147-153.

Metais, B. (1963), Criteria For Mixed Convection, Internal Report, Heat Transfer Laboratory, University of Minnesota, Minneapolis, Minnesota, HTL TR No. 51.

Metais, B. and Eckert, E. R. G. (1964), Forced, Mixed and Free Convection Regimes, J. Heat Transfer, Trans. ASME, v. 10, pp. 295-296.

Morcos, S. M. and Bergles, A. E. (1975), Experimental Investigation of Combined Forced and Free Laminar Convection in Horizontal Tubes, Int. J. Heat Mass Transfer Trans., v. 91, pp. 212-219.

Mori, Y., Futagami, K., Tokuda, S., and Nakamura, M. (1966), Forced Convective Heat Transfer in Uniformly Heated Horizontal Tubes, Int. J. Heat Mass Transfer, v. 9, pp. 453-463.

Ogawa, M. and Kawamura, H. (1987), Effects of Entrance Configuration on Pressure Loss and Heat Transfer of Transition Gas Flow in a Circular Tube, JSME Trans., v. 7, pp. 77-91.

Petukhov, B. S. and Polyakov, A. F. (1967a), Effect of Free Convection on Heat Transfer During Forced Flow in Horizontal Pipe, High Temperature, v. 5, pp. 75-81.

Petukhov, B. S. and Polyakov, A. F. (1967b), Effect of Free Convection on Heat Transfer During Forced Flow in Horizontal Pipe, High Temperature, v. 5, pp. 348-351.

Petukhov, B. S. and Popov, V. N. (1963), Theoretical Calculation of Heat Exchange and Frictional Resistance with Variable Physical Properties, Teplifiz. Vys. Temp, v. 1, pp. 85-101.

Readal, T. C. (1969), Effect of Density Gradients on the Rate of Heat Transfer for Flow Through a Horizontal Pipe, M.S. Thesis, University of Illinois, Urbana, Illinois.

Schiller, von L. (1922), Die Entwiklung Der Laminaren Geshwindigkeitverteilung und Ihre Bedeutung Fur Zahigkeitsmessungen. Z. Angew. Math. Mech. v. 2, pp. 96-106.

Shah, R. K. (1978), A Correlation for Laminar Hydrodynamic Entry Length Solutions for Circular and Non-Circular Ducts, J. of Fluid Engineering, Trans. ASME, v. 100, pp. 177-179.

Shah, R. K. and Johnson R. S. (1980), Correlations for Fully Developed Turbulent Flow Through Circular and Noncircular Channels, Proceeding of the 6th National Heat and Mass Transfer Conference, pp. D75-D96.

Shannon, R. L. and Depew, C. A. (1968), Combined Free and Forced Laminar Convection in a Horizontal Tube with Variable Viscosity and Free Convection Effect, J. Heat Transfer, Trans. ASME, v. 90, pp. 353-357.

Shannon, R. L. and Depew, C. A. (1969), Forced Laminar Flow Convection in a Horizontal Tube with Variable Viscosity and Free Convection Effects, J. Heat Transfer, v. 91, pp. 251-258.

Shapiro, A. H. and Smith, D. (1947), Friction Coefficients in the Inlet Length of Smooth, Round Tubes, N.A.C.A. TN No. 1785, pp. 1-43.

Sieder, E. N., and Tate, G. E. (1936), Heat Transfer and Pressure Drop in Liquids in Tubes, Ind. Eng. Chem, v. 29, pp. 1429-1435.

Siegal, R., Sparrow, E. M. and Hallman, T. M. (1958), Steady Laminar Heat Transfer in a Circular Tube with Prescribed Wall Heat Flux, Appl. Sci. Res., Sec. A, v. 7, pp. 386-392.

Siegwarth, D. P., Mikesell, R. D. Readal, T. C. and Hanratty, T. J. (1969), Effect of Secondary Flow on the Temperature Field and Primary Flow in a Heated Horizontal Tube, Int. Heat Mass Transfer, v. 12, pp. 1535-1552.

Strickland, D. T. (1990), Heat Transfer Measurement in the Transition Region for a Horizontal Circular Tube with a Square-Edged Entrance, M.S. Thesis, Oklahoma State University, Stillwater, Oklahoma.

Test, F.L., (1968), Laminar Flow Heat Transfer and Fluid Flow for Liquids with Temperature-Dependent Viscosity, J. Heat Transfer, v. 90, pp. 385-393.

Warnecker, D. (1995), Analysis of the Effect of Heating Rate and Inlet Configuration on the Pressure Drop Transition Boundaries for Square-edged and Reentrant Inlet Configurations Under Uniform Wall Heat Flux, Masters Report, Mechanical and Aerospace Engineering, Oklahoma State University, Stillwater, Oklahoma.

APPENDIX A

COMPUTER PROGRAMS

Program HNEW
Program RQ
Program FRIC

APPENDIX A

COMPUTER PROGRAMS

In this Appendix, a listing of the computer programs (HNEW, RQ, and FRIC) are presented.

A.1 Program HNEW

As mentioned in Chapter II, HNEW is the major data reduction program. The following is a complete listing of this program.

```
C ***********************************************************************
C *                  "HEAT"                    *
C *                                            *
C *  A PROGRAM TO CALCULATE THE INSIDE WALL TEMPERATURES AND
C *  LOCAL HEAT TRANSFER COEFFICIENTS FOR GIVEN OUTSIDE WALL
C *  TEMPERATURES FOR SINGLE PHASE HEAT TRANSFER STUDIES IN
C *  HORIZONTAL TUBES.  THE PROGRAM ALSO CALCULATES THE PERTINENT
C *  FLUID FLOW & HEAT TRANSFER DIMENSIONLESS NUMBERS.
C *
C *  THE MATHEMATICAL ALGORITHM OF THIS PROGRAM HAS BEEN DEVELOPED
C *  BY THE STUDENTS OF DR. J.D. PARKER & DR. K.J. BELL OF
C *  OKLAHOMA STATE UNIVERSITY.
C *
C *  THE PROGRAM WAS MODIFIED BY:
C *
C *          Y. H. ZURIGAT  (APRIL 1989)
C *                                        *
C *  AND REMODIFIED FOR INTERACTIVE USE ON PC's BY:
C *
C *          D. R. MAIELLO  (DECEMBER 1989)
C *
C *  UNDER THE SUPERVISION OF: DR. A.J. GHAJAR
C *                  SCHOOL OF MECHANICAL &
C *                    AEROSPACE ENGINEERING
C *                  OKLAHOMA STATE UNIVERSITY
C *                  STILLWATER, OK 74078
C *
C ***********************************************************************
C
C ***********************************************************************
C *
C *              SUBROUTINE LISTING
C *
C *    NAME      FUNCTION
C *   --------   ------------------------------------
C *   GEOM       Prompts for pipe dimensions and
C *              calculates geometry for finite
```

```
C *              differencing
C *
C *    BET        Calculates fluid Thermal Expansion Coefficient
C *
C *    CONDFL     Calculates fluid Thermal Conductivity
C *
C *    DENS       Calculates fluid Density
C *
C *    MEW        Calculates fluid Viscosity
C *
C *    PRNUM      Calculates fluid Prandtl Number
C *
C *    SPHEAT     Calculates fluid Specific Heat
C *
C *    PRNT       Prints calculated data to output files
C *
C ***********************************************************************
C
C
C ***********************************************************************
C *
C *                MAIN PROGRAM
C *
C ***********************************************************************
C
C
      CHARACTER INFILE*36,OUTFILE*11,SUMFILE*11,SUMDOC*11,FNAME*4
      DIMENSION TCHCK1(8),TCHCK2(8),QAVG(31),PWP(31),
     +     PRNU(31),CONDK(31,8),RSVTY(31,8)
C
      COMMON /PRINT/ IPICK,REN(31,8),TBULK(31),VEL,REYNO,PRNO,GW,
     +          HTCOFF(31,8),H(31),RENO(31),GRNO(31),PR(31),
     +          SNUS(31),VISBW(31),SHTHB(32),QFLXID(31,8),QFLXAV,
     +          QGEXPT,QBALC,QPCT,IGO,IPMAX,TAVG(31)
     +     /INPUT/ TROOM,VOLTS,TAMPS,RMFL,MFLUID,X2,FLOWRT,NRUN,VFLOW,
     +          TIN,TOUT,TOSURF(31,8),TISURF(31,8),IP(32),KST(32)
     +     /TEMP1/ TWALL(31,8),AMPS(31,8),RESIS(31,8),POWERS(32),
     +          TPOWER
     +     /MAIN1/ IST,KOUNT,NSTN
     +     /GEOM1/ XAREA(31),R(31),LTP(32),LTH(32),DELZ(31),LHEAT,
     +          LTEST,LOD(31),DOUT,DIN,DELR,NODES,NSLICE,PI
C
      REAL*4 LTH,LTP,LTEST,LHEAT,H,HAV,HTCOFF,HEF,HMIX,LOD
C
C -------------------------
C ----- PRINT HEADING -----
C -------------------------
C
      WRITE(*,1009)
C
      READ(*,1003)FNAME
C
C -------------------------------------------------
C ----- INITIALIZE OUTPUT DATA ARRAYS TO ZERO -----
C -------------------------------------------------
C
    1 DO 101 I=1,8
        DO 101 J=1,31
          TOSURF(J,I)=0.
          TISURF(J,I)=0.
```

```
      REN(J,I)=0.
      QFLXID(J,I)=0.
 101    HTCOFF(J,I)=0.
C
   G=32.174
C
C ---------------------------------------------------------------
C ----- PRINT EXPLANATIONS TO SCREEN & PROMPT FOR OUTPUT OPTION -----
C ---------------------------------------------------------------
C
   WRITE(*,1001)
C
   READ(*,*)IGO
C
C ------------------------------------------
C ----- PROMPT FOR INPUT DATA FILE NAME -----
C ------------------------------------------
C
   DO 2 J=1,18
  2 WRITE(*,*)' '
   WRITE(*,*)'  ENTER INPUT DATA FILE NAME:'
   WRITE(*,*)'   (COMPLETE PATH & EXTENSION; 36 CHARACTER MAX)'
   WRITE(*,*)'************************************'
   WRITE(*,*)' '
   READ(*,1002)INFILE
   OPEN(5,FILE=INFILE,STATUS='OLD')
C
C ------------------------------------------------
C ----- READ RUN NUMBER FROM INPUT DATA FILE -----
C ------------------------------------------------
C
   READ(5,1003)FNAME
   REWIND 5
C
C ---------------------------------------------------------------
C ----- ASSIGN FILE NAMES TO VARIABLES AND OPEN OUTPUT FILES -----
C ---------------------------------------------------------------
C
   OUTFILE='RN'//FNAME//'.OUT'
   SUMFILE='RN'//FNAME//'.SUM'
C
   OPEN(6,FILE=OUTFILE,STATUS='NEW')
   OPEN(9,FILE=SUMFILE,STATUS='NEW')
C
C ---------------------------------
C ----- PROMPT FOR UNITS INPUT -----
C ---------------------------------
C
   WRITE(*,*)' '
   WRITE(*,*)' '
  3 WRITE(*,*)'  SELECT ENGLISH OR S.I. UNITS FOR OUTPUT FILE:'
   WRITE(*,*)'      Enter "1" for English'
   WRITE(*,*)'      Enter "2" for S.I.'
   WRITE(*,*)' '
   READ(*,*)IPICK
   IF(IPICK.NE.1.AND.IPICK.NE.2)GO TO 3
C
C ------------------------------------------------------------
C ----- READ RUN NUMBER AND # STATIONS FROM INPUT FILE -----
C ------------------------------------------------------------
```

```
C
  4 READ(5,1004) NRUN,NSTN
C
C ---------------------------------
C ----- CHECK FOR END OF FILE -----
C ---------------------------------
C
    IF (NRUN .EQ. 0) GO TO 99
C
C -------------------------------------
C ----- READ DATA FROM INPUT FILE -----
C -------------------------------------
C
    X2=0.0
    IPMAX=0
    READ(5,1005)MFLUID,X2,FLOWRT,TAMPS,VOLTS,TIN,TOUT,TROOM
C
    IF(X2.LT.0.0.OR.X2.GT.1.0)THEN
     WRITE(*,*)' WARNING : MASS CONCENTRATION IS OUT OF RANGE'
     STOP
    END IF
C
    DO 5 IST=1,NSTN
     READ(5,1006)KST(IST),IP(IST),LTH(IST),
   +    (TOSURF(IST,IPR),IPR=1,IP(IST))
     IF(IST.NE.1)THEN
        IF(IP(IST).GE.IPMAX)IPMAX=IP(IST)
     ELSE
  5  ENDIF
C
    VFLOW=FLOWRT
C
C -----------------------------------------------------
C -----CALCULATION OF MASS FLOW RATE IN LBM/HR -----
C -----------------------------------------------------
C
    CALL DENS(TIN,MFLUID,X2,ROW)
    RMFL=VFLOW*0.133666*60.0*ROW
C
C -----         -----
     CALL GEOM
C -----         -----
C
    NNODE=NODES-1
C
C -------------------------------------------
C ----- START SOLUTION WITH STATION 1 -----
C -------------------------------------------
C
    DO 30 IST=1,NSTN
      IPP= IP(IST)
      DO 10 IPR=1,IPP
 10     TCHCK1(IPR)=0.0
C
C -------------------------------------------------
C -----  SET ALL RADIAL TEMPERATURES EQUAL  -----
C ----- TO THE OUTSIDE SURFACE TEMPERATURES -----
C -------------------------------------------------
C
      DO 11 ISL=1,NODES
```

```
        DO 11 IPR=1,IPP
  11        TWALL(ISL,IPR)=TOSURF(IST,IPR)
      KOUNT=1
C
C ---------------------------------------------------------------
C ----- CALCULATE THERMAL CONDUCTIVITY OF STAINLESS STEEL -----
C -----     FOR EACH NODE IN BTU/(HR-FT-DEGF)          -----
C ---------------------------------------------------------------
C
  12 DO 13 ISL=1,NODES
     DO 13 IPR=1,IPP
       CONDK(ISL,IPR)=7.27+0.0038*TWALL(ISL,IPR)
  13 CONTINUE
C
C ---------------------------------------------------------------
C ----- CALCULATE ELECTRICAL RESISTIVITY OF STAINLESS STEEL -----
C -----       FOR EACH NODE IN OHMS-SQIN/IN             -----
C ---------------------------------------------------------------
C
    DO 14 ISL=1,NODES
      IPP= IP(IST)
      DO 14 IPR=1,IPP
       RSVTY(ISL,IPR)=(27.67+0.0213*TWALL(ISL,IPR))/1.E6
  14 CONTINUE
C
C ---------------------------------------------------------------
C -----     CALCULATE RESISTANCE FOR EACH SEGMENT, ALSO     -----
C ----- CALCULATE EQUIVALENT RESISTANCE FOR PARALLEL CIRCUITS -----
C ---------------------------------------------------------------
C
    DELR = (DOUT-DIN)/2.0/NSLICE
    R(1) = DOUT/2.0
    DO 15  I=1,NSLICE
  15   R(I+1)=R(I)-DELR
    IPP= IP(IST)
    XAREA(1)=(R(1)-DELR/4.0)*PI*DELR/IPP
    XAREA(NODES)=(R(NODES)+DELR/4.0) *PI*DELR/IPP
    DO 16 I=2,NSLICE
  16   XAREA (I)= 2.0*R(I)*PI*DELR/IPP
C
    RINV = 0.0
    DO 17 ISL=1,NODES
      DO 17 IPR=1,IPP
        RESIS(ISL,IPR) = RSVTY(ISL,IPR)*DELZ(IST)/XAREA(ISL)
        RINV = RINV +1.0/RESIS(ISL,IPR)
  17 CONTINUE
C
C ------------------------------------------------
C ----- CALCULATE CURRENT FOR EACH SEGMENT -----
C ------------------------------------------------
C
    OHMS = 1.0/RINV
    AMP=0.0
    DO 18 ISL=1,NODES
      DO 18 IPR=1,IPP
        AMPS(ISL,IPR) = TAMPS*OHMS/RESIS(ISL,IPR)
        AMP=AMP+AMPS(ISL,IPR)
  18 CONTINUE
C
C ---------------------------------------------------------------
```

```
C -----          CALCULATE TEMPERATURES AT NODE 2          -----
C ----- TEMPERATURES AT NODE 1 ARE OUTSIDE WALL TEMPERATURES -----
C ---------------------------------------------------------------
C
      ISL=1
      DO 20 IPR=1,IPP
        ITHCTL=IPP
        IMINS=IPR-1
        IPLUS=IPR+1
        NMINS = ISL - 1
        NPLUS = ISL + 1
          IF(IMINS.EQ.0 .AND. IPP.EQ. ITHCTL) IMINS=ITHCTL
          IF(IPLUS.EQ.(ITHCTL+1) .AND.  IPP.EQ. ITHCTL) IPLUS=1
        A= 3.41214*12.0*AMPS(ISL,IPR)*AMPS(ISL,IPR)
     +          *RSVTY(ISL,IPR)/XAREA(ISL)
        B = IPP*DELR*(CONDK(ISL,IPR)+CONDK(ISL,IPLUS))
     +          *(TWALL(ISL,IPR)-TWALL(ISL,IPLUS))/(8.0*PI*R(ISL))
        C = IPP*DELR*(CONDK(ISL,IPR)+CONDK(ISL,IMINS))
     +          *(TWALL(ISL,IPR)-TWALL(ISL,IMINS))/(8.0*PI*R(ISL))
        X = PI*(R(ISL)-DELR/2.0)*(CONDK(ISL,IPR)+CONDK(NPLUS,IPR))
     +          /(IPP*DELR)
   20     TWALL(NPLUS,IPR) = TWALL(ISL,IPR)-(A-B-C)/X
C
C ------------------------------------------------
C ----- CALCULATE REMAINING NODAL TEMPERATURES -----
C ------------------------------------------------
C
      DO 21 ISL=2,NNODE
        DO 21 IPR=1,IPP
          ITHCTL=IPP
          IMINS=IPR-1
          IPLUS=IPR+1
          NMINS=ISL-1
          NPLUS=ISL+1
          IF(IMINS.EQ.0 .AND. IPP .EQ. ITHCTL) IMINS=ITHCTL
          IF(IPLUS.EQ.(ITHCTL+1) .AND. IPP .EQ. ITHCTL) IPLUS=1
          A= 3.41214*12.0*AMPS(ISL,IPR)*AMPS(ISL,IPR)
     +          *RSVTY(ISL,IPR)/XAREA(ISL)
          B =PI*(R(ISL)+DELR/2.)*(CONDK(ISL,IPR)+CONDK(NMINS,IPR))
     +          *(TWALL(ISL,IPR)-TWALL(NMINS,IPR))/(IPP*DELR)
          C = IPP*DELR*(CONDK(ISL,IPR)+CONDK(ISL,IPLUS))
     +          *(TWALL(ISL,IPR)-TWALL(ISL,IPLUS))/(4.0*PI*R(ISL))
          D = IPP*DELR*(CONDK(ISL,IPR)+CONDK(ISL,IMINS))
     +          *(TWALL(ISL,IPR)-TWALL(ISL,IMINS))/(4.0*PI*R(ISL))
          X =PI*(R(ISL)-DELR/2.)*(CONDK(ISL,IPR)+CONDK(NPLUS,IPR))
     +          /(IPP*DELR)
   21     TWALL(NPLUS,IPR) = TWALL(ISL,IPR)- (A-B-C-D)/X
C
C ---------------------------------------------------------
C ----- CHECK FOR THE CONVERGENCE OF THE WALL TEMPERATURES -----
C ---------------------------------------------------------
C
      TCHCK = 0.0
      DO 22 IPR=1,IPP
        TCHCK2(IPR)=TWALL(NODES,IPR)
   22     TCHCK = TCHCK + ABS(TCHCK2(IPR)-TCHCK1(IPR))
      IF (TCHCK .GT. 0.001) GO TO 23
      GO TO 26
   23   DO 24 IPR=1,IPP
   24     TCHCK1(IPR) = TCHCK2(IPR)
```

```
      IF (KOUNT .GT. 20) GO TO 25
      KOUNT = KOUNT+1
      GO TO 12
      WRITE(6,1007) IST,KOUNT
 25    WRITE(*,1007) IST,KOUNT
 26    DO 27 IPR=1,IPP
 27      TISURF( IST ,IPR)=TWALL(NODES,IPR)
C
C ---------------------------------------------------------------
C ----- CALCULATE POWER GENERATED IN EACH SEGMENT IN BTU/HOUR -----
C ---------------------------------------------------------------
C
      POWER =0.0
      DO 28 ISL=1,NODES
        DO 28 IPR=1,IPP
        POWER=POWER+AMPS(ISL,IPR)*AMPS(ISL,IPR)*RESIS(ISL,IPR)
 28    CONTINUE
C
      POWERS(IST)=POWER*3.41214
C
C ------------------------------------------------
C ----- CALCULATE HEAT FLUX AT INSIDE SURFACE -----
C ------------------------------------------------
C
    ISL=NODES
    IPP= IP(IST)
      ITHCTL=IPP
    DO 29 IPR=1,IPP
      IPLUS=IPR+1
      IMINS=IPR-1
      IF(IMINS.EQ.0 .AND. IPP .EQ. ITHCTL) IMINS=ITHCTL
      IF(IPLUS.EQ.(ITHCTL+1).AND. IPP.EQ. ITHCTL) IPLUS=1
      Q1 = PI*(CONDK(ISL-1,IPR)+CONDK(ISL,IPR))*(R(ISL-1)-DELR/2.0)*
     +      (TWALL(ISL,IPR)-TWALL(ISL-1,IPR))/(IPP*DELR)
      Q2 = IPP*(CONDK(ISL,IPLUS)+CONDK(ISL,IPR))*DELR
     +      *(TWALL(ISL,IPR)-TWALL(ISL,IPLUS))/(PI*R(ISL)*8.0)
      Q4 = IPP*(CONDK(ISL,IPR)+CONDK(ISL,IMINS))*DELR
     +      *(TWALL(ISL,IPR)-TWALL(ISL,IMINS))/(PI*R(ISL)*8.0)
      QGEN=3.41214*12.0*AMPS(ISL,IPR)*AMPS(ISL,IPR)
     +      *RSVTY(ISL,IPR)/XAREA(ISL)
 29   QFLXID(IST,IPR) =(QGEN-Q1-Q2-Q4)*IPP*12.0/(2.0*PI*R(ISL))
C
  30 CONTINUE
C
C ---------------------------------------------------------------
C ----- CALCULATE REYNOLDS NUMBERS AT INSIDE TUBE SURFACE -----
C ---------------------------------------------------------------
C
    DO 40 IST=1,NSTN
      IPP= IP(IST)
      DO 40 IPR=1,IPP
        TR=TISURF(IST,IPR)
        CALL MEW(TR,MFLUID,X2,VISS)
        REN(IST,IPR)=RMFL*48.0/(PI*DIN*VISS)
 40 CONTINUE
C
C ------------------------------------------------------
C ----- CALCULATE TOTAL POWER GENERATED IN BTU/HOUR -----
C ------------------------------------------------------
C
```

```
      TPOWER=0.0
      DO 45 IST=1,NSTN
   45 TPOWER=TPOWER+POWERS(IST)
C
C ---------------------------------------------------------------
C ----- CALCULATE BULK FLUID TEMPERATURE AT EACH STATION,DEG.F -----
C ---------------------------------------------------------------
C
      TBULK(1)=TIN+(TOUT-TIN)*LTP(1)/LTEST
      DO 50 IST =2,NSTN
   50   TBULK(IST) = TBULK(IST-1) + (TOUT-TIN)*LTP(IST)/LTEST
C
C ---------------------------------------------------------------
C ----- CALCULATION OF INPUT AND OUTPUT HEAT TRANSFER RATE,BTU/HR -----
C -----    AND OVERALL AVERAGE REYNOLDS AND PRANDTL NUMBERS      -----
C ---------------------------------------------------------------
C
      QGCALC=TPOWER
      QGEXPT =TAMPS*VOLTS*3.41214
      QIN=QGEXPT
      QFLXAV=QIN/(3.1416*DIN/12.0*(LHEAT/12.0))
C
C ----- CALCULATE FLUID PROPERTIES AT TAVE -----
C
      T=(TOUT+TIN)/2.0
      CALL SPHEAT(T,MFLUID,X2,SPHT)
      CALL MEW(T,MFLUID,X2,VISC)
      CALL CONDFL(T,MFLUID,X2,COND)
C
      QBALC=RMFL*SPHT*(TOUT-TIN)
      QPCT=(QIN-QBALC)*100.0/QIN
      AID=PI*DIN*DIN/4.0/144.0
      GW=RMFL/AID
      REYNO=GW*DIN/12.0/VISC
      PRNO=VISC*SPHT/COND
C
C ---------------------------------------------------------------
C ----- CALCULATION OF PERIPHERAL HEAT TRANSFER COEFFICIENT -----
C -----    FROM EXPERIMENTAL DATA,BTU/(HR-SQ.FT-DEG.F)     -----
C ---------------------------------------------------------------
C
      DO 55 IST=1,NSTN
        IPP= IP(IST)
        DO 55 IPR=1,IPP
        HTCOFF(IST,IPR) =QFLXID(IST,IPR)/(TISURF(IST,IPR)-TBULK(IST))
   55 CONTINUE
C
C ---------------------------------------------------------------
C ----- CALCULATE RATIO OF TOP/BOTTOM HEAT TRANSFER COEFFICIENTS -----
C ---------------------------------------------------------------
C
      DO 65 IST=1,NSTN
        IPP= IP(IST)
        IF (IPP.EQ. 4) GO TO 60
          SHTHB(IST)=HTCOFF(IST,1)/HTCOFF(IST,2)
          GO TO 65
   60   SHTHB(IST)=HTCOFF(IST,1)/HTCOFF(IST,3)
   65 CONTINUE
C
C ---------------------------------------------------------------
```

```
C ----- CALCULATION OF OVERALL HEAT TRANSFER COEFFICIENT -----
C ------------------------------------------------------------
C
    DO 75 IST=1,NSTN
      QQ=0.0
      TT=0.0
      IPP= IP(IST)
      DO 70 J=1,IPP
        TT=TT+TISURF(IST,J)
        QQ=QQ+QFLXID(IST,J)
 70   CONTINUE
      TAVG(IST)=TT/IPP
      QAVG(IST)=QQ/IPP
      H(IST)=QAVG(IST)/(TAVG(IST)-TBULK(IST))
 75 CONTINUE
C
C ---------------------------------------
C ----- CALCULATE FLUID PROPERTIES -----
C ---------------------------------------
C
    DO 85 IST=1,NSTN
      T=TBULK(IST)
      CALL MEW(T,MFLUID,X2,VISC)
      CALL SPHEAT(T,MFLUID,X2,SPHT)
      CALL CONDFL(T,MFLUID,X2,COND)
      CALL DENS(T,MFLUID,X2,ROW)
      CALL BET(T,MFLUID,X2,BETA)
      PR(IST) = VISC*SPHT/COND
      RENO(IST) = GW*DIN/12.0/VISC
      GRNO(IST)=G*BETA*ROW**2*(DIN/12)**3*(TAVG(IST)-TBULK(IST))
     +      /VISC**2 *3600.0**2
      TIS=0.0
      IPP= IP(IST)
      DO 80 IPR=1,IPP
 80     TIS=TIS+TISURF(IST,IPR)
      T=TIS/IPP
      CALL MEW(T,MFLUID,X2,VISWL)
      VISBW(IST) = VISC/VISWL
      SNUS(IST)=H(IST)*DIN/(12.0*COND)
      TWALL(IST,1)=TAVG(IST)
 85 CONTINUE
C
C ------------------------------------------------
C ----- CALCULATE FLUID VELOCITY IN FT/SEC -----
C ------------------------------------------------
C
      VEL = VFLOW/(2.462557*DIN*DIN)
C
C --------------------------
C ----- PRODUCE OUTPUT -----
C --------------------------
C
    CALL PRNT
C
C ------------------------------------------------------------
C ----- PROMPT USER FOR PROGRAM TERMINATION OR CONTINUATION -----
C ------------------------------------------------------------
C
    WRITE(*,1008)NRUN
    READ(*,*)KEEP
```

```
      IF(KEEP.EQ.1)GO TO 1
      GO TO 4
C
  99 STOP
C
 1001 FORMAT(///////,6X,'HEAT will automatically create output files'
     +     ' with',/,6X,'the following destinations: ',//,6X,
     +     '"RN(run #).OUT"    - Formatted Output Data File ',/,6X,
     +     '"RN(run #).SUM"    - Output Plot/Reduction File ',///,
     +   6X,'The Output Data File may be produced with a format',/,
     +   6X,'specifically created for Dr. Ghajar`s research project',/,
     +   6X,'using 26 stations with four T.C.`s.',/,
     +   6X,'You may select a more general format that will accept',/,
     +   6X,'up to 31 stations with up to eight T.C.`s per station.',//
     +  ,6X,'Enter "1" to select the restricted format (for Ghajar)',/,
     +   6x,'Enter "2" to select the generalized format',///)
 1002 FORMAT(A36)
 1003 FORMAT(A4)
 1004 FORMAT(I4,I3)
 1005 FORMAT(I2,F7.2,F7.4,5F7.2)
 1006 FORMAT(I3,I3,F9.2,8F7.2)
 1007 FORMAT(//5X,'TEMPERATURES AT STATION',I3,' DO NOT CONVERGE AFTER',
     +     I3,' ITERATIONS. JUMP TO NEXT STATION')
 1008 FORMAT(/////////////,6X,'DATA REDUCTION COMPLETED FOR RUN # ',I4,
     +    //6X,'To reduce a data set from another file, ENTER "1"',/,
     +     6x,'To continue program with current file, ENTER "2"',
     +     ///////)
 1009 FORMAT(////////,
     + 7X,'*****************************************************************',
     +/7X,'*                  "HEAT"                       *',
     +/7X,'*                                               *',
     +/7X,'*  A PROGRAM TO CALCULATE THE INSIDE WALL TEMPERATURES &  *',
     +/7X,'*  LOCAL HEAT TRANSFER COEFF.`s FOR GIVEN OUTSIDE WALL    *',
     +/7X,'*  TEMPERATURES FOR SINGLE PHASE HEAT TRANSFER STUDIES IN *',
     +/7X,'*  HORIZONTAL TUBES.  THE PROGRAM ALSO CALCULATES THE     *',
     +/7X,'*  FLUID FLOW & HEAT TRANSFER DIMENSIONLESS NUMBERS.      *',
     +/7X,'*                                               *',
     +/7X,'*  THE MATHEMATICAL ALGORITHM OF THIS PROGRAM HAS BEEN    *',
     +/7X,'*  DEVELOPED BY THE STUDENTS OF DR. J.D. PARKER &         *',
     +/7X,'*  DR. K.J. BELL OF OKLAHOMA STATE UNIVERSITY.            *',
     +/7X,'*                                               *',
     +/7X,'*  THE PROGRAM WAS MODIFIED BY: Y.H. ZURIGAT (APR 1989)  *',
     +/7X,'*                       D.R. MAIELLO (DEC 1989)  *',
     +/7X,'*                                               *',
     +/7X,'*  UNDER THE SUPERVISION OF:   DR. A.J. GHAJAR          *',
     +/7X,'*                       COLLEGE OF MECHANICAL    *',
     +/7X,'*                        & AREOSPACE ENGINEERING  *',
     +/7X,'*                       OKLAHOMA STATE UNIVERSITY *',
     +/7X,'*                                               *',
     +/7X,'*****************************************************************',
     + //,3X,'Press RETURN to Continue.')
C
      END
C
C
C ***********************************************************************
C *                                                     *
C *                SUBROUTINE GEOM                      *
C *                                                     *
C *              ALL LENGTH IN INCHES                   *
```

```
C *                                                                    *
C **********************************************************************
C
      SUBROUTINE GEOM
C
      COMMON /MAIN1/ IST,KOUNT,NSTN
     +     /GEOM1/ XAREA(31),R(31),LTP(32),LTH(32),DELZ(31),LHEAT,
     +          LTEST,LOD(31),DOUT,DIN,DELR,NODES,NSLICE,PI
C
      REAL*4 LTH,LTP,LTEST,LHEAT,LOD
C
      NSLICE=10
      NODES= NSLICE + 1
C
C --------------------------------
C ----- PROMPT FOR PIPE SIZE -----
C --------------------------------
C
    1 WRITE(*,*)' '
      WRITE(*,*)' '
      WRITE(*,*)' '
      WRITE(*,*)' '
      WRITE(*,*)'   SELECT DESIRED PIPE SIZE OPTION:'
      WRITE(*,*)' '
      WRITE(*,*)'      (1) USE "HEAT TRANSFER" DEFAULT VALUES'
      WRITE(*,*)'      (2) USE "PRESSURE DROP" DEFAULT VALUES'
      WRITE(*,*)'      (3) VIEW DEFAULT SETTINGS'
      WRITE(*,*)'      (4) INPUT YOUR OWN PIPE SIZE VALUES'
      READ(*,*)IPSO
C
      IF(IPSO.EQ.1)THEN
        DOUT=.748
        DIN=.624
        LHEAT=230.75
       ELSE
        IF(IPSO.EQ.2)THEN
          DOUT=.749
          DIN=.621
          LHEAT=230.75
         ELSE
          IF(IPSO.EQ.3)THEN
C
      WRITE(*,*)' '
      WRITE(*,*)' '
      WRITE(*,*)'    DEFAULT VALUES ARE (in inches):'
      WRITE(*,*)' '
      WRITE(*,*)'       PIPE       O.D.   I.D.   LENGTH '
      WRITE(*,*)'   ------------- ------ ------ ------'
      WRITE(*,*)'   HEAT TRANSFER   0.748   0.624  230.75 '
      WRITE(*,*)'   PRESSURE DROP   0.749   0.621  230.75 '
      WRITE(*,*)' '
C
           GO TO 1
           ELSE
            IF(IPSO.EQ.4)THEN
C
      WRITE(*,*)' '
      WRITE(*,*)' '
      WRITE(*,*)'  ENTER PIPE OUTSIDE DIAMETER (in inches):'
      READ(*,*)DOUT
```

```
      WRITE(*,*)' '
      WRITE(*,*)'  ENTER PIPE INSIDE DIAMETER (in inches):'
      READ(*,*)DIN
      WRITE(*,*)' '
      WRITE(*,*)'  ENTER PIPE LENGTH (in inches)'
      WRITE(*,*)'  (0.5 inches will be assumed & added for end plates):'
      READ(*,*)LHEAT
C
               ELSE
                 GO TO 1
               ENDIF
             ENDIF
           ENDIF
         ENDIF
C
C
      IF(DOUT.GT.DIN)GO TO 2
      WRITE(*,*)' '
      WRITE(*,*)' '
      WRITE(*,*)' ************* !!!!!! WARNING !!!!!! ***************'
      WRITE(*,*)'  YOU HAVE ENTERED PIPE DIAMETERS WHICH RESULT IN'
      WRITE(*,*)'  A WALL THICKNESS OF ZERO OR LESS. PLEASE TRY AGAIN!'
      WRITE(*,*)' ************************************************'
      GO TO 1
C
C -------------------------------------------------------
C ----- CALCULATE GEOMETRY FOR FINITE DIFFERENCING -----
C -------------------------------------------------------
C
    2 PI = 3.141593
      LTEST = LHEAT+0.5
C
      DO 3 I=1,NSTN
    3   LOD(I)=LTH(I)/DIN
      LTH(NSTN+1)=LHEAT
      LTP(1)=LTH(1)
        SUM=LTP(1)
      DO 4 I=2,NSTN
        LTP(I) =  LTH(I)-LTH(I-1)
    4   SUM=SUM+LTP(I)
        LTP(NSTN+1)=LHEAT-SUM
      DELZ(1) = LTH(1)+( LTH(2)-LTH(1))/2.0
      DO 5 I=2,NSTN
    5   DELZ(I) = ( LTH(I+1)-LTH(I-1))/2.0
      RETURN
      END
C
C
C ***********************************************************************
C *                                     *
C *              SUBROUTINE BET                 *
C *                                     *
C *  CALCULATES THE THERMAL EXPANSION COEFFICIENT (BETA) FOR PURE   *
C *  WATER AND ANY CONCENTRATION OF ETHYLENE GLYCOL/WATER SOLUTION.  *
C *  THE INPUT IS TEMPERATURE IN DEGREES F AND THE OUTPUT IS 1/F.   *
C *                                     *
C ***********************************************************************
C
      SUBROUTINE BET(TF,MFLUID,X,BETA)
      T = (TF-32.0)/1.8
```

```
C
C ----- PURE WATER -----
C
    IF(MFLUID.GT.1)GO TO 1
     PDRT=0.0615-0.01693*T+2.06E-4*T**2-1.77E-6*T**3+6.3E-9*T**4
      GO TO 2
C
C ----- ETHYLENE GLYCOL -----
C
   1  PDRTA = -1.2379*1.E-4 - 9.9189*1.E-4*X +4.1024*1.E-4*X*X
     PDRTB = 2.*((-2.9837E-06*T+2.4614E-06*X*T -9.5278E-8*X*X*T))
     PDRT=(PDRTA+PDRTB)*1000.
   2 CALL DENS(TF,MFLUID,X,ROW)
    ROW=ROW/.062427
    BETAC= -(1.0/ROW)*(PDRT)
    BETAF =(1.0/BETAC)*1.8
    BETA  = 1.0/BETAF
C
    RETURN
    END
C
C
C ***********************************************************************
C *                                                                     *
C *                 SUBROUTINE CONDFL                                   *
C *                                                                     *
C *    CALCULATES THE THERMAL CONDUCTIVITY (COND) FOR PURE WATER        *
C *     AND ANY CONCENTRATION OF ETHYLENE GLYCOL/WATER SOLUTION.        *
C *          THE INPUT IS TEMPERATURE IN DEGREES F                      *
C *           AND THE OUTPUT IS IN BTU/HR-FT-'F                         *
C *                                                                     *
C *        TEMPERATURE RANGE:                                           *
C *           PURE WATER        0 - 100 C                               *
C *           E.G. MIXTURES     0 - 150 C                               *
C *                                                                     *
C ***********************************************************************
C
     SUBROUTINE CONDFL(TF,MFLUID,X,COND)
C
    T=(TF-32.0)/1.8
    CONW=0.56276+1.874E-3*T-6.8E-6*T**2
C
    IF(MFLUID.GT.1) GO TO 1
C
C ----- PURE WATER -----
C
    IF(T.LT.0.0.OR.T.GT.100.0)THEN
     WRITE(*,*)' TEMPERATURE IS OUT OF RANGE IN SUBROUTINE CONDFL'
     STOP
    END IF
C
     COND=CONW*0.5778
      GO TO 2
C
C ----- ETHYLENE GLYCOL -----
C
   1 IF(T.LT.0.0.OR.T.GT.150.0)THEN
     WRITE(*,*)' TEMPERATURE IS OUT OF RANGE IN SUBROUTINE CONDFL'
     STOP
    END IF
```

```
C
      CETH=0.24511+0.0001755*T-8.52E-7*T*T
      CF=0.6635-0.3698*X-0.000885*T
      COND=(1.0-X)*CONW+X*CETH-CF*(CONW-CETH)*(1.0-X)*X
     COND=COND*0.5778
    2 RETURN
      END
C
C
C ***********************************************************************
C *                                                                     *
C *               SUBROUTINE DENS                                       *
C *                                                                     *
C *      CALCULATES THE FLUID DENSITY (ROW) FOR PURE WATER              *
C *    AND ANY CONCENTRATION OF ETHYLENE GLYCOL/WATER SOLUTION.         *
C * THE INPUT IS TEMPERATURE IN DEGREES F AND THE OUTPUT IS LB/FT**3.   *
C *                                                                     *
C *        TEMPERATURE RANGE:                                           *
C *           PURE WATER        0 - 100 C                              *
C *           E.G. MIXTURES     0 - 150 C                              *
C *                                                                     *
C ***********************************************************************
C
      SUBROUTINE DENS(TF,MFLUID,X,ROW)
      DIMENSION D(3,3),AD(3,3)
C
      T=(TF-32.0)/1.8
      IF(MFLUID.GT.1) GO TO 1
C
C ----- PURE WATER -----
C
      IF(T.LT.0..OR.T.GT.100.0)THEN
       WRITE(*,*)' TEMPERATURE IS OUT OF RANGE IN SUBROUTINE DENS'
       STOP
      END IF
C
C
      ROWSI=999.86+.061464*T-.0084648*T**2+6.8794E-5*T**3-4.4214E-7
     +     *T**4+1.2505E-9*T**5
      ROW=ROWSI*0.062427
      GO TO 4
C
C ----- ETHYLENE GLYCOL -----
C
    1 IF(T.LT.0.0.OR.T.GT.150.0)THEN
       WRITE(*,*)' TEMPERATURE IS OUT OF RANGE IN SUBROUTINE DENS'
       STOP
      END IF
C
      AD(1,1)=1.0004
      AD(1,2)=0.17659
      AD(1,3)=-0.049214
      AD(2,1)=-1.2379E-04
      AD(2,2)=-9.9189E-04
      AD(2,3)= 4.1024E-04
      AD(3,1)=-2.9837E-06
      AD(3,2)= 2.4614E-06
      AD(3,3)= -9.5278E-08
C
      DO 2 I=1,3
```

```
      DO 2 J=1,3
    2 D(I,J)=AD(I,J)*X**(J-1)*T**(I-1)
      SUM=0.0
      DO 3 I=1,3
      DO 3 J=1,3
    3 SUM=SUM+D(I,J)
      SUM=SUM*1.E6/1000.0
      ROW=SUM*0.062427
C
    4 RETURN
      END
C
C
C ***********************************************************************
C *                                                                     *
C *                SUBROUTINE MEW                                       *
C *                                                                     *
C *     CALCULATES THE DYNAMIC VISCOSITY (VISC) FOR PURE WATER          *
C *     AND ANY CONCENTRATION OF ETHYLENE GLYCOL/WATER SOLUTION.        *
C * THE INPUT IS TEMPERATURE IN DEGREES F AND THE OUTPUT IS LB/HR.FT.   *
C *                                                                     *
C *        TEMPERATURE RANGE:                                           *
C *           PURE WATER        10 - 100 C                             *
C *           E.G. MIXTURES      0 - 150 C                             *
C *                                                                     *
C ***********************************************************************
C
      SUBROUTINE MEW(TF,MFLUID,X,VISC)
      DIMENSION V(3,3),AV(3,3),V2(3)
C
      T=(TF-32.0)/1.8
      IF(MFLUID.GT.1) GO TO 1
C
C ----- PURE WATER -----
C
      IF(T.LT.10..OR.T.GT.100.0)THEN
       WRITE(*,*)' TEMPERATURE IS OUT OF RANGE IN SUBROUTINE MEW'
       STOP
      END IF
C
      VISC=2.4189*1.0019*10.0**((1.3272*(20.0-T)-0.001053*(20-T)
     +    **2)/(T+105.0))
       GO TO 4
C
C ----- ETHYLENE GLYCOL -----
C
    1 IF(T.LT.0..OR.T.GT.150.0)THEN
       WRITE(*,*)' TEMPERATURE IS OUT OF RANGE IN SUBROUTINE MEW'
       STOP
      END IF
C
      AV(1,1)=0.55164
      AV(1,2)=2.6492
      AV(1,3)=0.82935
      AV(2,1)=-0.027633
      AV(2,2)=-0.031496
      AV(2,3)= 0.0048136
      AV(3,1)= 6.0629E-17
      AV(3,2)= 2.2389E-15
      AV(3,3)= 5.879E-16
```

```
C
    DO 2 I=1,2
     DO 2 J=1,3
      V(I,J)=AV(I,J)*X**(J-1)*T**(I-1)
  2   V2(J)=AV(3,J)*X**(J-1)
C
      SUM=0.0
    DO 3 I=1,3
  3  SUM=SUM+V2(I)
     V3=SUM**0.25*T*T
     VISC=V3 + V(1,1)+V(1,2)+V(1,3)+V(2,1)+V(2,2)+V(2,3)
    VISC=EXP(VISC)*2.4189
C
  4 RETURN
    END
C
C
C ********************************************************************
C *                                                                  *
C *              SUBROUTINE PRNUM                                    *
C *                                                                  *
C *     CALCULATES THE PRANDTL NO.(PRN) FOR PURE WATER               *
C *   AND ANY CONCENTRATION OF ETHYLENE GLYCOL/WATER SOLUTION.       *
C *        THE INPUT IS TEMPERATURE IN DEGREES F.                    *
C *                                                                  *
C *        TEMPERATURE RANGE:                                        *
C *           PURE WATER        10 - 100 C                           *
C *           E.G. MIXTURES      0 - 150 C                           *
C *                                                                  *
C ********************************************************************
C
    SUBROUTINE PRNUM(TF,MFLUID,X,PRN)
    DIMENSION P(3,3),AP(3,3),P2(3)
C
    T=(TF-32.0)/1.8
    IF(MFLUID.GT.1) GO TO 1
C
C ----- PURE WATER -----
C
    IF(T.LT.10.OR.T.GT.100.0)THEN
     WRITE(*,*)' TEMPERATURE IS OUT OF RANGE IN SUBROUTINE PRNUM'
     STOP
    END IF
C
      CALL SPHEAT(TF,MFLUID,X,SPHT)
      CALL MEW(TF,MFLUID,X,VISC)
      CALL CONDFL(TF,MFLUID,X,COND)
      PRN=SPHT*VISC/COND
      RETURN
C
C ----- ETHYLENE GLYCOL -----
C
  1 IF(T.LT.0.0.OR.T.GT.150.0)THEN
     WRITE(*,*)' TEMPERATURE IS OUT OF RANGE IN SUBROUTINE PRNUM'
     STOP
    END IF
C
    AP(1,1)=2.5735
    AP(1,2)=3.0411
    AP(1,3)=0.60237
```

```
      AP(2,1)=-0.031169
      AP(2,2)=-0.025424
      AP(2,3)= 0.0037454
      AP(3,1)= 1.1605E-16
      AP(3,2)= 2.5283E-15
      AP(3,3)= 2.3777E-16
C
      DO 2 I=1,2
       DO 2 J=1,3
        P(I,J)=AP(I,J)*X**(J-1)*T**(I-1)
    2   P2(J)=AP(3,J)*X**(J-1)
C
       SUM=0.0
C
       DO 3 I=1,3
    3    SUM=SUM+P2(I)
      P3=SUM**0.25*T*T
      PRN=P3+P(1,1)+P(1,2)+P(1,3)+P(2,1)+P(2,2)+P(2,3)
      PRN=EXP(PRN)
C
      RETURN
      END
C
C
C ***********************************************************************
C *                                                                     *
C *                SUBROUTINE SPHEAT                                    *
C *                                                                     *
C *     CALCULATES THE SPECIFIC HEAT (SPHT) FOR PURE WATER              *
C *    AND ANY CONCENTRATION OF ETHYLENE GLYCOL/WATER SOLUTION.         *
C *         THE INPUT IS TEMPERATURE IN DEGREES F                       *
C *          AND THE OUTPUT IS IN BTU/(LBM-DEGF).                       *
C *                                                                     *
C *       TEMPERATURE RANGE:                                            *
C *          PURE WATER        0 - 100 C                                *
C *          E.G. MIXTURES     0 - 150 C                                *
C *                                                                     *
C ***********************************************************************
C
      SUBROUTINE SPHEAT(TF,MFLUID,X,SPHT)
C
      T=(TF-32.0)/1.8
      IF(MFLUID .GT. 1.0)GO TO 1
C
C ----- PURE WATER -----
C
      IF(T.LT.0.0.OR.T.GT.100.0)THEN
       WRITE(*,*)' TEMPERATURE IS OUT OF RANGE IN SUBROUTINE SPHT'
       STOP
      END IF
C
      SPHT=-1.475E-7*T**3+3.66E-5*T*T-.0022*T+4.216
      SPHT=SPHT/4.1868
      RETURN
C
C ----- ETHYLENE GLYCOL -----
C
    1 IF(T.LT.0.0.OR.T.GT.150.0)THEN
       WRITE(*,*)' TEMPERATURE IS OUT OF RANGE IN SUBROUTINE SPHT'
       STOP
```

```
      END IF
C
      CALL MEW(TF,MFLUID,X,VISC)
      CALL CONDFL(TF,MFLUID,X,COND)
      CALL PRNUM(TF,MFLUID,X,PRN)
      SPHT = PRN*COND/VISC
      RETURN
      END
C
C
C ***********************************************************************
C *                                                                     *
C *                 SUBROUTINE PRINT-OUT                                *
C *                                                                     *
C *         PRINTS DATA TO OUTPUT FILES:                                *
C *                                                                     *
C *              "RN(run #).OUT"    - Device #6                         *
C *              "RN(run #).SUM"    - Device #9                         *
C *                                                                     *
C ***********************************************************************
C
      SUBROUTINE PRNT
C
      DIMENSION SITOC(31,8),SITB(31),HAVG(31),PWP(31),
     +        SIH(31),SIHP(31,8),SIQIN(31,8),PRNU(31),SITIS(31,8)
C
      INTEGER IREN(31,8),IDFLX(31,8),IHCOF(31,8)
      COMMON /PRINT/ IPICK,REN(31,8),TBULK(31),VEL,REYNO,PRNO,GW,
     +           HTCOFF(31,8),H(31),RENO(31),GRNO(31),PR(31),
     +           SNUS(31),VISBW(31),SHTHB(32),QFLXID(31,8),QFLXAV,
     +           QGEXPT,QBALC,QPCT,IGO,IPMAX,TAVG(31)
     +     /INPUT/ TROOM,VOLTS,TAMPS,RMFL,MFLUID,X2,FLOWRT,NRUN,VFLOW,
     +           TIN,TOUT,TOSURF(31,8),TISURF(31,8),IP(32),KST(32)
     +     /TEMP1/ TWALL(31,8),AMPS(31,8),RESIS(31,8),POWERS(32),
     +           TPOWER
     +     /MAIN1/ IST,KOUNT,NSTN
     +     /GEOM1/ XAREA(31),R(31),LTP(32),LTH(32),DELZ(31),LHEAT,
     +           LTEST,LOD(31),DOUT,DIN,DELR,NODES,NSLICE,PI
C
      REAL*4 LTH,LTP,LTEST,LHEAT,H,HAV,HTCOFF,HEF,HMIX,LOD
C
C ------------------------------------------------
C ----- SET FLAG FOR STATION OUTPUT CONTROL -----
C ------------------------------------------------
C
      ATST=NSTN/9.
      IFST=INT(ATST)+1
C
C ---------------------------------------
C ----- PRINT RUN NUMBER & TUBE DATA -----
C ---------------------------------------
C
      IF(IPICK.EQ.2)GO TO 1
C
C ----- ENGLISH UNITS -----
C
      WRITE(6,2001)NRUN
C
C ----- PRINT FLUID-TYPE DESCRIPTION -----
C
```

```
      IF(MFLUID.EQ.1)THEN
        WRITE(6,2003)
          ELSE
          WRITE(6,2004)X2
      ENDIF
C
C ----- PRINT TUBE DATA -----
C
      IGW=GW
      IREYN=REYNO
      IFXA=QFLXAV
      IQEX=QGEXPT
      IQBL=QBALC
C
      WRITE(6,2016)VFLOW,RMFL,IGW,VEL,TROOM,TIN,TOUT,IREYN,PRNO,
     +          TAMPS,VOLTS,IFXA,IQEX,IQBL,QPCT
C
      GO TO 2
C
C ----- S.I. UNITS -----
C
    1 SRMFL=RMFL*.126
      FLOWRT=63.09*FLOWRT
      SITR=(TROOM-32.0)/1.8
      SITIN=(TIN-32.0)/1.8
      SITOUT=(TOUT-32.0)/1.8
      SITR=(TROOM-32.0)/1.8
      SIGW=GW/737.33806
      SIQAV=QFLXAV*3.154591
      SIQG=QGEXPT*0.2930711
      SIQBAL=QBALC*0.2930711
      SIVEL=VEL*.3048
      WRITE(6,2001)NRUN
C
C ----- PRINT FLUID-TYPE DESCRIPTION -----
C
      IF(MFLUID.EQ.1)THEN
        WRITE(6,2003)
          ELSE
          WRITE(6,2004)X2
      ENDIF
C
C ----- PRINT TUBE DATA -----
C
      IGW=SIGW
      IREYN=REYNO
      IFXA=SIQAV
      IQEX=SIQG
      IQBL=SIQBAL
C
      WRITE(6,2018)FLOWRT,SRMFL,IGW,SIVEL,SITR,SITIN,SITOUT,IREYN,PRNO,
     +          TAMPS,VOLTS,IFXA,IQEX,IQBL,QPCT
C
C ------------------------------------------------------
C ----- PRINT TUBE OUTSIDE SURFACE TEMPERATURES -----
C ------------------------------------------------------
C
    2 IF(IPICK.EQ.2)GO TO 8
C
C ----- ENGLISH UNITS -----
```

```
C
    DO 5 K=1,NSTN
    IF(IP(K).EQ.2)THEN
      TOSURF(K,3)=TOSURF(K,2)
      TOSURF(K,2)=0.0
      TOSURF(K,4)=0.0
     ELSE
  5 ENDIF
C
    WRITE(6,2005)
    DO 7 ICNT=1,IFST
     KMIN=1+(ICNT-1)*9
     KMAX=KMIN+8
     IF(NSTN.LT.KMAX)KMAX=NSTN
      DO 6 IPR=1,IPMAX
       IF(IPR.EQ.1)WRITE(6,2006)(KST(K),K=KMIN,KMAX)
       IF(IPR.EQ.1 .AND. KMAX.LT.(KMIN+8))WRITE(6,2007)
C
       IF((IPR.EQ.2.OR.IPR.EQ.4).AND.ICNT.EQ.IFST.AND.IGO.EQ.1)THEN
         WRITE(6,2008)IPR,(TOSURF(IST,IPR),IST=KMIN,KMAX-5)
           ELSE
           WRITE(6,2008)IPR,(TOSURF(IST,IPR),IST=KMIN,KMAX)
       ENDIF
C
  6   CONTINUE
  7  CONTINUE
C
    IF(IGO.EQ.1)WRITE(6,2002)
    GO TO 13
C
C ----- S.I. UNITS -----
C
  8 DO 9 IST=1,NSTN
      IPP= IP(IST)
      DO 9 IPR=1,IPP
        SITOC(IST,IPR) = (TOSURF(IST,IPR)-32.0)/1.8
  9 CONTINUE
C
    DO 10 K=1,NSTN
    IF(IP(K).EQ.2)THEN
      SITOC(K,3)=SITOC(K,2)
      SITOC(K,2)=0.0
      SITOC(K,4)=0.0
     ELSE
 10 ENDIF
C
    WRITE(6,2009)
    DO 12 ICNT=1,IFST
     KMIN=1+(ICNT-1)*9
     KMAX=KMIN+8
     IF(NSTN.LT.KMAX)KMAX=NSTN
      DO 11 IPR=1,IPMAX
       IF(IPR.EQ.1)WRITE(6,2006)(KST(K),K=KMIN,KMAX)
       IF(IPR.EQ.1 .AND. KMAX.LT.(KMIN+8))WRITE(6,2007)
C
       IF((IPR.EQ.2.OR.IPR.EQ.4).AND.ICNT.EQ.IFST.AND.IGO.EQ.1)THEN
         WRITE(6,2008)IPR,(SITOC(IST,IPR),IST=KMIN,KMAX-5)
           ELSE
           WRITE(6,2008)IPR,(SITOC(IST,IPR),IST=KMIN,KMAX)
       ENDIF
```

```
C
  11  CONTINUE
  12  CONTINUE
    IF(IGO.EQ.1)WRITE(6,2002)
C
C -----------------------------------------------------------
C ----- PRINT INSIDE SURFACE TEMPERATURES TO OUTPUT FILE -----
C -----------------------------------------------------------
  13 WRITE(6,2017)NRUN
    IF(IPICK.EQ.2)GO TO 17
C
C ----- ENGLISH UNITS -----
C
     DO 14 K=1,NSTN
     IF(IP(K).EQ.2)THEN
       TISURF(K,3)=TISURF(K,2)
       TISURF(K,2)=0.0
       TISURF(K,4)=0.0
      ELSE
   14 ENDIF
C
     WRITE(6,2010)
     DO 16 ICNT=1,IFST
      KMIN=1+(ICNT-1)*9
      KMAX=KMIN+8
      IF(NSTN.LT.KMAX)KMAX=NSTN
       DO 15 IPR=1,IPMAX
       IF(IPR.EQ.1)WRITE(6,2006)(KST(K),K=KMIN,KMAX)
       IF(IPR.EQ.1 .AND. KMAX.LT.(KMIN+8))WRITE(6,2007)
C
       IF((IPR.EQ.2.OR.IPR.EQ.4).AND.ICNT.EQ.IFST.AND.IGO.EQ.1)THEN
         WRITE(6,2008)IPR,(TISURF(IST,IPR),IST=KMIN,KMAX-5)
           ELSE
           WRITE(6,2008)IPR,(TISURF(IST,IPR),IST=KMIN,KMAX)
   15  ENDIF
C
   16  CONTINUE
C
     GO TO 22
C
C ----- S.I. UNITS -----
C
   17 DO 18 IST=1,NSTN
       IPP= IP(IST)
       DO 18 IPR=1,IPP
         SITIS(IST,IPR)=(TISURF(IST,IPR)-32.0)/1.8
   18 CONTINUE
C
     DO 19 K=1,NSTN
     IF(IP(K).EQ.2)THEN
       SITIS(K,3)=SITIS(K,2)
       SITIS(K,2)=0.0
       SITIS(K,4)=0.0
      ELSE
   19 ENDIF
C
     WRITE(6,2011)
     DO 21 ICNT=1,IFST
      KMIN=1+(ICNT-1)*9
      KMAX=KMIN+8
```

```
      IF(NSTN.LT.KMAX)KMAX=NSTN
       DO 20 IPR=1,IPMAX
        IF(IPR.EQ.1)WRITE(6,2006)(KST(K),K=KMIN,KMAX)
        IF(IPR.EQ.1 .AND. KMAX.LT.(KMIN+8))WRITE(6,2007)
C
        IF((IPR.EQ.2.OR.IPR.EQ.4).AND.ICNT.EQ.IFST.AND.IGO.EQ.1)THEN
          WRITE(6,2008)IPR,(SITIS(IST,IPR),IST=KMIN,KMAX-5)
            ELSE
            WRITE(6,2008)IPR,(SITIS(IST,IPR),IST=KMIN,KMAX)
  20    ENDIF
C
  21  CONTINUE
C
C ------------------------------------------------
C ----- PRINT REYNOLDS NUMBERS TO OUTPUT FILE -----
C ------------------------------------------------
  22 DO 29 K=1,NSTN
     IF(IP(K).EQ.2)THEN
       IREN(K,1)=INT(REN(K,1))
       IREN(K,3)=INT(REN(K,2))
       IREN(K,2)=0
       IREN(K,4)=0
      ELSE
       DO 28 L=1,IPMAX
  28    IREN(K,L)=INT(REN(K,L))
  29 ENDIF
C
      WRITE(6,2014)
      DO 31 ICNT=1,IFST
       KMIN=1+(ICNT-1)*9
       KMAX=KMIN+8
       IF(NSTN.LT.KMAX)KMAX=NSTN
        DO 30 IPR=1,IPMAX
         IF(IPR.EQ.1)WRITE(6,2006)(KST(K),K=KMIN,KMAX)
         IF(IPR.EQ.1 .AND. KMAX.LT.(KMIN+8))WRITE(6,2007)
C
        IF((IPR.EQ.2.OR.IPR.EQ.4).AND.ICNT.EQ.IFST.AND.IGO.EQ.1)THEN
          WRITE(6,2015)IPR,(IREN(IST,IPR),IST=KMIN,KMAX-5)
            ELSE
            WRITE(6,2015)IPR,(IREN(IST,IPR),IST=KMIN,KMAX)
  30    ENDIF
C
  31  CONTINUE
      IF(IGO.EQ.1)WRITE(6,2012)
C
C ------------------------------------------------
C ----- PRINT INSIDE HEAT FLUXES TO OUTPUT FILE -----
C ------------------------------------------------
C
  33 WRITE(6,2017)NRUN
     IF(IPICK.EQ.2)GO TO 38
C
C ----- ENGLISH UNITS -----
C
      DO 35 K=1,NSTN
      IF(IP(K).EQ.2)THEN
        IDFLX(K,1)=INT(QFLXID(K,1))
        IDFLX(K,3)=INT(QFLXID(K,2))
        IDFLX(K,2)=0
        IDFLX(K,4)=0
```

```
      ELSE
       DO 34 L=1,IPMAX
  34    IDFLX(K,L)=INT(QFLXID(K,L))
  35  ENDIF
C
     WRITE(6,2020)
     DO 37 ICNT=1,IFST
      KMIN=1+(ICNT-1)*9
      KMAX=KMIN+8
      IF(NSTN.LT.KMAX)KMAX=NSTN
       DO 36 IPR=1,IPMAX
       IF(IPR.EQ.1)WRITE(6,2006)(KST(K),K=KMIN,KMAX)
       IF(IPR.EQ.1 .AND. KMAX.LT.(KMIN+8))WRITE(6,2007)
C
       IF((IPR.EQ.2.OR.IPR.EQ.4).AND.ICNT.EQ.IFST.AND.IGO.EQ.1)THEN
         WRITE(6,2021)IPR,(IDFLX(IST,IPR),IST=KMIN,KMAX-5)
           ELSE
           WRITE(6,2021)IPR,(IDFLX(IST,IPR),IST=KMIN,KMAX)
  36    ENDIF
C
  37  CONTINUE
C
     GO TO 44
C
C ----- S.I. UNITS -----
C
  38 DO 39 IST=1,NSTN
       IPP= IP(IST)
       DO 39 IPR=1,IPP
         SIQIN(IST,IPR)=QFLXID(IST,IPR)*3.15491
  39 CONTINUE
C
     DO 41 K=1,NSTN
     IF(IP(K).EQ.2)THEN
       IDFLX(K,1)=INT(SIQIN(K,1))
       IDFLX(K,3)=INT(SIQIN(K,2))
       IDFLX(K,2)=0
       IDFLX(K,4)=0
      ELSE
       DO 40 L=1,IPMAX
  40    IDFLX(K,L)=INT(SIQIN(K,L))
  41 ENDIF
C
     WRITE(6,2022)
     DO 43 ICNT=1,IFST
      KMIN=1+(ICNT-1)*9
      KMAX=KMIN+8
      IF(NSTN.LT.KMAX)KMAX=NSTN
       DO 42 IPR=1,IPMAX
       IF(IPR.EQ.1)WRITE(6,2006)(KST(K),K=KMIN,KMAX)
       IF(IPR.EQ.1 .AND. KMAX.LT.(KMIN+8))WRITE(6,2007)
C
       IF((IPR.EQ.2.OR.IPR.EQ.4).AND.ICNT.EQ.IFST.AND.IGO.EQ.1)THEN
         WRITE(6,2021)IPR,(IDFLX(IST,IPR),IST=KMIN,KMAX-5)
           ELSE
           WRITE(6,2021)IPR,(IDFLX(IST,IPR),IST=KMIN,KMAX)
  42    ENDIF
C
  43  CONTINUE
C
```

```
C -------------------------------------------------------
C ---- PRINT PERIPHERAL HEAT TRANSFER COEFFICIENTS -----
C -------------------------------------------------------
C
  44 IF(IPICK.EQ.2)GO TO 49
C
C ----- ENGLISH UNITS -----
C
     DO 46 K=1,NSTN
     IF(IP(K).EQ.2)THEN
       IHCOF(K,1)=INT(HTCOFF(K,1))
       IHCOF(K,3)=INT(HTCOFF(K,2))
       IHCOF(K,2)=0
       IHCOF(K,4)=0
      ELSE
       DO 45 L=1,IPMAX
  45   IHCOF(K,L)=INT(HTCOFF(K,L))
  46 ENDIF
C
     WRITE(6,2023)
     DO 48 ICNT=1,IFST
      KMIN=1+(ICNT-1)*9
      KMAX=KMIN+8
      IF(NSTN.LT.KMAX)KMAX=NSTN
       DO 47 IPR=1,IPMAX
        IF(IPR.EQ.1)WRITE(6,2006)(KST(K),K=KMIN,KMAX)
        IF(IPR.EQ.1 .AND. KMAX.LT.(KMIN+8))WRITE(6,2007)
C
        IF((IPR.EQ.2.OR.IPR.EQ.4).AND.ICNT.EQ.IFST.AND.IGO.EQ.1)THEN
          WRITE(6,2021)IPR,(IHCOF(IST,IPR),IST=KMIN,KMAX-5)
            ELSE
            WRITE(6,2021)IPR,(IHCOF(IST,IPR),IST=KMIN,KMAX)
  47    ENDIF
C
  48  CONTINUE
C
C
     GO TO 55
C
C ----- S.I. UNITS -----
C
  49 DO 50 IST=1,NSTN
       IPP= IP(IST)
       DO 50 IPR=1,IPP
         SIHP(IST,IPR)=HTCOFF(IST,IPR)*5.678263
  50 CONTINUE
C
     DO 52 K=1,NSTN
     IF(IP(K).EQ.2)THEN
       IHCOF(K,1)=INT(SIHP(K,1))
       IHCOF(K,3)=INT(SIHP(K,2))
       IHCOF(K,2)=0
       IHCOF(K,4)=0
      ELSE
       DO 51 L=1,IPMAX
  51   IHCOF(K,L)=INT(SIHP(K,L))
  52 ENDIF
C
     WRITE(6,2024)
     DO 54 ICNT=1,IFST
```

```
      KMIN=1+(ICNT-1)*9
      KMAX=KMIN+8
      IF(NSTN.LT.KMAX)KMAX=NSTN
       DO 53 IPR=1,IPMAX
        IF(IPR.EQ.1)WRITE(6,2006)(KST(K),K=KMIN,KMAX)
        IF(IPR.EQ.1 .AND. KMAX.LT.(KMIN+8))WRITE(6,2007)
C
        IF((IPR.EQ.2.OR.IPR.EQ.4).AND.ICNT.EQ.IFST.AND.IGO.EQ.1)THEN
          WRITE(6,2021)IPR,(IHCOF(IST,IPR),IST=KMIN,KMAX-5)
            ELSE
            WRITE(6,2021)IPR,(IHCOF(IST,IPR),IST=KMIN,KMAX)
   53   ENDIF
C
   54  CONTINUE
C
C ----------------------------------------------
C ----- PRINT SUMMATION DATA FOR OUTPUT FILE -----
C ----------------------------------------------
C
   55 IF(IGO.EQ.1)WRITE(6,2012)
      WRITE(6,2028)NRUN
C
      WRITE(6,2029)
      DO 56 J=1,NSTN
      IF(IPICK.EQ.2)H(J)=H(J)*5.678263
      IF(IPICK.EQ.2)TBULK(J)=(TBULK(J)-32.0)/1.8
      IF(IPICK.EQ.2)TAVG(J)=(TAVG(J)-32.0)/1.8
      LRENO=INT(RENO(J))
      IGRNO=INT(GRNO(J))
      IHAV=INT(H(J))
      WRITE(6,2030)KST(J),LOD(J),TBULK(J),LRENO,PR(J),SNUS(J),IGRNO,
     +          VISBW(J),SHTHB(J),IHAV
   56  CONTINUE
C
C ----- PRINT NOTE GIVING UNITS -----
C
      IF(IPICK.EQ.1)WRITE(6,2032)
      IF(IPICK.EQ.2)WRITE(6,2034)
C
C ------------------------------------------------------
C -----      PRINT OUTPUT DATA FOR USE WITH:     -----
C ----- "MARQ" - A CURVE-FITTING ROUTINE         -----
C ----- "SIGMAPLOT" OR SIMULAR GRAPHICS PACKAGES -----
C ------------------------------------------------------
C
      DO 57 I=1,NSTN
       WRITE(9,2033)SNUS(I),RENO(I),PR(I),GRNO(I),LOD(I),VISBW(I),H(I),
     +          TBULK(I),TAVG(I)
   57     CONTINUE
C
C ----- PRINT END OF FILE FLAG TO FILE FOR USE WITH "MARQ" -----
C
          EOFF=0.00
          WRITE(9,2033)EOFF,EOFF,EOFF,EOFF,EOFF,EOFF,EOFF,EOFF,EOFF
C
      RETURN
C
 2001 FORMAT(//,18X,'*',41('-'),'*',/32X,'RUN NUMBER ',I4)
 2002 FORMAT(/////////////)
 2003 FORMAT(25X,'TEST FLUID IS DISTILLED WATER',/18X,'*',41('-'),'*')
```

```
2004 FORMAT(19X,'MASS FRACTION OF ETHYLENE GLYCOL =',F8.4,/18X,'*',
     +     41('-'),'*')
2005 FORMAT(////20X,'OUTSIDE SURFACE TEMPERATURES - DEGREES F')
2006 FORMAT(//,8X,I2,6X,I2,6X,I2,6X,I2,6X,I2,6X,I2,6X,I2,6X,I2,6X,I2,6X,I2,/)
2007 FORMAT(' ')
2008 FORMAT(3X,I1,1X,9F8.2)
2009 FORMAT(////20X,'OUTSIDE SURFACE TEMPERATURES - DEGREES C')
2010 FORMAT(///20X,'INSIDE SURFACE TEMPERATURES - DEGREES F')
2011 FORMAT(///20X,'INSIDE SURFACE TEMPERATURES - DEGREES C')
2012 FORMAT(////)
2013 FORMAT(4X,9F8.2)
2014 FORMAT(///20X,'REYNOLDS NUMBER AT THE INSIDE TUBE WALL')
2015 FORMAT(3X,I1,9I8)
2016 FORMAT(//,18X,'VOLUMETRIC FLOW RATE =',F9.2,3X,'GPM',
     +     /18X,'MASS FLOW RATE',7X,'=',F9.1,3X,'LBM/HR',
     +     /18X,'MASS FLUX',12X,'=',I9,3X,'LBM/(SQ.FT-HR)',
     +     /18X,'FLUID VELOCITY',7X,'=',F9.2,3X,'FT/S',
     +     /18X,'ROOM TEMPERATURE',5X,'=',F9.2,3X,'F',
     +     /18X,'INLET TEMPERATURE',4X,'=',F9.2,3X,'F',
     +     /18X,'OUTLET TEMPERATURE',3X,'=',F9.2,3X,'F',
     +     /18X,'AVERAGE RE NUMBER',4X,'=',I9,
     +     /18X,'AVERAGE PR NUMBER',4X,'=',F9.2,
     +     /18X,'CURRENT TO TUBE',6X,'=',F9.1,3X,'AMPS',
     +     /18X,'VOLTAGE DROP IN TUBE =',F9.2,3X,'VOLTS',
     +     /18X,'AVERAGE HEAT FLUX',4X,'=',I9,3X,'BTU/(SQ.FT-HR)'
     +     /18X,'Q=AMP*VOLT',11X,'=',I9,3X,'BTU/HR',
     +     /18X,'Q=M*C*(T2-T1)',8X,'=',I9,3X,'BTU/HR',
     +     /18X,'HEAT BALANCE ERROR',3X,'=',F9.2,3X,'%')
2017 FORMAT(//31X,'*',15('-'),'*',/32X,'RUN NUMBER ',I4,/31X,'*',
     +      15('-'),'*')
2018 FORMAT(//,18X,'VOLUMETRIC FLOW RATE =',F9.2,3X,'CC/SEC',
     +     /18X,'MASS FLOW RATE',7X,'=',F9.1,3X,'KG/SEC',
     +     /18X,'MASS FLUX',12X,'=',I9,3X,'KG/(SQ.M-SEC)',
     +     /18X,'FLUID VELOCITY',7X,'=',F9.2,3X,'M/S',
     +     /18X,'ROOM TEMPERATURE',5X,'=',F9.2,3X,'C',
     +     /18X,'INLET TEMPERATURE',4X,'=',F9.2,3X,'C',
     +     /18X,'OUTLET TEMPERATURE',3X,'=',F9.2,3X,'C',
     +     /18X,'AVERAGE RE NUMBER',4X,'=',I9,
     +     /18X,'AVERAGE PR NUMBER',4X,'=',F9.2,
     +     /18X,'CURRENT TO TUBE',6X,'=',F9.1,3X,'AMPS',
     +     /18X,'VOLTAGE DROP IN TUBE =',F9.2,3X,'VOLTS',
     +     /18X,'AVERAGE HEAT FLUX',4X,'=',I9,3X,'W/(SQ. M)'
     +     /18X,'Q=AMP*VOLT',11X,'=',I9,3X,'W',
     +     /18X,'Q=M*C*(T2-T1)',8X,'=',I9,3X,'W',
     +     /18X,'HEAT BALANCE ERROR',3X,'=',F9.2,3X,'%')
2020 FORMAT(///22X,'INSIDE SURFACE HEAT FLUXES BTU/HR/FT2')
2021 FORMAT(3X,I1,9I8)
2022 FORMAT(///22X,'INSIDE SURFACE HEAT FLUXES W PER SQ.M.')
2023 FORMAT(///14X,'PERIPHERAL HEAT TRANSFER COEFFICIENT BTU/',
     +     '(SQ.FT-HR-F)')
2024 FORMAT(///16X,'PERIPHERAL HEAT TRANSFER COEFFICIENT W/(SQ.M. K)')
2027 FORMAT(///18X,'AVERAGE HEAT TRANSFER COEFFICIENT-W/(SQ.M. K)')
2028 FORMAT(//31X,'*',15('-'),'*',/32X,'RUN NUMBER ',I4,/36X,
     +     'SUMMARY',/31X,'*',15('-'),'*',)
2029 FORMAT(///8X,'X/D',4X,'TBULK',4X,'RE',6X,'PR',
     +     6X,'NU',6X,'GR',5X,'MUB/',3X,'HTOP/',4X,'H',/,22X,
     +     'NUMBER',2X,'NUMBER',2X,'NUMBER',2X,'NUMBER',3X,'MUW',4X,
     +     'HBOT',4X,'AVG',/)
2030 FORMAT(2X,I2,2F8.2,I8,F8.2,F8.1,I8,F7.3,F7.2,I8)
2032 FORMAT(//,13X,'NOTE: TBULK IS GIVEN IN DEGREES "F"',/,
```

```
     +       19X,'H(AVG) IS GIVEN IN BTU/(FT^2*HR*F)')
 2033 FORMAT(3F10.3,F15.3,3F10.3,2F8.2)
 2034 FORMAT(///,13X,'NOTE: TBULK IS GIVEN IN DEGREES "C"',/,
     +       19X,'H(AVG) IS GIVEN IN W/(M^2*K)')
C
      END
```

A.2 Program RQ

The program RQ is a non-linear curve-fitting program. The following is a complete listing of this program.

```
C*************************************************************************
C*      PROGRAM : RQ.FOR
C*      A NON-LINEAR CURVE-FITTING PROGRAM
C*      THE ALGORITHM OF THIS PROGRAM HAS BEEN DEVELOPED BY
C*      DR. J. P. CHANDLER OF OSU COMPUTER SCIENCE DEPARTMENT
C*      ---------------------------------------------------------------------------
C*      MODIFIED BY : L. M. TAM AND D. R. MAIELLO (DECEMBER 1989)
C*
C*      UNDER THE SUPERVISION OF PROF. A. J. GHAJAR
C*              SCHOOL OF MECHANICAL&
C*              AEROSPACE ENGINEERING
C*              OKLAHOMA STATE UNIVERSITY
C*              STILLWATER, OK 74078
C*************************************************************************
    IMPLICIT REAL*8 (A-H,O-Z)
    INTEGER IFORM
    EXTERNAL EXFIT
    CHARACTER*20 NAME,NAMO
    DOUBLE PRECISION XMAX,XMIN,DELTX,DELMN,ERR,FOBJ,FLAMB,FNU,
   +          RELDF,RELMN,RZERO,XX,Y,YSIG,FIT
    DOUBLE PRECISION AMDA,X1,X2,X3,X4,X5,X6,A
C
    COMMON /CSTEP/ XMAX(20),XMIN(20),DELTX(20),DELMN(20),A(20),
   +          ERR(20,21),FOBJ,NV,NTRAC,MATRX,MASK(20),NFMAX,
   +          NFLAT,JVARY,NXTRA,KFLAG,NOREP,KERFL,KW,XX(20),
   +          NAME,NAMO,IPIC,NT
    COMMON /NLLS4/ FLAMB,FNU,RELDF,RELMN,METHD,KALCP,KORDF,MAXIT,
   +          LEQU,MXSUB,MXUPD
    COMMON /CDAT/  FIT(700),Y(700),YSIG(700),NPTS,IFORM
    COMMON /CSTOR/ X1(700),X2(700),X3(700),X4(700),X5(700),X6(700),
   +          AMDA(700)
    COMMON/TER/ITER,AAPD
C
C
C ---------------------------------
C ----- PRINT HEADER TO SCREEN -----
C ---------------------------------
C
    WRITE(*,9001)
    PAUSE 'Press ENTER to continue'
C
C --------------------------------
C ----- INITIALIZE VARIABLES -----
C --------------------------------
C
   1 I1=1
    I2=2
    I3=3
    I4=4
    I5=5
    I6=6
    IFORM=0
```

```
      IFLAG=0
      RZERO=0.
      NFMAX=32767
      MAXIT=40
      MXSUB=10
      METHD=1
      KALCP=0
      KORDF=1
      LEQU=0
      NFLAT=1
      MATRX=106
      NXTRA=0
      FLAMB=1.
      FNU=10.
      RELDF=1.E-8
      RELMN=1.E-6
      DO 10 JX=1,20
       DELTX(JX)=RZERO
       DELMN(JX)=RZERO
   10  CONTINUE
C
C ------------------------------------------
C ----- PROMPT USER FOR OUTPUT DEVICE -----
C ------------------------------------------
C
   21 WRITE(*,9002)
      WRITE(*,*)'  ENTER OUTPUT DESTINATION:'
      WRITE(*,*)'  '
      WRITE(*,*)'  Enter "0" to send output to screen'
      WRITE(*,*)'  Enter "1" to send output to data file'
      READ(*,9020,ERR=21)IPIC
      IF(IPIC.NE.0.AND.IPIC.NE.1)GO TO 21
      IF(IPIC.EQ.0)THEN
        KW=0
        GO TO 28
        ELSE
      GO TO 23
      ENDIF
   12    WRITE(*,9002)
         WRITE(*,9017)NAMO
         WRITE(*,*)' '
         WRITE(*,*)'   Do you wish to over-write this file?'
         WRITE(*,*)' '
         WRITE(*,*)'      YES, over-write this file - Enter "0"'
         WRITE(*,*)'       NO, use another filename - Enter "1"'
         READ(*,9020,ERR=12)IPCK
         IF(IPCK.EQ.0)GO TO 24
C
   23    WRITE(*,*)' '
         WRITE(*,*)' '
         WRITE(*,*)'  ENTER OUTPUT DATA FILENAME :'
         WRITE(*,*)'   [Example: C:\MARQ\OUT.DAT]'
         READ(*,9003)NAMO
         KW=5
         OPEN(5,FILE=NAMO,STATUS='NEW',FORM='FORMATTED',ERR=12)
         IF(IFLAG.EQ.1)GO TO 84
         GO TO 28
   24    OPEN(5,FILE=NAMO,STATUS='OLD',FORM='FORMATTED')
         IF(IFLAG.EQ.1)GO TO 84
C
```

```
C ---------------------------------------
C ----- PROMPT USER FOR OUTPUT MODE -----
C ---------------------------------------
C
  28 IF(IFLAG.EQ.1)GO TO 84
     WRITE(*,9002)
     WRITE(*,*)'   Select the amount of output from routine:'
     WRITE(*,*)' '
     WRITE(*,*)'   "1"  - to obtain trace output during minimumization'
     WRITE(*,*)'   "0"  - for initial and final output only'
     WRITE(*,*)'  "-1"  - for no output except error messages'
     READ(*,9020,ERR=28)NTRAC
     IF(NTRAC.NE.0.AND.NTRAC.NE.1.AND.NTRAC.NE.-1)GO TO 28
C
C ---------------------------------------
C ----- PROMPT USER FOR INPUT DEVICE -----
C ---------------------------------------
C
  22 WRITE(*,9002)
     WRITE(*,*)'   ENTER METHOD OF DATA INPUT:'
     WRITE(*,*)'   '
     WRITE(*,*)'   Enter "0" to read input data from file'
     WRITE(*,*)'   Enter "1" to input data with keyboard'
     READ(*,9020,ERR=22)NT
     IF(NT.NE.0.AND.NT.NE.1)GO TO 22
     IF(NT.EQ.1)GO TO 55
C
  27 WRITE(*,9002)
     WRITE(*,*)'   Select input file FORMAT option:'
     WRITE(*,*)'   '
     WRITE(*,*)'   Enter "0" - View HELP screen for this option'
     WRITE(*,*)'   Enter "1" - Select "HEAT" format'
     WRITE(*,*)'   Enter "2" - Select generalized format'
     READ(*,9020,ERR=27)INRED
     IF(INRED.LT.0.OR.INRED.GT.2)GO TO 27
     IF(INRED.EQ.0)THEN
       WRITE(*,9002)
       WRITE(*,9019)
       PAUSE 'Press ENTER to continue'
       GO TO 27
     ENDIF
C
C -----------------------------------------
C ----- PROMPT USER FOR INPUT FILE NAME -----
C -----------------------------------------
C
  39 WRITE(*,9002)
     GO TO 26
  25 WRITE(*,9002)
     WRITE(*,9018)NAME
     WRITE(*,*)' '
     WRITE(*,*)'  You must enter a valid filename of an EXISTING file.'
  26 WRITE(*,*)' '
     WRITE(*,*)' '
     WRITE(*,*)'   ENTER INPUT DATA FILENAME:'
     WRITE(*,*)'   [Example: C:\MARQ\IN.DAT]'
     READ(*,9003)NAME
     OPEN(10,FILE=NAME,STATUS='OLD',FORM='FORMATTED',ERR=25)
     GO TO 101
C
```

```
C ------------------------------------------------------------
C ----- PROMPT USER FOR FILE NAME TO SAVE KEYBOARD INPUT -----
C ------------------------------------------------------------
C
  93    WRITE(*,9002)
        WRITE(*,9017)NAME
        WRITE(*,*)' '
        WRITE(*,*)'   Do you wish to over-write this file?'
        WRITE(*,*)' '
        WRITE(*,*)'      YES, over-write this file - Enter "0"'
        WRITE(*,*)'       NO, use another filename - Enter "1"'
        READ(*,9020,ERR=12)IPCK
        IF(IPCK.EQ.0)GO TO 94
C
  55    WRITE(*,9002)
        WRITE(*,*)'  MARQ will create a data file to save your'
        WRITE(*,*)'    keyboard input data set.'
        WRITE(*,*)' '
        WRITE(*,*)'  ENTER INPUT DATA FILENAME :'
        WRITE(*,*)'   [Example: C:\MARQ\IN.DAT]'
        READ(*,9003)NAME
        OPEN(8,FILE=NAME,STATUS='NEW',FORM='FORMATTED',ERR=93)
        GO TO 101
  94    OPEN(8,FILE=NAME,STATUS='OLD',FORM='FORMATTED')
C
C
C ------------------------------------------------
C ----- PROMPT USER FOR EQUATION SELECTION -----
C ------------------------------------------------
C
 101 IF(IFLAG.EQ.1)GO TO 38
  95 WRITE(*,9002)
     WRITE(*,9004)
     READ(*,9020,ERR=55)IFORM
     IF(IFORM.LT.1.OR.IFORM.GT.12)GO TO 95
     IF(IFLAG.EQ.1)GO TO 85
C
  58 WRITE(*,*)' '
     WRITE(*,*)' '
     WRITE(*,*)'   Is this EQUATION OK ?'
     WRITE(*,*)' '
     WRITE(*,*)'   Enter "0" to re-enter'
     WRITE(*,*)'   Enter "1" to continue'
     READ(*,9020,ERR=21)IPICK
     IF(IPICK.EQ.0)GO TO 95
C
C ------------------------------------------------
C ----- PROMPT USER FOR NUMBER OF COEFFICIENTS -----
C ------------------------------------------------
C
  41 IF(IFORM.GT.1)GO TO 76
     WRITE(*,9002)
     WRITE(*,9005)
     GO TO 57
  56 WRITE(*,*)' '
     WRITE(*,*)' '
     WRITE(*,*)'  WARNING: YOU HAVE SELECTED MORE COEFFICIENTS THAN'
     WRITE(*,*)'          ARE AVAILABLE IN THE SELECTED EQUATION!'
     WRITE(*,*)' '
  57 WRITE(*,*)'  ENTER THE NUMBER OF COEFFICIENTS:'
```

```
      READ(*,9020,ERR=41)NV
      IF(NV.EQ.0)GO TO 41
      IF(NV.GT.6) GO TO 56
C
   71 WRITE(*,*)' '
      WRITE(*,*)' '
      WRITE(*,*)'  Do you wish to re-enter the NUMBER OF COEFFs ?'
      WRITE(*,*)' '
      WRITE(*,*)'   Enter "0" to re-enter'
      WRITE(*,*)'   Enter "1" to continue'
      READ(*,9020,ERR=71)IPICK
      IF(IPICK.EQ.0)GO TO 41
C
C ----- SET "NV" FOR APPROPRIATE EQUATION SELECTION -----
C
C ************************* E#@ *************************
C *                                                     *
C *              CHANGING EQUATIONS                     *
C *                                                     *
C * For the Equation # (IFORM) of the altered equation: *
C *                                                     *
C *   Set NV equal to the number of unknown constants   *
C *              in the new equation.                   *
C *                                                     *
C *******************************************************
C
   76 IF(IFORM.EQ.2) NV=3
      IF(IFORM.EQ.3) NV=2
      IF(IFORM.EQ.4) NV=3
      IF(IFORM.EQ.5) NV=4
      IF(IFORM.EQ.6) NV=5
      IF(IFORM.EQ.7) NV=5
      IF(IFORM.EQ.8) NV=8
      IF(IFORM.EQ.9) NV=4
      IF(IFORM.EQ.10)NV=5
      IF(IFORM.EQ.11)NV=3
      IF(IFORM.EQ.12)NV=3
      IF(IFLAG.EQ.1)GO TO 85
C
C ---------------------------------------------
C ----- PROMPT USER FOR NUMBER OF POINTS -----
C ---------------------------------------------
C
      IF(NT.EQ.0)GO TO 59
   77 WRITE(*,9002)
   78 WRITE(*,9006)
        WRITE(*,*)' '
        WRITE(*,*)' '
        WRITE(*,*)'  ENTER THE NUMBER OF DATA POINTS:'
        READ(*,9020,ERR=77)NPTS
C
      IF(NPTS.GT.700.OR.NPTS.LT.1)THEN
        WRITE(*,*)' '
        WRITE(*,*)' '
        WRITE(*,*)' NUMBER OF DATA POINTS IS LIMITED TO (1 <#< 700)!'
        WRITE(*,*)' '
        GO TO 78
      ENDIF
C
C ---------------------------------------------
```

```
C ----- PROMPT USER FOR DATA POINT VALUES -----
C ---------------------------------------------
C
    IF(NT.EQ.0)GO TO 59
   66 WRITE(*,9002)
    IF(IFORM.LT.5)GO TO 92
    WRITE(*,*)'  Be sure to enter your data in the following order.'
    WRITE(*,*)'  Omit data not required in your selected equation.'
    WRITE(*,*)' '
    WRITE(*,*)'     FIRST ENTRY - Nusselt  Number '
    WRITE(*,*)'     NEXT ENTRY - Reynolds Number '
    WRITE(*,*)'     NEXT ENTRY - Prandtl  Number '
    WRITE(*,*)'     NEXT ENTRY - Grashof  Number '
    WRITE(*,*)'     NEXT ENTRY - L/D '
    WRITE(*,*)'     NEXT ENTRY - MewB/MewW '
    WRITE(*,*)' '
    WRITE(*,*)'  For example, if you had selected Equation # 9,'
    WRITE(*,*)'  at the prompt:   Y(J), X1, X2, X3, X4:'
    WRITE(*,*)'  you would enter:  Nu , Re, Pr, L/D, MewB/MewW'
    WRITE(*,*)'  since the equation does not require the Grashof #.'
    PAUSE 'Press ENTER to begin data entry.'
    GO TO 192
   92  WRITE(*,*)'  ENTER DATA POINTS:'
     WRITE(*,*)' '
C
C ************************ E#@ *************************
C *                                 *
C *            CHANGING EQUATIONS            *
C *                                 *
C * For the Equation # (IFORM) of the altered equation:  *
C *                                 *
C *  At the following statements, check arguments:     *
C *    WRITE(*,9008)I,I1,I2,...In                *
C *    READ(*,*)AMDA(I),X1(I),...Xn(I)           *
C *    WRITE(8,9009)AMDA(I),X1(I),...Xn(I)         *
C *                                 *
C *    where "n" = NV                       *
C *                                 *
C ************************************************************
C
   192  DO 20 I=1,NPTS
      WRITE(*,9007)I
      IF(IFORM.GE.1.AND.IFORM.LE.4)THEN
       WRITE(*,9008)I,I1
       READ(*,*)AMDA(I),X1(I)
       WRITE(8,9009)AMDA(I),X1(I)
       ENDIF
      IF(IFORM.EQ.5)THEN
       WRITE(*,9008)I,I1,I2,I3,I4,I5,I6
       READ(*,*)AMDA(I),X1(I),X2(I),X3(I),X4(I),X5(I),X6(I)
       WRITE(8,9009)AMDA(I),X1(I),X2(I),X3(I),X4(I),X5(I),X6(I)
       ENDIF
      IF(IFORM.EQ.6)THEN
       WRITE(*,9008)I,I1,I2,I3,I4
       READ(*,*)AMDA(I),X1(I),X2(I),X3(I),X4(I)
       WRITE(8,9009)AMDA(I),X1(I),X2(I),X3(I),X4(I)
       ENDIF
      IF(IFORM.EQ.7)THEN
       WRITE(*,9008)I,I1
       READ(*,*)AMDA(I),X1(I)
```

```
      WRITE(8,9009)AMDA(I),X1(I)
      ENDIF
     IF(IFORM.EQ.8)THEN
      WRITE(*,9008)I,I1,I2,I3,I4,I5
      READ(*,*)AMDA(I),X1(I),X2(I),X3(I),X4(I),X5(I)
      WRITE(8,9009)AMDA(I),X1(I),X2(I),X3(I),X4(I),X5(I)
      ENDIF
     IF(IFORM.EQ.9)THEN
      WRITE(*,9008)I,I1,I2,I3,I4
      READ(*,*)AMDA(I),X1(I),X2(I),X3(I),X4(I)
      WRITE(8,9009)AMDA(I),X1(I),X2(I),X3(I),X4(I)
      ENDIF
     IF(IFORM.EQ.10)THEN
      WRITE(*,9008)I,I1,I2,I3,I4
      READ(*,*)AMDA(I),X1(I),X2(I),X3(I),X4(I)
      WRITE(8,9009)AMDA(I),X1(I),X2(I),X3(I),X4(I)
      ENDIF
     IF(IFORM.EQ.11)THEN
      WRITE(*,9008)I,I1,I2,I3
      READ(*,*)AMDA(I),X1(I),X2(I),X3(I)
      WRITE(8,9009)AMDA(I),X1(I),X2(I),X3(I)
      ENDIF
     IF(IFORM.EQ.12)THEN
      WRITE(*,9008)I,I1
      READ(*,*)AMDA(I),X1(I)
      WRITE(8,9009)AMDA(I),X1(I)
      ENDIF
 20   CONTINUE
C
  81 WRITE(*,*)' '
     WRITE(*,*)' '
     WRITE(*,*)'  Do you wish to re-enter the DATA POINT VALUES ?'
     WRITE(*,*)' '
     WRITE(*,*)'   Enter "0" to re-enter'
     WRITE(*,*)'   Enter "1" to continue'
     READ(*,9020,ERR=81)IPICK
     IF(IPICK.EQ.0)GO TO 66
  59 IF(NT.EQ.1)GO TO 69
C
C ---------------------------------------
C ----- READ DATA FROM INPUT FILE -----
C ---------------------------------------
C
C ----- READ USING "HEAT" FORMAT -----
C
  38 IF(INRED.EQ.1)THEN
      DO 31 I=1,700
      READ(10,9010)AMDA(I),X1(I),X2(I),X3(I),X4(I),X5(I)
      IF(AMDA(I).EQ.0..AND.X1(I).EQ.0.)GO TO 82
      GO TO 31
C
  82  NPT2=I-1
      WRITE(*,9002)
      WRITE(*,9021)NAME,NPT2
      READ(*,9020,ERR=82)IPICK
      IF(IPICK.NE.0.AND.IPICK.NE.1)GO TO 82
      IF(IPICK.EQ.0)STOP
      IF(IPICK.EQ.1)NPTS=NPT2
      GO TO 98
C
```

```
 31 CONTINUE
    ENDIF
C
C ----- READ USING GENERALIZED FORMAT -----
C
C
C ************************* E#@ **************************
C *                                 *
C *              CHANGING EQUATIONS             *
C *                                 *
C * For the Equation # (IFORM) of the altered equation:  *
C *                                 *
C *  At the following statement, check arguments:      *
C *                                 *
C *  READ(10,9009,END=89,ERR=89)AMDA(I),X1(I),...Xn(I)  *
C *                                 *
C *    where "n" = NV                        *
C *                                 *
C ***************************************************
C
    IF(INRED.EQ.1)GO TO 98
      DO 32 I=1,700
      IF(IFORM.GE.1.AND.IFORM.LE.4) THEN
      READ(10,9009,END=89,ERR=89)AMDA(I),X1(I)
      ENDIF
      IF(IFORM.EQ.5) THEN
      READ(10,9009,END=89,ERR=89)AMDA(I),X1(I),X2(I),X3(I),X4(I),X5(I)
      ENDIF
      IF(IFORM.EQ.6) THEN
      READ(10,9009,END=89,ERR=89)AMDA(I),X1(I),X2(I),X3(I),X4(I)
      ENDIF
      IF(IFORM.EQ.7) THEN
      READ(10,9009,END=89,ERR=89)AMDA(I),X1(I),X2(I)
      ENDIF
      IF(IFORM.EQ.8) THEN
      READ(10,9009,END=89,ERR=89)AMDA(I),X1(I),X2(I),X3(I),X4(I),X5(I)
      ENDIF
      IF(IFORM.EQ.9) THEN
      READ(10,9009,END=89,ERR=89)AMDA(I),X1(I),X2(I),X4(I),X5(I)
      ENDIF
      IF(IFORM.EQ.10)THEN
      READ(10,9009,END=89,ERR=89)AMDA(I),X1(I),X2(I),X4(I),X5(I)
      ENDIF
      IF(IFORM.EQ.11)THEN
      READ(10,9009,END=89,ERR=89)AMDA(I),X1(I),X2(I),X5(I)
      ENDIF
      IF(IFORM.EQ.12)THEN
      READ(10,9009,END=89,ERR=89)AMDA(I),X1(I)
      ENDIF
C
      GO TO 32
  89  NPT2=I-1
      WRITE(*,9002)
      WRITE(*,9021)NAME,NPT2
      READ(*,9020,ERR=89)IPICK
      IF(IPICK.NE.0.AND.IPICK.NE.1)GO TO 89
      IF(IPICK.EQ.0)STOP
      IF(IPICK.EQ.1)NPTS=NPT2
      GO TO 98
C
```

```
  32 CONTINUE
C
C ---------------------------------------------------
C ----- PROMPT USER FOR COEFFICIENT INITIAL VALUES -----
C ---------------------------------------------------
C
  98 IF(IFLAG.EQ.1)GO TO 84
C
  69 WRITE(*,9002)
     WRITE(*,9011)NV
     WRITE(*,*)'  ENTER THE INITIAL VALUES FOR COEFFICIENTS:'
     WRITE(*,*)' '
     WRITE(*,*)'  Enter "0" - begin value entry'
     WRITE(*,*)'  Enter "1" - set all initial values to 1'
     READ(*,*)IPICK
     IF(IPICK.NE.0.AND.IPICK.NE.1)GO TO 69
     DO 30 I=1,20
     IF(I.LE.NV)THEN
       IF(IPICK.EQ.0)THEN
         WRITE(*,9012)I
         READ(*,*)XX(I)
       ELSE
         XX(I)=1.
       ENDIF
     ELSE
       XX(I)=0.
     ENDIF
  30 CONTINUE
C
     IF(IFLAG.EQ.1)GO TO 85
     IF(IPICK.EQ.1)GO TO 65
     WRITE(*,*)' '
     WRITE(*,*)' '
     WRITE(*,*)'  Do you wish to re-enter the INITIAL VALUES ?'
     WRITE(*,*)' '
     WRITE(*,*)'   Enter "0" to re-enter'
     WRITE(*,*)'   Enter "1" to continue'
     READ(*,*)IPICK
     IF(IPICK.EQ.0)GO TO 69
C
C ---------------------------------------------------------------
C ----- PROMPT USER FOR COEFFICIENT MAXIMUM & MINIMUM VALUES -----
C ---------------------------------------------------------------
C
  65 WRITE(*,9002)
     WRITE(*,*)'  ENTER THE MAXIMUM & MINIMUM VALUES '
     WRITE(*,*)'    FOR COEFFICIENTS:'
     WRITE(*,*)' '
     WRITE(*,*)'  Enter "0" - begin value entry'
     WRITE(*,*)'  Enter "1" - set all maximum values to  1E+30'
     WRITE(*,*)'             and all minimum values to -1E+30'
     READ(*,*)IPICK
     DO 40 I=1,20
     IF(IPICK.EQ.1)THEN
       XMAX(I)=1.E+30
       XMIN(I)=-1.E+30
     ELSE
       IF(I.LE.NV)THEN
         GO TO 68
  67   WRITE(*,*)'  ******************************'
```

```
      WRITE(*,*)'  INVALID RANGE : RE-ENTER VALUES'
      WRITE(*,*)'  ******************************'
 68    WRITE(*,9013)I
       READ(*,9050,ERR=67)XMIN(I),XMAX(I)
       IF(XMIN(I).GT.XX(I).OR.XMAX(I).LT.XX(I))GO TO 67
      ELSE
       XMAX(I)=1.E+30
       XMIN(I)=-1.E+30
      ENDIF
     ENDIF
 40 CONTINUE
C
     IF(IFLAG.EQ.1)GO TO 85
     IF(IPICK.EQ.1)GO TO 63
     WRITE(*,*)' '
     WRITE(*,*)' '
     WRITE(*,*)'  Do you need re-enter the MIN/MAX VALUES ?'
     WRITE(*,*)' '
     WRITE(*,*)'   Enter "0" to re-enter'
     WRITE(*,*)'   Enter "1" to continue'
     READ(*,*)IPICK
     IF(IPICK.EQ.0)GO TO 65
C
C ------------------------------------------------
C ----- PROMPT USER FOR COEFFICIENT MASKING -----
C ------------------------------------------------
C
 63 WRITE(*,9002)
     WRITE(*,9015)
     WRITE(*,*)'  ENTER THE MASK FOR THE COEFFICIENTS:'
     WRITE(*,*)'  '
     WRITE(*,*)'  Enter "0" - begin individual value entry'
     WRITE(*,*)'  Enter "1" - set all MASK values to 0'
     READ(*,*)IPICK
     IF(IPICK.NE.0.AND.IPICK.NE.1)GO TO 63
     DO 60 I=1,20
      IF(I.LE.NV)THEN
       GO TO 79
 64    WRITE(*,*)' '
       WRITE(*,*)'  MASK variable must be 1 or 0.'
       WRITE(*,*)' '
 79    IF(IPICK.EQ.0)THEN
        WRITE(*,9016)I,XX(I)
        READ(*,*)MASK(I)
        IF(MASK(I).NE.0.AND.MASK(I).NE.1)GO TO 64
       ELSE
        MASK(I)=0
       ENDIF
      ELSE
       MASK(I)=1
      ENDIF
C
 60 CONTINUE
C
     IF(IFLAG.EQ.1)GO TO 85
     IF(IPICK.EQ.1.OR.IPICK.EQ.0)GO TO 129
     WRITE(*,*)' '
     WRITE(*,*)' '
     WRITE(*,*)'  Do you wish to re-enter the MASK parameters ?'
     WRITE(*,*)' '
```

```
      WRITE(*,*)'   Enter "0" to re-enter'
      WRITE(*,*)'   Enter "1" to continue'
      READ(*,*)IPICK
      IF(IPICK.EQ.0)GO TO 63
C
C
  129 DO 121 INP=1,NPTS
      Y(INP)=AMDA(INP)
  121 YSIG(INP)=0.01D0*DABS(Y(INP))
  122 CALL STEPT(EXFIT)
      PAUSE 'Press ENTER to continue.'
  115 WRITE(*,9002)
      WRITE(*,*)'      WHAT NEXT ?  Enter:'
      WRITE(*,*)' '
      WRITE(*,*)'   "0" - to terminate program'
      WRITE(*,*)'   "1" - to repeat iteration w/ current parameters'
      WRITE(*,*)'   "2" - to repeat iteration w/ new parameters'
      WRITE(*,*)'   "3" - to start over'
      WRITE(*,*)'   "4" - to view results of this run'
      READ(*,9020,ERR=115)ND
      IF(ND.LT.0.OR.ND.GT.4)GO TO 115
      IF(ND.EQ.1)GO TO 122
      IF(ND.EQ.3)GO TO 1
      IF(ND.EQ.4)THEN
        WRITE(*,9002)
        WRITE(*,9026)ITER
        DO 86 I=1,NV
   86   WRITE(*,9027)I,XX(I)
        WRITE(*,9028)
        DO 87 I=1,NPTS
   87   WRITE(*,9029)I,Y(I),FIT(I)
        WRITE(*,9030)AAPD
        WRITE(*,*)' '
        PAUSE 'Press ENTER to continue'
        GO TO 115
      ENDIF
      IF(ND.EQ.0)GO TO 110
   85 IFLAG=1
      WRITE(*,9002)
      IF(NT.EQ.0.AND.IPIC.EQ.1)WRITE(*,9022)NAME,NAMO
      IF(NT.NE.0.AND.IPIC.EQ.1)WRITE(*,9031)NAMO
      IF(NT.EQ.0.AND.IPIC.NE.1)WRITE(*,9032)NAME
      IF(NT.NE.0.AND.IPIC.NE.1)WRITE(*,9033)
      IF(IFORM.EQ.1)WRITE(*,9051)
      IF(IFORM.EQ.2)WRITE(*,9052)
      IF(IFORM.EQ.3)WRITE(*,9053)
      IF(IFORM.EQ.4)WRITE(*,9054)
      IF(IFORM.EQ.5)WRITE(*,9055)
      IF(IFORM.EQ.6)WRITE(*,9056)
      IF(IFORM.EQ.7)WRITE(*,9057)
      IF(IFORM.EQ.8)WRITE(*,9058)
      IF(IFORM.EQ.9)WRITE(*,9059)
      IF(IFORM.EQ.10)WRITE(*,9060)
      IF(IFORM.EQ.11)WRITE(*,9061)
      IF(IFORM.EQ.12)WRITE(*,9062)
      WRITE(*,9023)NV
      DO 90 INT=1,NV
   90 WRITE(*,9024)INT,XX(INT),XMAX(INT),XMIN(INT),MASK(INT)
      WRITE(*,*)' '
      PAUSE 'Press ENTER to continue'
```

```
 84   WRITE(*,9002)
      WRITE(*,9025)
      READ(*,9020,ERR=84)IPICK
      IF(IPICK.LT.1.OR.IPICK.GT.9)GO TO 84
      IF(IPICK.EQ.1)GO TO 95
      IF(IPICK.EQ.2)GO TO 41
      IF(IPICK.EQ.3)GO TO 69
      IF(IPICK.EQ.4)GO TO 65
      IF(IPICK.EQ.5)GO TO 63
      IF(IPICK.EQ.6) THEN
       CLOSE (10)
       GO TO 22
       ENDIF
      IF(IPICK.EQ.7) THEN
       CLOSE (5)
       GO TO 21
       ENDIF
      IF(IPICK.EQ.9)GO TO 85
      GO TO 122
 110 STOP
C
 9001 FORMAT(/////,
     +/9X,'************************************************************',
     +/9X,'**                                                        **',
     +/9X,'**              RQ.FOR(NOV 1991)                          **',
     +/9X,'**          NONLINEAR REGRESSION PROGRAM                  **',
     +/9X,'**                                                        **',
     +/9X,'**   THE MATHEMATICAL ALGORITHM OF THIS PROGRAM WAS       **',
     +/9X,'**     DEVELOPED BY:  J.P. CHANDLER                       **',
     +/9X,'**                OKLAHOMA STATE UNIVERSITY               **',
     +/9X,'**                                                        **',
     +/9X,'**   MODIFIED FOR INTERACTIVE USE ON P.C.s                 **',
     +/9X,'**     BY: DENNIS R. MAIELLO                              **',
     +/9X,'**                                                        **',
     +/9X,'**   EQUATION MODIFICATION                                **',
     +/9X,'**     BY: RAY L. M. TAM                                  **',
     +/9X,'**                                                        **',
     +/9X,'**   UNDER THE SUPERVISION OF:                            **',
     +/9X,'**                                                        **',
     +/9X,'**     PROFESSOR AFSHIN J. GHAJAR                         **',
     +/9X,'**     SCHOOL OF MECHANICAL & AEROSPACE ENGINEERING       **',
     +/9X,'**     OKLAHOMA STATE UNIVERSITY                          **',
     +/9X,'**                                                        **',
     +/9X,'************************************************************')
 9002 FORMAT(/////////////////////////)
 9003 FORMAT(A20)
C
C ************************* E#@ *************************
C *                                                      *
C *              CHANGING EQUATIONS                      *
C *                                                      *
C * For the Equation # (IFORM) of the altered equation:  *
C *                                                      *
C *  Change the form of the equation following the       *
C *    appropriate number in FORMAT STATEMENT 9004.      *
C *                                                      *
C ********************************************************
C
 9004 FORMAT(////14X,'***** HELP FOR SELECTION OF EQUATION *****',
     +/5X,'Standard Curve Fitting:',/,
```

```
     +/5X,' 1:  Y=A(1)+A(2)*X+A(3)*X**2+A(4)*X**3+A(5)*X**4+A(6)*X**5',
     +/5X,' 2:  Y=A(1)+A(2)*EXP(A(3)*X)',
     +/5X,' 3:  Y=A(1)+A(2)*DLOG(X)',
     +/5X,' 4:  Y=A(1)+A(2)*X**A(3)',/,
     +/5X,'Specialized Heat Transfer/Fluid Flow Curve Fitting:',/,
     +/5X,' 5:  Nu=A(1)*{[Re*Pr*(d/L)]+ A(2)*[(Gr*Pr)**A(3)]}**A(4)',
     +        '*(U/Uw)**0.14',
     +/5X,' 6:  Nu=A(1)*Re**A(2)*Pr**A(3)*Gr**A(4)*(d/L)**A(5)',
     +/5X,'*7:  Nu={A(1)*Nul**A(2)+[EXP((A(4)-Re)/A(5))]+'
     +/5X,'       1/Nut**A(3)**(-A(2)/A(3))}**(-A(2)/A(3))**(1/A(2))'
     +/5X,' 8:  Nu={NuL+A(1)*Re**A(2)*Pr**A(3)*[1+A(4)*EXP(A(5)*(L/d)]',
     +/5X,'      +A(6)*[(Gr*Pr)**.25]*[1-EXP(A(7)*L/d)]}*(Ub/Uw)**.14',
     +/5X,' 9:  Nu=A(1)*Re**A(2)*Pr**A(3)*(X/D)**A(4)*(Ub/Uw)**.14',
     +/5X,'10:  Nu=A(1)*Re**A(2)*Pr**A(3)*{1+A(4)*EXP[A(5)*(L/d)]}',
     +          '(Ub/Uw)**.14',
     +/5X,'11:  Nu=A(1)*Re**A(2)*Pr**A(3)*(Ub/Uw)**.14',
     +/5X,'12:  FRICTION FACTOR CORRELATION - f(Re) Only',//,
     +5X,'*Nul=1.224{RePr(D/X)+0.025(PrGr)**0.75}**(1/3)*(Ub/Uw)**.14',
     +/5X,'*Nut=0.023Re**0.8*Pr**0.385*(X/D)**(-0.0054)*(Ub/Uw)**.14',
     +//,2X,'Enter NUMBER corresponding to desired form of equation:')
 9005 FORMAT(7x,'Choose a number of coefficients that exist',
     +    /7x,'in the equation (A(1),A(2),...).If the number of',
     +    /7x,'coefficient which you enter is less than the',
     +    /7x,'number of coefficient in the equation, other',
     +    /7x,'coefficients automatically will be set "0".',//)
 9006 FORMAT(7X,'Enter the number of data points to be entered by',
     +    /7x,'keyboard input for use with curve fitting routine.')
 9007 FORMAT(//7X,'FOR DATA POINT #',I3,', ENTER:')
 9008 FORMAT(9X,'Y(',I3,'),',:,' X',I1,:,', X',I1,:,', X',I1,:,
     +    ', X',I1,:,', X',I1,:,', X',I1)
 9009 FORMAT(F15.5,:,F15.5,:,F15.5,:,F15.5,:,F15.5,:,F15.5)
 9010 FORMAT(3F10.3,F15.3,2F10.3)
 9011 FORMAT(7X,'Coefficients A(1) through A(',I1,') must be ',
     +    'initialized',/7x,'in this step.  Make your best guess',
     +    ' at this time or enter 1s or 0s.',/7X,'To fix one or more',
     +    ' variables, enter that value in this step',/7x,
     +    'and then set the mask for that variable to zero.',//)
 9012 FORMAT(//7x,'Enter initial value for coefficient A(',I1,'):')
 9013 FORMAT(//12x,'Enter max & min values for coefficient A(',I1,'):',
     + /9x,'[ Xmin, Xmax : must be REAL No.s separated with a comma]')
 9015 FORMAT(7X,'If you want to fix the value of one or more',
     +    /7X,'coefficients on initial guess, its mask should',
     +    /7X,'be "1".',//)
 9016 FORMAT(//7X,'Initial value for A(',I1,') is',F12.5,/7X,
     +        'Enter MASK (0=Vary, 1=Fixed):')
 9017 FORMAT(7X,'WARNING!  OUTPUT FILE ',A12,' ALREADY EXISTS!')
 9018 FORMAT(7X,'WARNING!  INPUT FILE ',A12,' DOES NOT EXIST!')
 9019 FORMAT(7X,'This version reads data from the input file'
     +    /7X,'using one of two formats.',/,
     +    /7X,'The first format is compatible with the output ',
     +    /7X,'generated by the "HEAT" program used at O.S.U.',/,
     +    /7X,'The second format is generalized and reads the',
     +    /7X,'data from the input file as follows:',/,
     +    /7X,'   COLUMN #1:  Experimental Y1    - F15.5 format',/,
     +    /7X,'   COLUMN #2:  Coefficient X1     - F15.5 format',
     +    /7X,'   COLUMN #3:  Coefficient X2     - F15.5 format',
     +    /7X,'     |  |     |      |     |',
     +    /7X,'   COLUMN #n:  Coefficient X(n+1) - F15.5 format',
     +    /7X,'Insure that your input file format is compatible!')
 9020 FORMAT(I2)
```

```
9021 FORMAT(10X,'Data file ',A20,' has been read.',//10X,'There were',
     +    I4,' data records found.',//10X,'Is this OK ?',//15X,
     +    'Enter "0" to terminate',/15X,'Enter "1" to continue')
C9021 FORMAT(10X,'WARNING : You have specified more data points',/21X,
C    +     'than are available in the data file.',//10X,
C    +     'You specified',I4,' data points, but there',/10X,
C    +     'are only',I4,' data points available in the',/10x,
C    +     'current data file:',A20,//7X,'Enter "0" to terminate',
C    +     ' program',/7X,'Enter "1" to continue with',I4,' points')
9022 FORMAT(7X,'You are currently attempting to fit your data:',//7X,
     +    'Input file:',A21,4X,'Output file:',A21,//7X,
     +    'to the following equation:',/)
9023 FORMAT(/7X,'using',I3,' coefficients.',//24X,'Initial',6x,
     +    'Maximum',6X,'Minimum',6X,'Mask')
9024 FORMAT(/5X,'Coefficient #',I1,':',2X,E11.4,2X,E11.4,2X,E11.4,6X,
     +    I1)
9025 FORMAT(12X,'***** EDIT MENU *****',/,
     +    /12X,'1.  Select new EQUATION',
     +    /12x,'2.  Select new NUMBER OF VARIABLES',
     +    /12x,'3.  Select new COEFFICIENT INITIAL VALUES',
     +    /12x,'4.  Select new COEFFICIENT MAX/MIN VALUES',
     +    /12x,'5.  Select new COEFFICIENT MASK VALUES',
     +    /12x,'6.  Change INPUT FILEname & read new data',
     +    /12x,'7.  Change OUTPUT FILEname ',
     +    /12x,'8.  Go with current parameters',
     +    /12x,'9.  View Current Settings',///////)
9026 FORMAT(//10X,'AFTER',I4,' ITERATIONS -',//10X,'THE CONSTANTS ',
     +    'HAVE BEEN CALCULATED AS:',/)
9027 FORMAT(10X,'A(',I1,') =',E14.5)
9028 FORMAT(/12X,'AND THE RESULTS ARE:',/12X,'No.',7X,'Y(I) EXP.',5X,
     +    'Y(I) CAL.',/)
9029 FORMAT(10X,I3,7X,F10.4,4X,F10.4)
9030 FORMAT(/10X,'THE AVE. ABSOLUTE DEVIATION FROM FIT =',E14.5,/)
9031 FORMAT(7X,'You are currently attempting to fit your data:',//7X,
     +    'Input file:  KEYBOARD',4X,'Output file:',A21,//7X,
     +    'to the following equation:',/)
9032 FORMAT(7X,'You are currently attempting to fit your data:',//7X,
     +    'Input file:',A21,4X,'Output file:  SCREEN',//7X,
     +    'to the following equation:',/)
9033 FORMAT(7X,'You are currently attempting to fit your data:',//7X,
     +    'Input file:  KEYBOARD',4X,'Output file:  SCREEN'.//7X,
     +    'to the following equation:',/)
9050 FORMAT(2E12.5)
9051 FORMAT(7X,'Y=A(1)+A(2)*X+A(3)*X**2+A(4)*X**3+A(5)*X**4+A(6)*X**5')
9052 FORMAT(7X,'Y=A(1)+A(2)*EXP(A(3)*X)')
9053 FORMAT(7X,'Y=A(1)+A(2)*DLOG(X)')
9054 FORMAT(7X,'Y=A(1)+A(2)*X**A(3)')
9055 FORMAT(7X,'Nu=A(1)*{[Re*Pr*(d/L)]+ A(2)*[(Gr*Pr)**A(3)]}**A(4)',
     +    '*(U/Uw)**0.14')
9056 FORMAT(7X,'Nu=A(1)*Re**A(2)*Pr**A(3)*Gr**A(4)*(d/L)**A(5)')
9057 FORMAT(7X,'Nu={A(1)*Nul**A(2)+[EXP((A(4)-Re)/A(5))]+'
     +    /10X,'1/Nut**A(3)**(-A(2)/A(3))}**(-A(2)/A(3))**(1/A(2))')
9058 FORMAT(7X,'Nu={NuL+A(1)*Re**A(2)*Pr**A(3)*[1+A(4)*EXP(A(5)*(L/d)]'
     +    ,/10X,'+A(6)*[(Gr*Pr)**.25]*[1-EXP(A(7)*L/d)]}*(Ub/Uw)**.14')
9059 FORMAT(7X,'Nu=A(1)*Re**A(2)*Pr**A(3)*(X/D)**A(4)*(Ub/Uw)**.14')
9060 FORMAT(7X,'Nu=A(1)*Re**A(2)*Pr**A(3)*{1+A(4)*EXP[A(5)*(L/d)]}',
     +    '(Ub/Uw)**.14')
9061 FORMAT(7X,'Nu=A(1)*Re**A(2)*Pr**A(3)*(Ub/Uw)**.14')
9062 FORMAT(7X,'f=2*{1/[(8/Re)**A(1)+(Re/A(3))**(2*A(1))]**A(2)/A(1)',
     +    /10X,'+[2.21*LN(Re/7)]**(2*A(2))}**(-1/A(2))')
```

```
C
      END
C
C------DATA NUMBER CHANGED                              ---C
C------P(700,20),FITSV(700)===> 700 TOTAL NUMBER OF DATA POINT  ---C
C------WHEN THE ARRAY HAS 700 ELEMENTS , IT MEANS THAT THE TOTAL---C
C------NUMBER OR DATA POINT CAN USE IS 700                ---C
C
      SUBROUTINE STEPT (FUNCON)
      IMPLICIT REAL*8 (A-H,O-Z)
      EXTERNAL FUNCON
      DOUBLE PRECISION FITSV,P
      DOUBLE PRECISION X1,X2,X3,X4,X5,X6,AMDA
      DIMENSION P(700,20),FITSV(700)
      COMMON /CSTOR/ X1(700),X2(700),X3(700),X4(700),X5(700),X6(700),
     +          AMDA(700)
      COMMON /CDAT/  FIT(700),Y(700),YSIG(700),NPTS,IFORM
C
      LPDMA=700
      LPDMB=20
      CALL MARQ (FUNCON,Y,YSIG,NPTS,FIT,FITSV,P,LPDMA,LPDMB,IFORM)
      RETURN
      END
C
      SUBROUTINE EXFIT(FITM)
      IMPLICIT REAL*8 (A-H,O-Z)
      DOUBLE PRECISION XX,FIT,FITM,FF,A,Y,YSIG
      DOUBLE PRECISION X1,X2,X3,X4,X5,X6,AMDA
      CHARACTER*20 NAME,NAMO
      DIMENSION FITM(1)
      COMMON /CSTEP/ XMAX(20),XMIN(20),DELTX(20),DELMN(20),A(20),
     +          ERR(20,21),FOBJ,NV,NTRAC,MATRX,MASK(20),NFMAX,
     +          NFLAT,JVARY,NXTRA,KFLAG,NOREP,KERFL,KW,XX(20),
     +          NAME,NAMO,IPIC,NT
      COMMON /CDAT/  FIT(700),Y(700),YSIG(700),NPTS,IFORM
      COMMON /CSTOR/ X1(700),X2(700),X3(700),X4(700),X5(700),X6(700),
     +          AMDA(700)
C
      FOBJ = 0.
      DO 200 J=1,NPTS
C
C ************************* E#@ **************************
C *                                 *
C *          CHANGING EQUATIONS          *
C *                                 *
C * For the Equation # (IFORM) of the altered equation:  *
C *                                 *
C *  Change the form of the FUNCTION following the     *
C *    appropriate number in DO LOOP 200.          *
C *                                 *
C ***************************************************
C
      GO TO (1,2,3,4,5,6,7,8,9,10,11,12),IFORM
    1 FF= XX(1)+XX(2)*X1(J)+XX(3)*X1(J)**2+XX(4)*X1(J)**3+
     +  XX(5)*X1(J)**4+XX(6)*X1(J)**5
      GO TO 1100
    2 FF= XX(1)+XX(2)*EXP(XX(3)*X1(J))
      GO TO 1100
    3 FF= XX(1)+XX(2)*DLOG(X1(J))
      GO TO 1100
```

```
   4 FF= XX(1)+XX(2)*X1(J)**XX(3)
     GO TO 1100
   5 FF= XX(1)*((X1(J)*X2(J)*(X4(J)**(-1))+XX(2)*(X3(J)*X2(J))**XX(3))
    +   **XX(4))*X5(J)**0.14
     GO TO 1100
   6 FF= XX(1)*X1(J)**XX(2)*X2(J)**XX(3)*X3(J)**XX(4)*X4(J)**(-XX(5))
     GO TO 1100
C
C-----MODIFIED CORRELATION IN THE TRANSITION REGION
C
   7 FF=((((1.2408*(X1(J)*X2(J)/X4(J)+0.024947*(X3(J)*X2(J))**0.75)
    +     **(1./3.)*X5(J)**0.14))*
    +     XX(1))**XX(2)+(EXP((XX(4)-X1(J))/XX(5))/XX(1)**XX(3)+
    +    1./((0.023*X1(J)**0.8*X2(J)**0.3847*X4(J)
    +    **(-0.00543)*X5(J)**0.14))
    +    **XX(3)**(-XX(2)/XX(3)))**(-XX(2)/XX(3)))**(1./XX(2))
     GO TO 1100
   8 FF=(XX(1)+(XX(2)*(X1(J)**XX(3))*(X2(J)**XX(4))*(1.+XX(5)*EXP(XX(6)
    +   *X4(J))))+(XX(7)*((X3(J)*X2(J))**.25)*(1.-EXP(XX(8)*X4(J)))))
    +   *(X5(J)**.14)
     GO TO 1100
C
C-----MODIFIED CORRELATION IN THE FORCED TURBULENT REGION
C
C    9 FF= XX(1)*X1(J)*X2(J)**XX(2)*(1+XX(3)*EXP(XX(4)*X4(J)))*X5(J)**.14
     9 FF=XX(1)*X1(J)**XX(2)*X2(J)**XX(3)*X4(J)**XX(4)*X5(J)**XX(5)
     GO TO 1100
    10 FF= XX(1)*X1(J)**XX(2)*X2(J)**XX(3)*(1+XX(4)*EXP(XX(5)*X4(J)))*
    +   X5(J)**.14
     GO TO 1100
    11 FF= XX(1)*X1(J)**XX(2)*X2(J)**XX(3)*X5(J)**.14
     GO TO 1100
    12 FF=2.*((1./(((8./X1(J))**XX(1)+(X1(J)/XX(3))**(2.*XX(1)))**
    + (XX(2)/XX(1))))+((2.21*DLOG(X1(J)/7.))**(2.*XX(2))))**(-1./XX(2))
C
  1100  FITM(J)=FF
  200 FOBJ = FOBJ +((FF-Y(J))/YSIG(J))**2
     RETURN
     END
C
     SUBROUTINE FOFX (JPT,NV,XX,F)
     DOUBLE PRECISION XX,F
     DIMENSION XX(20)
     DOUBLE PRECISION  X1,X2,X3,X4,X5,X6,AMDA
     COMMON /CSTOR/ X1(700),X2(700),X3(700),X4(700),X5(700),X6(700),
    +           AMDA(700)
     RETURN
     END
C
C
C
C
C
     SUBROUTINE CALCD (JPT,P,LPDMA,LPDMB)
     DOUBLE PRECISION P
     DIMENSION P(LPDMA,LPDMB)
     RETURN
     END
C
C
```

```
C
C
C
      SUBROUTINE MARQ (FUNCON,Y,YSIG,NPTS,FIT,FITSV,P,LPDMA,LPDMB,IFORM)
      EXTERNAL FUNCON
      DOUBLE PRECISION P,Y,YSIG,H,XMAX,XMIN,DELTX,DELMN,
     +    ERR,FOBJ,FLAMB,FNU,RELDF,QSQRT,ARG,CRIT,FLDEF,RELMN,
     +    RLTOL,FACCL,RZERO,RUNIT,RTWO,DELN,FMGN,FCUT,
     +    STFAC,PTERM,SCALJ,SA,PIVOT,EM,SUM,COSIN,SB,SC,HH,
     +    FRMIN,XMX,XMN,DENOM,FRAC,UPFAC,RLFAC,RSFAC,RMSDV,
     +    SDVMX,QMAX1,QMIN1,QABS,ARGB
      DOUBLE PRECISION XX,XSAVE,XTEMP,GRAD,FIT,FITSV,
     +            XSAV,SIG,RTERM,PHI,PHNEW,PHALF,XLIM
      DOUBLE PRECISION X1,X2,X3,X4,X5,X6,AMDA,A
      DOUBLE PRECISION AAPD,SSSUM
      CHARACTER*20 NAME,NAMO
      DIMENSION P(LPDMA,LPDMB)
      DIMENSION FITSV(1),FIT(1),Y(1),YSIG(1)
      DIMENSION XSAVE(20),H(20),GRAD(20),MASKT(20),XTEMP(20)
      COMMON /CSTEP/ XMAX(20),XMIN(20),DELTX(20),DELMN(20),A(20),
     +            ERR(20,21),FOBJ,NV,NTRAC,MATRX,MASK(20),NFMAX,
     +            NFLAT,JVARY,NXTRA,KFLAG,NOREP,KERFL,KW,XX(20),
     +            NAME,NAMO,IPIC,NT
      COMMON /NLLS4/ FLAMB,FNU,RELDF,RELMN,METHD,KALCP,KORDF,MAXIT,
     +            LEQU,MXSUB,MXUPD
      COMMON /CSTOR/ X1(700),X2(700),X3(700),X4(700),X5(700),X6(700),
     +            AMDA(700)
      COMMON/TER/ITER,AAPD
C
      QSQRT(ARG)=DSQRT(ARG)
      QABS(ARG)=DABS(ARG)
      QMAX1(ARG,ARGB)=DMAX1(ARG,ARGB)
      QMIN1(ARG,ARGB)=DMIN1(ARG,ARGB)
      NVMAX=20
      CRIT=.70711
      FLDEF=1.
      RLTOL=1.E-4
      FACCL=2.
      FNULM=2.
      RZERO=0.
      RUNIT=1.
      RTWO=2.
      KFLAG=0
      NOREP=0
      ITER=0
      PHI=1.E30
      SC=1.E30
      IF(NTRAC.GE.-1) WRITE(KW,10)
   10 FORMAT(//,9X,49H1MARQ.... BEGIN NONLINEAR LEAST SQUARES SOLUTION)
      NACTV=-99
      IF(KALCP.LT.0 .OR. NPTS.LE.LPDMA) GO TO 20
      KFLAG=-1
      GO TO 60
   20 NACTV=0
      DO 50 JX=1,NV
        DELN=QABS(DELMN(JX))
        IF(MASK(JX))50,30,50
   30   NACTV=NACTV+1
        IF(DELN.EQ.RZERO) DELN=QABS(RELMN*XX(JX))
        IF(DELN.EQ.RZERO) DELN=RELMN
```

```
40  XX(JX)=QMAX1(XMIN(JX),QMIN1(XMAX(JX),XX(JX)))
50  DELMN(JX)=DELN
  IF(NACTV.GT.0) GO TO 80
  KFLAG=-2
60 CONTINUE
  WRITE(KW,70)NV,NVMAX,NACTV,NPTS,LPDMA,LPDMB,KALCP
70 FORMAT(//29H ILLEGAL INPUT VALUE IN MARQ.,4X,5H NV =,I3,4X,
 +  8H NVMAX =,I3,4X,8H NACTV =,I3/10X,7H NPTS =,I5,4X,8H LPDMA =,
 +  I5,4X,8H LPDMB =,I5,4X,8H KALCP =,I3)
  STOP
80 CONTINUE
  IF(NTRAC.LT.-1) GO TO 150
  WRITE(KW,90)(MASK(J),J=1,NV)
90 FORMAT(/,9X,10H MASK   = ,5I5)
  WRITE(KW,100)(XX(J),J=1,NV)
100 FORMAT(/,9X,10H X      = ,5E10.3/(19X,5E10.3))
  WRITE(KW,110)(XMAX(J),J=1,NV)
110 FORMAT(/,9X,10H XMAX   = ,5E10.3/(19X,5E10.3))
  WRITE(KW,120)(XMIN(J),J=1,NV)
120 FORMAT(/,9X,10H XMIN   = ,5E10.3/(19X,5E10.3))
  WRITE(KW,130)(DELMN(J),J=1,NV)
130 FORMAT(/,9X,10H DELMN  = ,5E10.3/(19X,5E10.3))
  WRITE(KW,140)NV,NPTS,LPDMA,LPDMB,NTRAC,METHD,KALCP,KORDF,
 +    NFLAT,NFMAX,MAXIT,MXSUB,CRIT,RELDF,RELMN
140 FORMAT(//5H NV =,I4,5X,7H NPTS =,I6,5X,8H LPDMA =,I6,/,9X,
 +8H LPDMB =,I4,5X,8H NTRAC =,I2,5X,8H METHD =,I3,/,9X,8H KALCP =,
 +  I3//8H KORDF =,I2,5X,8H NFLAT =,I2,/,9X,8H NFMAX =,I7,5X,
 +  8H MAXIT =,I5,5X,8H MXSUB =,I4//7H CRIT =,E12.5,5X,8H RELDF =,
 +  E12.5,5X,8H RELMN =,E12.5)
150 JVARY=0
  FMGN=RUNIT
  UPNU=FNU
  DOWNU=FNU
  IF(FLAMB.LE.RZERO) FLAMB=FLDEF
  IF(METHD.LE.0) FLAMB=RZERO
  IF(METHD.NE.1) FACCL=RUNIT
  CALL FUNC (FUNCON,Y,YSIG,NPTS,FIT,PHI)
  NF=1
  IF(NTRAC.GE.-1) WRITE(KW,160)PHI,FLAMB
160 FORMAT(//,9X,27H PHI (THE SUM OF SQUARES) =,E15.8,/,9X,9H LAMBDA =
 +,E12.5//1H )
170 JSUB=0
  FCUT=RTWO
  ITER=ITER+1
  IF(NTRAC.GE.1) WRITE(KW,180)ITER,FMGN,FLAMB
180 FORMAT(//16H BEGIN ITERATION,I5,44X,7H FMGN =,E12.5,15X,
 +  9H LAMBDA =,E12.5)
  IF(NTRAC.GE.3) WRITE(KW,190)
190 FORMAT(/28H P (THE JACOBIAN MATRIX)..../1H )
  STFAC=RUNIT
  DO 200 JX=1,NACTV
       GRAD(JX)=RZERO
       DO 200 KX=1,JX
200    ERR(JX,KX)=RZERO
  SIG=YSIG(1)
  DO 270 JPT=1,NPTS
   KPT=JPT
       IF(KALCP.LT.0) GO TO 210
   IF(JPT.NE.1) GO TO 230
210  KPT=1
```

```
      IF(KORDF.LE.2) GO TO 220
           CALL CALCD (JPT,P,LPDMA,LPDMB)
      GO TO 230
220   CALL DERIV (JPT,FUNCON,NPTS,FIT,FITSV,P,LPDMA,LPDMB)
230   CONTINUE
           IF(NTRAC.GE.3) WRITE(KW,240)JPT,(P(KPT,JX),JX=1,NACTV)
240   FORMAT(1X,I3,2X,6E15.7/(6X,6E15.7))
      IF(LEQU.EQ.0) SIG=YSIG(JPT)
      RTERM=(FIT(JPT)-Y(JPT))/SIG**2
      DO 260 JX=1,NACTV
       GRAD(JX)=GRAD(JX)+P(KPT,JX)*RTERM
            PTERM=P(KPT,JX)/SIG**2
            DO 250 KX=1,JX
250        ERR(JX,KX)=ERR(JX,KX)+P(KPT,KX)*PTERM
260     CONTINUE
270   CONTINUE
     IF(KORDF.NE.2) GO TO 290
     IF(KALCP.NE.0) GO TO 280
     CALL FUNC (FUNCON,Y,YSIG,NPTS,FIT,PHI)
     NF=NF+1
280 NF=NF+NACTV
290 NF=NF+NACTV
     DO 300 JX=1,NACTV
      SCALJ=QSQRT(ERR(JX,JX))
      IF(SCALJ.EQ.RZERO) SCALJ=RUNIT
           DELTX(JX)=SCALJ
300   GRAD(JX)=GRAD(JX)/SCALJ
     IF(NTRAC.GE.1) WRITE(KW,310)(GRAD(JX),JX=1,NACTV)
310 FORMAT(/21H   SCALED GRADIENT = ,6E15.7/(21X,6E15.7))
     DO 355 JX=1,NACTV
      DO 350 KX=1,JX
            SA=ERR(JX,KX)/(DELTX(JX)*DELTX(KX))
            IF(KX.NE.JX) GO TO 320
            IF(SA.EQ.RZERO) GO TO 330
       SA=RUNIT
       GO TO 350
320     IF(QABS(SA).LT.RUNIT-RLTOL) GO TO 350
330     CONTINUE
       IF(NTRAC.GE.-2) WRITE(KW,340)JX,KX,SA,ITER
340     FORMAT(38H ******** POSSIBLY DANGEROUS VALUE OF ,
     +    16H COEFFICIENT....,5X,6H QSAV(,I3,1H,,I3,3H) =,E15.7,9X,
     +    10H ITERATION,I5)
350    ERR(JX,KX)=SA
355 CONTINUE
     IF(NTRAC.LT.2) GO TO 380
     WRITE(KW,360)
360 FORMAT(/49H QSAV (PT*P, SCALED, WHERE P IS THE JACOBIAN)..../1H )
     DO 370 JX=1,NACTV
370   WRITE(KW,240)JX,(ERR(JX,KX),KX=1,JX)
380 DO 390 JX=1,NV
390   XSAVE(JX)=XX(JX)
400 NACT=NACTV
     DO 410 JX=1,NV
410   MASKT(JX)=MASK(JX)
420 KRANK=0
     JQ=0
     JT=0
     DO 450 JX=1,NV
      IF(MASK(JX).NE.0) GO TO 450
      JQ=JQ+1
```

```
      IF(MASKT(JX).NE.0) GO TO 450
           JT=JT+1
      H(JT)=-GRAD(JQ)
      KQ=0
      KT=0
           DO 440 KX=1,JX
       IF(MASK(KX).NE.0) GO TO 440
       KQ=KQ+1
       IF(MASKT(KX).NE.0) GO TO 440
       KT=KT+1
       SA=ERR(JQ,KQ)
            IF(KX.NE.JX .OR. SA.EQ.RZERO) GO TO 430
            SA=RUNIT+FLAMB
            KRANK=KRANK+1
  430    ERR(KT,JT+1)=SA
  440    CONTINUE
  450  CONTINUE
     NSMAL=0
     NMU=NACT-1
     IF(NMU.EQ.0) GO TO 490
     DO 480 J=1,NMU
           PIVOT=ERR(J,J+1)
      IF(PIVOT.EQ.RZERO) GO TO 480
      JPU=J+1
      DO 470 K=JPU,NACT
            EM=ERR(J,K+1)/PIVOT
       IF(EM.EQ.RZERO) GO TO 470
       DO 460 L=K,NACT
  460      ERR(K,L+1)=ERR(K,L+1)-ERR(J,L+1)*EM
  470    H(K)=H(K)-H(J)*EM
  480  CONTINUE
  490 DO 530 JINV=1,NACT
           J=(NACT+1)-JINV
           PIVOT=ERR(J,J+1)
      IF(PIVOT.LE.RZERO) NSMAL=NSMAL+1
      IF(PIVOT.NE.RZERO) GO TO 500
      H(J)=RZERO
           GO TO 530
  500  SUM=RZERO
      IF(J.EQ.NACT) GO TO 520
      JPU=J+1
           DO 510 K=JPU,NACT
  510    SUM=SUM+ERR(J,K+1)*H(K)
  520  H(J)=(H(J)-SUM)/PIVOT
  530  CONTINUE
     MRANK=NACT-NSMAL
     IF(MRANK.EQ.NACT) GO TO 560
     COSIN=1.E30
     IF(NTRAC.GE.-2) WRITE(KW,540)MRANK,NACT,ITER
  540 FORMAT(/41H RANK-DEFICIENT NORMAL EQUATIONS IN MARQ.,9X,7H RANK =,
    +  I4,7X,18H ORDER OF MATRIX =,I4,9X,10H ITERATION,I5)
     IF(MRANK.GT.0) GO TO 550
     KFLAG=-4
     GO TO 1200
  550 IF(METHD.GT.0 .AND. MRANK.LT.KRANK) GO TO 860
  560 SA=RZERO
     SB=RZERO
     SC=RZERO
     KX=NV
     KQ=NACTV
```

```
      KT=NACT
      DO 590 JX=1,NV
       HH=RZERO
       IF(MASK(KX).NE.0) GO TO 580
       IF(MASKT(KX).NE.0) GO TO 570
            HH=H(KT)
       SA=SA-HH*GRAD(KQ)
       SB=SB+HH*HH
       SC=SC+GRAD(KQ)**2
       HH=HH*FMGN/DELTX(KQ)
       KT=KT-1
  570  KQ=KQ-1
  580  H(KX)=HH
  590  KX=KX-1
  600 CONTINUE
      IF(NTRAC.GE.1) WRITE(KW,610)(H(JX),JX=1,NV)
  610 FORMAT(/7X,14H CORRECTION = ,6E15.7/(21X,6E15.7))
      NACSV=NACT
      FRMIN=RUNIT
      NLOOP=0
      JXLIM=0
  620 DO 720 JX=1,NV
       IF(MASKT(JX).NE.0) GO TO 720
       XSAV=XSAVE(JX)
       XMX=XMAX(JX)
            XMN=XMIN(JX)
       HH=H(JX)
       IF((XSAV.LT.XMX .OR. HH.LE.RZERO) .AND.
     +    (XSAV.GT.XMN .OR. HH.GE.RZERO)) GO TO 640
       MASKT(JX)=1
       NACT=NACT-1
            XX(JX)=XSAV
            IF(NTRAC.GE.-1) WRITE(KW,630)JX,XSAV,ITER
  630  FORMAT(/8H FIX  X(,I3,4H) = ,E12.5,22H TEMPORARILY, TO AVOID,
     + 24H VIOLATING A CONSTRAINT.,26X,10H ITERATION,I5)
       GO TO 720
  640  XLIM=XSAV+HH*FRMIN
            IF(JX.NE.JXLIM) GO TO 650
       IF(KBND)680,660,660
  650  XX(JX)=XLIM
       IF(XLIM.LE.XMX) GO TO 670
  660  XX(JX)=XMX
       JBND=1
       GO TO 690
  670  IF(XLIM.GE.XMN) GO TO 720
  680  XX(JX)=XMN
       JBND=-1
  690  IF(JX.NE.JXLIM) GO TO 710
       IF(NTRAC.LT.-1) GO TO 720
       WRITE(KW,700)JX,XX(JX),FRMIN,ITER
  700  FORMAT(/26H CONSTRAINT VIOLATED BY X(,I3,18H).  VALUE RESET TO,
     + E15.7,23H USING CUTSTEP FACTOR =,E12.5,12H   ITERATION,I5)
            GO TO 720
  710  IF(NLOOP.NE.0) GO TO 720
       DENOM=XLIM-XSAV
       IF(DENOM.EQ.RZERO) GO TO 720
       FRAC=(XX(JX)-XSAV)/DENOM
            IF(FRAC.GE.FRMIN) GO TO 720
       FRMIN=FRAC
       JXLIM=JX
```

```
    KBND=JBND
720   CONTINUE
    IF(NACT.GT.0) GO TO 740
    KFLAG=3
    IF(NTRAC.LT.-2) GO TO 1200
    WRITE(KW,730)
730 FORMAT(////47H APPARENT CONSTRAINED OPTIMUM LIES IN A CORNER.)
    GO TO 1200
740 IF(NACT.LT.NACSV) GO TO 420
    IF(NLOOP.NE.0) GO TO 750
    NLOOP=1
    IF(JXLIM.NE.0) GO TO 620
750 CONTINUE
    IF(NTRAC.GE.1) WRITE(KW,760)(XX(JX),JX=1,NV)
760 FORMAT(/16X,5H X = ,6E15.7/(21X,6E15.7))
    CALL FUNC (FUNCON,Y,YSIG,NPTS,FIT,PHNEW)
    NF=NF+1
    IF(PHNEW-PHI)930,770,790
770 IF(NFLAT.EQ.0) GO TO 930
    KFLAG=2
    IF(NTRAC.LT.-1) GO TO 830
    WRITE(KW,780)
780 FORMAT(//,9X,45H CONVERGENCE ACHIEVED UNDER THE NFLAT OPTION.)
    GO TO 830
790 CONTINUE
    IF(NTRAC.GE.1) WRITE(KW,800)PHI,PHNEW
800 FORMAT(/33X,10H OLD PHI =,E15.8,5X,10H NEW PHI =,E15.8)
    JSUB=JSUB+1
    IF(JSUB.GT.MXSUB) GO TO 810
    IF(METHD)880,1090,850
810 KFLAG=-1
    IF(NTRAC.GE.-1) WRITE(KW,820)MXSUB
820 FORMAT(//43H EXCEEDED MAXIMUM NUMBER OF SUBITERATIONS =,I3,
   +  9H IN MARQ.)
830 DO 840 JX=1,NV
840   XX(JX)=XSAVE(JX)
    CALL FUNC (FUNCON,Y,YSIG,NPTS,FIT,PHI)
    GO TO 1200
850 DENOM=SB*SC
    IF(DENOM.LE.RZERO) GO TO 860
    COSIN=SA/QSQRT(DENOM)
    IF(COSIN.GT.CRIT) GO TO 880
860 UPFAC=UPNU
    UPNU=QMIN1(UPNU*RTWO,FNU)
    IF(METHD.EQ.1) UPFAC=QMIN1(UPFAC,FNULM+RUNIT/FLAMB)
    FLAMB=FLAMB*UPFAC
    IF(NTRAC.GE.1) WRITE(KW,870)JSUB,COSIN,FLAMB
870 FORMAT(/18H **** SUBITERATION,I3,4X,17H INCREASE LAMBDA.,4X,
   +  13H COS(GAMMA) =,E12.5,28X,9H LAMBDA =,E12.5)
    GO TO 400
880 STFAC=STFAC/FCUT
    IF(METHD.GE.0) GO TO 890
    FMGN=FMGN/FCUT
    GO TO 900
890 IF(METHD.EQ.1) FLAMB=FLAMB*RTWO
900 DO 910 JX=1,NV
910   H(JX)=(XX(JX)-XSAVE(JX))/FCUT
    FCUT=FCUT*FACCL
    IF(NTRAC.GE.1) WRITE(KW,920)JSUB,COSIN,STFAC
920 FORMAT(/18H **** SUBITERATION,I3,4X,16H TAKE CUT STEPS.,4X,
```

```
     +   13H COS(GAMMA) =,E12.5,5X,17H CUTSTEP FACTOR =,E12.5)
         GO TO 600
     930 IF(METHD.EQ.0 .OR. METHD.EQ.2) GO TO 1090
         DO 940 JX=1,NV
          XTEMP(JX)=XX(JX)
               IF(MASK(JX).NE.0) GO TO 940
          XX(JX)=XSAVE(JX)+(XX(JX)-XSAVE(JX))/RTWO
          XX(JX)=QMAX1(XMIN(JX),QMIN1(XMAX(JX),XX(JX)))
     940  CONTINUE
         DO 950 JPT=1,NPTS
     950  FITSV(JPT)=FIT(JPT)
         CALL FUNC (FUNCON,Y,YSIG,NPTS,FIT,PHALF)
         NF=NF+1
         RLFAC=RUNIT
         DENOM=RTWO*((PHNEW-PHALF)-(PHALF-PHI))
         STFAC=RZERO
         IF(DENOM.LE.RZERO) GO TO 960
         STFAC=(PHI-PHNEW)/DENOM
         RSFAC=(RUNIT+STFAC)/RTWO
         IF(STFAC.GE.RUNIT) STFAC=RZERO
     960 DO 970 JX=1,NV
               H(JX)=XX(JX)
     970  XX(JX)=XX(JX)+(XTEMP(JX)-XX(JX))*STFAC
         IF(PHALF.GE.PHNEW) GO TO 1010
         RLFAC=RUNIT/RTWO
         JSUB=JSUB+1
         DO 980 JX=1,NV
     980 XTEMP(JX)=H(JX)
         DO 990 JPT=1,NPTS
     990  FITSV(JPT)=FIT(JPT)
         IF(NTRAC.GE.1) WRITE(KW,1000)PHNEW,PHALF
    1000 FORMAT(/21H HALF STEP SUCCEEDED.,15X,8H PHNEW =,E15.8,18X,
        +   8H PHALF =,E15.8)
         PHNEW=PHALF
    1010 IF(STFAC.EQ.RZERO) GO TO 1020
         CALL FUNC (FUNCON,Y,YSIG,NPTS,FIT,PHI)
         NF=NF+1
         IF(PHI.LT.PHNEW) GO TO 1060
    1020 DO 1030 JX=1,NV
    1030  XX(JX)=XTEMP(JX)
         DO 1040 JPT=1,NPTS
    1040  FIT(JPT)=FITSV(JPT)
         IF(STFAC.EQ.RZERO) GO TO 1080
         IF(NTRAC.LT.1) GO TO 1080
         WRITE(KW,1050)RSFAC,PHI
    1050 FORMAT(/25H QUADRATIC INTERPOLATION.,22X,8H RSFAC =,E12.5,12X,
        +   6H PHI =,E15.8)
         GO TO 1080
    1060 RLFAC=RSFAC
         PHNEW=PHI
         IF(NTRAC.GE.1) WRITE(KW,1070)RLFAC,PHI
    1070 FORMAT(/35H QUADRATIC INTERPOLATION SUCCEEDED.,12X,8H RLFAC =,
        +   E12.5,12X,6H PHI =,E15.8)
    1080 IF(RLFAC.LE.RZERO) GO TO 1090
         FLAMB=FLAMB/RLFAC
         IF(METHD.LT.0) FMGN=FMGN*RLFAC
    1090 CONTINUE
         IF(NTRAC.GE.1) WRITE(KW,1100)ITER,PHNEW
    1100 FORMAT(/ ' END   ITERATION',I5,58X,' PHI =',E15.8)
         PHI=PHNEW
```

```
      IF(JXLIM.GT.0) GO TO 1130
      DO 1110 JX=1,NV
       IF(MASK(JX).NE.0) GO TO 1110
       IF(QABS(XX(JX)-XSAVE(JX)).GT.DELMN(JX)) GO TO 1130
 1110  CONTINUE
      KFLAG=1
      IF(NTRAC.LT.-1) GO TO 1200
      WRITE(KW,1120)
 1120 FORMAT(///,9X,38H CONVERGED WHEN THE STEP BECAME SMALL.)
      GO TO 1200
 1130 IF(ITER.LT.MAXIT) GO TO 1150
      KFLAG=-6
      IF(NTRAC.GE.-3) WRITE(KW,1140)MAXIT
 1140 FORMAT(1H1,//,9X,' MAXIMUM NUMBER OF ITERATIONS REACHED IN MARQ.'
     +,2X,8H MAXIT =,I3)
      GO TO 1200
 1150 IF(NF.GE.NFMAX) GO TO 1180
      IF(JSUB.GT.0) GO TO 1160
      FMGN=QMIN1(FMGN*RTWO,RUNIT)
      SCALJ=RUNIT+FLAMB
      IF(SCALJ.GT.RUNIT) FLAMB=FLAMB/DOWNU
      UPNU=DOWNU
      DOWNU=QMIN1(DOWNU*RTWO,FNU)
      GO TO 1170
 1160 IF(METHD.NE.1) GO TO 1170
      UPNU=FNULM
      DOWNU=FNULM
 1170 CONTINUE
      GO TO 170
 1180 KFLAG=-7
      IF(NTRAC.GE.-3) WRITE(KW,1190)NFMAX
 1190 FORMAT(//23H NF HAS REACHED NFMAX =,I7,9H IN MARQ.)
 1200 CONTINUE
      SC=QSQRT(SC)
      IF(NTRAC.LT.-1) GO TO 1290
      WRITE(KW,1210)ITER,NF,PHI,FMGN,FLAMB,SC
 1210 FORMAT(/10X,I4,11H ITERATIONS,7X,5H NF =,I5,9X,6H PHI =,E15.8,/,
     +  11X,7H FMGN =,E12.5,7X,9H LAMBDA =,E12.5//9X,15H NORM OF SCALED,
     +  18H GRADIENT VECTOR =,E12.5)
       WRITE(KW,69)
  69   FORMAT(9X,60(1H*),//)
C ------------------------------------
C      WRITE(KW,75) (A(I),I=1,70)
C  75 FORMAT(80A1,/)
C ------------------------------------
   76 FORMAT(14X,'A(',I2,') = ',E12.5)
      DO 771 NJK =1,NV
      WRITE(KW,76)NJK,XX(NJK)
  771 CONTINUE
      WRITE(KW,*)' '
      GO TO(1,2,3,4,5,6,7,8,9,11,12,13),IFORM
    1 WRITE(KW,9051)
      GO TO 1219
    2 WRITE(KW,9052)
      GO TO 1219
    3 WRITE(KW,9053)
      GO TO 1219
    4 WRITE(KW,9054)
      GO TO 1219
    5 WRITE(KW,9055)
```

```
      GO TO 1219
    6 WRITE(KW,9056)
      GO TO 1219
    7 WRITE(KW,9057)
      GO TO 1219
    8 WRITE(KW,9058)
      GO TO 1219
    9 WRITE(KW,9059)
      GO TO 1219
   11 WRITE(KW,9060)
      GO TO 1219
   12 WRITE(KW,9061)
      GO TO 1219
   13 WRITE(KW,9062)
C
C
C ************************* E#@ *************************
C *                                                     *
C *              CHANGING EQUATIONS                     *
C *                                                     *
C * For the Equation # (IFORM) of the altered equation: *
C *                                                     *
C *  Change the form of the equation following the      *
C *    appropriate number of FORMAT STATEMENT :         *
C *                                                     *
C *      EQUATION #        FORMAT #                     *
C *         1               9051                        *
C *         2               9052                        *
C *         3               9053                        *
C *         4               9054                        *
C *         5               9055                        *
C *         6               9056                        *
C *         7               9057                        *
C *         8               9058                        *
C *         9               9059                        *
C *        10               9060                        *
C *        11               9061                        *
C *        12               9062                        *
C *                                                     *
C *******************************************************
C
 9051 FORMAT(7X,'Y=A(1)+A(2)*X+A(3)*X**2+A(4)*X**3+A(5)*X**4+A(6)*X**5')
 9052 FORMAT(7X,'Y=A(1)+A(2)*EXP(A(3)*X)')
 9053 FORMAT(7X,'Y=A(1)+A(2)*DLOG(X)')
 9054 FORMAT(7X,'Y=A(1)+A(2)*X**A(3)')
 9055 FORMAT(7X,'Nu=A(1)*{[Re*Pr*(d/L)]+ A(2)*[(Gr*Pr)**A(3)]}**A(4)',
     +       '*(U/Uw)**0.14')
 9056 FORMAT(7X,'Nu=A(1)*Re**A(2)*Pr**A(3)*Gr**A(4)*(d/L)**A(5)')
 9057 FORMAT(7X,'Nu={A(1)*Nul**A(2)+[EXP((A(4)-Re)/A(5))]+'
     +     /10X,'1/Nut**A(3)**(-A(2)/A(3))}**(-A(2)/A(3))**(1/A(2))')

 9058 FORMAT(7X,'Nu={NuL+A(1)*Re**A(2)*Pr**A(3)*[1+A(4)*EXP(A(5)*(L/d)]'
     +    ,/10X,'+A(6)*[(Gr*Pr)**.25]*[1-EXP(A(7)*L/d)]}*(Ub/Uw)**.14')
 9059 FORMAT(7X,'Nu=A(1)*Re**A(2)*Pr**A(3)*(X/D)**A(4)*(Ub/Uw)**.14')
 9060 FORMAT(7X,'Nu=A(1)*Re**A(2)*Pr**A(3)*{1+A(4)*EXP[A(5)*(L/d)]}',
     +          '(Ub/Uw)**.14')
 9061 FORMAT(7X,'Nu=A(1)*Re**A(2)*Pr**A(3)*(Ub/Uw)**.14')
 9062 FORMAT(7X,'f=2*{1/[(8/Re)**A(1)+(Re/A(3))**(2*A(1))]**A(2)/A(1)',
     +    /10X,'+[2.21*LN(Re/7)]**(2*A(2))}**(-1/A(2))')
C
```

```
1219 IF(NTRAC.GE.0) WRITE(KW,1220)
1220 FORMAT(///6X,'No.',7X,'Y(I) EXP.',5X,'Y(I) CAL.',6X,'% DEV.'/)
   SIG=YSIG(1)
   RMSDV=RZERO
   SDVMX=RZERO
   JSMAX=1
   SSSUM=0.0D0
   DO 1240 I=1,NPTS
    IF(LEQU.EQ.0) SIG=YSIG(I)
    YY=Y(I)
    YX=FIT(I)
        PTERM=YY-YX
    RTERM=PTERM/(0.0100*Y(I))
        SSSUM=SSSUM+DABS(RTERM)
    IF(NTRAC.GE.0) WRITE(KW,1230)I,YY,YX,RTERM
1230 FORMAT(5X,I3,7X,F10.4,4X,F10.4,4X,E10.3)
    IF(QABS(RTERM).LE.SDVMX) GO TO 1240
        SDVMX=QABS(RTERM)
    JSMAX=I
1240  RMSDV=RMSDV+RTERM**2
   AAPD=SSSUM/NPTS
   DENOM=NPTS-NACTV
   IF(DENOM.LE.RZERO) GO TO 1270
   RMSDV=QSQRT(RMSDV/DENOM)
   WRITE(KW,1260)AAPD
1260 FORMAT(/,10X,43H AVE. ABSOLUTE PERCENT DEVIATION FROM FIT =,E12.5)
    WRITE(KW,69)
1270 CONTINUE
1290 CALL FUNC (FUNCON,Y,YSIG,NPTS,FIT,PHI)
   FOBJ=PHI
   IF(MATRX.EQ.0) RETURN
   CALL MQERR (NACTV,NPTS)
1300 RETURN
   END
C
   SUBROUTINE FUNC (FUNCON,Y,YSIG,NPTS,FIT,PHI)
   EXTERNAL FUNCON
   DOUBLE PRECISION Y,YSIG,XMAX,XMIN,DELTX,DELMN,ERR,FOBJ,
  +          FLAMB,FNU,RELDF,RELMN
   DOUBLE PRECISION XX,FIT,F,PHI,SIG
   DOUBLE PRECISION X1,X2,X3,X4,X5,X6,AMDA,A
   CHARACTER*20 NAME,NAMO
   DIMENSION Y(1),YSIG(1),FIT(1)
   COMMON /CSTEP/ XMAX(20),XMIN(20),DELTX(20),DELMN(20),A(20),
  +          ERR(20,21),FOBJ,NV,NTRAC,MATRX,MASK(20),NFMAX,
  +          NFLAT,JVARY,NXTRA,KFLAG,NOREP,KERFL,KW,XX(20),
  +          NAME,NAMO,IPIC,NT
   COMMON /NLLS4/ FLAMB,FNU,RELDF,RELMN,METHD,KALCP,KORDF,MAXIT,
  +          LEQU,MXSUB,MXUPD
   COMMON /CSTOR/ X1(700),X2(700),X3(700),X4(700),X5(700),X6(700),
  +          AMDA(700)
   RZERO=0.
   IF(KALCP.NE.0) GO TO 10
   CALL FUNCON (FIT)
   GO TO 30
 10 DO 20 JPT=1,NPTS
    CALL FOFX(JPT,NV,XX,F)
 20  FIT(JPT)=F
 30 PHI=RZERO
   SIG=YSIG(1)
```

```
      DO 50 JPT=1,NPTS
       IF(LEQU.EQ.0) SIG=YSIG(JPT)
       IF(SIG.GT.RZERO) GO TO 50
       WRITE(KW,40)LEQU,JPT,SIG
   40  FORMAT(/' ERROR IN MARQ....    LEQU = ',I1,5X,' JPT =',I5,5X,
     +  ' YSIG =',E13.5,' IS .LE. ZERO.')
       STOP
   50  PHI=PHI+((FIT(JPT)-Y(JPT))/SIG)**2
       RETURN
       END
C
       SUBROUTINE DERIV (JPT,FUNCON,NPTS,FIT,FITSV,P,LPDMA,LPDMB)
       DOUBLE PRECISION P,XMAX,XMIN,DELTX,DELMN,ERR,FOBJ,
      *    FLAMB,FNU,RELDF,RELMN,RZERO
       DOUBLE PRECISION XX,FIT,FITSV,DEL,TWODL,XSAVE,FX0,FX1,A
       DOUBLE PRECISION X1,X2,X3,X4,X5,X6,AMDA
       CHARACTER*20 NAME,NAMO
       DIMENSION FIT(1),FITSV(1),P(LPDMA,LPDMB)
       COMMON /CSTEP/ XMAX(20),XMIN(20),DELTX(20),DELMN(20),A(20),
      +          ERR(20,21),FOBJ,NV,NTRAC,MATRX,MASK(20),NFMAX,
      +          NFLAT,JVARY,NXTRA,KFLAG,NOREP,KERFL,KW,XX(20),
      +          NAME,NAMO,IPIC,NT
       COMMON /NLLS4/ FLAMB,FNU,RELDF,RELMN,METHD,KALCP,KORDF,MAXIT,
      +          LEQU,MXSUB,MXUPD
       COMMON /CSTOR/ X1(700),X2(700),X3(700),X4(700),X5(700),X6(700),
      +          AMDA(700)
C
       RZERO=0.
       JVARY=0
       IF(KALCP.LT.0) GO TO 20
       DO 10 J=1,NPTS
   10  FITSV(J)=FIT(J)
   20 KX=0
       DO 150 JX=1,NV
        IF(MASK(JX).NE.0) GO TO 150
        KX=KX+1
        DEL=RELDF*XX(JX)
        IF(DEL.EQ.RZERO) DEL=RELDF
        XSAVE=XX(JX)
            XX(JX)=XSAVE+DEL
        TWODL=DEL+DEL
            IF(KALCP)110,30,80
   30   CALL FUNCON (FIT)
        IF(KORDF.EQ.2) GO TO 50
        DO 40 J=1,NPTS
   40     P(J,KX)=(FIT(J)-FITSV(J))/DEL
        GO TO 140
   50   XX(JX)=XSAVE-DEL
        DO 60 J=1,NPTS
   60     FITSV(J)=FIT(J)
        JVARY=JX
        CALL FUNCON (FIT)
        JVARY=0
        DO 70 J=1,NPTS
   70     P(J,KX)=(FITSV(J)-FIT(J))/TWODL
        GO TO 140
   80   DO 100 J=1,NPTS
         CALL FOFX (J,NV,XX,FX1)
         IF(KORDF.EQ.2) GO TO 90
              P(J,KX)=(FX1-FITSV(J))/DEL
```

```
      GO TO 100
 90   XX(JX)=XSAVE-DEL
      CALL FOFX (J,NV,XX,FX0)
      P(J,KX)=(FX1-FX0)/TWODL
      XX(JX)=XSAVE+DEL
100   CONTINUE
      GO TO 140
110   FITSV(1)=FIT(JPT)
      CALL FOFX (JPT,NV,XX,FX1)
      IF(KORDF.EQ.2) GO TO 120
      P(1,KX)=(FX1-FITSV(1))/DEL
      GO TO 130
120   XX(JX)=XSAVE-DEL
      CALL FOFX (JPT,NV,XX,FX0)
      P(1,KX)=(FX1-FX0)/TWODL
130   FIT(JPT)=FITSV(1)
140   XX(JX)=XSAVE
150   CONTINUE
      IF(KALCP.LT.0) RETURN
      DO 160 J=1,NPTS
160   FIT(J)=FITSV(J)
      RETURN
      END
C
      SUBROUTINE MQERR (NACTV,NPTS)
      DOUBLE PRECISION X1,X2,X3,X4,X5,X6,AMDA,A
      DOUBLE PRECISION XMAX,XMIN,DELTX,DELMN,ERR,FOBJ,XX
      CHARACTER*20 NAME,NAMO
      COMMON /CSTEP/ XMAX(20),XMIN(20),DELTX(20),DELMN(20),A(20),
     +          ERR(20,21),FOBJ,NV,NTRAC,MATRX,MASK(20),NFMAX,
     +          NFLAT,JVARY,NXTRA,KFLAG,NOREP,KERFL,KW,XX(20),
     +          NAME,NAMO,IPIC,NT
      COMMON /CSTOR/ X1(700),X2(700),X3(700),X4(700),X5(700),X6(700),
     +          AMDA(700)
      RETURN
      END
```

A.3 Program FRIC

The program FRIC is developed for the pressure drop measurement and data reduction purposes. The following is a complete listing of this program.

```
/************************************************
Program FRIC.C  developed by Lap Mou Tam
  under the supervision of Prof. A. J. Ghajar for
  pressure drop measurement and data reduction purposes
************************************************/

#include <stdio.h>
#include <math.h>
#include <conio.h>
#include <stdlib.h>
#include <graphics.h>
#include <dos.h>
#include <ctype.h>

#define PI 3.141592653
#define   BASADR      0x300      /* Defining of Base address     */
#define   ADHI        BASADR+1   /* A/D Hi-byte conversion address*/
#define   STATUS      BASADR+2   /* Status register address      */
#define   NUMBER1     5
#define   NUMBER2     100
#define   MAXSTRING   100


/*                              */
/*  declaration of variables  and functions  */
/*                              */

double tbulk , twall , concen , fl , diam = 0.621 , dens , dense ;
double pdrt , pdrta , pdrtb , beta , betaf , betae , v3 , visc , abvisc;
double abvisce , kinvisc , kinvisce , pr , pran , kfactor ,pdrtc;
double kh2o , keth ,kk , ke , gr , re , mfe , vele , tde ,p3,cp,cpe;
double ad[3][3] , d[3][3] , av[3][3] , v[2][3] , v2[3] , ap[3][3] ;
double p[2][3] , p2[3] , ff[20] , dph[20] , dpm[20] , lnth[20] ;
double vavg[18];
double denhg , denh2o ,coef_a,coef_b;

main()
{

int i,j , m , gdriver = DETECT, gmode ;
int sth,type_of_gauge;
double sum=0 ;
char c;
int chno=5 , k, go ,del;          /* Declaration of Variables */
int lowbyte, hibyte, gage_no, sample_no ,check_gage_no ;
float sumv=0, data, da, dat, volt[NUMBER1][NUMBER2],check_volt;
FILE  *ofp ;
char name[MAXSTRING];

while(1) {  /****** for while loop ******/
system("cls");
window(1,1,80,25);
textbackground(BLUE);
clrscr();
```

```
window(1,1,80,1);
textbackground(MAGENTA);
textcolor(WHITE);
clrscr();
printf("            :::::::::::: FRIC PROGRAM MENU :::::::::::: ");
window(1,25,80,25);
textbackground(MAGENTA);
textcolor(WHITE);
clrscr();
printf("\t\t::::: By Ray under the supervision of Prof A. J. Ghajar :::::");
window(11,5,71,22);
textbackground(BLACK);
clrscr();
window(10,4,70,21);
textbackground(CYAN);
textcolor(BLACK);
clrscr();
gotoxy(5,2);
cprintf("D==> AD conversion ");
gotoxy(5,4);
cprintf("P==> properties of eth");
gotoxy(5,6);
cprintf("F==> Cf calculation ");
gotoxy(5,8);
cprintf("M==> run MRE  ");
gotoxy(5,10);
cprintf("C==> run CONVERT ");
gotoxy(5,12);
cprintf("A==> run ACQCOMP ");
gotoxy(5,14);
cprintf("Q==> Quit ");
window(40,4,70,21);
textbackground(RED);
textcolor(YELLOW);
clrscr();
gotoxy(5,2);
cprintf("H==> run HT ");
gotoxy(5,4);
cprintf("R==> run DTRED ");
gotoxy(5,6);
cprintf("S==> run PCPLUS ");
window(10,4,40,22);
textbackground(CYAN);
textcolor(RED);
gotoxy(5,16);
cprintf("Enter your choice : ");
scanf("%c",&c);

switch(c) {   /****** switch case brace ******/

case 'D' :


  do{
textbackground(BLUE);
  clrscr();
  window(6,6,74,19);
  textbackground(CYAN);
  textcolor(BLACK);
```

```
clrscr();
gotoxy(10,4);
cprintf("Specify the delay : ");
scanf("%d",&del);
gotoxy(10,6);
cprintf("Specify how many gage to use : ");
scanf("%d",&gage_no);
gotoxy(10,8);
cprintf("Specify the number of sample to average : ");
scanf("%d",&sample_no);
gotoxy(10,10);
printf("Specify the output file name : ");
scanf("%s",&name);
window(10,8,70,17);
textbackground(RED);
textcolor(WHITE);
clrscr();
gotoxy(5,1);
cprintf("The delay        = %d ",del);
gotoxy(5,3);
cprintf("The channel number =  %d ",gage_no);
gotoxy(5,5);
cprintf("The sample number  =  %d ",sample_no);
gotoxy(5,7);
cprintf("Ouput file name    =  %s ",name);
gotoxy(5,9);
cprintf("Enter '1' to run the program or '2' to re-enter : ");
scanf("%d",&go);
}while(go==2);

/*                                          */
/*    open a file to store the voltage in all the channels   */
/*                                          */

ofp = fopen(name,"w");
for(j=0;j< gage_no;++j)   {  /* loop to write the voltage in a file   */
window(1,1,80,25);
textbackground(CYAN);
textcolor(BLACK);
clrscr();
window(5,3,75,14);
textbackground(BLUE);
textcolor(YELLOW);
clrscr();
for(k=0;k<NUMBER1;++k)    {  /* sampling the same channel 5 times */
gotoxy(13,2);
cprintf("Sampling gage :%d  smapling time : %d",j+1,k+1);
sumv = 0.0;
for(i=0;i< sample_no ;++i) {  /* A/D conversion begins */

outportb(STATUS,chno);
outportb(ADHI,0);
while(inportb(STATUS) >= 128);
lowbyte = inportb(BASADR);
hibyte = inportb(ADHI);
da = hibyte*16+lowbyte/16;
dat = da*10/4096;
data =dat - 5.0;
sumv = sumv + data;
gotoxy(10,5);
```

```
cprintf("Voltage fluctuation  = %f ",data);
delay(del);                    /* A/D conversion ends after */
  }                          /* summing 20 values */
  gotoxy(10,7);

cprintf("Average voltage      = %f ",sumv/sample_no);
 volt[k][j] = sumv/sample_no;
 check_volt = volt[k][j];

  }    /*    end loop for the file    */
  gotoxy(10,11);
  textbackground(RED);
  cprintf("switch the channel and strike any key when ready !!");
  getch();
  check_gage_no = gage_no;
  if(check_volt > 4.5)
  break;
  }
  for(j=0;j<check_gage_no;++j)  {
  if (j==18) {
  fprintf(ofp,"%5d  %f %f %f %f %f\n",j+2,volt[0][j],volt[1][j],volt[2][j],volt[3][j],volt[4][j]);
  }
  else {
  fprintf(ofp,"%5d  %f %f %f %f %f\n",j+1,volt[0][j],volt[1][j],volt[2][j],volt[3][j],volt[4][j]);
  }
  }
getch();
break ;

case 'P' :

/* initialized the array */

ad[0][0] = 1.0004 ;      /* for density calculation */
ad[0][1] = .17659 ;
ad[0][2] = -0.049214 ;
ad[1][0] = -1.2379e-4 ;
ad[1][1] = -9.9189e-4 ;
ad[1][2] = 4.1024e-4 ;
ad[2][0] = -2.9837e-6 ;
ad[2][1] = 2.4614e-6 ;
ad[2][2] = -9.5278e-8 ;

av[0][0] = .55164 ;      /* for viscosity calculation */
av[0][1] = 2.6492 ;
av[0][2] = .82935 ;
av[1][0] = -0.027633 ;
av[1][1] = -0.031496 ;
av[1][2] = 0.0048136 ;
av[2][0] = 6.0629e-17 ;
av[2][1] = 2.2389e-15 ;
av[2][2] = 5.879e-16 ;

ap[0][0] = 2.5735 ;      /* for Prandtl number calculation */
ap[0][1] = 3.0411 ;
ap[0][2] = .60237 ;
ap[1][0] = -0.031169 ;
ap[1][1] = -0.025424 ;
ap[1][2] = .0037454 ;
ap[2][0] = 1.1605e-16 ;
```

```
ap[2][1] = 2.5283e-15 ;
ap[2][2] = 2.3777e-16 ;

   window(1,2,80,24);
   textbackground(BLACK);
   textcolor(WHITE);
   clrscr();

   gotoxy(10,2);
   printf("input the concentration : ");
   scanf("%lf",&concen);
   gotoxy(10,4);
   printf("input the bulk temperature : ");
   scanf("%lf",&tbulk);
   gotoxy(10,6);
   printf("input the wall temperature : ");
   scanf("%lf",&twall);
   gotoxy(10,8);
   printf("input the flow rate : ");
   scanf("%lf",&fl);

   diam = diam/12.0 ;        /* converted to feet */
   tbulk = (tbulk-32.)*5./9. ; /* convert deg. f to deg. c */

/* begin density calculation */

   sum = 0.0;
   for(i = 0 ; i<=2 ; i++)
   {
    for(j = 0 ; j<=2 ; j++)
     {
          d[i][j] = ad[i][j]*pow(concen,j)*pow(tbulk,i);
          sum = sum + d[i][j] ;
     }
   }
   dens = sum ;
   dense = dens*62.428 ;

/*  end of density calculation  */

/*  begin beta calculation  */

   pdrta = -1.2379e-4-9.9189e-4*concen+4.1024e-4*pow(concen,2) ;
   pdrtb = 2.*(-2.9837e-6*tbulk+2.4614e-6*concen*tbulk);
   pdrtc = 2.*(-9.5278e-8*concen*concen*tbulk);
   pdrt = pdrta + pdrtb + pdrtc ;
   beta = -(1./dens)*pdrt ;
   betaf = (1./beta)*1.8 ;
   betae = 1./betaf ;

/*  end of beta calculation  */

/*  begin viscosity calculation  */

   sum = 0.0 ;
   for(i=0;i<=1;i++)
   {
    for(j=0;j<=2;j++)
          {
           v[i][j] = av[i][j]*pow(concen,j)*pow(tbulk,i);
```

```
            sum = sum + v[i][j] ;
            v2[j] = av[2][j]*pow(concen,j);
           }
   }
   v3 = v2[0]+v2[1]+v2[2] ;
   v3 = pow(v3,0.25)*tbulk*tbulk ;
/*    visc = v[0][0]+v[0][1]+v[0][2]+v[1][0]+v[1][1]+v[1][2]+v3 ;  */
   visc = sum + v3 ;
   abvisc = exp(visc) ;
   abvisce = (abvisc/1000.)*.67197 ;
   kinvisc = (abvisc/dens) ;
   kinvisce = (abvisce/dense) ;

/*  end of viscosity calculation  */

/*  begin Prandtl number calculation  */

   sum = 0.0 ;
   for(i=0;i<=1;i++)
   {
    for(j=0;j<=2;j++)
          {
            p[i][j] = ap[i][j]*pow(concen,j)*pow(tbulk,i);
            p2[j] = ap[2][j]*pow(concen,j);
            sum = sum + p[i][j] ;
          }
   }

   p3 = pow((p2[0]+p2[1]+p2[2]),.25)*tbulk*tbulk ;
   pran = sum + p3 ;
   pr = exp(pran) ;

/*  end of Prandtl number calculation  */

/*  begin thermal conductivity     */
/*  cp , Grashof # , Reynolds #    */
/*  mass flow rate , velocity and  */
/*  thermal difusivity calculation */

   kh2o = .56276+0.001874*tbulk-0.0000068*pow(tbulk,2) ;
   keth = .24511+0.0001755*tbulk-8.52e-7*pow(tbulk,2) ;
   kfactor = .6635-0.3698*concen-0.000885*tbulk ;
   kk = (1-concen)*kh2o + concen*keth - kfactor*(kh2o-keth)*(1-concen)*concen ;
   ke = kk*.57818 ;
   cp = pr*kk/abvisc ;
   cpe = cp*0.23901 ;
   tbulk = tbulk*1.8 + 32. ;
   gr = ((32.174*betae*pow(0.05175,3)*(twall-tbulk))/pow(kinvisce,2))/10000. ;
   vele = (fl/7.48/(PI/4.*0.05175*0.05175))/60. ;
   re = vele*0.05175/kinvisce/1000. ;
   mfe = dense*(PI/4.*pow(0.05175,2))*vele*3600 ;
   tde = (ke/dense*cpe)*1000. ;

/*  end of ke , gr , re , vele , mfe and tde calculation  */

/*  scaling */

   kinvisce = kinvisce * 3600.*1000. ;
   abvisce = abvisce * 3600. ;
   betae = betae *1000. ;
```

```
   tde = (ke/dense/cpe)*1000. ;

/*  end of scaling  */

   clrscr();
   gotoxy(10,2);
   printf("Density (lbm/ft^3) = %lf",dense);
   gotoxy(10,4);
   printf("Prandtl number = %lf",pr);
   gotoxy(10,6);
   printf("Grashof number*10^-4 = %lf ",gr);
   gotoxy(10,8);
   printf("Reynolds number*10^-3 = %lf ",re);
   gotoxy(10,10);
   printf("velocity (ft/sec) = %lf ", vele);
   gotoxy(10,12);
   printf("mass flow rate (lbm/hr) = %lf",mfe);
   gotoxy(10,14);
   printf("abs. Visc. (lbm/ft*hr) = %lf", abvisce);
   gotoxy(10,16);
   printf("kin. Visc. (ft^2/hr)*10^3 = %lf",kinvisce);
   gotoxy(10,18);
   printf("Conductivity (btu/hr*ft*f) = %lf ",ke);
   gotoxy(10,20);
   printf("Beta (1/f)*10^3 = %lf",betae);
   gotoxy(10,22);
   printf("Th. Diff. (ft^2/hr)*10^3 = %lf",tde);
   getch();
   break ;

   case 'F' :
/***** initialized the lnth array *****/

   lnth[0] = 0.5 ;
   lnth[1] = 1.0 ;
   lnth[2] = 1.5 ;
   lnth[3] = 2.0 ;
   lnth[4] = 2.5 ;
   lnth[5] = 3.3 ;
   lnth[6] = 3.5 ;
   lnth[7] = 4.0 ;
   lnth[8] = 4.5 ;
   lnth[9] = 5.0 ;
   lnth[10] = 6.0 ;
   lnth[11] = 7.0 ;
   lnth[12] = 8.0 ;
   lnth[13] = 9.0 ;
   lnth[14] = 10.0 ;
   lnth[15] = 12.0 ;
   lnth[16] = 14.0 ;
   lnth[17] = 16.0 ;
   lnth[18] = 19.3021 ;

/*  test data */
   vavg[0] = 19.0;
   vavg[1] = 18.0;
   vavg[2] = 17.0;
   vavg[3] = 16.0;
   vavg[4] = 15.0;
   vavg[5] = 14.0;
```

```
  vavg[6] = 13.0;
  vavg[7] = 12.0;
  vavg[8] = 11.0;
  vavg[9] = 10.0;
  vavg[10] = 9.0;
  vavg[11] = 8.0;
  vavg[12] = 7.0;
  vavg[13] = 6.0;
  vavg[14] = 5.0;
  vavg[15] = 4.0;
  vavg[16] = 3.0;
  vavg[17] = 2.0;
  vavg[18] = 1.0;
    for(j=0;j<=18;j++)  {
   vavg[j] = (volt[j][1]+volt[j][2]+volt[j][3]+volt[j][4])/4. ;
 }
  window(1,2,80,24);
  clrscr();
  gotoxy(10,6);
  printf("correlation delp = a+b*volt , input the coefficient ");
  gotoxy(10,7);
  printf("input the coefficient a : ");
  scanf("%f",&coef_a);
  gotoxy(10,8);
  printf("input the coefficient b : ");
  scanf("%f",&coef_b);


   for(i=0;i<=18;i++)  {

/***** using the pressure transducer calibration equation *****/
    dph[i] = -0.253+2.755*vavg[i];
   }
  denh2o = 62.4 ;
  denhg = 852.13 ;

   window(1,2,80,24);
   textbackground(RED);
   textcolor(YELLOW);
   clrscr();
   window(10,3,60,5);
   textbackground(BLUE);
   textcolor(WHITE);
   clrscr();
   gotoxy(5,1);
   printf("Specify the output file name ");
   gotoxy(5,2);
   scanf("\n%s",&name);
   window(10,9,60,12);
   textbackground(BLUE);
   textcolor(WHITE);
   clrscr();
   gotoxy(5,1);
   cprintf("input the last station read by transducer : ");
   scanf("%d",&sth);
   ofp = fopen(name,"w");

/**** for the station read in inch of water ****/
   for(i=0;i<=sth;i++)
   {
```

```
    ff[i] = dph[i]*62.4*.621*2.*32.174/(lnth[i]*vele*vele*144.*dense);
   }
  m = sth+1 ;
    window(5,15,75,20);
    textbackground(BLUE);
    textcolor(WHITE);
    clrscr();
  for(i = m;i<=18;i++)
  {
    gotoxy(5,1);
    cprintf("for inches of water ==>1;for inches of mercury==>2 :");
    scanf("%d",&type_of_gauge);
    gotoxy(5,3);
    if(type_of_gauge==2) {
    cprintf("inches of mercury for station %d :",i);
    scanf("%lf",&dpm[i]);
    ff[i] = dpm[i]*denhg*.621*2*32.174/(lnth[i]*vele*vele*144.*dense);
    clrscr();
        }
    if(type_of_gauge==1) {
cprintf("inches of water read for station %d :",i);
    scanf("%lf",&dph[i]);
    clrscr();
    ff[i] = dph[i]*62.4*.621*2.*32.174/(lnth[i]*vele*vele*144.*dense);

   }

  }
  window(1,1,80,25);
  textbackground(BLUE);
  textcolor(YELLOW);
  clrscr();
  for(i=0;i<=sth;i++)
  {
  printf("\n%lf  %lf",lnth[i],ff[i]);
  fprintf(ofp,"\n%lf  %lf",lnth[i],ff[i]);
  }
  for(i=m;i<=18;i++)
  {
  printf("\n%lf  %lf",lnth[i],ff[i]);
  fprintf(ofp,"\n%lf  %lf",lnth[i],ff[i]);
  }
  getch();
  break ;

  case 'M' :
  window(1,2,80,24);
  textbackground(BLUE);
  textcolor(RED);
  clrscr();
  system("mre.exe");
  gotoxy(30,12);
  cprintf("hit any key to continue!");
  getch();
  break;

  case 'C' :
  system("cls");
  system("convert");
  getch();
```

```
break;

case 'A' :
system("cls");
system("c:\mac14\acqcomp");
getch();
break;

case 'H' :
window(1,2,80,24);
textbackground(BLUE);
textcolor(WHITE);
clrscr();
system("ht");
gotoxy(30,12);
cprintf("hit any key to continue!");
getch();
break;

case 'R' :
window(1,2,80,24);
textbackground(BLUE);
textcolor(WHITE);
clrscr();
system("dtred");
gotoxy(30,12);
cprintf("hit any key to continue!");
getch();
break;

case 's' :
window(1,2,80,24);
textbackground(BLUE);
textcolor(YELLOW);
clrscr();
system("c:\pcplus\pcplus");
gotoxy(30,12);
cprintf("hit any key to continue!");
getch();
break;

case 'Q' :
system("cls");
exit(1);



} /****** close brace for switch case *******/
} /****** close while loop ******/
} /*  end of main  */
```

APPENDIX B

UNCERTAINTY ANALYSIS

APPENDIX B

UNCERTAINTY ANALYSIS

The probable error in the experimental measurements of the heat transfer and skin friction coefficients are presented in this appendix. Calculation of the uncertainties is based on the method proposed by Kline and McClintock (1953).

B.1 Uncertainty Analysis of Heat Transfer Coefficient

The heat transfer coefficient is defined as:

$$h = \frac{\dot{q}''}{(T_{wi} - T_b)} \tag{B.1}$$

The percent probable error for h is given by:

$$U_h = \left[\left(\frac{d\dot{q}''}{\dot{q}''} \right)^2 + \left(\frac{d\Delta T}{\Delta T} \right)^2 \right]^{\frac{1}{2}} \tag{B.2}$$

The heat flux is the product of the voltage drop across the test section and the current carried by the tube. Therefore, the heat flux can be written as:

$$\dot{q}'' = \frac{VI}{\pi D L_h} \tag{B.3}$$

The uncertainty in the heat flux can then be calculated using the following equation :

$$U_{\dot{q}''} = \left[\left(\frac{dV}{V} \right)^2 + \left(\frac{dI}{I} \right)^2 + \left(-\frac{dD}{D} \right)^2 + \left(-\frac{dL_h}{L_h} \right)^2 \right]^{\frac{1}{2}} \quad \text{(B.4)}$$

The uncertainty of each variable was estimated as follows :

dV The volt meter has a manufacturer advertised accuracy of 1% of reading. The readings ranged from 2.67 to 24.97 volts giving an average error of 0.14 volts.

dI The ammeter was calibrated and had an error of less than 1% of full scale and was used from 150 to 450 Amps giving an average error of 2.5 Amps.

dD The inside diameter was measured accurately to 0.0005 inches using a micrometer and the inside diameter is 0.624 inches.

dL_h The heated length of the test section is 230.75 inches and was measured to within 0.0625 inches.

To evaluate the inside wall temperature (T_{wi}), the heat diffusion equation is solved by using the appropriate boundary conditions.

$$T_{wi} = T_{wo} - \left(\frac{\dot{q}}{2\pi (D_o^2 - D_i^2) K_s L_h} \right) \left[D_o^2 \ln(D_o / D_i) - \frac{1}{2} \left(D_o^2 - D_i^2 \right) \right] \quad \text{(B.5)}$$

The bulk temperature at the desired location x is determined by using the following equation :

$$T_b = T_{ba} - [(T_{ba} - T_{bi})(L_h - x)]/L_h \quad \text{(B.6)}$$

The uncertainty associated with the quantity (T_{wi} - T_b) can be estimated from the following equation :

$$U_t = \left[\left(\frac{|dT_{wo}| + |dT_{ba}| + |dT2| + |dT1|}{T_{wi} - T_b} \right)^2 \right]^{\frac{1}{2}} \quad \text{(B.7)}$$

where :

$$T1 = -\left(\frac{\dot{q}}{2Ak_sL_h}\right)\left[D_o^2 \ln(D_o / D_i) - \frac{1}{2}\left(D_o^2 - D_i^2\right)\right] \quad (B.8)$$

$$T2 = (T_{ba} - T_{bi})(L_h - x)/L_h \quad (B.9)$$

For this analysis the following uncertainties of each term are as follows :

dT_{wo} The assumed error in the outside wall temperature was estimated to be 0.3 °F from the calibration runs.

dT_{ba} The bulk average temperature deviation was assumed to be 0.3 °F from the calibration of the model 5100 datalogger.

dT2 The deviation ratio dT_2/T_2 was assumed to be 0.05.

dT1 The deviation ratio dT_1/T_1 was assumed to be 0.05.

Applying the following values :

$\dot{q} = 22738$ Btu / hr	$\dot{q}'' = 7238$ Btu / hr – ft^2
V = 19.04 volts	I = 350 Amps
$T_{bi} = 98.6$°F	$T_{ba} = 102.75$°F
$D_o = 0.748$ inches	$D_i = 0.624$ inches
$T_{wo} = 109.69$°F	$k_s = 7.686$ Btu/hr-ft-°F

Substitution of all values into the proper equations, we have

T1 = -0.6159 °F

T2 = 0.6913°F

$(T_{wi} - T_b) = 7.0154$°F

These values result in the expected experimental uncertainties of :

$$U_t = \{[(0.2 + 0.3 + 0.05 + 0.05)/7.0154]^2\}^{1/2}$$

$$= 0.0998$$

$$U_{\dot{q}''} = [(0.14/19.04)^2 + (2.5/350)^2 + (0.0005/0.624)^2 + (0.0625/230.75)^2]^{1/2}$$

$$= 0.0103$$

$$U_h = [(0.0998)^2 + (0.0103)^2]^{1/2}$$

Multiplying by 100 gives the percentage uncertainty for heat transfer coefficient calculations.

$$U_h = 10.03\%$$

From the uncertainty analysis, it can be seen that the maximum error corresponding to the experimental heat transfer coefficient is approximately 10%. The analysis shows that the uncertainty in heat transfer coefficient is predominated by the maximum error in the measurements of temperatures.

B.2 Uncertainty Analysis of Skin Friction Coefficient

The skin friction coefficient is defined as :

$$C_f = \frac{\tau_w}{1/2(\rho V^2)} \qquad (B.10)$$

The wall shear stress in the above equation may be obtained by evaluating the surface forces acting on the test section as follows :

$$SF_{surface} = DP\ A_c - t_w\ A_s \qquad (B.11)$$

$$t_w = (DP\ A_c)/A_s \qquad (B.12)$$

Some of the terms may be rewritten in terms of the measurable quantities :

$$V = \frac{\dot{Q}}{A_c} \tag{B.13}$$

$$A_c = \frac{\pi D^2}{4} \tag{B.14}$$

$$A_s = pD_iL \tag{B.15}$$

$$\dot{Q} = mF + b \tag{B.16}$$

Note that Equation (B.16) represents the turbine meter calibration for volume flow rate.

Substituting the equations and simplifying yields :

$$C_f = \frac{\pi^2 \Delta P D_i^5}{32\rho L(mF + b)^2} \tag{B.17}$$

Following the procedure outlined in Kline and McClintock (1953), the uncertainty interval for the skin friction coefficient may be obtained from the following equation :

$$U_{C_f} = \left[\left(\frac{d\Delta P}{\Delta P}\right)^2 + \left(\frac{4dD_i}{D_i}\right)^2 + \left(\frac{d\rho}{\rho}\right)^2 + \left(\frac{dL}{L}\right)^2 + \left(\frac{2mdF)}{mF + b}\right)^2\right]^{\frac{1}{2}} \tag{B.18}$$

The uncertainty for each variable was estimated as follows :

dDP/DP The uncertainty for the pressure transducer was specified by the manufacturer to be 0.0025, that is 0.25% of full scale.

dD_i The uncertainty interval for the test section tube diameter was estimated to be 0.0005 inches.

dr/r The uncertainty for density was estimated to be 0.0019 according to Bohn, et al. (1984).

dL The uncertainty interval for the pressure tap spacing was estimated to be 0.0005 inches.

dF The uncertainty interval for reading the frequency counter was estimated to be 4 Hz.

Substituting these values and the following values into (B.18)

m = 0.00418 gpm /Hz, F = 173 Hz, b = 0.024721 gpm,

D = 0.621 inches, L = 6 inches

$U_{Cf} = [(0.025)^2 + (0.0005/0.621)^2 + (0.0019)^2 + (0.0005/6)^2 + (0.0334/0.7479)^2]^{1/2}$

$U_{Cf} = 0.0511$

Multiplying by 100 gives the percentage uncertainty for skin friction coefficient calculations :

$U_{Cf} = 5.11\%$

From the uncertainty analysis, it can be seen that the maximum error corresponding to the experimental skin friction coefficient is approximately 5.11%. The greatest influence on the percentage uncertainty for the skin friction coefficient is seen to be the frequency counter readings.

APPENDIX C

SUMMARY OF EXPERIMENTAL DATA

APPENDIX C

SUMMARY OF EXPERIMENTAL DATA

In this appendix, the data summaries of heat transfer and pressure drop for the reentrant, square-edged and bell-mouth inlets are presented.

C.1 Heat Transfer Data Summary

The following tables are the data summary for heat transfer measurements. The subscript "22" indicates test station 22 (x/D = 192).

Reentrant inlet

RUN#	Re_{22}	Pr_{22}	Nu_{22}	Gr_{22}
1002	49939	4.52	271.7	188452
1003	29538	4.56	174	154089
1004	22983	4.94	146.3	147400
1007	12537	4.65	69	233942
1009	11049	4.39	68.8	289222
1010	16760	4.27	92.1	317174
1011	9602	4.57	60	228270
1012	13312	4.12	75.3	428724
1013	48337	4.43	237.1	158236
1014	39098	4.78	203	96027
2603	2693	43.97	38	5224
2605	3609	41.5	53.6	4443
2607	5497	35.21	85	20275
2608	3838	41.97	64.9	13931
2609	2408	45.97	27.1	11196
2612	7526	29.01	117.7	50998
2614	3482	38.53	54.8	24049
2615	2053	46.98	14.5	12841
2616	1746	42.51	14.4	15506
2617	2494	46.92	32.7	8433
2618	1642	45.31	19.1	15698
2619	1689	47.79	14	12484
2620	2898	45.28	44.1	10753

RUN#	Re_{22}	Pr_{22}	Nu_{22}	Gr_{22}
2621	2784	46.54	40.3	4543
2622	2431	46.83	35.1	5149
2623	1659	46.75	14.3	12819
2626	1852	45.24	14.4	13622
2627	2156	46.94	14	12966
2632	2089	44.63	15.4	13299
2633	2262	42.59	22.7	16592
2638	2207	39.35	19.2	33471
2640	2337	38.46	18.8	29530
2646	9476	27.62	129.6	42972
2647	8599	26.42	118.9	51544
2648	9144	26.2	123.9	50287
2649	7707	25.41	105	63561
2650	6170	25.16	89.4	76550
2651	4844	26.25	71.7	70696
2652	7343	23.66	99.2	78357
2653	7343	23.66	99.2	78357
2654	6723	23.76	92.5	83451
2655	4144	27.25	60.7	47641
2656	3215	30.31	46.4	39222
2657	6021	26.03	87.5	58644
2660	11562	25.97	155.9	44906
2661	13314	25.09	171.2	47830
2662	15408	21.96	182.3	62170
2663	2533	36.46	43.6	20317
2664	15246	20.38	183.8	67627
2665	11937	27.17	155.1	26953
2666	12731	20.42	159.4	77831
2667	7279	40.76	68.8	4197
2668	3030	32.33	60.8	26635
2669	2538	38.47	28.5	14592
2670	2260	39.25	18.5	15715
2904	1315	95.8	14.6	5415
2905	1232	95.39	14.3	5585
2907	1368	98.3	14.9	5018
2911	900	100.91	13.6	4784
2912	668	94.1	14.8	5022
2913	872	95.38	13.9	5174

Square-edged inlet

RUN#	Re_{22}	Pr_{22}	Nu_{22}	Gr_{22}
1001	15228	4.81	91.4	210453
1002	28232	4.44	149.2	331511

RUN#	Re_{22}	Pr_{22}	Nu_{22}	Gr_{22}
1003	31964	4.76	208.8	186013
1004	38587	4.8	197	203011
1005	46001	4.97	229	158734
1006	44873	5.04	236.8	104157
1007	33168	5.28	153.8	95489
1008	25912	5.09	150.1	103246
1009	11980	4.83	74.6	188670
1010	10728	4.67	69	223828
1012	8791	4.79	58.2	206356
1013	7727	4.6	51.2	263216
1014	30918	5.5	167.5	77841
1015	24353	5.37	140	100342
1016	14567	4.36	91.6	403636
1017	6147	4.69	39.8	302495
1018	5448	4.61	35.2	338924
1019	4634	4.77	29.7	298395
2001	349	121.54	14.3	3837
2002	1049	139.49	16.3	3971
2003	640	138.54	15.1	3503
2004	1308	132.62	19.3	5925
2005	830	137.6	16.2	4129
2006	1578	112.93	21.6	10468
2007	1757	110.48	22.1	11523
2008	2088	114.13	21.9	10119
2009	2284	114.66	25.2	8637
2010	2583	111.58	46.6	5517
2011	2982	107.28	61.3	5301
2601	6889	26.88	93.2	38358
2602	6626	26.51	88.9	42078
2603	2734	27.4	21.6	96339
2604	2307	24.72	22.4	115567
2605	1650	24.79	21.3	92017
2606	1953	24.04	22.8	112054
2607	2725	23.94	23.1	137076
2608	3519	22.38	41.9	111790
2609	4013	21.57	48.3	114820
2610	6359	25.68	86.6	43162
2611	2536	23.7	22.8	132786
2612	3151	21.85	25.5	173170
2613	3295	30.4	43.3	28716
2614	4582	21.9	58.5	91341
2651	3123	36.79	27.5	10496
2652	4409	38.48	54.3	5014
2653	6953	39.47	66.4	3738
2654	11349	29.3	152.4	23116

RUN#	Re_{22}	Pr_{22}	Nu_{22}	Gr_{22}
2655	5087	35.3	76.2	22533
2656	4975	34.99	74	23641
2657	4738	34.46	70.1	25810
2658	4532	34.12	66.5	27817
2659	6644	35.75	99.4	16755
2660	6263	35.59	93.1	18072
2667	1539	40.89	12.8	20840
2668	1718	41.57	13.2	20119
2669	1893	41.79	13.8	23200
2670	2137	40.87	15.1	27485
2671	2225	42.89	13.8	21486
2672	2012	44.42	13	16924
2673	2305	45.1	12.9	16512
2674	2438	43.58	14.2	22556
2675	2690	39.74	17.6	39181
2676	2863	37.29	20.5	54468
2677	2720	41.38	17.4	34687
2678	2562	44.81	14.5	20810
2679	2513	46.32	12.4	15482
2680	2735	46.45	25	8055
2681	2588	44.44	15.3	21536
2682	2725	41.53	17.9	33513
2683	3586	38.99	45.3	21840
2684	3185	37.77	39.4	26922
2685	3886	41.65	50.9	17715
2686	4933	36.32	68.3	29436
2687	6171	34.27	86.1	33408
2688	3140	40.08	41.5	24136
2689	2524	51.87	13.9	14358
2690	2813	47.75	32.1	13720
2691	3311	48.98	41	10153
2692	2983	48.26	36.9	11653

Bell-mouth inlet

RUN#	Re_{22}	Pr_{22}	Nu_{22}	Gr_{22}
1200	7853	11.81	17.6	169330
1201	9671	9.41	86.2	56532
1202	9040	10.11	75	55550
1203	8601	9.11	29	184064
1204	8529	10.84	17.9	204533
1206	10876	9.39	90.6	54010

RUN#	Re_{22}	Pr_{22}	Nu_{22}	Gr_{22}
1207	11536	8.15	101.6	65690
1208	9522	9.46	19.3	255128
1211	13029	9.66	128.6	35732
1214	9861	9.14	80.9	64243
1215	10650	9.09	81.5	64598
1216	11479	9.08	94	56022
1217	3811	8.04	17.8	384894
1218	4444	8.69	17.2	337253
1219	5282	8.77	20.9	274277
1220	5184	8.78	17.9	314238
1221	8521	10.25	52	77274
1222	9101	10.37	49.4	79394
1223	9095	10.38	65	60106
1224	9083	10.39	67.6	57614
1225	10066	10.45	98.3	39077
2503	4138	15.62	21.2	163454
2504	9532	16.88	87.7	32845
2505	8844	16.98	21.1	137856
2506	8517	17.21	101.9	27096
2507	7979	17.09	52.3	53861
2508	7424	16.91	32.1	90451
2509	9012	17.3	118.5	23048
2510	8829	17.41	115.8	23272
2512	6159	17.77	42.4	64693
2513	5890	17.72	40.8	67668
2514	5656	17.86	32	85225
2515	5444	17.76	29.6	93319
2516	9413	16.73	106.6	28241
2517	8973	17.31	85.2	32936
2518	8821	17.49	63.5	43347
2519	8665	17.52	54.5	50313
2520	8511	17.6	55.7	48735
2521	8257	18.56	83.5	31328
2522	8157	18.54	68	38640
2523	8049	18.58	57.1	45828
2524	7953	18.54	46.8	56268
2525	7557	19.29	37.4	65004
2527	7785	18.71	55.6	46430
2528	7672	18.69	48.6	53356
2529	7668	18.52	23.6	113302
2530	7461	18.45	23.3	115901
2531	7246	18.48	22.7	118568
2532	7113	18.51	20.3	132375
2533	6827	18.54	20.8	129098
2534	6484	18.62	20.2	131384
2539	36295	6.09	281.2	20482

RUN#	Re_{22}	Pr_{22}	Nu_{22}	Gr_{22}
2540	15624	5.99	117.9	50926
2541	9951	5.9	18.4	345807
2542	17728	5.86	153.7	41107
2543	16837	5.94	116.3	52807
2544	15592	5.98	98.4	61422
2545	14634	5.96	81.6	74531
2546	13732	5.95	69.4	88252
2547	13120	5.93	42.8	144738
2548	12008	5.94	37.1	166561
2549	10434	6.21	26.4	211672
2601	4448	28.65	20.1	65084
2602	4853	27.66	57	32639
2603	2209	24.29	22.4	110545
2604	4780	27.44	22.7	86142
2605	3967	26.44	22.9	92302
2606	4332	27.07	22.5	89895
2607	4594	27.2	22.5	88923
2608	5226	27.45	22.6	86979
2609	4815	25.92	22.7	97665
2610	5055	24.65	22.8	107893
2611	5389	23.96	23.1	112919
2612	6130	21.02	84.8	67934
2613	6133	21.01	85	67817
2614	3555	34.45	18.4	29789
2615	4720	28.13	22.8	79617
2616	3108	32.9	17.7	32543
2617	3190	33.03	17.7	32320
2618	3463	33.56	17.5	31493
2619	3799	33.44	17.6	31591
2620	4320	32.24	17.8	33823
2621	5730	17.22	21	155674
2622	5977	17.65	21	147825
2623	4052	17.75	19.5	158055
2624	6807	15.24	21.3	198617
2625	3141	19.15	13.8	51213
2626	7291	12.82	21.7	265772
3801	11400	12.55	112.9	73094
3802	10480	12.72	106.8	75199
3804	8931	12.2	89.8	97821
4301	18426	13.37	159.4	73219
4302	17337	12.95	156.3	80038
4304	16135	12.75	148.1	87418
4305	15218	13.16	141.7	77367
4306	14372	13.02	134.4	83385
7305	3958	45.84	22.5	43997
7306	3913	43.87	23.9	49174
7308	5388	36.8	73.9	30772

RUN#	Re_{22}	Pr_{22}	Nu_{22}	Gr_{22}
7316	5652	39.71	76.3	22641
7317	5197	38.78	66.9	27217
7322	7673	33.3	103	30318
7323	7439	32.6	99	33013
7325	7033	31.94	94.4	36218
7329	5421	35.97	71.9	31176
7330	5643	37.45	76.1	27006
7335	3804	48.68	21.6	33912
7340	4403	40.01	27.7	55033
7341	4061	39.57	32	48512
7342	4492	40.5	31.2	49446
7343	4473	40.31	41.8	37974
7344	4898	40.32	49.1	32149
7345	4645	39.87	52.3	30879
7346	4136	41.62	31.9	43165
7347	4161	41.35	34.3	41868
7348	4281	40.21	48.1	33039
8002	3293	69.86	22	20701
8107	3649	63.46	22.5	25135
8109	2764	68.04	20.6	21370
8110	3946	57.66	24.1	33919
8406	3787	70.46	22.9	20607

C.2 Pressure Drop Data Summary

The following tables are the summary for pressure drop measurements. The subscript "18" indicates test station 18 (x/D = 310).

Reentrant inlet

RUN#	Re_{18}	C_{f18}		RUN#	Re_{18}	C_{f18}
1001	1286.10	0.01370		1002	1205.37	0.01470
1003	1423.44	0.01218		1004	1495.27	0.01157
1005	1594.08	0.01095		1006	1681.30	0.01046
1007	1791.16	0.00980		1008	1909.51	0.00914
1009	2007.13	0.00882		1010	2102.73	0.00843
1011	2194.52	0.00811		1012	2299.68	0.00768
1013	2411.27	0.00734		1014	2520.40	0.00707
1015	2575.89	0.00689		1016	2670.95	0.00665
1017	2773.15	0.00641		1018	4024.52	0.00965

RUN#	Re_{18}	C_{f18}		RUN#	Re_{18}	C_{f18}
1019	3921.76	0.00967		1020	3814.04	0.00965
1021	3702.47	0.00964		1023	3465.08	0.00934
1024	3348.78	0.00926		1025	3198.89	0.00788
1026	3026.74	0.00680		1027	2938.24	0.00652
1031	4191.42	0.00957		1032	4385.00	0.00949
1034	4635.25	0.00941		1035	4478.92	0.00947
2001	1949.73	0.01030		2002	1853.17	0.01122
2003	1753.70	0.01206		2004	1656.41	0.01334
2005	2030.04	0.00955		2006	2216.17	0.00881
2007	2329.54	0.00839		2008	2420.23	0.00801
2009	2556.10	0.00749		2010	2614.06	0.00718
2011	2726.79	0.00687		2012	2904.22	0.00658
2013	2998.39	0.00636		2014	3114.67	0.00610
2015	3227.82	0.00589		2020	3311.05	0.00578
2021	3655.58	0.00616		2022	3789.39	0.00777
2023	3850.44	0.00861		2024	4081.04	0.00889
2025	4238.02	0.00904		2026	4392.83	0.00906
2027	4525.02	0.00908		2028	4678.26	0.00909
3023	3055.21	0.00910		3043	3308.33	0.00745
3041	3419.05	0.00707		3040	3493.27	0.00675
3039	3585.77	0.00639		3036	3856.83	0.00592
3014	3914.46	0.00571		3024	3936.58	0.00579
3035	4033.15	0.00567		3010	4138.69	0.00539
3026	4178.95	0.00538		3030	4327.67	0.00522

Square-edged inlet

RUN#	Re_{18}	C_{f18}		RUN#	Re_{18}	C_{f18}
1001	3074.85	0.00597		1003	2838.84	0.00646
1004	2731.77	0.00672		1005	2598.76	0.00695
1006	2467.87	0.00739		1007	2350.51	0.00772
1009	2082.00	0.00858		1015	2926.99	0.00621
1016	2211.87	0.00817		1018	1899.18	0.00984
1019	1648.44	0.01149		1020	1386.05	0.01425
1021	3163.13	0.00577		1022	3257.67	0.00560
1023	3366.72	0.00544		1024	3455.58	0.00534
1025	3538.76	0.00528		1026	3656.80	0.00578
1027	3743.81	0.00676		1028	3817.50	0.00773
1029	3926.62	0.00905		1030	4019.51	0.00955
1031	4114.42	0.00976		1032	4211.41	0.00977
1033	4309.67	0.00975		1034	4397.57	0.00979

RUN#	Re_{18}	C_{f18}		RUN#	Re_{18}	C_{f18}
1035	4479.60	0.00976		1040	4722.41	0.00971
1041	4617.66	0.00970		2001	3483.07	0.00560
2004	3200.01	0.00610		2005	3091.51	0.00634
2006	2991.57	0.00648		2009	2794.36	0.00706
2010	2699.35	0.00730		2011	2613.72	0.00760
2012	2511.91	0.00797		2013	2424.39	0.00830
2016	1978.58	0.01085		2017	1871.10	0.01170
2018	2302.29	0.00876		2019	2144.34	0.00957
2020	2915.22	0.00668		2022	3326.92	0.00583
2024	3585.80	0.00539		2025	3689.59	0.00522
2026	3749.92	0.00516		2027	3839.81	0.00503
2029	4036.84	0.00497		2031	4189.33	0.00710
2032	4106.52	0.00612		2033	3950.01	0.00488
2034	4342.00	0.00850		2035	4430.19	0.00891
2036	4555.61	0.00919		2037	4657.19	0.00921
2038	4721.71	0.00922		2039	4806.87	0.00925
2040	4922.96	0.00923		2041	5048.95	0.00925
2042	5168.35	0.00922		2044	5413.90	0.00922
2045	5524.70	0.00927		2046	5620.50	0.00919
3001	4184.70	0.00506		3004	3550.98	0.00616
3005	3432.93	0.00645		3006	3309.47	0.00675
3007	3192.45	0.00709		3008	3112.78	0.00735
3011	2749.90	0.00924		3012	2828.62	0.00876
3013	2931.11	0.00820		3014	3059.11	0.00771
3015	3617.53	0.00604		3016	3720.11	0.00578
3017	3816.35	0.00565		3018	3880.06	0.00551
3019	3962.68	0.00542		3020	4057.40	0.00525
3021	4322.49	0.00489		3024	4009.83	0.00532
3027	4564.06	0.00462		3028	4677.91	0.00448
3030	4472.19	0.00471		3032	4829.94	0.00472
3033	4919.45	0.00530		3034	4964.65	0.00709
3035	5119.44	0.00816		3036	5209.44	0.00861
3037	5257.59	0.00866		3038	5420.35	0.00871
3039	5525.93	0.00872		3040	5640.08	0.00872
3041	5863.41	0.00877		3042	6038.48	0.00870
3044	6862.15	0.00863		3045	7119.06	0.00861
3046	7315.21	0.00855		3047	7512.17	0.00848
3048	7753.08	0.00848		3049	6670.02	0.00871
3051	6421.64	0.00874				

Bell-mouth inlet

RUN#	Re_{18}	C_{f18}		RUN#	Re_{18}	C_{f18}
1601	4107.71	0.00456		1602	4394.95	0.00433
1603	4698.35	0.00412		1604	4469.32	0.00428
1605	6073.68	0.01099		1606	9553.89	0.00798
1608	10959.75	0.00765		1609	13629.11	0.00736
1610	8728.59	0.00825		1611	7597.49	0.00820
1612	7058.46	0.00804		1613	6269.80	0.00783
1614	5646.19	0.00329		1615	6067.31	0.00655
1616	5929.81	0.00326		1617	6016.54	0.00426
1618	6106.37	0.00763		1619	6457.14	0.00795
1620	5178.57	0.00355		1621	4651.78	0.00399
1622	3929.28	0.00487		1623	3929.28	0.00476
1624	3610.21	0.00530		1625	2917.22	0.00642
2501	16254.27	0.00709		2502	15392.87	0.00721
2503	11996.92	0.00756		2504	10992.86	0.00761
2505	10372.46	0.00773		2506	9108.89	0.00787
2507	8610.86	0.00789		2508	8223.25	0.00793
2509	7678.60	0.00787		2510	7244.81	0.00792
2511	7365.90	0.00842		2512	6915.01	0.00751
2513	6380.36	0.00319		2514	6483.73	0.00310
2515	6708.43	0.00624		2516	6747.14	0.00833
2517	6713.40	0.00814		2518	6550.22	0.00503
2519	5990.66	0.00334		2520	5053.44	0.00401
2521	4337.27	0.00479		2522	3934.96	0.00522
2523	3940.59	0.00508		3501	17084.83	0.00710
3502	15456.95	0.00715		3503	13784.02	0.00748
3504	12394.22	0.00762		3505	10926.62	0.00776
3506	9557.48	0.00793		3507	8091.11	0.00797
3508	7814.74	0.00765		3509	7323.61	0.00280
3510	7420.64	0.00550		3511	7433.14	0.00481
3512	7964.04	0.00771		3513	7544.51	0.00605
3514	6908.30	0.00315		3515	6772.74	0.00328
3516	6403.58	0.00345		3517	5500.59	0.00411
3518	4827.51	0.00466		3519	4187.55	0.00531

VITA

Lap Mou Tam

Candidate for the Degree of

Doctor of Philosophy

Thesis: AN EXPERIMENTAL INVESTIGATION OF HEAT TRANSFER AND PRESSURE DROP IN THE TRANSITION REGION FOR A HORIZONTAL TUBE WITH DIFFERENT INLETS AND UNIFORM WALL HEAT FLUX

Major Field: Mechanical Engineering

Biographical:

Personal Data: Born in Macau, on August 3, 1966, the son of Kuok Kuong Tam and Mei Heng Chau.

Education: Graduated from Anglican Choi Ko High School, Macau, in June, 1984; received the Bachelor of Science degree in Mechanical Engineering from National Chiao Tung University, Taiwan, in June, 1989; received the Master of Science degree in Mechanical Engineering from Oklahoma State University in December, 1990; completed the requirements for the Doctor of Philosophy degree at Oklahoma State University in December 1995.

Professional Experience: Graduate Research Assistant and Teaching Assistant, School of Mechanical and Aerospace Engineering, Oklahoma State University, 1990 to 1995.